Charles University
First Faculty of Medicine

Study section: Biomedicine
Academic program: Biochemistry and Pathobiochemistry

UNIVERZITA KARLOVA
1. lékařská fakulta

Mgr. Hana Štufková
(Kratochvílová)

Molekulární podstata deficitu F_1F_o-ATP syntázy a jeho dopad na energetický metabolismus buňky

Molecular basis of deficit of F_1F_o-ATP synthase and its impact on energy metabolism of a cell

Ph.D. Thesis

Supervisor: Ing. Markéta Tesařová, Ph.D.

Consultant: prof. MUDr. Tomáš Honzík, Ph.D.

Prague, 2022

PROHLÁŠENÍ

Prohlašuji, že jsem závěrečnou práci zpracovala samostatně a že jsem řádně uvedla a citovala všechny použité prameny a literaturu. Současně prohlašuji, že práce nebyla využita k získání jiného nebo stejného titulu.

Souhlasím s trvalým uložením elektronické verze mé práce v databázi systému meziuniverzitního projektu Theses.cz za účelem soustavné kontroly podobnosti kvalifikačních prací.

V Praze, Mgr. Hana Štufková

IDENTIFIKAČNÍ ZÁZNAM

ŠTUFKOVÁ, Hana. *Molekulární podstata deficitu F_1F_o-ATP syntázy a jeho dopad na energetický metabolismus buňky.* [*Molecular basis of deficit of F_1F_o-ATP synthase and its impact on energy metabolism of a cell*]. Praha, 2022. 107 stran., 7 příloh, Disertační práce. Univerzita Karlova, 1. lékařská fakulta, Klinika pediatrie a dědičných poruch metabolismu. Vedoucí práce: Ing. Markéta Tesařová, Ph.D. Konzultant: prof. MUDr. Tomáš Honzík, Ph.D.

IDENTIFICATION RECORD

ŠTUFKOVÁ, Hana. *Molecular basis of deficit of F_1F_o-ATP synthase and its impact on energy metabolism of a cell.* [*Molekulární podstata deficitu F_1F_o-ATP syntázy a jeho dopad na energetický metabolismus buňky*]. Prague, 2022. 107 pages., 7 supplements, Ph.D. thesis. Charles University, First Faculty of Medicine, Department of Pediatrics and Inherited Metabolic Disorders. Supervisor: Ing. Markéta Tesařová, Ph.D. Consultant: prof. MUDr. Tomáš Honzík, Ph.D.

ACKNOWLEDGEMENTS

I would like to thank my supervisor Ing. Markéta Tesařová, Ph.D. for her patience, a lot of useful advice, support, and kind guidance during my doctoral studies. Special thanks belong to RNDr. Hana Hansíková CSc, prof. MUDr. Jiří Zeman, DrSc, and prof. MUDr. Tomáš Honzík, Ph.D. who allowed me to participate in mitochondrial research. Furthermore, I would like to thank all my colleagues from Laboratory for the Study of Mitochondrial Disorders and all collaborating colleagues. Last but not least, I am grateful for patience and support of my family.

This Ph.D. thesis was completed during the author´s doctoral studies in biochemical sciences at the First Faculty of Medicine, Charles University, between the years 2009-2022 (interrupted by maternity leave, 2017-2021). The studies involved in this thesis were carried out within the framework of institutional research programs from Charles University: GAUK 37710; PRVOUK-P24/LF1/3; the Cooperatio Program, research area Pediatrics; and SVV260516. Specific support was provided by grants AZV 17-30965A and NU22-01-00499 from the Ministry of Health of the Czech Republic, and GAČR 14-36804G from the Czech Science Fundation.

ABSTRACT

Mitochondria's primary function is to produce energy through the process of oxidative phosphorylation. ATP synthase is a macromolecular rotary machine located in the inner mitochondrial membrane that catalyzes the synthesis of adenosine triphosphate (ATP) from adenosine diphosphate (ADP) and inorganic phosphate (Pi).

The mitochondrial disorders due to ATP synthase deficiency represent a heterogeneous group of diseases characterized by variable severity of the phenotype with onset at birth or later in life till adulthood. Mutations in both, mitochondrial or nucelar DNA encoded genes, may result in ATP synthase impairment, either isolated or combined with deficits of other complexes of oxidative phosphorylation.

The aims of the thesis were to characterize TMEM70 protein, an ATP synthase assembly factor, and to analyze the impact of novel disease variants leading to ATP synthase deficiency in patients´ derived samples.

TMEM70 is a 21 kDa hairpin structure protein localized in the inner mitochondrial membrane, with both termini oriented into the matrix, which forms higher oligomer structures. Our results demonstrated that the absence of TMEM70 protein leads to an isolated deficiency of complex V followed in some stage by adaptive/compensatory effect of respiratory chain complexes. Different severities of ATP synthase deficiency were observed in muscle mitochondria due to extremely rare heteroplasmic variants of *MT-ATP6*. While m.8851T>C (p.Trp109Arg) variant lead only to mild reduction of ATP synthase, m.8719G>A (p.Gly65*) variant resulted in diminished levels of ATP synthase holoenzyme and the presence of assembly intermediates. Similarly, a profound impact on ATP synthase was observed in the case of novel variants in *MTTK* and *PUS1* genes, which was accompanied by deficiency of other oxidative phosphorylation system complexes.

Keywords: mitochondria, oxidative phosphorylation system, ATP synthase, mitochondrial diseases, mitochondrial DNA, *MT-ATP6*, *MTTK*, *TMEM70*

ABSTRAKT

Hlavní funkcí mitochondrií je produkce energie prostřednictvím procesu oxidační fosforylace. ATP syntáza je makromolekulární rotační stroj lokalizovaný ve vnitřní mitochondriální membráně katalyzující syntézu adenosintrifosfátu (ATP) z adenosindifosfátu (ADP) a anorganického fosfátu (Pi).

Mitochondrialní poruchy ATP syntázy představují heterogenní skupinu onemocnění charakterizovanou různou závažností klinického fenotypu s nástupem od narození nebo v pozdějších fázích života. Mutace v mitochondriální nebo jaderné DNA mohou vést k poruše ATP syntázy, a to buď izolovaně, nebo v kombinaci s defekty dalších komplexů systému oxidační fosforylace.

Cílem práce bylo charakterizovat protein TMEM70, asemblační faktor ATP syntázy, a studovat vliv nových variant vedoucích k deficitu ATP syntázy v pacientských vzorcích.

TMEM70 je 21 kDa velký protein vnitřní mitochondriální membrány s orientací obou konců do mitochondriální matrix, který tvoří v membráně vyšší oligomerní struktury. Naše výsledky ukázaly, že absence proteinu TMEM70 vede ke vzniku izolovaného deficitu komplexu V, s přítomností adaptačního/kompenzačního efektu komplexů dýchacího řetězce. Ve svalových mitochondriích byly pozorovány různé stupně deficitu ATP syntázy způsobené extrémně vzácnými heteroplazmatickými variantami v genu *MT-ATP6*. Zatímco varianta m.8851T>C (p.Trp109Arg) vede jen k mírnému snížení množství holoenzymu ATP syntázy, varianta m.8719G>A (p.Gly65*) má za následek výrazné snížení hladiny komplexu V s přítomnosti několika asemblačních intermediátů. Podobně těžký dopad na hladinu ATP syntázy byl pozorován i u nových variant v genech *MTTK* a *PUS1*, což bylo doprovázeno deficitem dalších komplexů systému oxidační fosforylace.

Klíčová slova: mitochondrie, systém oxidační fosforylace, ATP syntáza, mitochondriální poruchy, mitochondriální DNA, *MT-ATP6*, *MTTK, TMEM70*

LIST OF CONTENTS

ABBREVIATIONS

AA: Amino Acid

ADP: Adenosinediphosphate

ANT: Adenine Nucleotide Translocator

ATP: Adenosinetriphosphate

ATPAF1-2: ATP synthase mitochondrial F_1 complex Assembly Factor 1-2

bp: base pair

BN-PAGE: Blue Native Polyacrylamide Gel Electrophoresis

BSN: Bilateral Striatal Necrosis

Ca^{2+}: Calcium ion

cDNA: complementary Deoxyribonucleic Acid

CJ: Cristae Junction

CMT: Charcot-Marie-Tooth syndrome

CoQ: Ubiquinone-coenzyme Q

CO_2: Carbon dioxide

COX: Cytochrome c Oxidase

CS: Citrate Synthase

Cyt b: Cytochrome b

Cyt c: Cytochrome c

CI: Complex I

CII: Complex II

CIII: Complex III

CIV: Complex IV

CV: Complex V

DAPIT: Diabetes Associated Protein in Insulin sensitive Tissues

DMEM: Dulbecco's Modified Eagle's Medium

DNA: Deoxyribonucleic Acid

dNTP: deoxy Nucleoside Triphosphate

D-loop: Displacement loop

EC: Enzyme Commission number

EDTA: Ethylenediaminetetraacetic Acid

ELAC2: ElaC Ribonuclease Z 2

ER: Endoplasmic Reticulum

F: Female

FAD: Flavin Adenine Dinucleotide

FADH2: reduced form of Flavin Adenine Dinucleotide

FBS: Fetal Bovine Serum

[Fe-S]: Iron-Sulfur Cluster

FH: Fumarate Hydratase

FMN: Flavin Mononucleotide

FMC1: Formation Of Mitochondrial Complex V Assembly Factor 1 Homolog

GFP: Green Fluorescent Protein

H: Heavy Strand of Mitochondrial deoxyribonucleic Acid

H^+: Hydrogen ion

H_2S: Hydrogen sulfide

HEK293: Human Embryonic Kidney 293 cells

HSP70: Heat Shock Protein 70

IF1: Inhibitory Factor 1

IMB: Inner Boundary Membrane

IMM: Inner Mitochondrial Membrane

IMS: Intermembrane Space

IP: Immunoprecipitates

kb: kilobase

kDa: kilodalton

KO: Knockout

L: Light Strand of Mitochondrial Deoxyribonucleic acid

LHON: Leber Hereditary Optic Neuropathy

LP: Like Pathogenic

LS: Leigh Syndrome

M: Mitochondria

M: Male

MAM: Mitochondria Associated Endoplasmic Reticulum Membrane

MGME1: Mitochondrial Genome Maintenance Exonuclease 1

MIDD: Maternally Inherited Diabetes and Deafness syndrome

MILS: Maternally Inherited Leigh Syndrome

MLASA: Myopathy, Lactic Acidosis, and Sideroblastic Anemia

MOPS: N-morpholino-propanesulfonic acid

mRNA: messenger Ribonucleic Acid

mt: mitochondrial

MT-ATP6: Mitochondrial gene for subunit a, encoded by mtDNA

***MT-ATP8*:** Mitochondrial gene for subunit A6L, encoded by mtDNA

mtDNA: mitochondrial Deoxyribonucleic Acid

mt-mRNA: mitochondrial messenger Ribonucleic Acid

mt-PAP: mitochondrial Poly(A) Polymerase

mt-rRNA: mitochondrial ribosomal Ribonucleic Acid

mt-SSB: mitochondrial Single-Stranded DNA Binding protein

mt-tRNA: mitochondrial transfer Ribonucleic Acid

MTTC: mitochondrial gen, tRNA for cysteine

MTTK: mitochondrial gen, tRNA for lysine

***MTTV*:** mitochondrial gen, tRNA for valine

MTTY: mitochondrial gen, tRNA for tyrosine

Mx: matrix

NADH: Reduced form of Nicotinamide Adenine Dinucleotide

NAD^+: Nicotinamide Adenine Dinucleotide

NARP: Neurogenic muscle weakness, Ataxia, and Retinitis Pigmentosa syndrome

ND1-6: NADH dehydrogenase subunit 1-6, mtDNA encoded

ND4L: NADH dehydrogenase subunit 4L, mtDNA encoded

nDNA: nuclear Deoxyribonucleic acid

NDUFAB1: NADH ubiquinone oxidoreductase subunit AB1

NDUFA4: mitochondrial complex associated, COXFA4

NQR: NADH: coenzyme Q reductase

NRF1-2: Nuclear Respiratory Factor 1-2

OH^-: Hydroxide ion

OMM: Outer Mitochondrial Membrane

OPA1: mitochondrial dynamin like GTPase

OSCP: Oligomycin-Sensitivity Conferring Protein

OXPHOS: Oxidative Phosphorylation System

O_2: Oxygen

P: Patient

PBS: Phosphate Buffered Saline

PGC-1α; β: Peroxisome proliferator-activated receptor Gamma Coactivator 1-α; β

Pi: Inorganic phosphate

PiC: Inorganic Phosphate Carrier

PIC: Protease Inhibitor Cocktail

pmf: proton motive force

POLG: DNA Polymerase Subunit Gamma

POLRMT: monomeric mitochondrial RNA polymerase

PRC: PGC-1-related coactivator

PTP: Permeability Transition Pore

PUS1: Pseudouridylate Synthase 1

PVDF: Polyvinylidene Difluoride

Q: Ubiquinone-coenzyme Q

QCR: Cytochrome c Oxidoreductase

QH2: Ubiquinol

RC: Respiratory Chain

RIPA: Radioimmunoprecipitation Assay Buffer

RNA: Ribonucleic Acid

RNASeH1: Ribonuclease H1

ROS: Reactive Oxygen Species

rRNA: ribosomal Ribonucleic Acid

S: Svedberg unit

S: Solubilized proteins

SA: Sideroblastic anemia

SDH: Succinate Dehydrogenase

SDHA-D: Succinate Dehydrogenase complex flavoprotein subunit A-D

SDS: Sodium Dodecyl Sulfate

SDS-PAGE: Sodium Dodecyl Sulfate–Polyacrylamide Gel Electrophoresis

STE: Sodium Chloride-Tris-EDTA pufr

TCA: Tricarboxylic Acid Cycle

TFB1-2M: Initiation Transcription Factor B 1-2, Mitochondrial

TEFM: Transcription Elongation Factor, Mitochondrial

TFAM: Transcription factor A, mitochondrial

TMEM242: Transmembrane Protein 242

TMEM70: Transmembrane Protein 70

tRNA: transfer Ribonucleic Acid

TX-100: Triton X-100

UTR: Untranslated Region

VDAC: Voltage Dependent Anion-selective Channel

VUS: Variant of Uncertain Significance

WB: Western Blot

WT: Wilde Type

6.8PL: 6.8 kDa Proteolipid

1. LITERATURE REVIEW

1.1. Mitochondria

Mitochondria are semiautonomic organelles with their own deoxyribonucleic acid (DNA). They play a central role in energy generation in almost all eukaryotic cells. They produce more than 95% of the cellular adenosinetriphosphate (ATP) from metabolic fuels through the oxidative phosphorylation system (OXPHOS) (Henze and Martin 2003; Papa 1996). In addition, mitochondria are involved in the metabolisms of amino acids (AA), lipids and nucleotides, biosynthesis of heme, in the maturation of cellular iron-sulfur clusters [Fe-S]. They are also the site of the tricarboxylic acid cycle (TCA) and key steps of gluconeogenesis and the urea cycle. Mitochondria serve as a calcium storage and play a key role in apoptosis and the production of reactive oxygen species (ROS). Furthermore, mitochondria control proliferation, motility, and redox status of the cell (Craig et al. 1999; Lemasters et al. 2009; Murphy et al. 2016; Weinberg et al. 2015).

According to the endosymbiotic theory, mitochondria are the direct descendent of a eubacterial endosymbiont (Gray 2017; Margulis 1968). The protoeukaryotic host cell with an anaerobic heterotrophic metabolism engulfed aerobic bacteria α-proteobacterium in the process of endocytosis (Degli Esposti 2014; Gray et al. 1999). The major part of the original bacterial genome was transferred to the nucleus thus bacteria became fully dependent on the host cell. However, several proteins uniquely stay encoded by the mitochondrial DNA (mtDNA).

1.1.1. Mitochondrial structure

Mitochondria are commonly depicted as bean-like structures, but they form highly dynamic networks in the majority of cells where they constantly undergo fission and fusion (Kleele et al. 2021; van der Bliek et al. 2013). The fusion/fission process controls mitochondrial morphology and functions (Westermann 2012; Yu et al. 2020). Different tissues contain various numbers and structures of mitochondria reflecting their variable energetic demand (Benard et al. 2006; Garesse and Vallejo 2001).

The pleiotropic role of mitochondria in energy conversion, apoptosis, calcium homeostasis, intermediary metabolism, and cell differentiation is consistent with their morphological and ultrastructural complexity (Favaro et al. 2019; Pernas and Scorrano 2016).

Mitochondria as double membrane organelles have a complex internal structure consisting of several functionally distinct compartments: outer mitochondrial membrane, inner mitochondrial membrane, intermembrane space, cristae, inner boundary membrane, cristae junctions and matrix (Figure 1).

The outer mitochondrial membrane is a smooth and loosely permeable for molecules up to 5 kDa. The metabolites flow by numerous integral proteins called porins, voltage dependent anion-selective channels (VDAC). Large molecules can pass the outer mitochondrial membrane by active transport through special transport proteins (calcium uniporter, sodium/calcium exchanger, etc.) (Crompton et al. 1999; Rizzuto et al. 2009). While transport of nuclear-encoded proteins with mitochondrial targeting signal is facilitated and regulated by the translocase of the outer membrane complex (Neupert and Herrmann 2007; Su et al. 2022; Tucker and Park 2019).

The outer mitochondrial membrane also contains enzymes linked with various processes (transport of long chain fatty acids: carnitine palmitoyltransferase I, oxidation of adrenaline: monoamine oxidase, etc). In addition, the outer mitochondrial membrane may associate with the endoplasmic reticulum (ER) membrane in a structure called the mitochondria associated ER-membrane (MAM). MAMs are essential for calcium signalling between ER and mitochondria and are involved in lipid transport (Cartes-Saavedra et al. 2021; Rieger et al. 2019; Rizzuto et al. 1998; Ruby et al. 1969).

The intermembrane space is the area between the inner mitochondrial membrane and the outer mitochondrial membrane (Chipuk et al. 2006; Neupert and Herrmann 2007). Only about 5% of the mitochondrial proteome is located in this region, yet it is endowed with the greatest variability in protein import mechanisms (Edwards et al. 2021).

The inner mitochondrial membrane forms an impermeable barrier for all molecules except oxygen, water, carbon dioxide (CO_2), and hydrogen sulfide (H_2S) (Fu et al. 2012; Kohl et al. 2019). The inner mitochondrial membrane is the main compartment for the conversion of cellular energy by the OXPHOS system, transport of metabolites e.g. pyruvate, fatty acids, nucleotides, ions, and small molecules. The nuclear-encoded proteins are passed through the membrane by translocase of the inner membrane protein complex (Valpadashi et al. 2021; Wasilewski et al. 2017). The structure of the inner mitochondrial membrane is specifically compartmentalized into the inner boundary membrane, cristae, and cristae junctions (Cogliati et al. 2016). The inner boundary membrane exactly copies the shape of outer mitochondrial membrane. The cristae are formed by the inner mitochondrial membrane, which protrudes into the matrix, significantly increasing its

surface area. The cristae and inner boundary membrane are connected by the cristae junction, a specific microcompartment, with a difference in membrane composition, especially in lipid, protein contents and pH value (Busch et al. 2013). Cristae membrane is mainly enriched in the respiratory chain complexes, whereas ATP synthase appears to be localized predominantly in the flexures of the cristae membrane. The ATP synthase dimers play a role in the cristae membrane formation and hence in establishing the morphology of the cristae (Davies et al. 2012; Klecker and Westermann 2021) (see chapter 1.2.6.2.). In addition, the complex mitochondrial ultrastructure is a marker of mitochondrial quality.

The matrix is the space inside the mitochondria. It contains mainly enzymes/metabolites of following pathways: oxidation of pyruvate and fatty acids, heme metabolism, TCA cycle, and part of the urea cycle. The mitochondrial matrix contains components of metabolic processes required for, mtDNA replication, repair, and mitochondrial proteosynthesis.

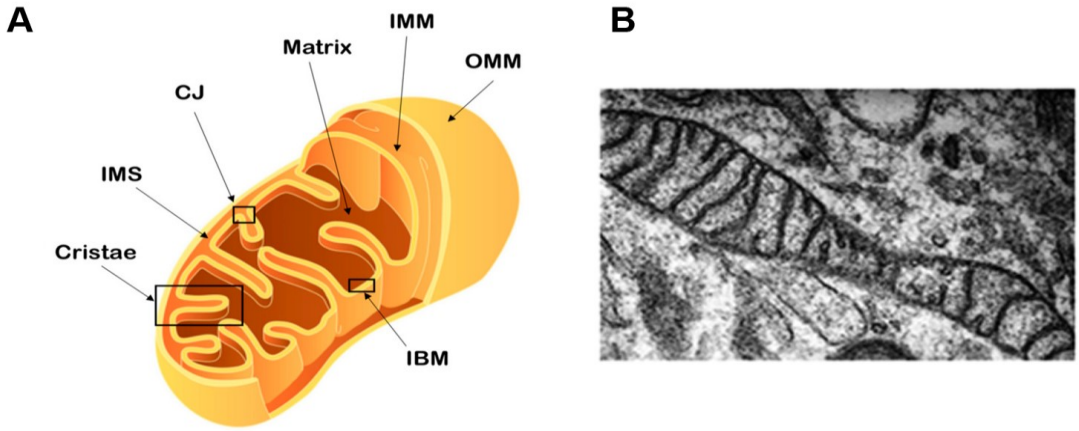

Figure 1: A) Schematic structure of the mitochondria. The outer mitochondrial membrane (OMM), inner mitochondrial membrane (IMM), inner boundary membrane (IBM), cristae junctions (CJ), intermembrane space (IMS), cristae and mitochondrial matrix are indicated (Protasoni and Zeviani 2021). B) Mitochondria in control cultivated fibroblast visualized by transmission electron microscopy, original magnification 44,000x (Brantová et al. 2006).

1.1.2. Mitochondrial genome

The mtDNA was discovered in 1963 (Nass and Nass 1963) and the complete sequence was published in 1981 (Anderson et al. 1981). MtDNA is a circular double-stranded molecule, consisting of 16 569 bp encoding 37 genes: 13 structural proteins, 2 rRNAs, and 22 tRNAs which fully ensure mitochondrial translation (Figure 2). The heavy (H) strand

contains genes encoding 2 rRNAs, 14 tRNAs, and 12 proteins, the light (L) strand encodes 8 tRNAs and a single protein. The displacement loop (D-loop) ~1 kb represents regulatory elements for replication and transcription of mtDNA (Falkenberg et al. 2007; Zhang et al. 2022).

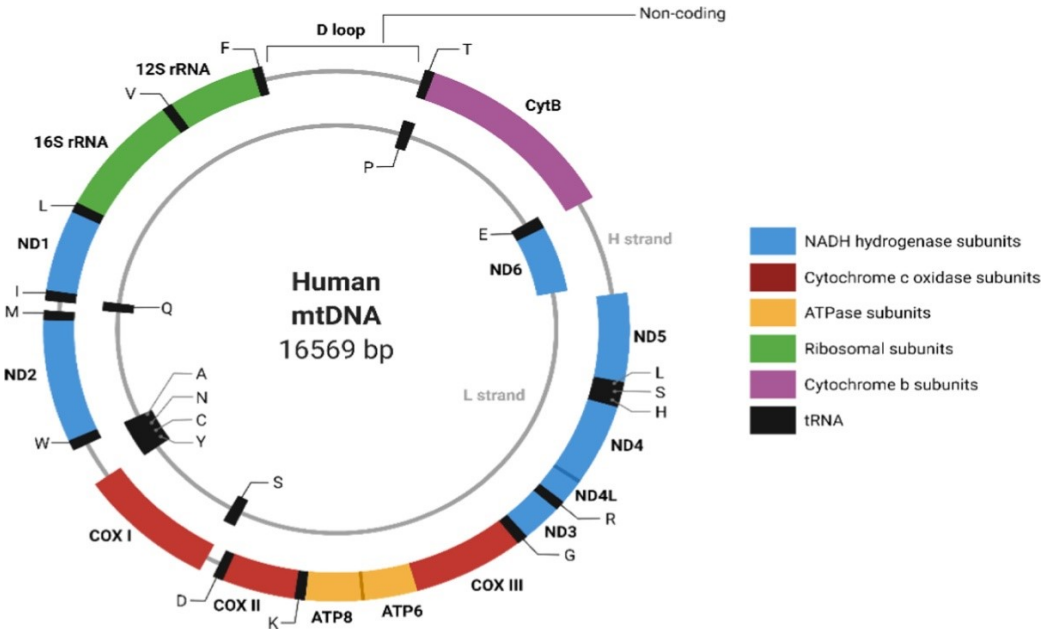

Figure 2: The human mitochondrial genome is organized as double-stranded a light (L) (inner) and a heavy (H) (outer) circular molecule containing 37 genes. 13 of these genes encode different OXPHOS complexes subunits, 2 genes encoded mitochondrial ribosomal RNAs (mt-rRNAs) and 22 remainings are for mitochondrial transfer RNAs (mt-tRNAs). The displacement loop (D-loop), non-coding control region, contains sequences that are essential for the initiation of mtDNA replication and transcription. Adapted from (Aldossary et al. 2022).

The human mtDNA encoded 13 proteins are parts of the OXPHOS complex I, complex III, complex IV, and complex V. Complex II is encoded entirely by the nuclear genome. The remaining mitochondrial proteins ~1200 are encoded by the nuclear genome, synthesized in the cytosol, and imported into the mitochondria (Calvo and Mootha 2010; Rath et al. 2021).

The cell contains hundreds of mitochondria, depending on the type, each possesses 2-10 molecules of mtDNA. A single cell contains from ten to several thousand copies of mtDNA (Burger et al. 2003; Robin and Wong 1988). A single mtDNA molecule is packaged into DNA-protein assemblies called “nucleoids” tethered to the inner mitochondrial membrane, this clustering is thought to facilitate mtDNA segregation (Bonekamp and Larsson 2018).

Sequences of the individual mtDNA may be identical (homoplasmy) or distinct (heteroplasmy) within a single cell, organ, or individual. The proportion of mutated mtDNA affects the biochemical phenotype, with a threshold level of heteroplasmy specific for each variant (DiMauro 2013; Parakatselaki and Ladoukakis 2021).

The mitochondrial genome differs from the nuclear genome in several ways. The mtDNA is built of 16,569 bp, while the nuclear genome is made of 3.3 billion bp. The mtDNA is very compact due to the lack of introns and the absence of significant 5′ and 3′ untranslated regions (UTRs). Unlike the nuclear genome, the mitochondrial genome is inherited exclusively in the maternal line, but there are also studies pointing to the possibility of biparental transmission of mtDNA (Luo et al. 2018). The mitochondrial genome is circular, whereas the nuclear genome is linear. One cell contains several thousand copies of its mtDNA, but only one copy of its nDNA. MtDNA is not packaged into chromatin, but is enveloped by specific proteins. The reduction of the mitochondrial genome has led to overlapping genes (*MT-ATP8/6*, *MT-ND4/4L* and *MTTY/MTTC*). Mitochondrial genes on both DNA strands are transcribed in a polycistronic manner: large mitochondrial mRNAs contain the instructions to build many different proteins, which are encoded one after the other along the mRNA. In contrast, nuclear genes are usually transcribed one at a time from their mRNA (Lynch et al. 2006; Rackham and Filipovska 2022).

Mitochondrial replication, transcription, and translation take place in the matrix (Antonicka and Shoubridge 2015; Bogenhagen et al. 2014; Rackham and Filipovska 2022). All these processes are regulated by nuclear-encoded proteins imported into mitochondria.

The replication of mtDNA is different from that of the nuclear genome. Its mechanism is still not fully understood. Mitochondrial replication is initiated from a small non-coding region (D-loop), and unlike nDNA, it is not cell cycle dependent and proceeds continuously (Bogenhagen and Clayton 1977). Mammalian mtDNA replicates by an asynchronous shift mechanism involving two separate origins, with the synthesis of the leading strand starting at a specific site and proceeding to approximately two-thirds of the way around the molecule before the synthesis of the second DNA strand is initiated (Ciesielski et al. 2016; Clayton 1982; Falkenberg and Gustafsson 2020).

There are two other proposed models describing the process of mitochondrial replication. The second model is “ribonucleotide incorporation throughout the lagging strand“, where processed RNA molecules produced by transcription hybridize with the parent heavy chain. These, according to the results of metabolic labeling experiments, are

not generated during replication, but pre-existing molecules have been used (Reyes et al. 2013).

In 2000, another replication model was suggested, the so called “strand-coupled“. According to this model, replication starts from many origins in a broad region called the ori zone and proceeds bidirectionally on both strands, continuously on the leading strand and using Okazaki fragments on the lagging strand, as in the nucleus (Holt et al. 2000).

MtDNA replication depends on the cooperation of several specific factors: DNA polymerase γ (catalytic subunit is encoded by *POLG* gene), mitochondrial single-stranded DNA binding protein (mtSSB), Twinkle mtDNA helicase, mitochondrial RNA polymerase (RNAseH1), mitochondrial DNA ligase III, and mitochondrial genome maintenance exonuclease 1 (MGME1) (Young and Copeland 2016). Moreover, the pool of dNTP is necessary for the replication process (Saada 2004).

MtDNA transcription results in the production of two long transcripts, one transcript from each strand. The mitochondrial genome is transcribed by specialized machinery that includes a monomeric mitochondrial RNA polymerase (POLRMT), the mitochondrial transcription factor A (TFAM), one of the two mitochondrial initiation transcription factor B paralogues (TFB1M or TFB2M), and mitochondrial transcription elongation factor (TEFM) (D'Souza and Minczuk 2018; Shi et al. 2012).

Transcription mitochondrial products are processed to individual mRNAs, rRNAs, and mt-tRNAs by a protein-RNase P complex (Holzmann et al. 2008) and Zinc phosphodiesterase ELAC2 (Brzezniak et al. 2011). The resulting RNAs (except mRNA for *ND6*) undergo post-transcriptional modifications. The maturation of pre-transcripts includes methylation of rRNAs, adenylation of mRNAs catalyzed by mitochondrial poly(A) polymerase (mtPAP) (Tomecki et al. 2004), and the addition of the CCA sequence to the 3′end of tRNAs, and other tRNAs modification. Several proteins have been described to be involved in these processes (Ali et al. 2019; Hällberg and Larsson 2014).

The modifications occur at different positions within mitochondrial tRNAs and have different functions. Methylation, pseudouridylation or dihydrouridylation of residues in the body of mt-tRNAs provides structural stability (Bohnsack and Sloan 2018). Mitochondrial pseudouridylate synthase 1 (PUS1) converts uridine into pseudouridine in tRNA positions and increases the efficiency of protein synthesis. Moreover, pseudouridine may have a functional role in tRNAs, and may assist in the peptidyl transfer reaction of rRNAs (Sibert and Patton 2012).

The mitochondrial transcription is activated by many transcriptional activators and coactivators (PGC-1α, PGC-1β, and PRC) associated with the targeting of specific transcription factors (e.g. NRF-1, NRF-2, and ERRα) (Huertas et al. 2019; Jornayvaz and Shulman 2010; Scarpulla 2012).

The mitochondrial translation system is similar to the translation system in prokaryotes. The 13 mitochondrial genes encode highly hydrophobic transmembrane proteins that are translated, and assembled into complexes I, III, IV, and V of OXPHOS. The mitochondrial 22 tRNAs encoded by mtDNA are essential for mitochondrial translation. The mitochondrial protheosynthesis takes place on mitochondrial ribosomes. The mammalian mitochondrial ribosome (55S) is composed of a small mitochondrial subunit (28S) and a large subunit (39S). The small mitoribosomal subunit is composed of 12S rRNAs and over 28 mitoribosomal proteins, while large mitoribosomal subunit consists of 16S rRNAs and more than 50 mitoribosomal proteins (Hällberg and Larsson 2014; Mai et al. 2017). The mt-tRNA for valine (*MTTV*) is also present as a structural component of the mitoribosome (Amunts et al. 2015).

Mitochondrial translation can be separated into several phases – initiation, elongation, termination, peptide release and mitochondrial ribosome dissociation. For each phase are required many ancillary specific factors (D'Souza and Minczuk 2018; Mai et al. 2017).

1.1.3. Mitochondrial proteome

As already mentioned, 13 mitochondrial genes for structural subunits of OXPHOS complexes are encoded by mtDNA (Falkenberg et al. 2007). The remaining subunits and all other mitochondrial proteins are encoded by nDNA and synthesized in the cytoplasm. All the proteins targeting to the mitochondria are synthesized as precursors and imported into the mitochondria by specialized transporters. Thus mitochondrial targeting signal, located at the N-terminus of the polypeptide, is required (Wasilewski et al. 2017). In addition, other supplementary signals that subsequently target protein to different regions in the mitochondria such as inner mitochondrial membrane, intermembrane space, outer mitochondrial membrane or mitochondrial matrix can occur.

Based on several methodical integrative approaches has been estimated that the mammalian mitochondrial proteome consists of ~1200 individual proteins (Calvo and Mootha 2010). The most common strategies for mitochondrial protein identification are searching for mitochondrial targeting signals, mass spectrometry, microscopy, and analysis of sequence homology. Nowadays, the mitochondrial protein catalog MitoCarta combining

literature information and various experimental techniques is available. The original database from 2008 includes 1013 human genes and 1098 mouse genes (Pagliarini et al. 2008). In 2015, the MitoCarta inventory was updated to MitoCarta 2.0 containing 1158 human genes and 1158 mouse genes encoding mitochondrial proteins (Calvo et al. 2016) and then updated yet again to MitoCarta+ (1166 human mitochondrial proteins) (Floyd et al. 2016). The latest update removed 100 human genes from the previous version and 78 genes were added. MitoCarta3.0 contains 1136 human genes, including 1058 genes that were previously in MitoCarta2.0, and a very similar list of 1140 mouse genes (Rath et al. 2021).

1.2. Oxidative phosphorylation system

The main role of mitochondria is energy provision by aerobic respiration and producing the bulk of cellular ATP by oxidative phosphorylation system (OXPHOS) (Figure 3) (Saraste 1999). Electrons provided by the oxidation of fatty acids and carbohydrates are shuttled to oxygen along four respiratory chain (RC) complexes (CI–CIV) embedded in the inner mitochondrial membrane, producing water and releasing the energy necessary to pump protons from the mitochondrial matrix to the intermembrane space. This leads to the formation of a transmembrane electrochemical ion gradient across the IMM, also called the proton motive force (pmf) thus the outer side of the IMM is positively charged while the inner side is negatively charged. The pmf enables the ATP synthase to produce ATP from ADP and Pi (Boyer 1997). Human five OXPHOS complexes contain ~90 different types of structural proteins (Table 1) (Pinke et al. 2020; Vercellino and Sazanov 2022).

The OXPHOS complexes and the mitoribosome are built through a series of orchestrated steps that require the help of additional proteins that are not part of the mature complex, called assembly factors. Not all assembly factors directly promote assembly, the controlled coalescence of subunits into complexes through stabilization of assembly intermediates, but many instead provide critical services in the form of maturation and delivery of cofactors such as heme, copper and [Fe-S] clusters, post-translational modification of subunits, and regulation of translation. Furthermore, transcription of mtDNA, mitochondrial mRNA processing, mitochondrial tRNA maturation, mitoribosome assembly, and translation all directly influence OXPHOS complex biogenesis and/or function.

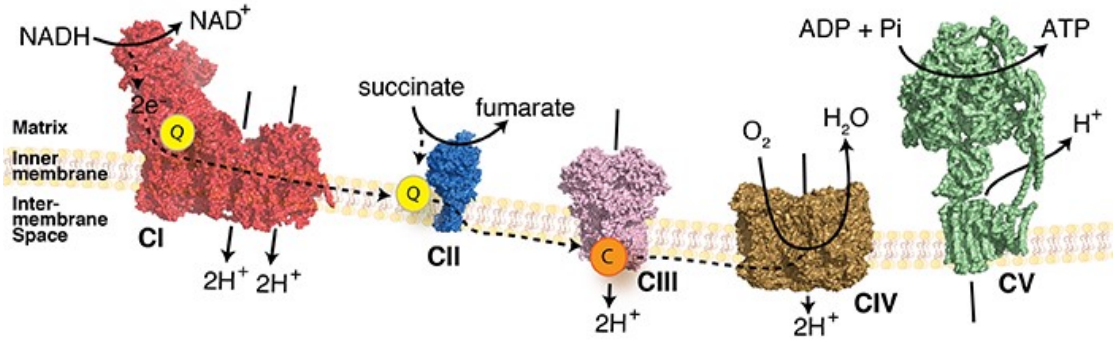

Figure 3: Schematic representation of the OXPHOS system. Complex I (CI) oxidizes NADH to NAD+ to reduce ubiquinone (Q) to ubiquinol (QH2). The electron transfer is coupled to the transport of protons from the mitochondrial matrix to the inner membrane space (IMS). Complex II (CII) oxidizes succinate to fumarate and reduces Q without proton translocation. The electrons are then transferred from QH2 to cytochrome c via complex III (CIII) accompanied by the translocation of protons. Finally, cytochrome c is used to reduce oxygen to water in complex IV (CIV) coupled to the transport protons. The electrochemical proton gradient is dissipated by the complex V (CV) to generate ATP. Adapted from (Hock et al. 2020).

Table 1: Human OXPHOS complexes I-V: name, approximate molecular weight (kDa), the number of different type subunits, subunits encoded by mtDNA, and prosthetic groups. Adapted from (Pinke et al. 2020; Vercellino and Sazanov 2022).

	Enzyme	**Mass (kDa)**	**Number of different types subunits**	**Number of mtDNA encoded subunits**	**Prosthetics groups**
Complex I	*NADH dehydrogenase EC 1.6.5.3*	*~1000*	*44*	*7*	*FMN, 8 [Fe-S] clusters*
Complex II	*Succinate dehydrogenase EC 1.3.5.1*	*~140*	*4*	*0*	*FAD, 3 [Fe–S] clusters, heme b*
Complex III	*Cytochrome c oxidoreductase EC 1.10.2.2*	*~240*	*11*	*1*	*heme b and c1, 2 [Fe–S]*
Complex IV	*Cytochrome c oxidase EC 1.9.3.1*	*~200*	*14*	*3*	*heme a and a3, CuA, CuB*
Complex V	*ATP synthase EC 7.1.2.2*	*~650*	*18*	*2*	-

1.2.1. Complex I

Complex I (NADH dehydrogenase, NADH: ubiquinone oxidoreductase, CI, NQR) represents the largest (~1 Mda) multi-subunits enzyme of the OXPHOS complexes. It catalyzes the oxidation of NADH to NAD+ by a non-covalently bound flavin mononucleotide (FMN) and passes the electrons to carrier ubiquinone-coenzyme Q (CoQ, Q) over a distance of around 100 Å by a chain of [Fe-S] clusters. By coupling the transfer of two electrons with the translocation of four protons (H^+) across the inner mitochondrial membrane, the enzyme contributes to the generation of the pmf that drives ATP synthase (Brandt 2006; Sharma et al. 2009; van Belzen et al. 1997). Moreover, complex I has been shown as a major source of mitochondrial reactive oxygen species (ROS) (Brand et al. 2004; Yin et al. 2021).

The L-shaped complex I consists of a hydrophobic membrane arm, that is linked to the hydrophilic peripheral part protruding into the mitochondrial matrix by the stalk region. The stalk represents part of the electron transfer pathway linking to the NADH binding site in the hydrophilic arm with the ubiquinone binding site in the membrane domain (Grigorieff 1998; Parey et al. 2020; Zhu et al. 2016).

In human, the complex I consists of 45 subunits (44 distinct subunits as one subunit, NDUFAB1 is present in two locations within the complex) (Vinothkumar et al. 2014). Seven subunits are encoded by the mitochondrial genome. Fourteen central subunits, conserved from bacteria to humans, form the catalytic core of the enzyme. The core subunits that are sufficient for the function are assigned to three functional modules: the N module for NADH oxidation, the Q module for ubiquinone reduction, and the P module for proton pumping (Kampjut and Sazanov 2020; Leif et al. 1993).

In addition, the enzyme complex comprises over 30 accessory subunits surrounding the central subunits that are not directly associated with energy conservation (Lazarou et al. 2009; Wirth et al. 2016). They are thought to be involved in the assembly and stability of the complex, or the protection from oxidative damage and ROS production (Guerrero-Castillo et al. 2017; Hirst 2013; Stroud et al. 2016; Vogel et al. 2007; Wang et al. 2021).

1.2.2. Complex II

Complex II (succinate dehydrogenase, succinate: ubiquinone oxidoreductase, CII, SDH,) catalyzes the oxidation of succinate to fumarate with electron transfer via its iron sulfur [Fe–S] clusters from FADH2 to ubiquinone-coenzyme Q (CoQ). In addition

complex II is a component of the TCA cycle, making a functional link between these two essential processes in mitochondria (Cecchini 2003; Lussey-Lepoutre et al. 2015).

Complex II represents a parallel electron transport pathway to complex I, but unlike complex I, no protons are transported to the intermembrane space in this pathway. Therefore, the pathway through complex II contributes less energy to the overall electron transport chain process (Rutter et al. 2010).

Complex II is the smallest (~140 kDa) enzyme of the OXPHOS complexes. It is composed of two domains, the hydrophilic head protruding to the matrix, and the hydrophobic tail anchoring enzyme complex to the membrane (Rutter et al. 2010). It consists of four subunits encoded by nuclear DNA and five prosthetic groups. The catalytic core of the enzyme represents two subunits SDHA and SDHB, which form the heterodimer localized on the matrix side of the inner mitochondrial membrane, prosthetic group FAD, and three [Fe–S] clusters. Moreover, the catalytic core comprised the binding site for succinate. The other two subunits, SDHC and SDHD serve as anchors of the catalytic core to the inner mitochondrial membrane (Sun et al. 2005).

1.2.3. Complex III

Mitochondrial complex III (Cytochrome c oxidoreductase, ubiquinol: cytochrome c oxidoreductase, CIII, QCR) transfers the electrons from coenzyme Q to cytochrome c (cyt c). Human complex III (~240 kDa) localized in the inner mitochondrial membrane is a tightly bound symmetrical dimer (~480 kDa) with 11 subunits per monomer, only one of which is encoded by mtDNA (cytochrome b) (Guo et al. 2017; Iwata et al. 1998; Schägger et al. 1986).

The catalytically active core consists of mitochondrially encoded cytochrome b, which contains two hemes (bL and bH), cytochrome c1 subunit, and iron sulfur clusters [Fe–S] wrapped by an iron-sulphur protein (Rieske protein) (Yang and Trumpower 1986). There are two CoQ binding sites at either end of cytochrome b that are embedded in the inner mitochondrial membrane, one of which is the ubiquinol (QH2) oxidation site located on the cytoplasmic side that is related to the low potential cytochrome bL. The other is the matrix-side Q reduction site, which is related to the high potential cytochrome bH (Gao et al. 2003; Xia et al. 2013).

The core subunits (subunit 1 and 2) are homologous to the matrix processing peptidase (MPP) subunits. MPP is a metalloprotease responsible for removing leader sequences of imported proteins. In plants, the core proteins are the MPP enzyme. In vertebrates and in

yeast there are separate genes encoding core proteins and MPP (Berry et al. 2013; Xia et al. 2013). Function of the core proteins in non-plant species is not fully understood but they could be involved in mitochondrial import protein processing (Deng et al. 2001). In addition, transmembrane subunits 10 and 11 control the contact of cytochrome c1 with the Rieske protein (Iwata et al. 1998).

1.2.4. Complex IV

Complex IV (cytochrome c oxidase, CIV, COX) is a copper-heme A terminal enzyme complex embedded in the mitochondrial inner membrane (Soto et al. 2012). It catalyzes the electron transfer from reduced cytochrome c to molecular oxygen in a process coupled to the transfer of protons across the inner membrane, thus contributing to the generation of the proton gradient that is used by complex V to drive ATP synthesis (Ludwig et al. 2001).

Mammalian complex IV (~200 kDa) is a multimeric enzyme consisting of 14 subunits of dual genetic origin. The three subunits forming the catalytic core of the enzyme (COX1, COX2, and COX3) are encoded by the mtDNA. The core structure of the subunits is conserved from α-proteobacteria to humans. COX1 and COX3 are highly hydrophobic, integral membrane proteins with no substantial extramembrane domains. COX2, on the other hand, consists of a β barrel extramembrane domain anchored by two transmembrane helices that bind to COX1, opposite from the side of COX1 that binds COX3. Subunits COX1 and COX2 contain the redox metal active centers of the enzyme. The extramembrane domain of COX2 extends into IMS to bind soluble cytochrome c. A di-copper center termed CuA accepts the electrons from soluble cytochrome c. The CuA center is located in the loop region at the bottom of the extramembrane domain of COX2, at the interface of COX1 and COX2. Electrons flow from CuA to heme and in COX1, which transfers the electrons to the binuclear heme a3-CuB center, where O_2 is reduced to water (Soto et al. 2012).

Up to eleven smaller subunits (in mammals) have been added to the catalytic core. This has presumably allowed coping with evolving energetic requirements of eukaryotic cells over time, to adapting to oxygen-rich environments, and to regulate complex IV activity to coordinate energy production with timely cellular needs (Pierron et al. 2012). The last subunit of the mammalian complex to be identified was NDUFA4 (Balsa et al. 2012; Pitceathly and Taanman 2018; Vercellino and Sazanov 2022). NDUFA4 was absent from the crystal structures (Tsukihara et al. 1996) and had been mistakenly assigned as a subunit of complex I. The mammalian cytochrome c oxidase has multiple tissue-specific isoforms

of nuclear encoded subunits, indicating a key regulatory role complex IV on OXPHOS (Hüttemann et al. 2003; Kadenbach 2017; Pierron et al. 2012; Sinkler et al. 2017).

1.2.5. Organization of respiratory chain complexes

The respiratory chain complexes interact to form higher order structures, known as the supercomplex or respirasome. Defined associations of complexes I, III, and IV are found when mitochondrial membrane extracts are solubilized with mild detergent digitonin and separated through Blue Native Polyacrylamide Gel Electrophoresis (BN-PAGE) (Acín-Pérez et al. 2008; Schägger 2002). Thus, according to their molecular size and subunit composition, the main supercomplexes have been assigned the following stoichiometries: $CIII_2$-CIV, CI-$CIII_2$, CI-$CIII_2$-CIV, and CI_2-$CIII_2$-CIV_{1-2}. Supercomplex CI-$CIII_2$-CIV is termed the "respirasome" and supercomplex CI_2-$CIII_2$-CIV_2 has been named "respiratory megacomplex" (Guo et al. 2017; Lobo-Jarne et al. 2020; Vercellino and Sazanov 2021, 2022).

Several roles of the supercomplexes have been proposed, ranging from regulators of ROS production (Lopez-Fabuel et al. 2016; Maranzana et al. 2013), to regulators of the OXPHOS system efficiency through turnover rates (Moe et al. 2021), and in particular as major players in the putative substrate channeling (Calvo et al. 2020; Lapuente-Brun et al. 2013).

1.2.6. Complex V

1.2.6.1. Structure of complex V

Human mitochondrial ATP synthase (F_1F_o-ATP synthase, complex V, CV) is a unique macromolecular rotary machine of ~650 kDa located in the inner mitochondrial membrane. It consists of 18 different protein subunits (α3, β3, γ, δ, ε, a, b, c8, d, e, f, g, F6, A6L, OSCP, IF1, 6.8 kDa proteolipid, and DAPIT) (Figure 4) organized in membrane-extrinsic F_1 catalytic and membrane-embedded F_o domains, which are connected via peripheral and central stalk (Abrahams et al. 1994; Ackerman and Tzagoloff 2005; Pinke et al. 2020; Walker 2013; Wittig and Schägger 2008).

A central stalk composed of δ, ε, and γ subunits connects the c-subunits ring (8 in humans) to the catalytic unit F_1, which consists of a hexamer of alternating α and β subunits, where ATP synthesis and hydrolysis takes place. Finally, peripheral stalk containing the subunits b, d, and F6 and the oligomycin-sensitivity

conferring protein (OSCP) connects the lateral portion of F_o to the top of the F_1 domain (Walker 2013).

Other specific subunits e and g induce either directly or indirectly the formation of ATP synthase dimers that self-assemble in longer ribbons important for cristae formation (Davies et al. 2012; Hahn et al. 2016; Parsons 1963; Strauss et al. 2008). Accessory subunits, DAPIT (diabetes associated protein in insulin sensitive tissues) and 6.8PL (6.8 kDa proteolipid) were identified in the membrane-embedded F_o domain (Chen et al. 2007; Meyer et al. 2007; Ohsakaya et al. 2011). One regulatory subunit IF1 (inhibitory factor 1) binds to the F_1 domain at low pH to prevent hydrolysis of ATP. Two ATP synthase subunits (a and A6L) are encoded by mtDNA (Fearnley and Walker 1986).

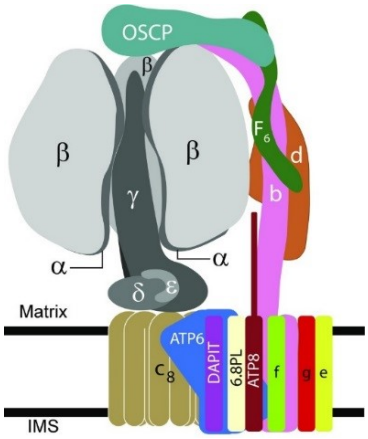

Figure 4: Organization of subunits in monomeric ATP synthase in mammalian mitochondria. Black horizontal lines represent the inner mitochondrial membrane (IMS). The peripheral stalk consists of subunits OSCP, F6, b, and d. The membrane domain of subunit b is associated with mitochondrially encoded subunits a (ATP6) and A6L (ATP8). Subunit b interacts directly or indirectly with subunits e, f, g, DAPIT, and 6.8PL. The ATP6 contacts c8-ring. The central stalk contains subunits γ, δ, and ε and form with α3β3 F_1 domain. Adapted from (He et al. 2018).

ATP synthase requires a supply of the substrates (ADP and Pi) for its function, which is mediated by two specialized transporters. Adenine nucleotide translocator (ANT) transports ADP into the mitochondrial matrix (Itoh et al. 2004). The inorganic phosphate carrier (PiC) catalyzes the transport of Pi into the mitochondrial matrix. This transport is electroneutral and occures either in symport with H^+ or by exchange for OH^- (Seifert et al. 2015). ATP synthase, ANT, and PiC form a structure of ATP synthasome, the mitochondrial ADP-phosphorylating apparatus (Bernardi and Di Lisa 2015; Bernardi et al. 2015).

1.2.6.2. Function of complex V

Complex V catalyzes the synthesis of ATP from ADP and Pi in the F_1 domain during the final step of oxidative phosphorylation. While the main function of ATP synthase is to synthesize ATP, it can also run in reverse to hydrolyze ATP under certain physiological and pathological conditions.

The synthesis is made possible by the energy derived from the gradient of protons that cross the inner mitochondrial membrane from the inter membrane space into the mitochondrial matrix through the F_o domain of ATP synthase. The proton gradient establishes a pmf, that has two components: the pH differential and the electrical membrane potential ($\Delta\psi m$) (Campanella et al. 2009). The energy released causes the rotation of two rotary motors: the ring of c subunits in F_o (relative to subunit a), along with subunits γ, δ, and ε in the F_1 domain, to which it is attached (Cox et al. 1984).

The protons pass the inner mitochondrial membrane and drive the c-oligomer rotation, which is transmitted by the central stalk to the catalytic F_1 domain which cyclically changes the conformation of the α3β3 hexamer (Cox et al. 1984; Walker 2013; Wittig and Schägger 2008). This is called "rotary catalysis" (Devenish et al. 2008) and can be explained by the "binding-change" mechanism, first proposed by Boyer (Boyer 1975). For uncovering the mechanisms of ATP synthesis by complex V, Paul D. Boyer and John E. Walker were awarded the Nobel Prize in chemistry in 1997. The mechanism of proton translocation coupled to ADP phosphorylation has been extensively studied and was recently visualized using high-resolution cryo-EM structures of various intact ATP synthase (Pinke et al. 2020; Spikes et al. 2020).

Briefly, the pmf powers the rotation of the membrane-embedded c-ring. Passing through the two half-channels formed at the interface between subunit a and the c-ring, protons reach the conserved glutamate in the middle of the c-ring and subsequently leave on the opposite side of the membrane. Crucial for the unidirectional transfer of protons to and from the glutamate of the c-ring and to prevent leakage in the opposite direction is a conserved arginine residue of subunit a, sitting at the convergence of the two oblique hydrophilic half-channels, essentially formed by subunit a, with contributions from subunits b, c and f (Pinke et al. 2020; Spikes et al. 2020). The central stalk transmits the rotation to F_1, held in place by the peripheral stalk, driving the conformational changes in the αβ subunits that perform ADP phosphorylation.

This mechanism describes ATP synthesis and ATP hydrolysis at the catalytic sites, located in each of the three β subunits at the interface with an adjacent α subunit. In the case of ATP synthesis, each site cooperatively switches through conformations in which ADP and Pi bind, ATP is formed, and then released. ATP hydrolysis uses the same pathway, but in reversible manner (Adachi et al. 2007). These transitions are caused by rotation of the γ subunit. The α3β3 hexamer must remain fixed relative to subunit a during catalysis; this occurs via a peripheral stalk. Thus, complex V can be mechanically divided into "rotor" (c-ring, γ, δ, ε) and "stator" (α3β3, a, b, d, F6, OSCP) parts (Devenish et al. 2008).

ATP synthase forms dimers and higher oligomers (Arnold et al. 1998; Davies et al. 2012; Schägger and Pfeiffer 2000; Wittig and Schägger 2005) and thus contributes to the formation of the inner mitochondrial membrane. The interaction between the two monomers of ATP synthase is mainly through the F_o sector by subunits a and accessory subunits (e, g, b, and A6L) stabilize the monomer-monomer interface (Bisetto et al. 2008; Wagner et al. 2010; Wittig and Schägger 2008). Subunits DAPIT and 6,8PL also play an important role in ATP synthase dimerization (Wittig and Schägger 2008). Another protein that plays a role in the stabilization of di- and oligomers is IF1. IF1 links two ATP synthases via the F_1 sector (Devenish et al. 2008). Mature IF1 is only bound to di- and oligomeric ATP synthase in mammals (Wittig et al. 2010).

Dimerization provides stabilization of ATP synthase and facilitates ATP synthesis. ATP synthase appears to be localized predominantly in the flexures of the cristae membrane. The clustering of ATP synthase dimers at the apex of the cristae creates a strong local positive curvature that generates a proton trap. The role of ATP synthase dimers in mitochondria cristae formation was first described in yeast models where downregulation of ATP synthase (Lefebvre-Legendre *et al.* 2005) or altered ATP synthase dimer formation due to deficiency of the subunits e or g (Paumard *et al.* 2002) led to the absence of cristae and the appearance of mitochondria as "onion-like" structures.

ATP synthase is also implicated in the formation of the permeability transition pore (PTP), which triggers cell death (Giorgio et al. 2013). Mitochondrial PTP is a large conductance channel in the inner mitochondrial membrane. Prolonged opening of PTP collapses mitochondrial membrane potential ($\Delta\Psi m$) and ultimately leads to cell death (Bernardi et al. 2015; Giorgio et al. 2013; He et al. 2017b).

1.2.6.3. Biogenesis of complex V

ATP synthase formation is a not fully understood modular process that requires specific assembly factors and depends on the coordinated expression of the nuclear and mitochondrial genomes. Description of ATP synthase biogenesis is mainly based on the yeast model (Ackerman and Tzagoloff 2005; Rak et al. 2011; Rühle and Leister 2015). But the assembly of complex V has been also studied in eukaryotic cells using subunit incorporation dynamics (Nijtmans et al. 1995), analysis of mtDNA-deficient cell lines (Carrozzo et al. 2006; Wittig et al. 2010), and more recently by creating knock-out eukaryotic cell lines for specific ATP synthase subunits (He et al. 2017a; He et al. 2017b; He et al. 2018). Findings in patient cells and tissues deficient/defective in some subunit of complex V or assembly factors are also helpful in revealing the process of the ATP synthase assembly.

The biogenesis of human ATP synthase is a process (Figure 5) in which subcomplexes are formed independently, required presence of several assembly factors ATPAF1, ATPAF2, TMEM70, FMC1 and TMEM242 (Carroll et al. 2021; Cízková et al. 2008b; Li et al. 2017; Wang et al. 2001). The assembly of human ATP synthase occurs through several modules corresponding to the F_1 particle, c8-ring, and peripheral stalk. However, recent studies in knockout models of individual subunits demonstrated that it can proceed via alternative pathways to form subcomplexes whose composition is incompatible with the strictly linear assembly scheme (He et al. 2017a; He et al. 2017b; He et al. 2018; Vercellino and Sazanov 2022).

De novo biogenesis (Figure 5) of complex V starts the formation of the soluble F_1 domain together with the central stalk (α3, β3, γ, δ and ε). Three assembly factors are involved in this process. ATPAF1 (ATP synthase mitochondrial F_1 complex assembly factor 1) and ATPAF2 (ATP synthase mitochondrial F_1 complex assembly factor 2) bind specifically to the α and β subunits to prevent the subunits from forming unproductive homooligomers during enzyme assembly (Wang et al. 2001). Human FMC1 is also required for the assembly of human ATP synthase and interacts with ATPAF2 (Li et al. 2017).

The assembly of the c8-ring of human ATP synthase is influenced by TMEM70 (Bahri et al. 2021), which is located in the inner mitochondrial membrane, but is not a component of the ATP synthase itself; and a second inner mitochondrial membrane protein, TMEM242 (Carroll et al. 2021).

A subcomplex containing subunits of the peripheral stalk is also pre-formed. After joining the c8-ring and the F_1 subcomplex, the peripheral stalk is incorporated in two steps, subunits (b, d, F6, and OSCP) are added, followed by (e, f, g) (Fujikawa et al. 2015; He et al. 2018). The peripheral stalk can also join the F_1 subcomplex in absence of the c8-ring (He et al. 2017b).

During the initial steps, the inhibitory protein IF1 binds to the intermediates and is released with the insertion of two mtDNA-encoded subunits (He et al. 2018). In cases where the mitochondrially encoded a (*MT-ATP6*) and A6L (*MT-ATP8*) subunits are missing, the previous assembly intermediate readily accumulates (He et al. 2017b; Nijtmans et al. 1995; Wittig et al. 2010). The interaction of mitochondrial subunits is stabilized by the addition of 6.8PL and DAPIT subunits (Fujikawa et al. 2015). The assembly factor TMEM242 appears to be required for these last two steps (Carroll et al. 2021).

One of the human ATP synthase assembly factor TMEM70 was determined by integrative genomics (Calvo et al. 2006). Its homologs were found in higher eukaryotes but not in yeasts and fungi. Expression level of TMEM70 is very low as typically for ancillary factors (Cízková et al. 2008b; Hejzlarová et al. 2011). *TMEM70* gene is located on chromosome 8 and encodes 260 AA. The protein precursor (29 kDa) contains mitochondrial targeting N-terminal sequence. Processed TMEM70 is a 21 kDa transmembrane protein localized in the inner mitochondrial membrane (Hejzlarová et al. 2011). Mature TMEM70 protein consists of 179 AA (Hejzlarová et al. 2011), contains conserved DUF1301 domain and two transmembrane regions with both termini facing the mitochondrial matrix (Jonckheere et al. 2011; Kratochvílová et al. 2014).

TMEM70 forms dimers and higher oligomers and a stable interaction with ATP synthase subunits has not been detected (Kratochvílová et al. 2014). Recently, however, thanks to new methodological approaches, several studies have demonstrated the presence of an interaction between TMEM70 and the subunit c (Bahri et al. 2021; Kovalčíková et al. 2019; Sánchez-Caballero et al. 2020).

The absence/defect of TMEM70 protein results in reduced content/activity of ATP synthase but not absolutely. Therefore, TMEM70 has been characterized as an accessory assembly factor for ATP synthase but is not essential for its biogenesis. The role of the TMEM70 protein has been intensively studied in recent years. TMEM70 is localized restrictedly in cristae where it assembles into large oligomers that interact specifically with the subunit c of ATP synthase and provide a scaffold for c-ring assembly prior to its

incorporation into the functional complex (Bahri et al. 2021; Carroll et al. 2021; Kovalčíková et al. 2019). Interestingly, the model cell line shows an improvement in the impact of the TMEM70 defect on ATP synthase levels when the subunit c is overexpressed (Kovalčíková et al. 2019). Another assembly factor described in 2021, TMEM242, is also involved in the c8-ring assembly. TMEM70 and TMEM242 have similar overlapping functions in the c8-ring assembly, but TMEM242 may additionally influence the incorporation of the a, A6L, DAPIT, and 6.8PL subunits (Carroll et al. 2021).

The study from 2020 delineates the function of TMEM70, using a combination of proximity-dependent biotin identification process, complexome profiling and coevolutionary analyses. Furthermore, TMEM70 interacts with subunit c and as well as mitochondrial assembly complex I intermediates (Sánchez-Caballero et al. 2020). They proposed that TMEM70 interacts with complex I and V and for both complexes, loss of TMEM70 leads to accumulation of an assembly intermediate followed by reduction of the next assembly intermediate in the biogenesis pathway. This indicates that TMEM70 has a specific role in the stability of membrane-bound subassemblies or in the membrane recruitment of subunits into the forming complex I (Sánchez-Caballero et al. 2020).

Recently, the *TMEM70* gene was shown to be hypermethylated and its mRNA downregulated in the liver of rats treated with hepatocarcinogen thiocetamid for 28 days. It determined that aberrant epigenetic regulation of *TMEM70* gene leads to the shift of metabolism from oxidative phosphorylation to glycolysis. This may indicate that this gene is involved in tumorigenesis (Mizukami et al. 2017). These findings are consistent with the previously described downregulation of ATP synthase in many types of carcinomas (Isidoro et al. 2004).

Recently, two animal models of TMEM70 deficiency were developed. The first is an inducible knockout of TMEM70 in mice, that exhibit a progressive onset of phenotype and predominantly liver associated pathology, which serve as a good patient model during metabolic crisis. The second is a model of spontaneously hypertensive rats with a targeted TMEM70 gene (SHR-Tmem70ko/ko) with heart associated pathology, which is representative for patients at the onset of disease. In a recent study, complementation of the gene using a transgenic rescue approach led to efficient complementation of ATP synthase deficiency and thus in successful genetic treatment of an otherwise fatal mitochondrial disorder (Marković et al. 2022; Vrbacký et al. 2016).

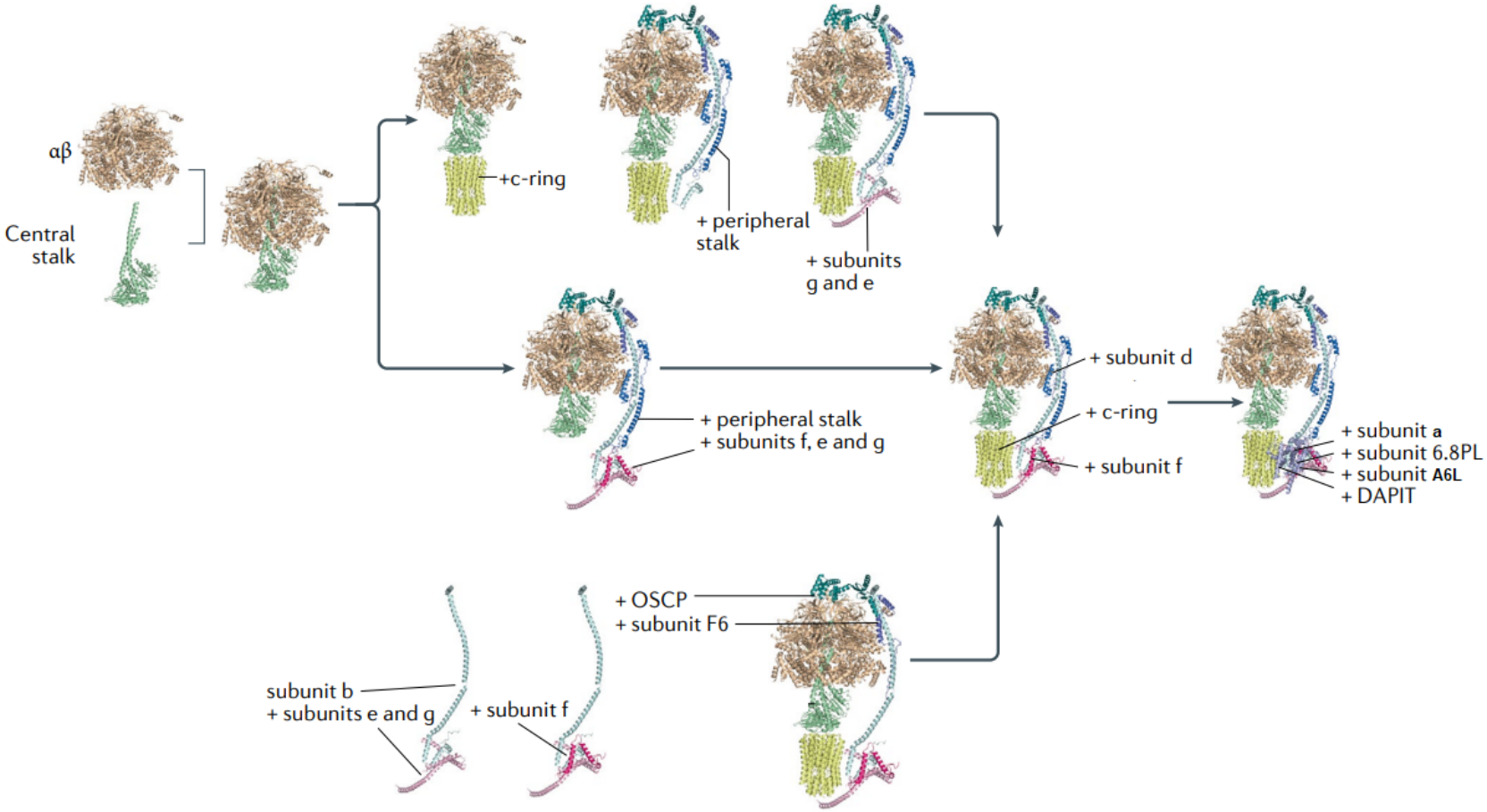

Figure 5: The human ATP synthase assembly model. Adapted from (Vercellino and Sazanov 2022). The αβ heterooligomer assembles with the central stalk followed by two possible pathways: either the c-ring or the full peripheral stalk, with subunits f, g and e. The last assembly step involves the addition of the two mtDNA encoded subunits a and A6L and the module made of accessory subunits 6.8PL and DAPIT. Different intermediates contain subunits b, g and e attach to subunit f, then they attach other assembly intermediates with OSCP and subunit F6, and finally, the peripheral stalk is completed with subunit d. Finally, pathway 2 was further elaborated, describing the sequential addition of subunits g and e and then subunit f after the OSCP module.

1.3. Mitochondrial disorders

Mitochondrial disease is a summary term for a clinically heterogeneous group of disorders whose common feature is impaired mitochondrial functions and aberrant energy metabolism. Nowadays, more than 400 genes, either in nDNA or mtDNA, mutations are known to cause mitochondrial disease (Stenton et al. 2022). Due to dual genetic origin, mitochondrial disorders can be inherited with any inheritance pattern: sporadic (de-novo), maternal (mtDNA), autosomal dominant, autosomal recessive or X-linked.

Mitochondria are the largest producer of energy in the cell, so their dysfunctions mainly affect tissues and organs with high energy demand (heart, brain, liver, eyes, and skeletal muscle). Mitochondrial diseases cause a wide range of health problems, including fatigue, weakness, metabolic strokes, seizures, arrhythmias, cardiomyopathy, developmental or cognitive delay, impairment of hearing, vision, growth, liver, gastrointestinal, or kidney function, and more. Clinical symptoms arise in childhood or later in life, affect one organ or multiple organs (Lightowlers et al. 2015). The prevalence of mitochondrial disease in adults is 1: 8 000 and 1: 5 000 in childhood (Rahman 2020; Watson et al. 2020)

Mitochondrial diseases of nuclear origin are caused by mutations in structural genes of OXPHOS complexes as well as in their specific assembly factors (Shoubridge 2001; Thompson et al. 2020). Moreover, nuclear origin defects have been demonstrated in upstream pathways generating substrates for OXPHOS (pyruvate dehydrogenase complex, Krebs cycle, fatty acid beta-oxidation or substrate import) or in genes encoding factors involved in mtDNA expression. Mitochondrial proteosynthesis requires proteins involved in mtDNA maintenance, transcription, RNA processing/maturation, translation and posttranslational modification. Furthermore, all of these proteins must be correctly targeted and imported into the mitochondria. Thus, any defects in mitochondrial protein import or structure, caused by aberrant cristae formation or abnormal membrane lipid composition, as well as factors affecting mitochondrial fission/fusion or quality control negatively impact the OXPHOS complexes (Russell et al. 2020; Thompson et al. 2020).

Mutations in the maternally transmitted mtDNA occur in structural as well as mt-tRNA, and mt-rRNA genes. More than 600 different pathogenetic variants in mtDNA are involved in human diseases. An overview of all variants in mtDNA is published in the MITOMAP compendium https://www.mitomap.org (Lott et al. 2013). Clinical and biochemical phenotypes of the patients with mtDNA variants depend on the level of heteroplasmy. Heteroplasmic mutations often have a variable threshold, the level to which

the cell can tolerate defective mtDNA molecules (Stewart and Chinnery 2015; Yang et al. 2022). When the mutation load exceeds this threshold, metabolic dysfunction and associated clinical symptoms occur.

The heterogeneous nature of mitochondrial diseases, their individual rarity, genotypic and phenotypic variability and overlapping presentations with other genetic disorders, make diagnosis very challenging. However, whole exome sequencing approaches have markedly improved diagnostic yield, highlighted the genetic variability of diseases, facilitated the diagnosis of mitochondrial disorders and advanced understanding of mitochondrial biology/metabolism, opening potential therapeutic avenues (Legati et al. 2016; McCormick et al. 2018; Schoonen et al. 2019; Theunissen et al. 2018; Thompson et al. 2020). Biochemical/histological investigation and approaches are reserved for the identification of tissue-specific variants and functional validation of novel variants.

The mitochondrial disorders affecting OXPHOS complexes in patient derived cells and tissues can be isolated (defect in single complexes) or combined (impact on multiple complexes). The combined defects of OXPHOS complexes are usually caused by aberrant molecular mechanisms: mtDNA (replication, transcription, RNA processing, and modification, translation, large mtDNA deletions), cofactor biosynthesis (coenzyme Q, [Fe-S] clusters, heme/cytochromes, riboflavin), maintenance of mitochondrial homeostasis (mitochondrial protein import, lipid metabolism, division/fusion, mitophagy/quality control) or supercomplex formation (Mayr et al. 2015).

1.3.1. Defects of ATP synthase

Mitochondrial disorders of ATP synthase are caused by mutations in mtDNA or nDNA. ATP synthase disorders are divided into primary defects caused by a mutation in genes encoding structural subunits or assembly factors and secondary defects caused by mutations in genes related to mitochondrial replication, transcription, processing, modification, or translation.

Primary defects of ATP synthase represent the most severe metabolic diseases, usually manifested by encephalo-cardiomyopathies, and predominantly affect the pediatric population. Interestingly, mitochondrial disorders caused by a mutation in ATP synthase structural subunits or assembly factors are less frequent than other OXPHOS-related diseases (Dautant et al. 2018). Secondary ATP synthase defects in the cells/tissues manifest as combined defects of multiple OXPHOS complexes (Mayr et al. 2015).

1.3.1.1. Primary defects of ATP synthase due to mutation in mtDNA

Two structural subunits of ATP synthase, subunit a, encoded by *MT-ATP6* gene, and subunit A6L encoded by *MT-ATP8* gene, are encoded by mtDNA. Primary disorders of ATP synthase by mitochondrial origin can be caused by mutations in both of them. However, the mutations in the *MT-ATP6* gene are much more frequent. Subunit a and subunit A6L are synthesized from a bi-cistronic mRNA unit. The genes show an overlap of 46 nucleotides. Mutations in this unit can therefore affect either subunit a or A6L, or both.

Currently, over 70 different variants in *MT-ATP6*, 10 various mutation in *MT-ATP8* and 8 in the overlapping region have been reported in MITOMAP compendium (Lott et al. 2013). In this database, a "confirmed" (Cfrm) status indicates that at least two or more independent laboratories have published report on the pathogenicity of a particular variant. These variants are generally accepted by the mitochondrial research community as being pathogenic (Table 2). "Reported" status indicates that one or more publications have considered the mutation as possibly pathogenic.

The mtDNA defects of ATP synthase typical clinically manifest as neuropathy, ataxia, retinitis pigmentosa (NARP), Leigh syndrome (LS), maternally inherited Leigh's syndrome (MILS), Leber hereditary optic neuropathy (LHON) (Baracca et al. 2007) or hypertrophic cardiomyopathy (Jonckheere et al. 2008). The wide variability in clinical outcomes likely resides in the levels of heteroplasmy and different distributions of mtDNA mutations in cells and tissues. In addition to ; ATP deficiency, defects in ATP synthase may have a number of secondary effects, such as increased production of ROS and changes in upstream metabolic processes, which together unpredictably influence the disease process.

Mutations in mtDNA genes encoding ATP synthase subunits can result in impaired F_o proton channel function, complex stability or protein-protein interactions can be damaged (Wittig et al. 2010). Defects in *MT-ATP6* often affected ATP production (Baracca et al. 2007; Blanco-Grau et al. 2013; Dautant et al. 2018; Pallotti et al. 2004; Sgarbi et al. 2006; Sikorska et al. 2009). Steady-state ATP synthase levels were reduced and/or incomplete forms of ATP synthase were present in patient cells/tissues (Carrozzo et al. 2006; Nijtmans et al. 1995). However, the absence of these subcomplexes has also been reported (Honzik et al. 2013; Verny et al. 2011).

Table 2: Confirmed pathogenic variants in MT-ATP8 and MT-ATP6 genes and associated disease(s)/syndrome(s), modified by MITOMAP https://www.mitomap.org/MITOMAP (Lott et al. 2013).

Gene	Variant	AA change	Disease/syndrome
MT-ATP8/6	m.8528T>C	*MT-ATP8*:p.Trp55Arg *MT-ATP6*:p.Met1Thr	Infantile cardiomyopathy / hyperammonemia
MT-ATP6	m.8851T>C	p.Trp109Arg	BSN / LS
MT-ATP6	m.8969G>A	p.Ser148Asn	MLASA / IgG nephropathy
MT-ATP6	m.8993T>C	p.Leu156Pro	NARP / LS / MILS / other
MT-ATP6	m.8993T>G	p.Leu156Arg	NARP / LS / MILS / other
MT-ATP6	m.9035T>C	p.Leu170Pro	Ataxia syndromes
MT-ATP6	m.9155A>G	p.Gln210Arg	MIDD / renal insufficiency
MT-ATP6	m.9176T>G	p.Leu217Arg	LS / Spastic Paraplegia / Spinocerebellar Ataxia
MT-ATP6	m.9176T>C	p.Leu217Pro	FBSN / LS / Spinocerebellar Ataxia
MT-ATP6	m.9185T>C	p.Leu220Pro	LS / Ataxia syndromes / NARP-like disease / Episodic weakness and CMT
MT-ATP6	m.9191T>C	p.Leu222Pro	LS
MT-ATP6	m.9205_9206del	Ter-Met	Encephalopathy / Seizures / LA

BSN: Bilateral Striatal Necrosis, CMT: Charcot-Marie-Tooth syndrome, LA: Lactic Acidosis, LS: Leigh Syndrome, MIDD: Maternally Inherited Diabetes and Deafness syndrome, MILS: Maternally Inherited Leigh Syndrome MLASA: Mitochondrial myopathy, lactic acidosis and sideroblastic anemia, NARP: Neurogenic muscle weakness, Ataxia, and Retinitis Pigmentosa syndrome.

1.3.1.2. Primary defects of ATP synthase due to mutation in nDNA

Primary ATP synthase defects caused by nuclear mutations belong to the most severe metabolic diseases, usually manifesting as early-onset mitochondrial encephalo-cardiomyopathies. Mitochondrial disorders caused by mutations in nDNA present as an isolated deficit of ATP synthase with often fatal consequences (Houstek et al. 2006). Deficiency of complex V causes insufficient ATP production, a significant decrease in the content of fully assembled enzyme complex, and an increase in ROS (Baracca et al. 2007; Cízková et al. 2008b). Energy deprivation together with oxidative stress represents key factors in the pathogenesis of isolated deficit of ATP synthase (Mrácek et al. 2006). It results in damage to tissues with high energy demands (heart, skeletal muscles, brain, etc.) (Houstek et al. 2004; Mrácek et al. 2006). The most common phenotypes of these disorders are lactate acidosis, 3-methylglutaconic aciduria, hypertrophic cardiomyopathy and central nervous system disorder (Galber et al. 2021; Magner et al. 2014; Sperl et al. 2006).

Up to now, mutations in eight nuclear genes related to primary nuclear defects of ATP synthase were found. Six of them, *ATP5F1A*, *ATP5F1E*, *ATP5F1D*, *ATP5MK*, *ATP5PO,* and *ATP5MC3* encode structural subunits α, ε, δ, DAPIT, OSCP, and c, while the other two *ATPAF2* and *TMEM70* genes encode specific ancillary factors of biosynthesis of ATP synthase. However, differences can be found in the frequency of mutations. While the first seven types of nuclear ATP synthase defects are extremely rare, various mutations in the *TMEM70* gene are very frequent.

The autosomal recessively inherited c.985C>T (p.Arg329Cys) mutation was found in the *ATP5F1A* gene, encoding the structural subunit α, in two siblings with severe neonatal encephalopathy, who died in the first week of life (Jonckheere et al. 2013). The mother expressed only the wild-type variant while the asymptomatic father was a heterozygous carrier for the mutation. The severity of this phenotype was due to the fact that the maternal wild-type allele was not expressed. The only polymorphism found was c.-49+418C>T variant in the *ATP5F1A* gene but there was no evidence that it could affect the gene expression/regulation. Probands fibroblasts showed a reduction in the oxygen consumption rate. There was significantly reduced level of fully assembled ATP synthase without accumulation of F_1 subcomplexes, as well as decreased levels of individual ATP synthase subunits. Complementation with wild-type variant restored ATP synthase deficit in the patient´s fibroblasts, confirming the pathogenicity of the defect (Jonckheere et al. 2013).

The homozygous mutation c.962A>G (p.Tyr321Cys) in the *ATP5F1A* gene was described in two siblings born from a consanguineous relationship. Both patients with microcephaly, pulmonary hypertension, failure to thrive, hypotonia, encephalopathy, and heart failure died 15 months/3 months after birth. Deficiency of OXPHOS complexes and mtDNA depletion were described in muscle. Moreover, mutation affected a highly conserved residue. Expression of an analogous yeast variant in the ATP1 knockout strain led to an equally severe phenotype with a loss of mtDNA, and a decrease in mitochondrial membrane potential (Lieber et al. 2013).

A novel heterozygous for a recurrent de novo substitution, c.620G>A (p.Arg207His) in *ATP5F1A*, was described in three neonates with failure to thrive, hyperammonemia, development delay and lactate acidosis. Probands fibroblasts exhibited multiple deficits in complex V function and expression (Lines et al. 2021). The autors modelled the potential structural consequences of the recurrent p.Arg207His substitution. In the model, the sidechain of residue 207 resides at the α-β subunit interface, opposite the nearby β subunit's active site. At matrix pH, replacement of Arg207 with a histidine is a nonconservative substitution predicted to create a negatively-charged patch at the α–β interaction surface. The possibility that *ATP5F1A* (p.Arg207His) is dominant-negative with respect to the assembly, stability, or function of complex V remains to be tested in a suitable animal model (Lines et al. 2021).

Using whole-exome sequencing in cohorts of patients with suspected mitochondrial disease, three individuals were found with three different de novo heterozygous missense variants in *ATP5F1A* gene. The same mutation as in the previous study (Lines et al. 2021) was found in a 14-year-old proband, who presented during the first few months of life with developmental delay, failure to thrive, and lactic acidosis; subsequently, she recovered and had no persistent neurologic phenotype. Enzymatic analysis of OXPHOS complexes and citrate synthase in muscle tissue shows a decrease in ATP synthase activity (Zech et al. 2022). The second individual, a 17-year-old boy, harbored a c.545G>A (p.Arg182Gln) variant, presented with psychomotor delay, intellectual disability, ataxia, spastic paraparesis, and dystonia. The last patient from this study, a 12-year-old girl, heterozygous for c.1037C>T (p.Ser346Phe), had psychomotor retardation, spastic tetraparesis, generalized dystonia, absent speech, swallowing problems, and increased blood lactate concentrations (Zech et al. 2022).

In 2010 homozygous missense mutation c.35A>G (p.Tyr12Cys) in *ATP5F1E* gene encoded ATP synthase structural subunit ε was found in the 22-years-old proband (Mayr et

al. 2010). The pathogenic variant led to early-onset lactate acidosis, 3-methylglutaconic aciduria, but no cardiac involvement, followed by mild mental retardation, exercise intolerance, and peripheral neuropathy. Analysis of the patient´s fibroblast showed decreased oligomycin-sensitive ATP synthase activity and reduction of ATP synthesis. The amount of fully assembled ATP synthase, containing the mutated subunit ε, was reduced, as well as the level of individual ATP synthase subunits, with exception of subunit c, which accumulated (Mayr et al. 2010). Analysis of knock-down Human Embryonic Kidney 293 cells (HEK293) indicated reduced activity and content of ATP synthase as well as accumulation of subunit c (Havlícková et al. 2010). These results revealed that subunit ε is essential for the assembly and/or stability of the F_1 part of ATP synthase.

The same homozygous c.35A>G (p.Tyr12Cys) mutation in *ATP5F1E* was described in 2022 in two other patients from two unrelated families. A 16-month-old infant presented after birth with vomiting, severe respiratory distress, seizures, and impaired consciousness associated with lactate acidisis, developing generalized dystonia, and visual and hearing deficits. A 13-year-old girl manifested lactate acidosis with transient respiratory failure, developmental delay, and episodes of generalized tonic-clonic seizures, gait ataxia, and peripheral neuropathy. Reduced ATP synthase levels have been confirmed by immunocytochemistry (Neilson et al. 2022).

Two different homozygous missense mutations, c.245C>T (p.Pro82Leu) and c.317T>G (p.Val106Gly) in *ATP5F1D* gene encoded subunit δ, were found in two unrelated individuals manifest with episodic lethargy, metabolic acidosis, 3-methylglutaconic aciduria and hyperammonemia (Oláhová et al. 2018). Analysis of cultured skin fibroblasts revealed impaired ATP synthase assembly and subsequently reduced activity. Western blot and immunodetection in fibroblasts showed that steady-state levels of the δ subunit were unaffected. While the other ATP synthase subunits α, β, and OSCP were strongly reduced. In contrast, other OXPHOS complexes showed normal levels in both patients. A significant disruption of mitochondrial ultrastructure was also revealed in both patients (Oláhová et al. 2018). Results obtained from fibroblast analysis were confirmed in skeletal muscle. The steady-state levels of RC native complexes and subunits were not affected, whereas the amounts of ATP synthase subunit α and fully assembled complex V were markedly decreased. Authors hypothesize that the missense mutations present in both individuals did not alter the amount of subunit δ but instead led to an inability of subunit δ to properly bind to the other F_1 subunits, and thus reducing amount of ATP synthase (Oláhová et al. 2018).

In 2018 group of authors reported four individuals from three unrelated families carried a homozygous splicing mutation c.87+1G>C in *ATP5MK* gene encoded DAPIT subunit (Barca et al. 2018). All patients clinically manifest with Leigh syndrome. Interestingly, the mutation negatively affects enzyme dimerization and ATP synthesis rate. Furthermore, an altered shape of mitochondrial cristae with increased mitochondrial volume was found in the muscles (Barca et al. 2018). The complementation in patient fibroblast enhanced ATP synthase dimers and ATP production rate (Barca et al. 2018). Knock-down of DAPIT subunit in HeLA cells leads to reduced level and activity of ATP synthase (Ohsakaya et al. 2011). In addition, DAPIT protein plays role in ATP synthase dimerization (He et al. 2018; Meyer et al. 2007). ATP synthase dimers are linked back-to-face by DAPIT to form long oligomers along the edges of the cristae and thus helping to form mitochondrial ultrastructure (see chapter 1.2.6.2.).

Recently, a rare homozygous splice variant (c.87+3A>G) in the *ATP5PO* gene, encoding a subunit OSCP, was described in three individuals from two unrelated families with clinically suspected mitochondrial disorders. These individuals had a similar, severe infantile and often fatal multisystem disorder that included hypotonia, delayed development, hypertrophic cardiomyopathy, progressive epileptic encephalopathy, progressive cerebral atrophy, lactic acidosis, and white matter abnormalities on the brain consistent with Leigh syndrome (Ganapathi et al. 2022). Fibroblasts from the affected individuals demonstrated reduced OSCP protein, altered ATP synthase assembly with significantly reduced peripheral stalk subunits, and reduced ATP synthase hydrolytic activity (Ganapathi et al. 2022).

In 2022, compound heterozygous variants c.34C>T and c.329-20A>G (p.Gln12*/-) in *ATP5PO* were described in one individual. The girl presented during the neonatal period with fever-induced partial seizures, hypotonia, and elevated cerebrospinal fluid lactate concentrations; examination at 2 years of age revealed acquired microcephaly, global developmental delay, and dystonia. Magnetic resonance imaging (MRI) studies documented progressive brain atrophy. Following a period of initial stabilization, she developed seizure deterioration and died after several episodes with super-refractory status epilepticus at the age of 6 years. Using RNA-seq, proteomics and immunoblotting on the patient's fibroblasts, were demonstrated that these are loss-of-function variants that lead to a reduction in ATP synthase levels (Zech et al. 2022).

Three different heterozygous de novo variants in the *ATP5MC3* gene, encoding the subunit c, were identified in 3 individuals. The first proband, heterozygous for c.318C>G

(p.Asn79Lys), was a 12-year-old boy, who presented with isolated upper limb dystonia (Neilson et al. 2022; Zech et al. 2022). Fibroblast showed impaired ATP generation, and oxygen consumption. Drosophila model carrying orthologous mutations also exhibited impaired mitochondrial function and displayed reduced mobility (Neilson et al., 2022; Zech et al., 2022). The second individual, heterozygous for c.319C>G (p.Pro107Ala) variant, 15-year-old girl had delayed milestone development, pyramidal symptoms and general dystonia with marked upper body involvement (Zech et al. 2022). A third individual with de novo heterozygous variant c.236G>T (p.Gly79Val), 6-year-old boy manifested with delayed psychomotor development, lower limb spasticity and elevated blood lactate levels. Reduced ATP synthase activity and levels were found in the patient's fibroblasts without accumulation of the assembly subcomplex (Zech et al. 2022).

The homozygous missense mutation c.280T>A (p.Trp94Arg) in the *ATPAF2* gene for assembly factor ATPAF2, was found in the patient with severe neonatal encephalopathy (De Meirleir et al. 2004). Both parents (consanguineous) and unaffected siblings were heterozygous carriers of the variant, resulting in altered dynamic properties of the assembly factor (Meulemans et al. 2010). The patient presented dysmorphic features, cortical-subcortical brain atrophy followed by basal ganglia atrophy, 3-methylglutaconic aciduria, and lactate acidosis, and died at the age of 14 months (De Meirleir et al. 2004). The activity and level of native complex V, without accumulation of the F_1 part, were strongly reduced in liver more than in skeletal muscle. The reduced levels of individual ATP synthase subunits suggest that the assembly of the F_1 part may have been disorganized at an early stage, and thus the unassembled subunits were rapidly degraded (De Meirleir et al. 2004). In a yeast model, this variant has been shown to affects the solubility of the ATPAF2 protein (Meulemans et al. 2010).

In a group of patients with isolated ATP synthase deficiency, severe neonatal lactic acidosis, and encephalocardiomyopathy, the presence of a mutation in the *TMEM70* gene was identified as the cause of the disease (Cízková et al. 2008b). The homozygous splicing mutation c.317-2A>G was found in the second intron preventing the synthesis of TMEM70 protein (Cízková et al. 2008b; Houstek et al. 2009). The patient´s fibroblasts presented decreased ADP-stimulated respiration, decreased ATP synthase activities and significantly reduced amount of ATP synthase. All defects in fibroblasts were corrected after complementation with wild-type *TMEM70.* TMEM70 protein was determined as a specific assembly factor of human ATP synthase (Cízková et al. 2008b; Houstek et al. 2009). Within the last 14 years, numerous patients with mutations in the *TMEM70* gene,

either homozygous or compound heterozygous, have been described with a wide range of clinical manifestations (Galber et al. 2021; Hejzlarová et al. 2014).

The prevalent homozygous splicing mutation c.317-2A>G, which leads to multiple unstable and incomplete transcripts to prevent protein synthesis, has been described in more than 50 patients. Clinically, TMEM70 protein deficiency was manifested in patients mainly as hypertrophic cardiomyopathy, 3-methylglutaconic aciduria, lactate acidosis, dysmorphism, hypotonia, ataxia, and psychomotor retardation. Less common symptoms include oligohydramnios, prematurity, low birth weight, intrauterine growth restriction, persistent pulmonary hypertension, Wolff-Parkinson-White syndrome, and hyperuricemia.

The severity of the disease is very vast, a high percentage of individuals dying within the first few years and mostly in the first few months of life. On contrary, some patients can survive significantly longer. In 2010 Honzik et al. suggested in a retrospective clinical study, that if the patient survive the critical early postnatal period of the first weeks and months of life, metabolic imbalance and cardiac disorders might improve (Honzík et al. 2010).

The majority of the patients with prevalent homozygous c.317-2A>G mutation have been of Roma origin (Baban et al. 2020; Braczynski et al. 2015; Catteruccia et al. 2014; Diodato et al. 2014; Honzík et al. 2010; Magner et al. 2014; Stojanović and Doronjski 2013; Torraco et al. 2012; Wortmann et al. 2009), but it is not the norm (Catteruccia et al. 2014; Diodato et al. 2014; Sarajlija et al. 2017).

The predominant mutation c.317-2A>G was found in combination with other variants in the *TMEM70* gene. The c.317-2A>G and c.118_119insGT (p.SerCfsX11) lead to a formation of premature stop codon and a presumed 40 AA short protein (Cameron et al. 2011; Cízková et al. 2008b; Honzík et al. 2010; Magner et al. 2014).

Several patients have a combination of prevalent homozygous splicing mutation c.317-2A>G and a missense mutations c.494G>A (p.Gly165Asp) (Shchelochkov et al. 2010) or c.628A>C (p.T210Pro) (Catteruccia et al. 2014; Magner et al. 2014; Torraco et al. 2012). The combination of mutations c.317-2A>G and c.494G>A was found in patient presenting other symptoms with mild Reye-like syndrome (Shchelochkov et al. 2010). The compound heterozygote patients c.317-2A>G and c.628A>G (p.Thr210Pro) were severely affected by metabolic acidosis and cardiomyopathy, pulmonary arterial hypertension and Wolf-Parkinson-White preexcitation syndrome (Catteruccia et al. 2014; Magner et al. 2014; Torraco et al. 2012).

The c.317-2A>G variant was also found in combination with c.349_352del (p.Ile117Alafs*36) and c.783A>G (p.*261Trpext*17) in two probands with similar phenotypes: intrauterine growth retardation, lactate acidosis, psychomotor retardation, hypertrophic cardiomyopathy and dysmorphism (Diodato et al. 2014).

Different type of homozygous splicing mutation c.316+1G>T was detected in two siblings of consanguineous parents presented with typical manifestation of isolated deficit of ATP synthase but without 3-methylglutaconic aciduria (Magner et al. 2014; Spiegel et al. 2011). The translated abnormal protein is lacking 34 AA. Mutated protein has defective membrane assembly and/or import into mitochondria.

Splice site variant c.316+1G>A and deletion variant c.141delG (p.Pro48Argfs*2), were described in an individual who had metabolic acidosis, hyperalaninemia, developmental delay, undescended testicle, lactate acidosis, 3-methylglutaconic acidicuria and left ventricular noncompaction (Hirono et al. 2019).

Several different homozygous frameshift mutations creating premature stop codon, leading to the synthesis of potentially incompleted TMEM70 protein were reported. Two siblings of consanguineous parents were positive for c.578_579delCA (p.Asn198*) deletion, which results in synthesis of a 197 AA long protein missing almost two third of mature protein (Magner et al. 2014; Spiegel et al. 2011).

Because of c.336T>A (p.Tyr112*) variant is synthetized 112 AA premature TMEM70 protein (Magner et al. 2014; Spiegel et al. 2011), while c.211–450_317–568del (2290bp deletion) mutation deleting the whole exon 2 (Tort et al. 2011) thus produces a protein only 71 AA long. Patients carrying these variants presented with hypertrophic cardiomyopathy, metabolic acidosis, mental retardation and facial dysmorphism (Magner et al. 2014; Spiegel et al. 2011; Tort et al. 2011). The frameshift mutation c.238C>T (p. Arg80*) in the second exon led to formation of an incomplete 80 AA long protein. This variant manifested in the severe phenotype characterized by with encephalopathy, hypotonia, metabolic acidosis, intrauterine growth retardation, early onset hypotonia, laclate acidosis, elevated level of 3-methylglutaconic acid, hyperamonnemia, hypertrophic cardiomyopathy, multiorgan failure and dysmorphism (Diodato et al. 2014; Magner et al. 2014; Spiegel et al. 2011).

Another type of *TMEM70* homozygous mutation g.2436–3789 (1353bp deletion) resulting in transcript lacking of the second exon was described in proband of consanguineous parents (Jonckheere et al. 2011).

The homozygous frameshift c.105dupT (p.Val36Cysfs*52) variant was reported in 2019 (Staretz-Chacham et al. 2019). The mutation resides within the first exon and results in loss-of-function of the encoded protein (via nonsense-mediated decay). Two siblings of consanguineous parents presented mitochondrial encephalo-cardiomyopathy, accompanied by elevated lactate and hyperammonemia, dysmorphic features, hypotonia, developmental delay and brain anomalies, congenital heart defects and mild cardiac hypertrophy and antenatal intrauterine growth restriction. Hypercitrullinemia during decompensation has been described as a novel finding in this condition. Elevated citrulline has been reported previously in different inborn errors of metabolism (Haviv et al. 2014; Rabier et al. 1998), while uncommonly associated with *TMEM70* mutations.

The homozygous missense mutation c.535C>T (p.Tyr179His) has been described in patient presenting with neonatal lactic acidemia, severe hypotonia and hypertrophic cardiomyopathy, mild mental retardation and intrauterine growth retardation dysmorphism, bilateral cataract and hyperammonemia (Atay et al. 2013; Magner et al. 2014). Cataract and neonatal mitochondrial encephalo-cardiomyopthy also occurred in a patient with the same mutation (Kars et al. 2021).

The homozygous missense point mutation c.701A>C (p.His234Pro) manifests in patient of non-consanguinity parents in early onset of elevated 3-methylglutaconic acid level, hyperammonemia, lactic acidosis, psychomotor retardation, intrauterine growth retardation, dysmorphism, leukoencephalopathy, hypotonia, hypertrophic cardiomyopathy and pulmonary arterial hypertension (Catteruccia et al. 2014; Diodato et al. 2014).

Magner and colleagues reported, among others, one homozygous c.359delC (p. Thr120Asnfs*34) mutations and two heterozygous varaints (c.317-2A>G/c.251delC (p.Thr84Serfs*11) and c.317-2A>G/c.470T>A) (p.Val157Glu), which had not been found previously. The clinical course of probands with these mutations was not significantly different from other *TMEM70* patients (Magner et al. 2014).

In a study from 2021, fibroblasts from a cardiomyopathy patient carrying a homozygous frameshift mutation c.497_498del (p.Tyr166Cysfs*7) in the *TMEM70* gene were used. This variant results in a truncated protein downstream of its second transmembrane segment (Bahri et al. 2021).

In recent years, thanks to whole-exome sequencing, new homozygous mutations c.479A>C (p.His160Pro) in the *TMEM70* gene have been found in large cohorts of patients of pediatric cardiomyopathy patients (Al-Hassnan et al. 2020). The same mutation was also found in three siblings in a family with consanguineous parents. The proband described in

this study presented with developmental delay, high ammonia, and metabolic acidosis (AlFaris et al. 2021).

Another homozygous mutation was found by whole-exome sequencing in a cohort of adults with neurological symptoms with a high degree of consanguinity rate. The homozygous c.289A>C (p.Thr97Pro) missense variant in *TMEM70* results in splice site changes. The mutation manifested with mitochondrial encephalocardiomyopathy, development delay, intellectual disability failure to thrive, hyperammonemia, lactic acidosis, short stature, renal anomalies and hypotonia (Mu et al. 2019).

The study performed on fibroblasts prom a patient carrying the prevalent homozygous splicing mutation c.317-2A>G showed an increased level of complex III and complex IV. Surprisingly, the increase in these enzyme complexes was detected only at the protein level, while not at mRNA level. Thus, the compensatory increase in complex III and complex IV proteins appears to be due to specific adaptive changes in mitochondrial biogenesis that occur during posttranslational phase (Havlickova Karbanova et al. 2012).

Mitochondrial ultrastructure is often impaired in *TMEM70* patient´s cells and tissues, because ATP synthase plays important role in the formation of mitochondrial cristae (see chapter 1.2.6.2). Defective morphological features have been observed in the skeletal muscle mitochondria of patients with two different compound heterozygous mutations c.317-2A>G and c.118_119insGT (p.Ser40Cysfs*11) (Cameron et al. 2011); c.317-2A>G and c.783A>G (p.*261Trpext*17) (Diodato et al. 2014) and patients´ fibroblast and myoblasts (Braczynski et al. 2015; Diodato et al. 2014; Jonckheere et al. 2011; Sládková et al. 2015). Several swollen and irregularly shaped mitochondria with disruption of the central part and complete loss of cristae were reported. Furthermore, some mitochondria were small with simplified cristae. Reduction of ATP synthase levels results in the absence of cristae and formation of an ”onion-like” mitochondrial ultrastructure characterized by concentric rings of the inner mitochondrial membrane (Diodato et al. 2014). A spectrum of mild to more severe pathological changes have been observed in patients with the prevalent mutation, including giant mitochondria, subsarcolemmal accumulation of mitochondria, globular inclusions, concentric cristae formation, cristae fragmentation, and crystalloid inclusions (Braczynski et al. 2015). The ultrastructural morphology of affected mitochondria is restored by complementation (Jonckheere et al. 2011).

Increased fragmentation of the mitochondrial network, suggesting altered fission/fusion dynamic,s was observed also in fibroblast patient with compound heterozygous mutation

c.317-2A>G; c.349_352del (p.Ile117Alafs*36) and homozygous splicing c.317-2A>G (Diodato et al. 2014).

Light microscopy analysis did not reveal any ragged-red or COX-deficient fibers, usual for mitochondrial disease in muscle (Braczynski et al. 2015; Diodato et al. 2014; Magner et al. 2014). Interestingly, muscle biopsy from a non-Roma patient with compound heterozygous *TMEM70* mutations (c.317-2A>G and c.494G>A) demonstrated the presence of ragged-red fibers (Shchelochkov et al. 2010).

In the Human Gene Mutation Database (HGMD), other variants in assembly factors or structural subunits of ATP synthase are listed. However, there was no evidence of causality associated with patients´ phenotype (Stenson et al. 2003).

2. AIMS OF STUDY

Mitochondrial diseases represent one of the most common groups of inherited metabolic disorders affecting children and adults (Lightowlers et al. 2015; Thompson et al. 2020). Due to the dual genetic control of mitochondria, defects in mitochondrial processes can be caused by mutations in the mtDNA or nDNA. Inheritance of mitochondrial disorders is either maternal (mtDNA), sporadic (de-novo), autosomal recessive, autosomal dominant, or X-linked. Genetic defects affecting mitochondrial functions have so far been identified in more than 400 genes (Frazier et al. 2019; Stenton et al. 2022; Thompson et al. 2020).

The aim of this study was to characterize the protein TMEM70, an ATP synthase assembly factor and specifically to characterize the impact of identified novel disease variants leading to primary or secondary ATP synthase deficiency in patients´ cell lines or tissues samples.

The specific aims:

A) **To characterize TMEM70 protein, the assembly factor of human mitochondrial F_1F_o-ATP synthase**

B) **To study the impact of prevalent splicing homozygous mutation c.317-2A>G in *TMEM70* gene on OXPHOS complexes and mitochondrial ultrastructure**

C) **To study the impact of various *MT-ATP6* variants on OXPHOS complexes and energy metabolism**

D) **To study the molecular and biochemical aspects of selected mitochondrial diseases with complex V deficiency**

3. MATERIAL AND METHODS

I. Ad published results, see individual articles/manuscripts in the Supplement

II. Material and methods related to my participation on articles/manuscripts

3.1. Material

A summary of the patient materials I used for my experiments is shown in Table 3. The model cell lines that I prepared and analysed are summarized in Table 4.

3.2. Tissues and cell cultures

Fibroblast cultures were established from skin biopsy/autopsy. Cells were grown in high-glucose (4.5 g/l) Dulbecco's modified Eagle's medium (DMEM) supplemented with 10% (v/v) fetal bovine serum (FBS) (Sigma-Aldrich), penicillin (100 U/mL) and streptomycin (100 μg/mL) at 37°C in 5% CO_2 in air. Skin fibroblasts were grown to 80% - 90% confluence and harvested using 0.05% (w/v) trypsin and 0.02% (w/v) EDTA. Detached cells were diluted with an ice-cold culture medium, sedimented by centrifugation (600 g and 4°C for 15 min) and washed twice in Phosphate Buffered Saline (PBS) (Sigma-Aldrich, 8 g/L NaCl, 0.2 g/L KCl, 1.15 g/L Na_2HPO_4, 0.20 g/L KH_2PO_4).

HEK293 cells (CRL-1573, ATCC) were grown in high-glucose (4.5 g/l) DMEM medium supplemented with 10% (v/v) FBS (Sigma-Aldrich), penicillin (100 U/mL) and streptomycin (100 μg/mL) at 37 °C in 5% CO_2 atmosphere. HEK293 cells (~1×10^7) were harvested by trypsinization 0.05% (w/v) and washed twice in PBS.

3.3. Expression vectors and transfections

TMEM70-FLAG cDNA expression vector the full-length human TMEM70 coding sequence was amplified from the IMAGE clone 3631570 and inserted into the C-FLAG fusion mammalian expression pIRESpuro3 (Clontech). The fidelity of the constructs was confirmed by sequencing.

Plasmids were transfected into the HEK293 cell lines (2 μg of DNA/5×10^5 cells) by Nucleofector device and nucleofection Kit V (Amaxa/Lonza) following standard protocols. TMEM70-GFP cDNA expression vector (Calvo et al. 2006) was provided by Prof. V.K. Mootha. TMEM70-GFP cDNA expression vector were transiently transfected into the HEK293 expressed stabile TMEM70-FLAG fussion protein by Express-In Transfection Reagent (Open Biosystems).

Table 3: Patients´ material related to my participation on articles/manuscripts

	age of onset	**geneder**	**gene**	**mutation**	**AA change**	**tissue and derivated cells, (A: autopsy; B: biopsy)**
patient	<1 week	M	*TMEM70*	c.[317-2A>G];[317-2A>G]	Splicing	muscle (A); heart (A); liver (A); brain* (A); fibroblasts (A)
patient	<1 week	F	*TMEM70*	c.[317-2A>G];[317-2A>G]	Splicing	muscle (B); heart (A); liver (A); brain* (A); fibroblasts (B)
patient	<1 week	M	*TMEM70*	c.[317-2A>G];[317-2A>G]	Splicing	muscle (A); heart (A); liver (A); fibroblasts (A)
patient	<1 week	M	*TMEM70*	c.[317-2A>G];[317-2A>G]	Splicing	muscle (B); heart (A); brain* (A)
patient	<1 week	M	*TMEM70*	c.[317-2A>G];[317-2A>G]	Splicing	muscle (A); heart (A); liver (A); brain* (A)
patient	<1 week	M	*TMEM70*	c.[317-2A>G];[317-2A>G]	Splicing	muscle (B); heart (A); fibroblasts (B)
patient	<1 week	M	*TMEM70*	c.[317-2A>G];[317-2A>G]	Splicing	muscle (A); heart (B); fibroblasts (A)
patient	<1 week	F	*TMEM70*	c.[317-2A>G];[317-2A>G]	Splicing	myoblasts (A); fibroblasts (A)
patient	8 months	F	*MT-ATP6*	m.8851T>C	p.Trp109Arg	muscle (B); fibroblasts (B)
patient	57 years	M	*MT-ATP6*	m.8719G>A	p.Gly65*	muscle (B)
patient	39 years	F	*MTTK*	m.8315A>C	-	muscle (B)
patient	<1 week	F	*PUS1*	c.[896+2551_1061delinsATTTTACCA]; [896+2551_1061delinsATTTTACCA]	p.Gly148ValfsX41/ p.Gly148ValfsX41	muscle (B); liver (A)
patient	5 years	M	*PUS1*	c.[896+2551_1061delinsATTTTACCA]; [896+2551_1061delinsATTTTACCA]	p.Gly148ValfsX41/ p.Gly148ValfsX41	muscle (B); liver (A)
patient	<1 week	F	*COX10*	c. [610A>G]; [674C>T]	p.Asn204Asp/ p.Pro225Leu	muscle (B); liver (A)

*frontal cortex

Table 4: Model cell lines related to my participation on articles/manuscripts

cell lines	fussion protein	transfetion	expression
HEK293	TMEM70-FLAG	nucleofection	stabile
HEK293	TMEM70-FLAG-GFP	lipofection	transient

3.4. Isolation of mitochondria

Mitochondria were isolated from cultured skin fibroblast and HEK293 cells. Cells were harvested by trypsinization, washed three times with PBS, re-suspended in an isotonic Sodium Chloride-Tris-EDTA (STE) buffer (250 mM sucrose, 10 mM Tris–HCl (pH 7.4), 1 mM EDTA, 1% (v/v) Protease Inhibitor Cocktail (PIC, Sigma-Aldrich) and disrupted on ice using a Dounce homogenizer. The unbroken cells and nuclei, the homogenate was centrifuged at 600 g and 4°C for 15 min. The post-nuclear supernatant was centrifuged at 10 000 g and 4°C for 25 min. The resulting mitochondrial pellet was twice washed with STE buffer. Protein concentration were determined with the Bio-Rad Protein Assay Kit (Bio-Rad Laboratories). The isolated mitochondria were stored at -80°C.

3.5. Trypsinization of the endogenous or C-terminal tagged TMEM70 protein in cells and mitochondria

To analyze the effect of trypsin on isolated organelle, mitochondria isolated from HEK293 cells stabile expressing TMEM70-FLAG fusion protein were exposed to hypotonic shock (Tang et al. 2009). Briefly, 150 µg of mitochondrial protein were resuspended in 100 µl of 5 mM MOPS-KOH, pH 7.2, and incubated for 20 min at 4°C on a rotator. Swollen mitochondria with disrupted outer membrane were treated with trypsin (4 µg/100 µg of protein) for 20 min at 4°C on a rotator in the presence or absence of 1% Triton X-100. Digestion was stopped with 100 µg/mL of soybean trypsin inhibitor and 1% (v/v) PIC (Sigma-Aldrich). Samples were analyzed by 12% Sodium Dodecyl Sulfate–Polyacrylamide Gel Electrophoresis (SDS-PAGE) and western blot (WB) analysis.

3.6. Immunoprecipitation

For TMEM70-FLAG immunoprecipitation, 1.3 mg protein of freshly isolated mitochondria from cultured cells were lysed with 0.35 ml buffer containing 0.5% Triton X-100, 150 mM NaCl and 50mM Tris–HCl (pH 7.4) and 1% PIC for 30 min at 4°C on a rotator and centrifuged at 12 000 g for 10 min. The lysate (0.32 ml) was incubated overnight at 4°C with previously washed 40 µl of an EZ View ANTI-FLAG M2 affinity agarose resin (Sigma-Aldrich). Subsequently the resin was washed three times with buffer containing 150 mM NaCl and 50 mM Tris–HCl (pH 7.4). The bound protein was eluted by competition with 3×FLAG peptide (Sigma-Aldrich). The eluted immunoprecipitate

was combined with Sodium Dodecyl Sulfate (SDS) sample buffer and analyzed by 12% SDS-PAGE and WB.

3.7. Electrophoresis, Western blot and Immunoblot Analysis

SDS-PAGE was carried out under standard conditions (Schägger et al. 1986) performed on 10% or 12% polyacrylamide minigels using Mini-Protean system (Bio-Rad). Mitochondria or tissue/cell homogenates were incubated for 20 min on ice with radioimmunoprecipitation assay buffer (RIPA) (50 mM Tris/HCl (pH 7.4), 150 mM NaCl, 1 mM PMSF, 1 mM EDTA, 1% Triton X-100 and 0,1% SDS (v/v), 1% (v/v) PIC) and centrifuged at 51 000 g for 25 min, 4°C. Samples were dissociated in 50 mM Tris/HCl (pH 6.8), 12% (v/v) glycerol, 4% SDS, 2% (v/v) 2-mercaptoethanol, and 0.01% (w/v) Bromphenol Blue for 30 min at 37°C. 2,5-20 μg of protein was loaded in each lane. Serial dilutions of control sample (25-100%) were loaded on the same gels. Electrophoresis was performed at 50 V for 30 min and then at 90 V.

BN-PAGE was performed on 8–15% or 6-15% polyacrylamide minigels (Schägger and von Jagow 1991). Isolated mitochondria were solubilized with DDM (1 g/g of protein) or digitonin (2 g/g of protein) for 15 min on ice in 1.5 M aminohexanoic acid, 2 mM EDTA and 50 mM Bis-Tris, pH 7.0. The samples were centrifuged for 20 min at 4 °C and 30,000 g and Coomassie Brilliant Blue G-250 dye (Serva, 0.1 g/g of detergent) and 5% (v/v) glycerol were added to supernatants before electrophoresis. 2-30 μg of protein prepared was loaded in each lane. Serial dilutions of control mitochondrial sample (10%-100%) were loaded on the same gels. Electrophoresis was performed at 50 V for 30 min and then at 90 V.

For two-dimensional BN/SDS-PAGE, strips of the first dimensions gels were incubated in a 2-diomensional buffer containing 1% 2-mercaptoethanol and 1% SDS and then resolved in the second dimension on SDS-PAGE.

WB analysis using semidry electrotransfer of proteins was performed by standard protocols (Jesina et al. 2004b; Stiburek et al. 2005). Proteins were electroblotted from the gels on to Immobilon^{TM}-PVDF Membranes (Merck-Millipore) using semi-dry transfer for 1 h at a constant current of 0.6 mA/cm^2. Membranes were air-dried overnight, rinsed with 100% methanol (v/v) and blocked in TBS (Tris-buffer saline) with 5% non-fat dried milk for 2 hours.

For immunodetection we used specific antibodies to FLAG (Sigma-Aldrich), OPA1 (BD Biosciences), fumarate hydratase (FH), GFP (Santa Cruz Biotechnology), TMEM70

(Proteintech Group), NDUFB6 (Abcam), NDUFA9 (Abcam), SDH70 (Abcam), SDH30 (Abcam), CORE2 (Abcam), COX1 (Abcam), COX2 (Abcam), COX5a (Abcam), F_1-α (Abcam), F_1-β (Abcam), Fo-c Abcam, Fo-a (Abcam), OSCP (Abcam), IF1 (Abcam), F6 (Abcam), Fo-d (Abcam), MtHSP70 (Alexis Biochemicals), α-Tubulin (Cell Signaling), VDAC1 (Abcam). The immunoblots were detected with peroxidase conjugated secondary antibodies and SuperSignalWest Femto Maximum Sensitivity Substrate (Thermo Scientific Pierce) using VersaDoc 4000 Imaging System (Bio-Rad) or G:Box system (Syngene).

4. RESULTS AND DISCUSSION

4.1. Results and discussion related to the specific aim A) To characterize TMEM70 protein, the assembly factor of human mitochondrial F_1F_o-ATP synthase

I. Publications related to the specific aim A):

1) Hejzlarová, K., Tesařová, M., Vrbacká-Čížková, A., Vrbacký, M., Hartmannová, H., Kaplanová, V., Nosková, L., **Kratochvílová, H**., Buzková, J., Havlíčková, V., Zeman, J., Kmoch, S., Houštěk, J. (2011). Expression and processing of the TMEM70 protein. Biochimica et biophysica acta 1807, 144-149. IF = 4.843, Quartile Score = Q1 (2011).
   Supplement 1)

2) **Kratochvílová, H.** *, Hejzlarová, K. *, Vrbacký, M., Mráček, T., Karbanová, V., Tesařová, M., Gombitová, A., Cmarko, D., Wittig, I., Zeman, J., Houštěk, J. (2014). Mitochondrial membrane assembly of TMEM70 protein. Mitochondrion 15, 1-9. * Equal contribution, IF = 3.249, Quartile Score = Q2 (2014).
   Supplement 2)

   Author's contribution: plasmid cloning (1, 2), transfection of transient and stable cell lines (1, 2), analysis of protein localization (1) and orientation (2), immunoprecipitation (2), co-immunoprecipitation (2), two-dimensional electrophoretic analysis and manuscript preparation (2).

Hejzlarová, K., Tesařová, M., Vrbacká-Čížková, A., Vrbacký, M., Hartmannová, H., Kaplanová, V., Nosková, L., **Kratochvílová, H**., Buzková, J., Havlíčková, V., Zeman, J., Kmoch, S., Houštěk, J. (2011). **Expression and processing of the TMEM70 protein.** Biochimica et biophysica acta; 1807: 144-149. IF = 4.843, Quartile Score = Q1 (2011).

The *TMEM70* gene encoding a mitochondrial membrane protein was first identified by integrative genomics in 2006 (Calvo et al. 2006). In 2008, the TMEM70 protein was determined as an assembly factor of mammalian ATP synthase (Cízková et al. 2008b). In this study, we investigated the import, localization, sublocalization, and processing of this factor in human cells using GFP- and FLAG-tagged forms of TMEM70 protein.

TMEM70 was found to be synthesized as a 29 kDa precursor protein processed to a 21 kDa mature form. Mitochondrial localization was demonstrated by immunocytochemical colocalization of TMEM70-FLAG, mitochondrial dye (MitoTracker Red), and ATP synthase subunit β. Furthermore, TMEM70 was found only in isolated mitochondria from the cells expressing the TMEM70-FLAG protein, while it was absent in the cytosolic fraction (Figure 6A). Moreover, we fractionated the isolated mitochondria by sonication and treated the mitochondrial membranes with Na_2CO_3. Pellet and supernatant after centrifugation (100,000*g)* were analyzed by SDS-PAGE and WB (Figure 6B). TMEM70-FLAG was found only in the sediment, similar to the cytochrome *c* oxidase subunit (COX1), indicating its localization in the mitochondrial membrane. The efficacy of the treatment was verified by heat shock protein 70 (HSP70) protein (matrix) that was recovered in the supernatant fractions.

The mass spectroscopy analysis confirmed the mitochondrial location of TMEM70 and further indicated low cellular content of the TMEM70 protein as well as ATP synthase assembly factors ATPAF1 and ATPAF2 (Ackerman and Tzagoloff 2005). Although the TMEM70 protein has been described as an ATP synthase assembly factor, in this study we did not identify a direct interaction of TMEM70 with ATP synthase, but we did identify the presence of a dimeric form of the TMEM70 protein.

In this study, we only tested the possible interaction of TMEM70 protein with the subunit α/β and possible subassembly complexes in which these subunits are present (F_1, F_1-c). As later shown, the TMEM70 protein interacts with the subunit c and helps in the assembly of the c8 ring, which is present in the inner mitochondrial membrane (Bahri et al. 2021; Carroll et al. 2021; Kovalčíková et al. 2019; Sánchez-Caballero et al. 2020).

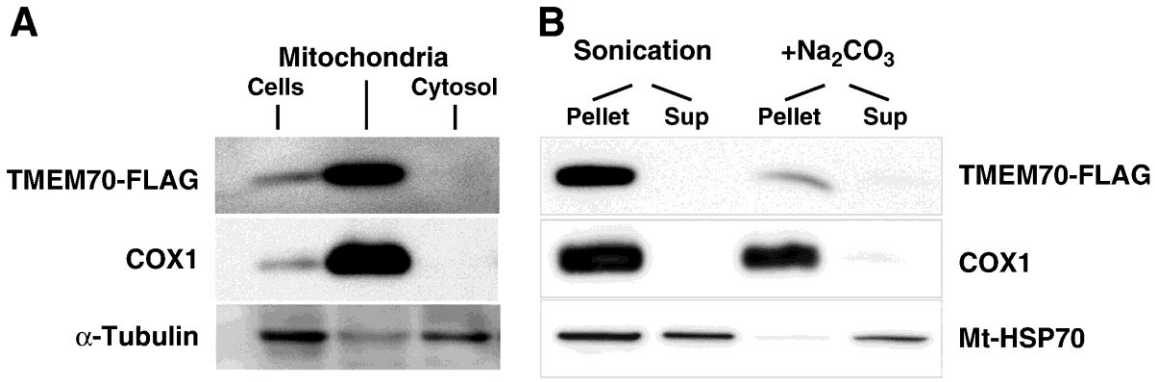

Figure 6: A) TMEM70 is a membrane mitochondrial protein. HEK293 cells expressed TMEM70-FLAG and cell homogenate, isolated mitochondria and cytosolic fractions were analyzed. TMEM70-FLAG signal was found in the mitochondrial fraction while it was absent in the cytosol. B) Isolated mitochondria were sonicated and extracted with Na_2CO_3 and 100,000*g* pellet and supernatant were prepared. WB was performed with indicated antibodies (Hejzlarová et al. 2011).

Kratochvílová, H. *, Hejzlarová, K. *, Vrbacký, M., Mráček, T., Karbanová, V., Tesařová, M., Gombitová, A., Cmarko, D., Wittig, I., Zeman, J., Houštěk, J. * Equal contribution, (2014). **Mitochondrial membrane assembly of TMEM70 protein.** Mitochondrion 15: 1-9. IF = 3.249, Quartile Score = Q2 (2014).

In this study, we focused on description of TMEM70 protein structure, to elucidate its function. Therefore, we characterized the membrane topology of TMEM70 protein in the inner mitochondrial membrane by several independent approaches using GFP, FLAG and MYC-FLAG as the C-terminal tags of the protein.

TMEM70 protein sequence contains two highly conserved transmembrane domains spanning 21 AA each, separated by a short sequence of 18 mostly hydrophilic AA. This structure is predicted to form a hairpin-like membrane assembly of the protein. Based on the accessibility to membrane impermeable protease (trypsin) (Figure 7A) and to the dye (Trypan blue) at differently permeabilized mitochondria we demonstrated that TMEM70 has a hairpin structure with the N- and C-termini oriented towards the mitochondrial matrix (Figure 7B). Such conformation is also consistent with previous computational predictions (Jonckheere et al. 2011).

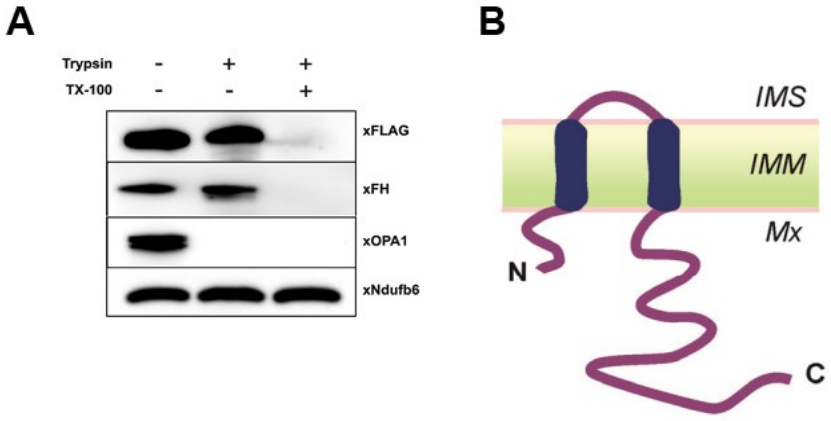

Figure 7: Accessibility of the C-terminal FLAG to protease in mitochondria from HEK293 cells expressing TMEM70-FLAG. The outer membrane of isolated mitochondria was disrupted by hypotonic shock and mitochondria were treated with 4 μg of trypsin/100 μg of protein in the presence or absence of 1% Triton X-100 (TX-100) as indicated. Samples were separated by SDS-PAGE and probed with antibodies to FLAG, OPA1 (representative of intermembrane space proteins), fumarate hydratase (FH, representative of matrix proteins) and Ndufb6 (inner membrane protein protected from protease digestion). B) The schematic orientation of TMEM70 protein in mitochondria, IMS: intermembrane space, IMM: inner mitochondrial membrane, Mx: matrix. Adapted from (Kratochvílová et al. 2014).

Two-dimensional electrophoresis and co-imunnoprecipitation analysis of different tagged forms confirmed our previous findings that TMEM70 protein forms dimers and higher oligomer structures (Hejzlarová et al. 2011). Nevertheless, no evidence of a specific association with the ATP synthase complex or the F_1 subcomplexes was found.

To confirm that TMEM70 forms oligomers, the tagged forms of TMEM70 were used. We have analyzed HEK293 cells expressing either TMEM70-GFP or TMEM70-FLAG alone or coexpressing both constructs simultaneously (TMEM70-FLAG + TMEM70-GFP) (Figure 8). Mitochondria from these cells were solubilized with Triton X-100 (TX-100) immunoprecipitated with anti-FLAG antibody. Immunoprecipitate from cells coexpressing both tagged forms, the FLAG- and the GFP-tagged TMEM70 was detected (Figure 8). These experiments demonstrated that TMEM70 protein forms oligomers.

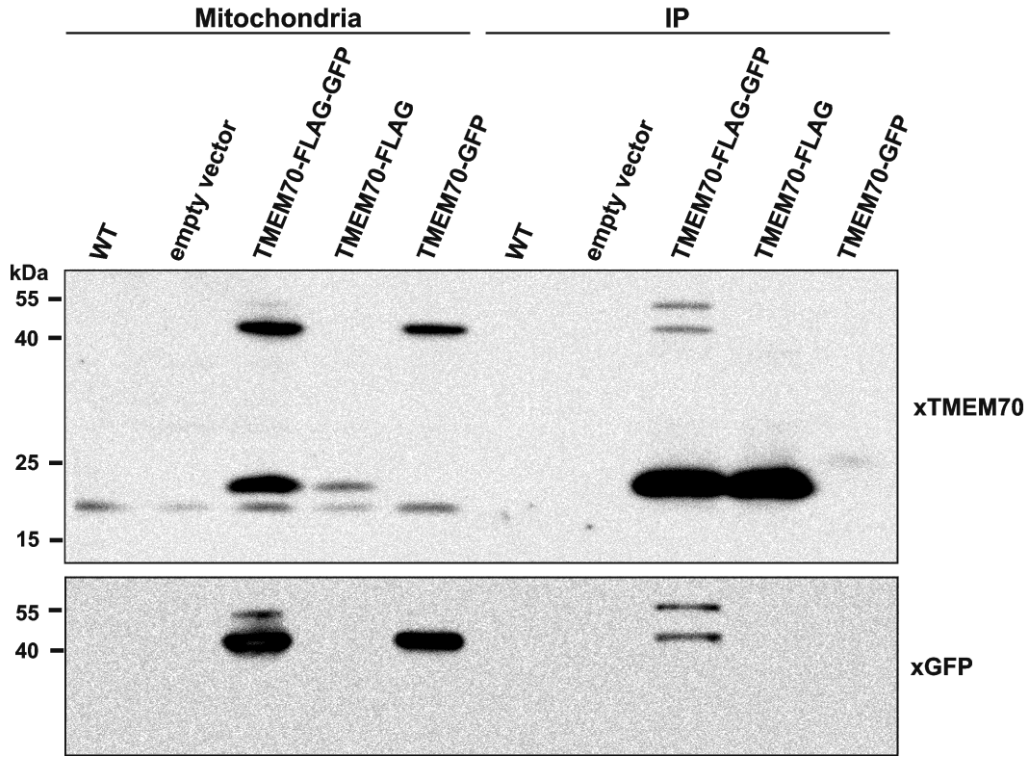

Figure 8: Detection of TMEM70 oligomers by immunoprecipitation. Isolated mitochondria from wilde type HEK293 cells (WT), cells expressing TMEM70-FLAG, TMEM70-GFP, cells expressing both TMEM70-FLAG and TMEM70-GFP, as well as cells transfected with empty vector were solubilized with 0.5% Triton X-100 and for immunoprecipitation antibody to FLAG was used. Original mitochondria (M) solubilized proteins (S) and the immunoprecipitates (IP) were separated by SDS-PAGE and Western blot detection using antibodies to TMEM70 or GFP (Kratochvílová et al. 2014).

A key question for understanding the biological function of the TMEM70 protein, however, is to reveal physiological interactions with the ATP synthase components, assembly intermediates or other specific assembly factors. Neither immunoprecipitation nor electron microscopy studies with immunogold labeling uncovers a direct interaction of TMEM70 protein with ATP synthase or its intermediates. And although we tested the interactions with the subunit c by immunocapture of an antibody against ATP synthase, no signal of TMEM70 protein was observed.

However, as later shown, TMEM70 interacts with the subunit c and helps its, along with another assembly factor TMEM242, to organize the subunits c in the inner mitochondrial membrane by assembling into larger oligomeric structures (Bahri et al. 2021; Carroll et al. 2021). Our work has thus provided the first steps towards unraveling the function of this protein.

4.2. Results and discussion related to the specific aim B) To study the impact of prevalent splicing homozygous mutation c.317-2A>G in *TMEM70* gene on OXPHOS complexes and mitochondrial ultrastructure

I. Manuscript (prepared for submission) related to the specific aim B):

1) **Štufková, H.,** Hůlková, H., Stránecký, V., Smíšková, Z., Pavrovská, S., Wenchich, L., Hansíková, H., Honzík, T., Mráček, T., Houštěk, J., Zeman, J., Tesařová, M. The impact of prevalent homozygous splicing c.317-2A>G *TMEM70* mutation on OXPHOS complexes, mitochondrial reticulum, and ultrastructure in patient tissues, fibroblasts and myoblasts.
   Supplement 3)

   Author's contribution: biochemical analyses of steady-state level of OXPHOS complexes (1) and manuscript preparation (1).

Štufková, H., Hůlková, H., Stránecký, V., Smíšková, Z., Pavrovská, S., Wenchich, L., Hansíková, H., Honzík, T., Mráček, T., Houštěk, J., Zeman, J., Tesařová, M. **The impact of prevalent homozygous splicing c.317-2A>G *TMEM70* mutation on OXPHOS complexes, mitochondrial reticulum, and ultrastructure in patient tissues, fibroblasts, and myoblasts** (manuscript prepared for submission).

This study represents a detailed analysis of the impact of the prevalent homozygous splicing mutation c.317-2A>G in the *TMEM70* gene on the amount, stability, and activity of OXPHOS complexes and mitochondrial ultrastructure in predominantly affected tissues (brain, muscle, heart, and liver), in myoblasts, and fibroblasts.

TMEM70 was found to be involved in the assembly of the c8-ring in the inner mitochondrial membrane. In other studies (Carroll et al. 2021; Sánchez-Caballero et al. 2020), the authors suggested that TMEM70 is not only involved in the assembly of complex V but also has a role in the stabilization and assembly of complex I.

In a set of patient tissues (muscle, heart, liver, brain), steady-state level of individual OXPHOS complexes in mitochondria were determined by BN-PAGE/WB (Figure 9A-D). In all analyzed tissues, a significant deficiency of complex V was detected. Accumulation of the F_1 part was detected in only a few of them. The decreased levels of complex I were observed in all patient muscle samples. While, no specific pattern was observed in the levels of other OXPHOS complexes. SDS-PAGE/WB analysis revealed significantly reduced level of all ATP synthase subunits analysed, including subunit c.

In the case of fibroblasts, a compensatory effect was observed in all cases, but this phenomenon was not apparent in all available tissues. In cardiomyocytes, an increase in mitochondrial mass and increased OXPHOS activity was observed based on SDH, COX staining. Increased levels and activities of OXPHOS complexes, associated with compensatory effect, have been previously reported in several mitochondrial defects (Kovářová et al. 2012; Mayr et al. 2010). The adaptive response is probably enabled by post-transcriptional events (Havlickova Karbanova et al. 2012) in addition a compensatory effect was also observed in the TMEM70 KO mouse model (Kovalčíková et al. 2019; Vrbacký et al. 2016).

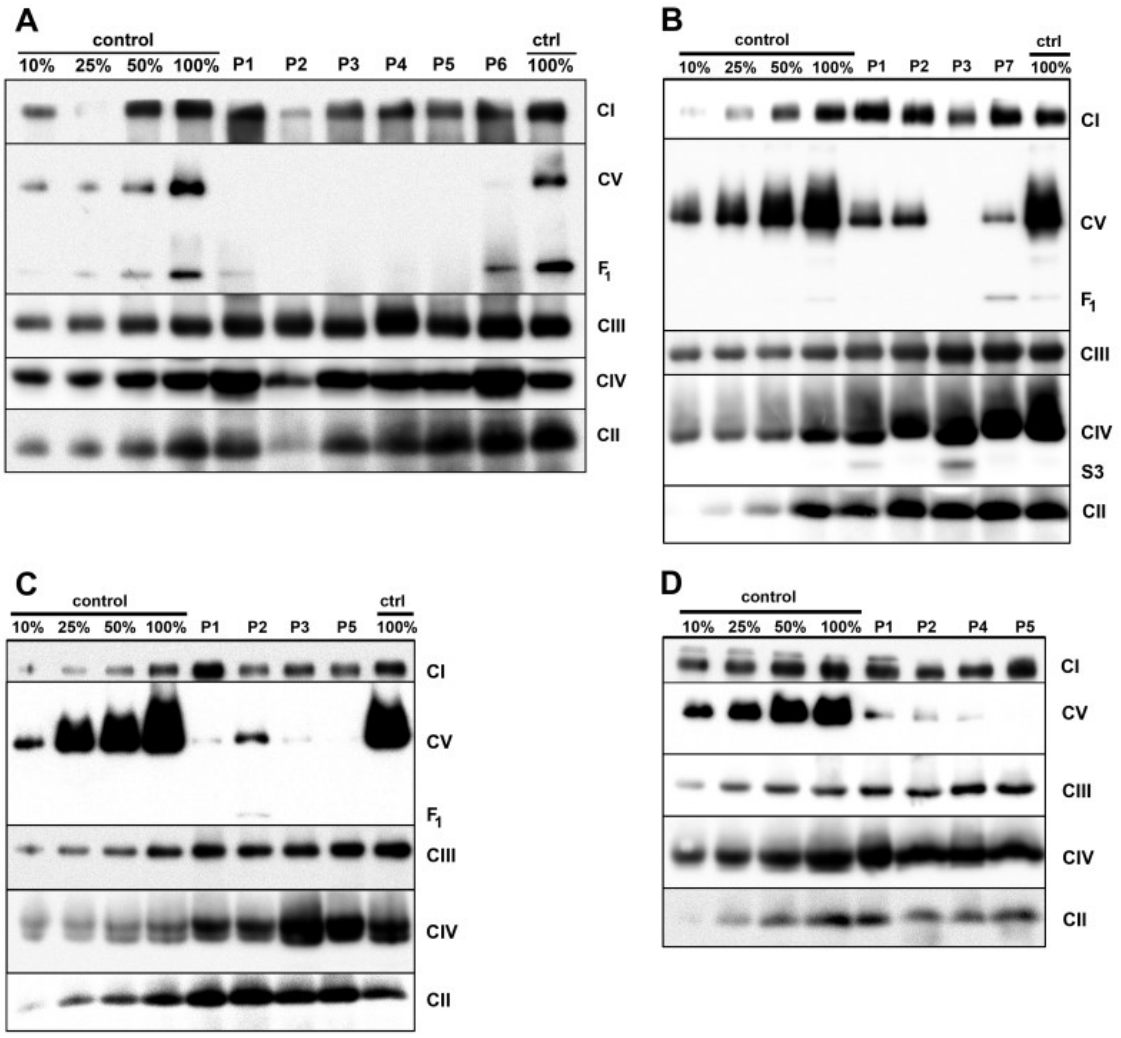

Figure 9: Steady-state levels of OXPHOS complexes in muscle, heart, liver and brain mitochondria: Mitochondrial fraction (2-20 µg) from the muscle (A), heart (B), liver (C) and brain (D) from patients carrying c.317-2A>G homozygous splicing *TMEM70* mutation were resolved using 6-15% BN-PAGE, electroblotted and probed with specific antibodies (CI: NDUFB6, CII: SDH70, CIII: CORE2, CIV: COX1, CV: F1-α).

The mitochondrial ultrastructure was analyzed in, among others, patient myoblasts (P12) (Figure 10). Elongated mitochondria were predominant in control myoblasts, whereas structural changes, including unusually aberrant and sparse cristae, were common in patient myoblasts. Moreover, mitochondria with concentric cristae were also found in the myoblasts of patient P12. Dimerization of complex V plays a pivotal role in cristae formation and thus in determining the morphology of the inner mitochondrial membrane (Davies et al. 2012). The role of ATP synthase dimers in mitochondria cristae formation was first described in yeast models, where a downregulation of ATP synthase (Lefebvre-Legendre et al. 2005) or altered formation of ATP synthase dimers due to deficiency of the subunits e or g (Paumard et al. 2002) led to the absence of cristae and

formation of concentric (“onion-like”) membrane structures. Both in tissues from TMEM70 patients and in cultured cells, strongly altered mitochondrial cristae and "onion-like" mitochondria were present. Our data confirmed previously published findings (Bahri et al. 2021; Braczynski et al. 2015; Cameron et al. 2011; Diodato et al. 2014; Holme et al. 1992; Sládková et al. 2015). Similar changes in mitochondrial ultrastructure have also been demonstrated in TMEM70 deficient models (Bahri et al. 2021; Vrbacký et al. 2016). However, deficiency of the mitophilin protein has also led to aberrant mitochondrial morphology and the formation of concentric cristae (“onion-like“ morphology) in HeLa cells (John et al. 2005), thus this morphological feature is not exclusive to TMEM70 defects.

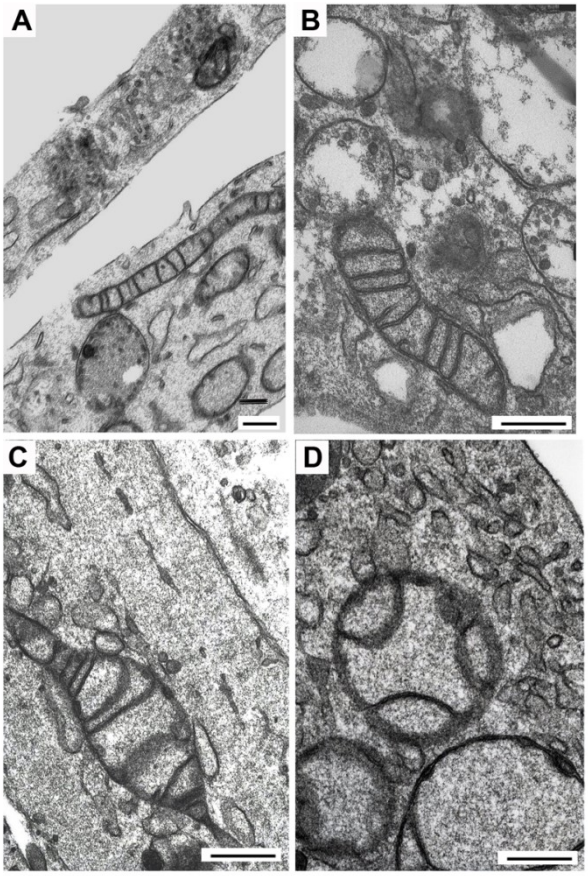

Figure 10: Mitochondrial ultrastructure in myoblast in TMEM70 deficient patients: The normal mitochondria with number of cristae were observed in the control cell (A, B). In patient P12 (C, D) enlarged sphere mitochondria with the concentric shape of cristae were observed. Scale bars represent 250 nm.

It was shown, that in the absence of TMEM70 protein, minimal ammounts of ATP synthase are assembled and therefore the existence of an additional assembly factor was assumed. The hypothesis of a second protein required for the c8-ring assembly was recently confirmed by the Walker's group (Carroll et al. 2021). Carroll and coauthors showed that assembly of the c8-ring requires not only TMEM70 but also a second protein TMEM242. TMEM242 is directly involved in the assembly of ATP synthase and both TMEM242 and TMEM70 interact specifically with subunit c (Carroll et al. 2021). TMEM70 and TMEM242 have similar overlapping functions, but in addition, TMEM242 may influence the incorporation of subunits a, A6L, DAPIT, and 6.8PL (Carroll et al. 2021). Finally, in our previous study, we obtained gene expression data in a set of 10 TMEM70 patient fibroblasts (Cízková et al. 2008a). In this group, we analysed the mRNA expression level of TMEM242. However, data does not show any specific trend in the expression levels of TMEM242 in the patients.

Furthermore, TMEM70 and TMEM242 interact with the subunit c as well as with the mitochondrial assembly intermediates of complex I (Carroll et al. 2021; Sánchez-Caballero et al. 2020). Nevertheless, this functional connection needs to be further studied as reduction of complex I is not a consistent feature (Havlickova Karbanova et al. 2012; Kovalčíková et al. 2019) including this study. Across various types of patient tissues, a decreased of complex I levels were rather individual and seem to be tissue specific. Moreover, no assembly intermediates were observed.

4.3. Results and discussion related to the specific aim C) To study the impact of various *MT-ATP6* variants on OXPHOS complexes and energy metabolism

I. Publication related to the specific aim C):

1) Honzík, T., Tesařová, M., Vinšová, K., Hansíková, H., Magner, M., **Kratochvílová, H.**, Zámečník, J., Zeman, J., and Ješina, P. (2013). Different laboratory and muscle biopsy findings in a family with an m.8851T>C mutation in the mitochondrial *MT-ATP6* gene. Mol Genet Metab 108, 102-105. IF = 2.827, Quartile Score = Q2 (2013).
   Supplement 4)

II. Manuscript (prepared for submission) related to the specific aim C):

2) **Štufková, H**., Kelifová, S., Kousal, B., Lokvencová, K., Hansiková, H., Zámečník, J., Vaněčková, M., Zeman, J., Lišková, P., Honzík, T., Tesařová, M. Clinical and laboratory findings in a rare maternally inherited variant m.8719G>A in *MT-ATP6* gene.
   Supplement 5)

   Author's contribution: biochemical analyses of the steady-state level of OXPHOS complexes (1, 2) and manuscript preparation (2).

Honzík, T., Tesařová, M., Vinšová, K., Hansíková, H., Magner, M., **Kratochvílová, H.**, Zámečník, J., Zeman, J., and Ješina, P. (2013). **Different laboratory and muscle biopsy findings in a family with an m.8851T>C mutation in the mitochondrial *MT-ATP6* gene**. Mol Genet Metab 108, 102-105. IF = 2.827, Quartile Score = Q2 (2013).

In this study, we reported a very rare maternally inherited missense m.8851T>C (p.Trp109Arg) mutation in the mitochondrial *MT-ATP6* gene. In 2013 a second family with this mtDNA variant was reported so far. Several additional patients have been reported (Ganetzky et al. 2019; Lott et al. 2013; Poole et al. 2021; Wong et al. 2020).

In our study, clinical symptoms such as a failure to thrive, microcephaly, psychomotor retardation and hypotonia were present in a 3-year-old girl (proband) with a high mtDNA mutational load (87–97%). LS findings on magnetic resonance imaging were documented. Her 36-year-old mother (68% blood heteroplasmy) developed peripheral neuropathy and muscle weakness at the age of 22 years.

We uncover pathological features in the proband´s muscle sample. Enzyme histochemical analysis revealed focal subsarcolemmal accumulation of SDH reaction products in up to 5% of muscle fibers. Typical COX-negative fibers were not observed. Electron microscopy revealed a focal increase in subsarcolemmal mitochondria without altered morphology. The energy-generating capacity of OXPHOS in the muscle sample, indicated diminished OXPHOS activity due to disrupted complex V. Analysis of RC enzyme activities in a muscle homogenate and isolated mitochondria showed normal or even increased activities of complexes I, II, III, I+III, II+III, and IV and CS compared to age-matched controls. Muscle mitochondrial proteins were separated by BN-PAGE. There was a significant decrease in steady-state levels of complex V and the accumulation of its subcomplexes (Figure 11A).

In skin fibroblasts, BN-PAGE followed by WB and immunodetection revealed a slight decrease (80% of controls) amount of complex V. However, no assembly subcomplexes were observed (Figure 11B), similar to that observed in the patient´s fibroblasts with the prevalent variant m.8993T>G (p.Leu156Arg) in the *MT-ATP6* gene, with a high level of heteroplasmy (97%). Unfortunately, the level of heteroplasmy in the proband´s fibroblasts was not analysed and therefore cannot be determined whether the absence of ATP synthase subcomplexes is due to a low levels of heteroplasmy or to the effect of the mutation in the fibroblasts.

Decreased complex V holoenzyme and the presence of assembly subcomplexes were common phenotypic features of the *MT-ATP6* variant in patient tissues or fibroblasts (Castagna et al. 2007; Dautant et al. 2018; Ganetzky et al. 2019; Hao et al. 2015; López-Gallardo et al. 2009; Pitceathly and Taanman 2018). However, studies have been reported where ATP synthase holoenzyme was not reduced, despite high heteroplasty load (García et al. 2000; Verny et al. 2011). The inconsistency of complex V assembly in individuals with the same genotype and similar levels of heteroplasmy points to biochemical variability caused by pathogenic variants in *MT-ATP6*. Our result suggests that the treshold effect varies according to the type of material analysed.

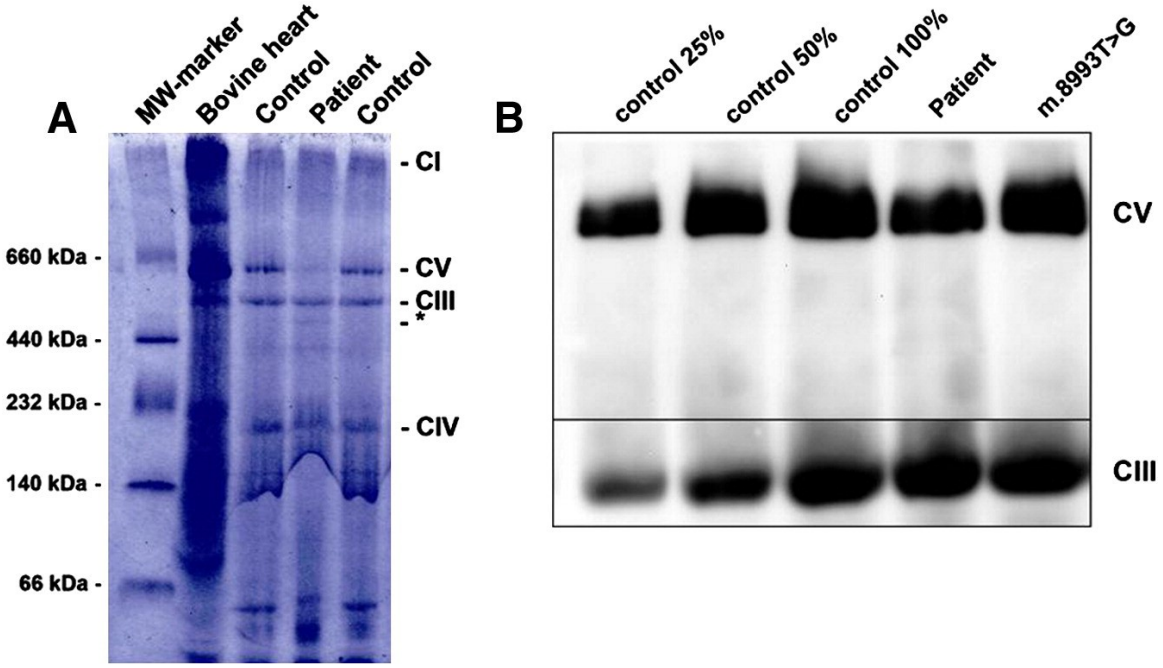

Figure 11: Steady-state level of OXPHOS complexes in muscle and fibroblasts. A) BN-PAGE in muscle mitochondria revealed a marked decrease of the steady-state level of complex V (CV) and the accumulation of its subcomplex (*). Levels of complex I (CI), complex III (CIII) and complex IV (CIV) showed identical pattern in patient and control samples. The migration of molecular mass standards is indicated on the left side B) BN-PAGE, WB and immunodetection with a monoclonal antibody showed a mild decrease level (80% of control) of complex V (CV) in fibroblasts. Free F_1-part and/or other subcomplexes were not detected. Complex III (CIII) was normal content in the patient and control. No change in the level of complex V and complex III was observed in the patient m. 8993T>G (p.Leu156Arg). The series of the dilution control sample is indicated, (CV-F_1- α, CIII-CORE2) (Honzik et al. 2013).

Our findings extend the clinical and laboratory phenotype associated with the m.8851T>C (p.Trp109Arg) mutation in the *MT-ATP6* gene. We classified this variant as

pathogenic in 2013. However, in 2018 this classification was changed to like pathogenetic (LP). Recently, this variant was indicated as “Cfrm” in MITOMAP database (Lott et al. 2013), indicating that at least two or more independent laboratories have published report on the pathogenicity of this particular variant. However, this variant has also been reported as “Variant of Uncertain Significance” (VUS), due to the high variability of clinical symptoms in patients with the same variant and a similar level of heteroplasmy (Ganetzky et al. 2019; Wong et al. 2020). Recently, one individual was described who lived to the 9th decade despite carrying 98% m.8851T>C levels, a mutant load. Although this variant has been previously associated with severe pediatric phenotypes (De Meirleir et al. 1995; Honzik et al. 2013). However, this may be due to overall unique aspect of each patient and the different levels of heteroplasmy.

Furthermore, studies with a yeast model have revealed that m.8851T>C (p.Trp109Arg) variant leads to major drops (95%) in mitochondrial ATP synthesis due to a block in Fo-mediated proton transfer (Kucharczyk et al. 2013).

Štufková, H., Kelifová, S., Kousal, B., Lokvencová, K., Hansíková, H., Zámečník, J., Vaněčková, M., Zeman, J., Lišková, P., Honzík, T., Tesařová, M. **Clinical and laboratory findings in a rare maternally inherited variant m.8719G>A in *MT-ATP6* gene** (manuscript prepared for submission).

In the second study related to the third specific aim, we study the effect of the m.8719G>A variant in *MT-ATP6* (p.Gly65*) on the OXPHOS complexes, in particular on the complex V assembly. This extremely rare variant was found in a 57-year-old patient with cataract, pigmentary retinopathy, hearing loss, and leukoencephalopathy.

Tested tissues (blood, buccal swab, skin fibroblasts, skeletal muscle) showed a variable heteroplasmy load from 9% in fibroblasts to 70% in muscle. Normal or elevated activities of respiratory chain complexes were observed in muscle mitochondria. Analysis of the mitochondrial energy-generating system indicated a complex V deficiency.

Separation of muscle mitochondria by BN-PAGE followed by WB and immunodetection revealed reduced amounts of complex V (approx. 20% of controls) with accumulated subcomplexes, V* (F_1-part with c8-ring) and free F_1-part (Figure 12A). In addition, steady-state levels of complex IV holoenzyme were also diminished in patient mitochondria (approx. 70% of control, Figure 12A).

Compositional analysis of assembly/stability subcomplexes is performed by 2D electrophoresis (Figure 12B). The approximately 390 kDa subcomplex containing the subunit β presumably the F_1-part of ATP synthase, a larger 460 kDa subcomplex containing the subunit β and the subunit c were found in muscle mitochondria. Additionally, another complex containing only the subunit c was observed with a molecular mass of approximately 120 kDa, which likely represents the c8-ring itself. In addition, the presence of lower oligomers of the subunit c was detected. However, none of the above complexes showed detectable presence of subunit a or subunit d. A similar profile was found in a patient carrying 2 bp microdeletion m.9205_9206delTA in mtDNA (Jesina et al. 2004a).

The maternally inherited missense variant m.8719G>A (p.Gly65*) has so far been reported only once in a patient (without clinical and laboratory findings) from a cohort of more than 10,000 patients with suspected mitochondrial disease (Tang et al. 2013). Our findings thus provide for the first time the clinical and biochemical phenotypes associated with this ultra rare pathogenic mtDNA variant.

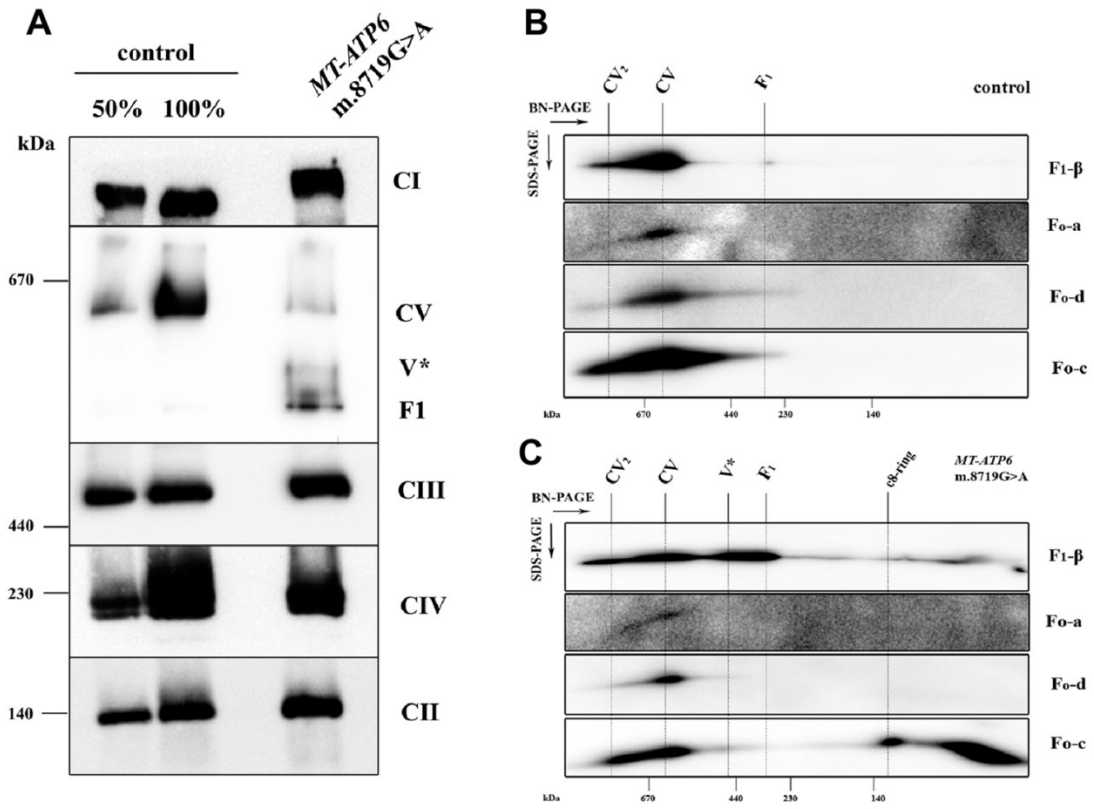

Figure 12: A) Steady-state levels of OXPHOS complexes in muscle mitochondria in *MT-ATP6* m.8719G>A patient and control. The mitochondrial fractions (5-10 μg) were resolved using 6-15% BN-PAGE, electroblotted, and probed with specific antibodies (CI-NDUFA9, CII-SDH70, CIII-CORE2, CIV-COX1, CV-F_1-β). Two aliquots of control mitochondria corresponding to the indicated dilutions of control samples were loaded on the same gels. B) and C) 2D electrophoretic analysis and immunodetection of selected ATP synthase subunits in control (B) and patient (C) (*MT-ATP6* m.8719G>A) muscle mitochondria. Mitochondrial muscle fractions (10 μg) were separated in the first dimension by BN-PAGE and in the second dimension by SDS-PAGE. Final gels were electroblotted and probed with specific antibodies against the ATP synthase β (F_1-β), subunit a (F_o-a), subunit d (F_o-d) and subunit c (F_o-c).

4.4. Results and discussion related to the specific aim D) To study the molecular and biochemical aspects of selected mitochondrial diseases with complex V deficiency

I. Publication related to the specific aim D):

1) Tesařová, M., Vondráčková, A., **Štufková, H**., Vepřeková, L., Stránecký, V., Beránková, K., Hansíková, H., Magner, M., Galoová, N., Honzík, T., Vodičková, E., Starý, J., Zeman, J. (2019). Sideroblastic anemia associated with multisystem mitochondrial disorders. Pediatr Blood Cancer 66. IF = 2.355, Quartile Score = Q2 (2019).
   Supplement 6)

2) **Štufková, H.**, Kolářová, H., Lokvencová, K., Honzík, T., Zeman, J., Hansíková, H., and Tesařová, M. (2022). A Novel *MTTK* Gene Variant m.8315A>C as a Cause of MERRF Syndrome. Genes (Basel) 13. IF = 4.141, Quartile Score = Q2 (2021).
   Supplement 7)

Author's contribution: biochemical analyses of steady-state level of OXPHOS complexes (1, 2) and manuscript preparation (2).

Tesařová, M., Vondráčková, A., **Štufková, H**., Vepřeková, L., Stránecký, V., Beránková, K., Hansíková, H., Magner, M., Gáloová, N., Honzík, T., Vodičková, E., Starý, J., Zeman, J. (2019). **Sideroblastic anemia associated with multisystem mitochondrial disorders**. Pediatr Blood Cancer 66, e27591. IF = 2.355, Quartile Score = Q2 (2019).

Sideroblastic anemia (SA) is a heterogeneous group of inherited or acquired diseases with disrupted iron utilization in erythroblast, ineffective erythropoiesis, and variable systemic iron overload (Bottomley and Fleming 2014). Inherited SA can be caused by mutations in various genes associated with heme biosynthesis, [Fe-S] biosynthesis/transport with the thiamine-transport cluster, structural subunits of the OXPHOS complexes or mutations in mtDNA (Bergmann et al. 2010; Bykhovskaya et al. 2004; Diaz et al. 1999; Lichtenstein et al. 2016; Riley et al. 2010; Riley et al. 2016; Schmitz-Abe et al. 2015; Wiseman et al. 2013).

In a cohort of 421 patients with multisystem mitochondrial diseases, SA was found in 8 individuals. Two patients developed SA with ring sideroblasts at the ages of three and six years, respectively. Both had mitochondrial myopathy, lactic acidosis, and SA due to homozygous 6-kb deletion of all of exon 4, a partial deletion of exon 5, and a 9-bp insertion derived from intron 3 (c.896+2551_1061delinsATTTTACCA) resulting in a putative truncation of the PUS1 protein (p.Gly148ValfsX41). Large deletions represent a novel cause of presumed PUS1 loss-of-function phenotype.

The PUS1 protein is essential for proper postransriptional modification of tRNA mitochndrial proteosynthesis (Chen and Patton 1999). PUS1 converts uridine into pseudouridine. Pseudouridine may have a functional role in tRNAs and may assist in the peptidyl transfer reaction of rRNAs. Mutations in the *PUS1* gene have been associated with mitochondrial myopathy and SA (Bykhovskaya et al. 2004; Fernandez-Vizarra et al. 2009).

In our study, SA was also found in a child with heterozygous composed mutations c.610A>G (p.Asn204Asp) and c.674C>T (p.Pro225Leu) in the *COX10* gene that encodes the COX10 protein, an assembly factor for complex IV. The insertion of heme A is a two-step process performed by COX10 (Valnot et al. 2000). Mutations in the assembly factors *COX10* have been reported to cause variable severe phenotypes including lactic acidosis, Leigh syndrome, hypertrophic cardiomyopathy and hypotonia (Antonicka et al. 2003).

In our study the activity of respiratory chain complexes III and IV in the muscles of *PUS1* patients was significantly reduced. In addition, the activity of I + III was also reduced in one of them. The patient with mutation in the *COX10* gene showed low activities of complexes I + III and IV in muscles. Reduced activities of complexes I + III and IV were also found in all three analyzed patients with mtDNA deletion. All patients, except one with mtDNA deletion, had very low COX/CS ratios.

Protein analyses of the OXPHOS complexes revealed reduced levels of complex IV in muscle and liver mitochondria in the patient with *COX10* variant (P8) (Figure 13 A, B). Steady-state levels of complexes I, IV and V were markedly reduced in liver mitochondria of *PUS1* patients (P1, P2). The combined deficiency of OXPHOS complexes was more profound in the muscle mitochondria of these two patients, where reduced levels of complexes I, III, IV, and V were observed (Figure 13 A, B). In addition, we also found an increased number of intermediates of complex V assembly in both muscle and liver tissue of *PUS1* patients (P1, P2).

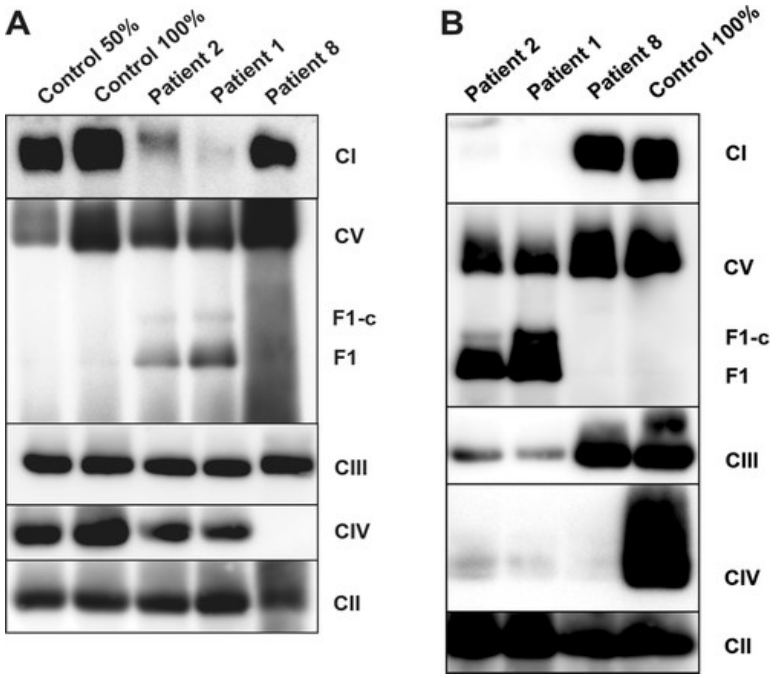

Figure 13: Steady-state levels of OXPHOS complexes in liver (A) and muscle (B) mitochondria of patients 1, 2 (*PUS1*) and patient 8 (COX10) separated by BN-PAGE followed by immunoblotting. In both tissues patients 1 and 2, a profound, combined OXPHOS complex deficiency (complexes I, III, IV, and V) was found with an accumulation of assembly intermediates of complex V (F_1-part of the complex and F_1-c, which is F_1-part associated with the c-subunits). Patient 8 mitochondria revealed an isolated deficiency of complex IV in liver and muscle as well (Tesarova et al. 2019).

Our results confirm that defects in complex V are primarily caused by defects in structural subunits or ATP synthase assembly factors, but also in genes providing other mitochondrial functions. In this case, we observe a combined defect in multiple OXPHOS complexes in muscle and liver tissue in *PUS1* patients. While the defect in complex IV assembly factor primarily disrupts complex IV biogenesis. Moreover, the presence of ATP synthase assembly intermediates is also evident in liver and muscle. The combined defect was also observed in other *PUS1* patients (Fernandez-Vizarra et al. 2009).

Štufková, H., Kolářová, H., Lokvencová, K., Honzík, T., Zeman, J., Hansíková, H., and Tesařová, M. (2022). **A Novel *MTTK* Gene Variant m.8315A>C as a Cause of MERRF Syndrome**. Genes (Basel) 13 (7) IF = 4.141, Quartile Score = Q2 (2021).

ATP synthase disorders can be caused by primary defects in structural subunits or assembly factors, but also by secondary defects in genes important for other mitochondrial functions. These include genes for mt-tRNA encoded by mtDNA. Which are essential for mitochondrial proteosynthesis of all subunits of mitochondrially encoded OXPHOS complexes. Damage to mt-tRNAs commonlly leads to combined defects in the OXPHOS complexes (Richter et al. 2021).

In this study, we report a novel pathogenic variant in mtDNA in mt-tRNA gene for lysin. Since first description in 1990, the number of pathogenic variants in mt-tRNA genes has steadily increased (Lott et al. 2013; Richter et al. 2021). Mt-tRNA-Lys is encoded by the *MTTK* gene, which is the second most common site of pathogenic variants in mtDNA. To date, 28 pathogenic variants have been described (Lott et al. 2013).

Our proband, a 39-year-old woman with myoclonus, epilepsy, muscle weakness, and hearing impairment carried the heteroplasmic m.8315A>C variant in the *MTTK* gene with a mutation load ranging from 71% to >96% in the tested tissues.

In the muscle sample, analysis of the capacity of the mitochondrial energy-generating system showed impaired OXPHOS activity with reduced ADP stimulation. The activities of respiratory chain enzymes in isolated muscle mitochondria showed significantly reduced activities of complexes I + III and complex IV as well as the COX/CS ratio. Interestingly, the activities of RC complexes II and complexes II + III were slightly increased, suggesting a compensatory effect.

Analysis of steady-state muscle mitochondrial protein levels using BN-PAGE followed by WB and immunodetection revealed mildly reduced amounts of complex I and complex V with accumulated sub-complexes, most likely V* (ATP synthase with several subunits c) and F_1 domain. In addition, the steady-state level of complex IV holoenzyme was significantly reduced (Figure 14A). A similar effect of mutations in the *MTTK* gene on OXPHOS complexes in muscle mitochondria was observed in our previous study (Fornuskova et al. 2008) (Figure 14B). Two patients with pathogenic *MTTK* variants (m.8363G>A and m.8344A>G) showed the same pattern of combined OXPHOS

complexes deficiency (diminished CIV level, with a profound decrease in CI and CV, and accumulated CV sub-complexes). Interestingly, even though the individual variants are localized in different parts of the mt-tRNA the effect on OXPHOS remains the similar (Fornuskova et al. 2008). The pattern is distinct from m.3243A>G in *MT-TL1* gen for mt-tRNA-Leu in muscle mitochondria (Fornuskova et al. 2008)

The variant m.8315A>C, is localized in the linker between the D-loop arm and the anticodon stem, which has not been previously predicted as a mutation hotspot. Based on *MTTK* sequence alignment, there is only a single purine nucleotide, either adenine or guanine, found in this position among 40 species (Pütz et al. 2007). Thus, the substitution of adenine for cytosine at position m.8315 may disrupt interactions that stabilize the secondary structure of mt-tRNA-Lys.

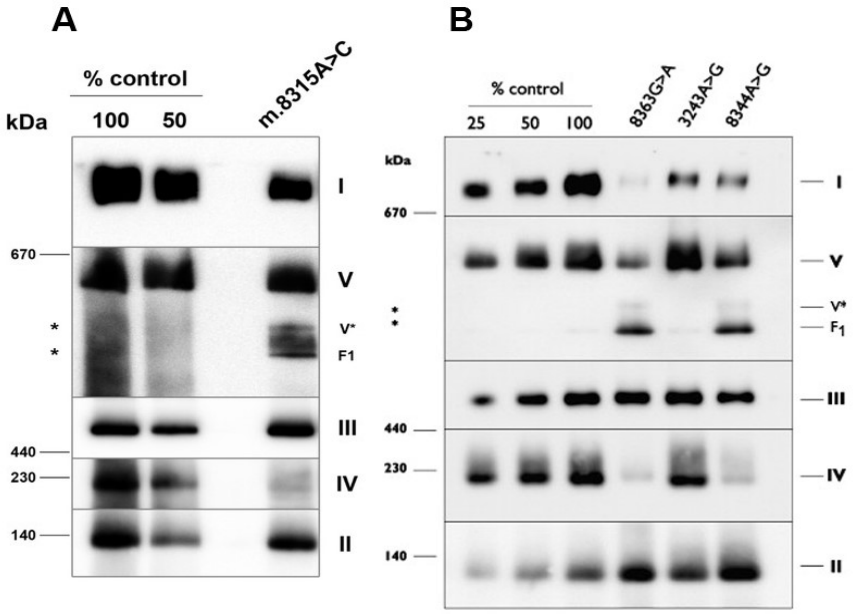

Figure 14: Analysis of the assembly of OXPHOS complexes by immunoblotting of BN-PAGE in muscle mitochondria patient with (m.8315A>C (A), m.8363G>A m.8344A>G variant in *MTTK* and 3243A>G in MT-TL1 gene (B)). BN-PAGE of lauryl maltoside-solubilized mitochondria was electroblotted onto PVDF membranes and probed with monoclonal antibodies that detect the native forms of the OXPHOS complexes. Two/three aliquots of control mitochondria corresponding to the indicated dilutions of control samples were loaded on the same gels. I—complex I; II—complex II; III—complex III; IV—complex IV; V—complex V; V*—complex V subcomplex composed of F_1-ATP synthase with several c-subunits; F_1—F_1-ATP synthase; *-expected migration of complex V subcomplexes. The migration of holoenzymes (I–V) and molecular mass standards (kDa) are indicated; the actual position of sub-complex V∗ and/or F_1 of complex V (∗) in muscle mitochondria is directly below complex III (around 370–470 kDa) (Fornuskova et al. 2008; Štufková et al. 2022).

5. CONCLUSIONS

The overall aim of the presented thesis was to study the biochemical and molecular genetic aspects of primary and secondary ATP synthase deficiency and its impact on mitochondrial energy metabolism. Furthermore, the study of the structural characteristics of the TMEM70 protein, whose defects are the most common cause of primary nuclear mitochondrial ATP synthase disorders.

The core of the thesis is based on the five published articles by the author and coauthors, extended by two manuscripts prepared for submission. Four specific aims of the thesis have been proposed and each has been addressed in its corresponding section (see chapters 4.1.- 4.4.).

The first specific aim focused on the characterizationof the protein TMEM70, an assembly factor of human mitochondrial ATP synthase. It was found that the 21 kDa TMEM70 protein localized in the inner mitochondrial membrane forms a higher oligomeric structure. TMEM70 has a hairpin structure with the N- and C-termini oriented into the mitochondrial matrix. Our results contributed to the later discovery of the function of TMEM70 protein in the assembly of ATP synthase.

Secondly, we were able to characterize the impact of the prevalent splicing homozygous mutation c.317-2A>G in the *TMEM70* gene on OXPHOS complexes and mitochondrial ultrastructure in board spectrum of tissues and cells. Our results demonstrate that prevalent *TMEM70* mutation leads to a certain degree of adaptive/compensatory effect, which is especially evident in fibroblasts, and affects mitochondrial reticulum and ultrastructure. The absence of TMEM70 protein always leads to an isolated deficiency of complex V, but only to the inconsistent formation of a combined defect in OXPHOS complexes.

The third specific aim was to study the effect of various *MT-ATP6* variants on OXPHOS complexes and energy metabolism. Our results extend the clinical, biochemical, and laboratory phenotype associated with two rare variants m.8851T>C (p.Trp109Arg) and m.8719G>A (p.Gly65*) in the *MT-ATP6* gene. Our findings may contribute to further diagnosis of maternally inherited ATP synthase disorders.

In the last section, we focus on the molecular and biochemical aspects of selected mitochondrial diseases with combinated OXPHOS defects including complex V deficiency. We observed combined defects of OXPHOS complexes in tissues of patients with *PUS1* and *MTTK* . The novel results extend the knowledge of secondary ATP synthase defects in combination with defects in other OXPHOS complexes.

In conclusion, the proposed aims of the Ph.D. Thesis were accomplished.

6. SUMMARY

- TMEM70 is a 21 kDa mitochondrial protein localised in the inner mitochondrial membrane, has hairpin structure with the N- and C-termini oriented into the mitochondrial matrix, and forms higher oligomer structures.

- The prevalent mutation of the *TMEM70* gene leads to a some stage of adaptive/compensatory effect, which is especially evident in fibroblasts; the absence of TMEM70 protein always leads to an isolated deficiency of complex V, but only to an inconsistent combined defects of OXPHOS complexes.

- The findings extend the clinical and biochemical description of the phenotype associated with two rare maternally inherited variants in *MT-ATP6* gene: m.8851T>C (p.Trp109Arg) and m.8719G>A (p.Gly65*).

- Pathogenic mutations in *PUS1* and *MTTK* genes lead to a specific pattern of combined OXPHOS complexes deficit in tissues´mitochondria.

7. SHRNUTÍ

- TMEM70 je mitochondriální protein o velikosti 21 kDa lokalizovaný ve vnitřní mitochondriální membráně, se strukturou vlásenky a oběma konci orientovaný do mitochondriáklní matrix, tvořící vyšší oligomerní struktury.

- Prevalentní mutace v genu *TMEM70* vede k určitému stupni adaptačního/kompenzačního efektu, který je patrný zejména u fibroblastů; absence proteinu TMEM70 vždy vede k izolovanému deficitu komplexu V, ale pouze v některých případech ke vzniku kombinovaného deficitu komplexů systému OXPHOS.

- Výsledky rozšiřují klinický a biochemický popis fenotypu spojeného se dvěma vzácnými maternálně dědičnými variantami mtDNA v genu *MT-ATP6*: m.8851T>C (p.Trp109Arg) a m.8719G>A (p.Gly65*).

- Patogenní mutace v genech *PUS1* a *MTTK* mají za následek vznik specifického kombinovaného deficitu komplexů systému OXPHOS v pacientských tkáních.

8. LIST OF ORIGINAL ARTICLES

Publications *in extenso*, that constitutes the basis of the PhD thesis:

Hejzlarová, K., Tesařová, M., Vrbacká-Čížková, A., Vrbacký, M., Hartmannová, H., Kaplanová, V., Nosková, L., **Kratochvílová, H**., Buzková, J., Havlíčková, V., Zeman, J., Kmoch, S., Houštěk, J. (2011). **Expression and processing of the TMEM70 protein**. Biochimica et biophysica acta 1807, 144-149. IF = 4.843, Quartile Score = Q1 (2011).

Honzík, T., Tesařová, M., Vinšová, K., Hansíková, H., Magner, M., **Kratochvílová, H.**, Zámečník, J., Zeman, J., and Ješina, P. (2013). **Different laboratory and muscle biopsy findings in a family with an m.8851T>C mutation in the mitochondrial *MT-ATP6* gene**. Mol Genet Metab 108, 102-105. IF = 2.827, Quartile Score = Q2 (2013).

Kratochvílová, H. *, Hejzlarová, K. *, Vrbacký, M., Mráček, T., Karbanová, V., Tesařová, M., Gombitová, A., Cmarko, D., Wittig, I., Zeman, J., Houštěk, J. (2014). **Mitochondrial membrane assembly of TMEM70 protein**. Mitochondrion 15, 1-9. * Equal contribution, IF = 3.249, Quartile Score = Q2 (2014).

Tesařová, M., Vondráčková, A., **Štufková, H**., Vepřeková, L., Stránecký, V., Beránková, K., Hansíková, H., Magner, M., Galoová, N., Honzík, T., Vodičková, E., Starý, J., Zeman, J. (2019). **Sideroblastic anemia associated with multisystem mitochondrial disorders**. Pediatr Blood Cancer 66. IF = 2.355, Quartile Score = Q2 (2019).

Štufková, H., Kolářová, H., Lokvencová, K., Honzík, T., Zeman, J., Hansíková, H., and Tesařová, M. (2022). **A Novel *MTTK* Gene Variant m.8315A>C as a Cause of MERRF Syndrome**. Genes (Basel) 13 (7). 1245. IF = 4.141, Quartile Score = Q2 (2021).

Other publications *in extenso*:

Vondráčková, A., Veselá, K., **Kratochvílová, H**., Kučerová Vidrová, V., Vinšová, K., Stránecký, V., Honzík, T., Hansíková, H., Zeman, J., and Tesařová, M. (2014). **Large copy number variations in combination with point mutations in the TYMP and SCO2 genes found in two patients with mitochondrial disorders**. Eur J Hum Genet 22, 431-434. IF = 4.349, Quartile Score = Q1 (2014).

Kratochvílová, H., Rodinová, M., Sládková, J., Klempíř, J., Lišková, I., Motlík, J., Zeman, J., Hansíková, H., Tesařová, M. (2015). **Acyl-CoA Binding Domain Containing 3 (ACBD3) Protein in Huntington's Disease Human Skin Fibroblasts.** Cesk Slov Neurol N 78/111, (Suppl 2) 2S34-2S38. IF = 0.209, Quartile Score = Q4 (2015).

Ng, Y.S., Alston, C.L., Diodato, D., Morris, A.A., Ulrick, N., Kmoch, S., Houštěk, J., Martinelli, D., Haghighi, A., Atiq, M., Gamero, M. A., Garcia-Martinez, E., **Kratochvílová, H**. ,Santra, S., Brown, R. M., Brown, G. K., Ragge, N., Monavari, A., Pysden, K., Ravn, K., Casey, J. P., Khan, A., Chakrapani, A., Vassallo, G., Simons, C., McKeever, K., O'Sullivan, S., Childs, A. M., Østergaard, E., Vanderver, A., Goldstein, A., Vogt, J., Taylor, R. W., McFarland, R (2016). **The clinical, biochemical and genetic features associated with RMND1-related mitochondrial disease**. J Med Genet 53, 768-775. IF = 5.451, Quartile Score = Q1 (2016).

Křížová, J., **Štufková, H.**, Rodinová, M., Macáková, M., Bohuslavová, B., Vidínská, D., Klíma, J., Ellederová, Z., Pavlok, A., Howland, D.S., Zeman, J., Motlik, J., Hansíková, H. (2017). **Mitochondrial Metabolism in a Large-Animal Model of Huntington Disease: The Hunt for Biomarkers in the Spermatozoa of Presymptomatic Minipigs**. Neurodegener Dis 17, 213-226. IF = 2.785, Quartile Score = Q2 (2017).

Askeland, G., Rodinová, M., **Štufková, H.**, Dosoudilová, Z., Baxa, M., Smatlíková, P., Bohuslavová, B., Klempíř, J., Nguyen, T.D., Kuśnierczyk, A., Bjørås, M., Klungland, A., Hansíková, H., Ellederová, Z., Eide, L. (2018). **A transgenic minipig model of Huntington's disease shows early signs of behavioral and molecular pathologies**. Dis Model Mech 11. IF = 4.028, Quartile Score = Q1 (2018).

Rodinová, M., Křížová, J., **Štufková, H**., Bohuslavová, B., Askeland, G., Dosoudilová, Z., Juhas, S., Juhasová, J., Ellederová, Z., Zeman, J., Eide, L., Motlík, J., Hansíková, H. (2019). **Deterioration of mitochondrial bioenergetics and ultrastructure impairment in skeletal muscle of a transgenic minipig model in the early stages of Huntington's disease**. Dis Model Mech 12. IF = 4.651, Quartile Score = Q1 (2019).

Daňhelovská, T., Zdražilová, L., **Štufková, H**., Vanišová, M., Volfová, N., Křížová, J., Kuda, O., Sládková, J., and Tesařová, M. (2021). **Knock-Out of ACBD3 Leads to Dispersed Golgi Structure, but Unaffected Mitochondrial Functions in HEK293 and HeLa Cells.** Int J Mol Sci 22. IF = 6.208, Quartile Score = Q1 (2021).

Vanišová, M., **Štufková, H.**, Kohoutová, M., Rakosníková, T., Křížová, J., Klempíř, J., Ryšánková, I., Roth, J., Zeman, J., Hansíková, H. (2022). **Mitochondrial organization and structure are compromised in fibroblasts from patients with Huntington's disease**. Ultrastruct Pathol. 1-14. IF= 1.385, Quartile Score = Q4 (2021).

9. REFERENCES

Abrahams JP, Leslie AG, Lutter R, Walker JE (1994) Structure at 2.8 A resolution of F1-ATPase from bovine heart mitochondria. Nature 370: 621-628

Ackerman SH, Tzagoloff A (2005) Function, structure, and biogenesis of mitochondrial ATP synthase. Prog Nucleic Acid Res Mol Biol 80: 95-133

Acín-Pérez R, Fernández-Silva P, Peleato ML, Pérez-Martos A, Enriquez JA (2008) Respiratory active mitochondrial supercomplexes. Mol Cell 32: 529-539

Adachi K, Oiwa K, Nishizaka T, Furuike S, Noji H, Itoh H, Yoshida M, Kinosita K (2007) Coupling of rotation and catalysis in F(1)-ATPase revealed by single-molecule imaging and manipulation. Cell 130: 309-321

Al-Hassnan ZN, Almesned A, Tulbah S, Alakhfash A, Alhadeq F, Alruwaili N, Alkorashy M, Alhashem A, Alrashdan A, Faqeih E, Alkhalifi SM, Al Humaidi Z, Sogaty S, Azhari N, Bakhaider AM, Al Asmari A, Awaji A, Albash B, Alhabdan M, Alghamdi MA, Alshuaibi W, Al-Hassnan RZ, Alshenqiti A, Alqahtani A, Shinwari Z, Rbabeh M, Takroni S, Alomrani A, Albert Brotons DC, AlQwaee AM, Almanea W, Alfadley FA, Alfayyadh M, Alwadai A (2020) Categorized Genetic Analysis in Childhood-Onset Cardiomyopathy. Circ Genom Precis Med 13: 504-514

Aldossary AM, Tawfik EA, Alomary MN, Alsudir SA, Alfahad AJ, Alshehri AA, Almughem FA, Mohammed RY, Alzaydi MM (2022) Recent advances in mitochondrial diseases: From molecular insights to therapeutic perspectives. Saudi Pharm J 30: 1065-1078

AlFaris HS, Rahbeeni ZA, Peake RWA, Almontashiri NAM (2021) A Child with Progressive Hypertrophic Cardiomyopathy and Lactic Acidosis. Clin Chem 67: 912-914

Ali AT, Boehme L, Carbajosa G, Seitan VC, Small KS, Hodgkinson A (2019) Nuclear genetic regulation of the human mitochondrial transcriptome. Elife 8

Amunts A, Brown A, Toots J, Scheres SHW, Ramakrishnan V (2015) Ribosome. The structure of the human mitochondrial ribosome. Science 348: 95-98

Anderson S, Bankier AT, Barrell BG, de Bruijn MH, Coulson AR, Drouin J, Eperon IC, Nierlich DP, Roe BA, Sanger F, Schreier PH, Smith AJ, Staden R, Young IG (1981) Sequence and organization of the human mitochondrial genome. Nature 290: 457-465

Antonicka H, Leary SC, Guercin GH, Agar JN, Horvath R, Kennaway NG, Harding CO, Jaksch M, Shoubridge EA (2003) Mutations in COX10 result in a defect in mitochondrial heme A biosynthesis and account for multiple, early-onset clinical phenotypes associated with isolated COX deficiency. Hum Mol Genet 12: 2693-2702

Antonicka H, Shoubridge EA (2015) Mitochondrial RNA Granules Are Centers for Posttranscriptional RNA Processing and Ribosome Biogenesis. Cell Rep 10: 920-932

Arnold I, Pfeiffer K, Neupert W, Stuart RA, Schägger H (1998) Yeast mitochondrial F1F0-ATP synthase exists as a dimer: identification of three dimer-specific subunits. EMBO J 17: 7170-7178

Atay Z, Bereket A, Turan S, Haliloglu B, Memisoglu A, Khayat M, Shalev SA, Spiegel R (2013) A novel homozygous TMEM70 mutation results in congenital cataract and neonatal mitochondrial encephalo-cardiomyopathy. Gene 515: 197-199

Baban A, Adorisio R, Corica B, Rizzo C, Calì F, Semeraro M, Taurisano R, Magliozzi M, Carrozzo R, Parisi F, Dallapiccola B, Vaz FM, Drago F, Dionisi-Vici C (2020) Delayed appearance of 3-methylglutaconic aciduria in neonates with early onset metabolic cardiomyopathies: A potential pitfall for the diagnosis. Am J Med Genet A 182: 64-70

Bahri H, Buratto J, Rojo M, Dompierre JP, Salin B, Blancard C, Cuvellier S, Rose M, Ben Ammar Elgaaied A, Tetaud E, di Rago JP, Devin A, Duvezin-Caubet S (2021) TMEM70 forms oligomeric scaffolds within mitochondrial cristae promoting in situ assembly of mammalian ATP synthase proton channel. Biochim Biophys Acta Mol Cell Res 1868: 118942

Balsa E, Marco R, Perales-Clemente E, Szklarczyk R, Calvo E, Landázuri MO, Enríquez JA (2012) NDUFA4 is a subunit of complex IV of the mammalian electron transport chain. Cell Metab 16: 378-386

Baracca A, Sgarbi G, Mattiazzi M, Casalena G, Pagnotta E, Valentino ML, Moggio M, Lenaz G, Carelli V, Solaini G (2007) Biochemical phenotypes associated with the mitochondrial ATP6 gene mutations at nt8993. Biochimica et biophysica acta 1767: 913-919

Barca E, Ganetzky RD, Potluri P, Juanola-Falgarona M, Gai X, Li D, Jalas C, Hirsch Y, Emmanuele V, Tadesse S, Ziosi M, Akman HO, Chung WK, Tanji K, McCormick EM, Place E, Consugar M, Pierce EA, Hakonarson H, Wallace DC, Hirano M, Falk MJ (2018) USMG5 Ashkenazi Jewish founder mutation impairs mitochondrial complex V dimerization and ATP synthesis. Hum Mol Genet 27: 3305-3312

Benard G, Faustin B, Passerieux E, Galinier A, Rocher C, Bellance N, Delage JP, Casteilla L, Letellier T, Rossignol R (2006) Physiological diversity of mitochondrial oxidative phosphorylation. Am J Physiol Cell Physiol 291: C1172-1182

Bergmann AK, Campagna DR, McLoughlin EM, Agarwal S, Fleming MD, Bottomley SS, Neufeld EJ (2010) Systematic molecular genetic analysis of congenital sideroblastic anemia: evidence for genetic heterogeneity and identification of novel mutations. Pediatr Blood Cancer 54: 273-278

Bernardi P, Di Lisa F (2015) The mitochondrial permeability transition pore: molecular nature and role as a target in cardioprotection. J Mol Cell Cardiol 78: 100-106

Bernardi P, Di Lisa F, Fogolari F, Lippe G (2015) From ATP to PTP and Back: A Dual Function for the Mitochondrial ATP Synthase. Circ Res 116: 1850-1862

Berry EA, De Bari H, Huang LS (2013) Unanswered questions about the structure of cytochrome bc1 complexes. Biochim Biophys Acta 1827: 1258-1277

Bisetto E, Picotti P, Giorgio V, Alverdi V, Mavelli I, Lippe G (2008) Functional and stoichiometric analysis of subunit e in bovine heart mitochondrial F(0)F(1)ATP synthase. J Bioenerg Biomembr 40: 257-267

Blanco-Grau A, Bonaventura-Ibars I, Coll-Cantí J, Melià MJ, Martinez R, Martínez-Gallo M, Andreu AL, Pinós T, García-Arumí E (2013) Identification and biochemical characterization of the novel mutation m.8839G>C in the mitochondrial ATP6 gene associated with NARP syndrome. Genes Brain Behav 12: 812-820

Bogenhagen D, Clayton DA (1977) Mouse L cell mitochondrial DNA molecules are selected randomly for replication throughout the cell cycle. Cell 11: 719-727

Bogenhagen DF, Martin DW, Koller A (2014) Initial steps in RNA processing and ribosome assembly occur at mitochondrial DNA nucleoids. Cell Metab 19: 618-629

Bohnsack MT, Sloan KE (2018) The mitochondrial epitranscriptome: the roles of RNA modifications in mitochondrial translation and human disease. Cell Mol Life Sci 75: 241-260

Bonekamp NA, Larsson NG (2018) SnapShot: Mitochondrial Nucleoid. Cell 172: 388-388.e381

Bottomley SS, Fleming MD (2014) Sideroblastic anemia: diagnosis and management. Hematol Oncol Clin North Am 28: 653-670, v

Boyer PD (1975) A model for conformational coupling of membrane potential and proton translocation to ATP synthesis and to active transport. FEBS Lett 58: 1-6

Boyer PD (1997) The ATP synthase--a splendid molecular machine. Annu Rev Biochem 66: 717-749

Braczynski AK, Vlaho S, Müller K, Wittig I, Blank AE, Tews DS, Drott U, Kleinle S, Abicht A, Horvath R, Plate KH, Stenzel W, Goebel HH, Schulze A, Harter PN, Kieslich M, Mittelbronn M (2015) ATP synthase deficiency due to TMEM70 mutation leads to ultrastructural mitochondrial degeneration and is amenable to treatment. Biomed Res Int 2015: 462592

Brand MD, Affourtit C, Esteves TC, Green K, Lambert AJ, Miwa S, Pakay JL, Parker N (2004) Mitochondrial superoxide: production, biological effects, and activation of uncoupling proteins. Free Radic Biol Med 37: 755-767

Brandt U (2006) Energy converting NADH:quinone oxidoreductase (complex I). Annu Rev Biochem 75: 69-92

Brantová O, Tesarová M, Hansíková H, Elleder M, Zeman J, Sládková J (2006) Ultrastructural changes of mitochondria in the cultivated skin fibroblasts of patients with point mutations in mitochondrial DNA. Ultrastruct Pathol 30: 239-245

Brzezniak LK, Bijata M, Szczesny RJ, Stepien PP (2011) Involvement of human ELAC2 gene product in 3' end processing of mitochondrial tRNAs. RNA Biol 8: 616-626

Burger G, Gray MW, Lang BF (2003) Mitochondrial genomes: anything goes. Trends Genet 19: 709-716

Busch KB, Deckers-Hebestreit G, Hanke GT, Mulkidjanian AY (2013) Dynamics of bioenergetic microcompartments. Biol Chem 394: 163-188

Bykhovskaya Y, Casas K, Mengesha E, Inbal A, Fischel-Ghodsian N (2004) Missense mutation in pseudouridine synthase 1 (PUS1) causes mitochondrial myopathy and sideroblastic anemia (MLASA). Am J Hum Genet 74: 1303-1308

Calvo E, Cogliati S, Hernansanz-Agustín P, Loureiro-López M, Guarás A, Casuso RA, García-Marqués F, Acín-Pérez R, Martí-Mateos Y, Silla-Castro JC, Carro-Alvarellos M, Huertas JR, Vázquez J, Enríquez JA (2020) Functional role of respiratory supercomplexes in mice: SCAF1 relevance and segmentation of the Q. Sci Adv 6: eaba7509

Calvo S, Jain M, Xie X, Sheth SA, Chang B, Goldberger OA, Spinazzola A, Zeviani M, Carr SA, Mootha VK (2006) Systematic identification of human mitochondrial disease genes through integrative genomics. Nat Genet 38: 576-582

Calvo SE, Clauser KR, Mootha VK (2016) MitoCarta2.0: an updated inventory of mammalian mitochondrial proteins. Nucleic Acids Res 44: D1251-1257

Calvo SE, Mootha VK (2010) The mitochondrial proteome and human disease. Annu Rev Genomics Hum Genet 11: 25-44

Cameron JM, Levandovskiy V, Mackay N, Ackerley C, Chitayat D, Raiman J, Halliday WH, Schulze A, Robinson BH (2011) Complex V TMEM70 deficiency results in mitochondrial nucleoid disorganization. Mitochondrion 11: 191-199

Campanella M, Parker N, Tan CH, Hall AM, Duchen MR (2009) IF(1): setting the pace of the F(1)F(o)-ATP synthase. Trends Biochem Sci 34: 343-350

Carroll J, He J, Ding S, Fearnley IM, Walker JE (2021) TMEM70 and TMEM242 help to assemble the rotor ring of human ATP synthase and interact with assembly factors for complex I. Proc Natl Acad Sci U S A 118

Carrozzo R, Wittig I, Santorelli FM, Bertini E, Hofmann S, Brandt U, Schägger H (2006) Subcomplexes of human ATP synthase mark mitochondrial biosynthesis disorders. Ann Neurol 59: 265-275

Cartes-Saavedra B, Macuada J, Lagos D, Arancibia D, Andrés ME, Yu-Wai-Man P, Hajnóczky G, Eisner V (2021) OPA1 Modulates Mitochondrial Ca. Front Cell Dev Biol 9: 774108

Castagna AE, Addis J, McInnes RR, Clarke JT, Ashby P, Blaser S, Robinson BH (2007) Late onset Leigh syndrome and ataxia due to a T to C mutation at bp 9,185 of mitochondrial DNA. Am J Med Genet A 143A: 808-816

Catteruccia M, Verrigni D, Martinelli D, Torraco A, Agovino T, Bonafé L, D'Amico A, Donati MA, Adorisio R, Santorelli FM, Carrozzo R, Bertini E, Dionisi-Vici C (2014) Persistent pulmonary arterial hypertension in the newborn (PPHN): a frequent manifestation of TMEM70 defective patients. Mol Genet Metab 111: 353-359

Cecchini G (2003) Function and structure of complex II of the respiratory chain. Annu Rev Biochem 72: 77-109

Chen J, Patton JR (1999) Cloning and characterization of a mammalian pseudouridine synthase. RNA 5: 409-419

Chen R, Runswick MJ, Carroll J, Fearnley IM, Walker JE (2007) Association of two proteolipids of unknown function with ATP synthase from bovine heart mitochondria. FEBS Lett 581: 3145-3148

Chipuk JE, Bouchier-Hayes L, Green DR (2006) Mitochondrial outer membrane permeabilization during apoptosis: the innocent bystander scenario. Cell Death Differ 13: 1396-1402

Ciesielski GL, Oliveira MT, Kaguni LS (2016) Animal Mitochondrial DNA Replication. Enzymes 39: 255-292

Clayton DA (1982) Replication of animal mitochondrial DNA. Cell 28: 693-705

Cogliati S, Enriquez JA, Scorrano L (2016) Mitochondrial Cristae: Where Beauty Meets Functionality. Trends Biochem Sci 41: 261-273

Cox GB, Jans DA, Fimmel AL, Gibson F, Hatch L (1984) Hypothesis. The mechanism of ATP synthase. Conformational change by rotation of the beta-subunit. Biochimica et biophysica acta 768: 201-208

Craig EA, Voisine C, Schilke B (1999) Mitochondrial iron metabolism in the yeast Saccharomyces cerevisiae. Biol Chem 380: 1167-1173

Crompton M, Virji S, Doyle V, Johnson N, Ward JM (1999) The mitochondrial permeability transition pore. Biochem Soc Symp 66: 167-179

Cízková A, Stránecký V, Ivánek R, Hartmannová H, Nosková L, Piherová L, Tesarová M, Hansíková H, Honzík T, Zeman J, Divina P, Potocká A, Paul J, Sperl W, Mayr JA, Seneca S, Houstěk J, Kmoch S (2008a) Development of a human mitochondrial oligonucleotide microarray (h-MitoArray) and gene expression analysis of fibroblast cell lines from 13 patients with isolated F1Fo ATP synthase deficiency. BMC Genomics 9: 38

Cízková A, Stránecký V, Mayr JA, Tesarová M, Havlícková V, Paul J, Ivánek R, Kuss AW, Hansíková H, Kaplanová V, Vrbacký M, Hartmannová H, Nosková L, Honzík T, Drahota Z, Magner M, Hejzlarová K, Sperl W, Zeman J, Houstek J, Kmoch S (2008b) TMEM70 mutations cause isolated ATP synthase deficiency and neonatal mitochondrial encephalocardiomyopathy. Nat Genet 40: 1288-1290

D'Souza AR, Minczuk M (2018) Mitochondrial transcription and translation: overview. Essays Biochem 62: 309-320

Dautant A, Meier T, Hahn A, Tribouillard-Tanvier D, di Rago JP, Kucharczyk R (2018) ATP Synthase Diseases of Mitochondrial Genetic Origin. Front Physiol 9: 329

Davies KM, Anselmi C, Wittig I, Faraldo-Gómez JD, Kühlbrandt W (2012) Structure of the yeast F1Fo-ATP synthase dimer and its role in shaping the mitochondrial cristae. Proc Natl Acad Sci U S A 109: 13602-13607

De Meirleir L, Seneca S, Lissens W, De Clercq I, Eyskens F, Gerlo E, Smet J, Van Coster R (2004) Respiratory chain complex V deficiency due to a mutation in the assembly gene ATP12. J Med Genet 41: 120-124

De Meirleir L, Seneca S, Lissens W, Schoentjes E, Desprechins B (1995) Bilateral striatal necrosis with a novel point mutation in the mitochondrial ATPase 6 gene. Pediatr Neurol 13: 242-246

Degli Esposti M (2014) Bioenergetic evolution in proteobacteria and mitochondria. Genome Biol Evol 6: 3238-3251

Deng K, Shenoy SK, Tso SC, Yu L, Yu CA (2001) Reconstitution of mitochondrial processing peptidase from the core proteins (subunits I and II) of bovine heart mitochondrial cytochrome bc(1) complex. J Biol Chem 276: 6499-6505

Devenish RJ, Prescott M, Rodgers AJ (2008) The structure and function of mitochondrial F1F0-ATP synthases. Int Rev Cell Mol Biol 267: 1-58

Diaz GA, Banikazemi M, Oishi K, Desnick RJ, Gelb BD (1999) Mutations in a new gene encoding a thiamine transporter cause thiamine-responsive megaloblastic anaemia syndrome. Nat Genet 22: 309-312

DiMauro S (2013) Mitochondrial DNA mutation load: chance or destiny? JAMA Neurol 70: 1484-1485

Diodato D, Invernizzi F, Lamantea E, Fagiolari G, Parini R, Menni F, Parenti G, Bollani L, Pasquini E, Donati MA, Cassandrini D, Santorelli FM, Haack TB, Prokisch H, Ghezzi D, Lamperti C, Zeviani M (2014) Common and Novel TMEM70 Mutations in a Cohort of Italian Patients with Mitochondrial Encephalocardiomyopathy. JIMD Rep

Edwards R, Eaglesfield R, Tokatlidis K (2021) The mitochondrial intermembrane space: the most constricted mitochondrial sub-compartment with the largest variety of protein import pathways. Open Biol 11: 210002

Falkenberg M, Gustafsson CM (2020) Mammalian mitochondrial DNA replication and mechanisms of deletion formation. Crit Rev Biochem Mol Biol 55: 509-524

Falkenberg M, Larsson NG, Gustafsson CM (2007) DNA replication and transcription in mammalian mitochondria. Annu Rev Biochem 76: 679-699

Favaro G, Romanello V, Varanita T, Andrea Desbats M, Morbidoni V, Tezze C, Albiero M, Canato M, Gherardi G, De Stefani D, Mammucari C, Blaauw B, Boncompagni S, Protasi F, Reggiani C, Scorrano L, Salviati L, Sandri M (2019) DRP1-mediated mitochondrial shape controls calcium homeostasis and muscle mass. Nat Commun 10: 2576

Fearnley IM, Walker JE (1986) Two overlapping genes in bovine mitochondrial DNA encode membrane components of ATP synthase. EMBO J 5: 2003-2008

Fernandez-Vizarra E, Berardinelli A, Valente L, Tiranti V, Zeviani M (2009) Nonsense mutation in pseudouridylate synthase 1 (PUS1) in two brothers affected by myopathy, lactic acidosis and sideroblastic anaemia (MLASA). BMJ Case Rep 2009

Floyd BJ, Wilkerson EM, Veling MT, Minogue CE, Xia C, Beebe ET, Wrobel RL, Cho H, Kremer LS, Alston CL, Gromek KA, Dolan BK, Ulbrich A, Stefely JA, Bohl SL, Werner KM, Jochem A, Westphall MS, Rensvold JW, Taylor RW, Prokisch H, Kim JP, Coon JJ, Pagliarini DJ (2016) Mitochondrial Protein Interaction Mapping Identifies Regulators of Respiratory Chain Function. Mol Cell 63: 621-632

Fornuskova D, Brantova O, Tesarova M, Stiburek L, Honzik T, Wenchich L, Tietzeova E, Hansikova H, Zeman J (2008) The impact of mitochondrial tRNA mutations on the amount of ATP synthase differs in the brain compared to other tissues. Biochim Biophys Acta 1782: 317-325

Frazier AE, Thorburn DR, Compton AG (2019) Mitochondrial energy generation disorders: genes, mechanisms, and clues to pathology. J Biol Chem 294: 5386-5395

Fu M, Zhang W, Wu L, Yang G, Li H, Wang R (2012) Hydrogen sulfide (H2S) metabolism in mitochondria and its regulatory role in energy production. Proc Natl Acad Sci U S A 109: 2943-2948

Fujikawa M, Sugawara K, Tanabe T, Yoshida M (2015) Assembly of human mitochondrial ATP synthase through two separate intermediates, F1-c-ring and b-e-g complex. FEBS Lett 589: 2707-2712

Galber C, Carissimi S, Baracca A, Giorgio V (2021) The ATP Synthase Deficiency in Human Diseases. Life (Basel) 11

Ganapathi M, Friocourt G, Gueguen N, Friederich MW, Le Gac G, Okur V, Loaëc N, Ludwig T, Ka C, Tanji K, Marcorelles P, Theodorou E, Lignelli-Dipple A, Voisset C, Walker MA, Briere LC, Bourhis A, Blondel M, LeDuc C, Hagen J, Cooper C, Muraresku C, Ferec C, Garenne A, Lelez-Soquet S, Rogers CA, Shen Y, Strode DK, Bizargity P, Iglesias A, Goldstein A, High FA, Network UD, Sweetser DA, Ganetzky R, Van Hove JLK, Procaccio V, Le Marechal C, Chung WK (2022) A homozygous splice variant in ATP5PO, disrupts mitochondrial complex V function and causes Leigh syndrome in two unrelated families. J Inherit Metab Dis

Ganetzky RD, Stendel C, McCormick EM, Zolkipli-Cunningham Z, Goldstein AC, Klopstock T, Falk MJ (2019) MT-ATP6 mitochondrial disease variants: Phenotypic and biochemical features analysis in 218 published cases and cohort of 14 new cases. Hum Mutat 40: 499-515

Gao X, Wen X, Esser L, Quinn B, Yu L, Yu CA, Xia D (2003) Structural basis for the quinone reduction in the bc1 complex: a comparative analysis of crystal structures of mitochondrial cytochrome bc1 with bound substrate and inhibitors at the Qi site. Biochemistry 42: 9067-9080

García JJ, Ogilvie I, Robinson BH, Capaldi RA (2000) Structure, functioning, and assembly of the ATP synthase in cells from patients with the T8993G mitochondrial DNA mutation. Comparison with the enzyme in Rho(0) cells completely lacking mtdna. J Biol Chem 275: 11075-11081

Garesse R, Vallejo CG (2001) Animal mitochondrial biogenesis and function: a regulatory cross-talk between two genomes. Gene 263: 1-16

Giorgio V, von Stockum S, Antoniel M, Fabbro A, Fogolari F, Forte M, Glick GD, Petronilli V, Zoratti M, Szabó I, Lippe G, Bernardi P (2013) Dimers of mitochondrial ATP synthase form the permeability transition pore. Proc Natl Acad Sci U S A 110: 5887-5892

Gray MW (2017) Lynn Margulis and the endosymbiont hypothesis: 50 years later. Mol Biol Cell 28: 1285-1287

Gray MW, Burger G, Lang BF (1999) Mitochondrial evolution. Science 283: 1476-1481

Grigorieff N (1998) Three-dimensional structure of bovine NADH:ubiquinone oxidoreductase (complex I) at 22 A in ice. J Mol Biol 277: 1033-1046

Guerrero-Castillo S, Baertling F, Kownatzki D, Wessels HJ, Arnold S, Brandt U, Nijtmans L (2017) The Assembly Pathway of Mitochondrial Respiratory Chain Complex I. Cell Metab 25: 128-139

Guo R, Zong S, Wu M, Gu J, Yang M (2017) Architecture of Human Mitochondrial Respiratory Megacomplex I. Cell 170: 1247-1257.e1212

Hahn A, Parey K, Bublitz M, Mills DJ, Zickermann V, Vonck J, Kühlbrandt W, Meier T (2016) Structure of a Complete ATP Synthase Dimer Reveals the Molecular Basis of Inner Mitochondrial Membrane Morphology. Mol Cell 63: 445-456

Hao X, Liu S, Wu X, Hao Y, Chen Y (2015) Infantile mitochondrial disorder associated with subclinical hypothyroidism is caused by a rare mitochondrial DNA 8691A>G mutation: a case report. Neuroreport 26: 588-592

Haviv R, Zeharia A, Belaiche C, Haimi Cohen Y, Saada A (2014) Elevated plasma citrulline: look for dihydrolipoamide dehydrogenase deficiency. Eur J Pediatr 173: 243-245

Havlickova Karbanova V, Cizkova Vrbacka A, Hejzlarova K, Nuskova H, Stranecky V, Potocka A, Kmoch S, Houstek J (2012) Compensatory upregulation of respiratory chain complexes III and IV in isolated deficiency of ATP synthase due to TMEM70 mutation. Biochim Biophys Acta 1817: 1037-1043

Havlícková V, Kaplanová V, Nůsková H, Drahota Z, Houstek J (2010) Knockdown of F1 epsilon subunit decreases mitochondrial content of ATP synthase and leads to accumulation of subunit c. Biochimica et biophysica acta 1797: 1124-1129

He J, Carroll J, Ding S, Fearnley IM, Walker JE (2017a) Permeability transition in human mitochondria persists in the absence of peripheral stalk subunits of ATP synthase. Proc Natl Acad Sci U S A 114: 9086-9091

He J, Ford HC, Carroll J, Ding S, Fearnley IM, Walker JE (2017b) Persistence of the mitochondrial permeability transition in the absence of subunit c of human ATP synthase. Proc Natl Acad Sci U S A 114: 3409-3414

He J, Ford HC, Carroll J, Douglas C, Gonzales E, Ding S, Fearnley IM, Walker JE (2018) Assembly of the membrane domain of ATP synthase in human mitochondria. Proc Natl Acad Sci U S A 115: 2988-2993

Hejzlarová K, Mráček T, Vrbacký M, Kaplanová V, Karbanová V, Nůsková H, Pecina P, Houštěk J (2014) Nuclear genetic defects of mitochondrial ATP synthase. Physiol Res 63 Suppl 1: S57-71

Hejzlarová K, Tesařová M, Vrbacká-Čížková A, Vrbacký M, Hartmannová H, Kaplanová V, Nosková L, Kratochvílová H, Buzková J, Havlíčková V, Zeman J, Kmoch S, Houštěk J (2011) Expression and processing of the TMEM70 protein. Biochimica et biophysica acta 1807: 144-149

Henze K, Martin W (2003) Evolutionary biology: essence of mitochondria. Nature 426: 127-128

Hirono K, Ichida F, Nishio N, Ogawa-Tominaga M, Fushimi T, Feichtinger RG, Mayr JA, Kohda M, Kishita Y, Okazaki Y, Ohtake A, Murayama K (2019) Mitochondrial complex deficiency by novel compound heterozygous. Clin Case Rep 7: 553-557

Hirst J (2013) Mitochondrial complex I. Annu Rev Biochem 82: 551-575

Hock DH, Robinson DRL, Stroud DA (2020) Blackout in the powerhouse: clinical phenotypes associated with defects in the assembly of OXPHOS complexes and the mitoribosome. Biochem J 477: 4085-4132

Holme E, Greter J, Jacobson CE, Larsson NG, Lindstedt S, Nilsson KO, Oldfors A, Tulinius M (1992) Mitochondrial ATP-synthase deficiency in a child with 3-methylglutaconic aciduria. Pediatr Res 32: 731-735

Holt IJ, Lorimer HE, Jacobs HT (2000) Coupled leading- and lagging-strand synthesis of mammalian mitochondrial DNA. Cell 100: 515-524

Holzmann J, Frank P, Löffler E, Bennett KL, Gerner C, Rossmanith W (2008) RNase P without RNA: identification and functional reconstitution of the human mitochondrial tRNA processing enzyme. Cell 135: 462-474

Honzik T, Tesarova M, Vinsova K, Hansikova H, Magner M, Kratochvilova H, Zamecnik J, Zeman J, Jesina P (2013) Different laboratory and muscle biopsy findings in a family with an m.8851T>C mutation in the mitochondrial MTATP6 gene. Mol Genet Metab 108: 102-105

Honzík T, Tesarová M, Mayr JA, Hansíková H, Jesina P, Bodamer O, Koch J, Magner M, Freisinger P, Huemer M, Kostková O, van Coster R, Kmoch S, Houstêk J, Sperl W, Zeman J (2010) Mitochondrial encephalocardio-myopathy with early neonatal onset due to TMEM70 mutation. Arch Dis Child 95: 296-301

Houstek J, Kmoch S, Zeman J (2009) TMEM70 protein - a novel ancillary factor of mammalian ATP synthase. Biochimica et biophysica acta 1787: 529-532

Houstek J, Mrácek T, Vojtísková A, Zeman J (2004) Mitochondrial diseases and ATPase defects of nuclear origin. Biochimica et biophysica acta 1658: 115-121

Houstek J, Pícková A, Vojtísková A, Mrácek T, Pecina P, Jesina P (2006) Mitochondrial diseases and genetic defects of ATP synthase. Biochimica et biophysica acta 1757: 1400-1405

Huertas JR, Casuso RA, Agustín PH, Cogliati S (2019) Stay Fit, Stay Young: Mitochondria in Movement: The Role of Exercise in the New Mitochondrial Paradigm. Oxid Med Cell Longev 2019: 7058350

Hällberg BM, Larsson NG (2014) Making proteins in the powerhouse. Cell Metab 20: 226-240

Hüttemann M, Schmidt TR, Grossman LI (2003) A third isoform of cytochrome c oxidase subunit VIII is present in mammals. Gene 312: 95-102

Isidoro A, Martínez M, Fernández PL, Ortega AD, Santamaría G, Chamorro M, Reed JC, Cuezva JM (2004) Alteration of the bioenergetic phenotype of mitochondria is a hallmark of breast, gastric, lung and oesophageal cancer. Biochem J 378: 17-20

Itoh H, Takahashi A, Adachi K, Noji H, Yasuda R, Yoshida M, Kinosita K (2004) Mechanically driven ATP synthesis by F1-ATPase. Nature 427: 465-468

Iwata S, Lee JW, Okada K, Lee JK, Iwata M, Rasmussen B, Link TA, Ramaswamy S, Jap BK (1998) Complete structure of the 11-subunit bovine mitochondrial cytochrome bc1 complex. Science 281: 64-71

Jesina P, Tesarova M, Fornuskova D, Vojtiskova A, Pecina P, Kaplanova V, Hansikova H, Zeman J, Houstek J (2004a) Diminished synthesis of subunit a (ATP6) and altered function of ATP synthase and cytochrome c oxidase due to the mtDNA 2 bp microdeletion of TA at positions 9205 and 9206. Biochem J 383: 561-571

Jesina P, Tesarová M, Fornůsková D, Vojtísková A, Pecina P, Kaplanová V, Hansíková H, Zeman J, Houstek J (2004b) Diminished synthesis of subunit a (ATP6) and altered function of ATP synthase and cytochrome c oxidase due to the mtDNA 2 bp microdeletion of TA at positions 9205 and 9206. Biochem J 383: 561-571

John GB, Shang Y, Li L, Renken C, Mannella CA, Selker JM, Rangell L, Bennett MJ, Zha J (2005) The mitochondrial inner membrane protein mitofilin controls cristae morphology. Mol Biol Cell 16: 1543-1554

Jonckheere AI, Hogeveen M, Nijtmans LG, van den Brand MA, Janssen AJ, Diepstra JH, van den Brandt FC, van den Heuvel LP, Hol FA, Hofste TG, Kapusta L, Dillmann U, Shamdeen MG, Smeitink JA, Rodenburg RJ (2008) A novel mitochondrial ATP8 gene mutation in a patient with apical hypertrophic cardiomyopathy and neuropathy. J Med Genet 45: 129-133

Jonckheere AI, Huigsloot M, Lammens M, Jansen J, van den Heuvel LP, Spiekerkoetter U, von Kleist-Retzow JC, Forkink M, Koopman WJ, Szklarczyk R, Huynen MA, Fransen JA, Smeitink JA, Rodenburg RJ (2011) Restoration of complex V deficiency caused by a novel deletion in the human TMEM70 gene normalizes mitochondrial morphology. Mitochondrion 11: 954-963

Jonckheere AI, Renkema GH, Bras M, van den Heuvel LP, Hoischen A, Gilissen C, Nabuurs SB, Huynen MA, de Vries MC, Smeitink JA, Rodenburg RJ (2013) A complex V ATP5A1 defect causes fatal neonatal mitochondrial encephalopathy. Brain 136: 1544-1554

Jornayvaz FR, Shulman GI (2010) Regulation of mitochondrial biogenesis. Essays Biochem 47: 69-84

Kadenbach B (2017) Regulation of Mammalian 13-Subunit Cytochrome c Oxidase and Binding of other Proteins: Role of NDUFA4. Trends Endocrinol Metab 28: 761-770

Kampjut D, Sazanov LA (2020) The coupling mechanism of mammalian respiratory complex I. Science 370

Kars ME, Başak AN, Onat OE, Bilguvar K, Choi J, Itan Y, Çağlar C, Palvadeau R, Casanova JL, Cooper DN, Stenson PD, Yavuz A, Buluş H, Günel M, Friedman JM, Özçelik T (2021) The genetic structure of the Turkish population reveals high levels of variation and admixture. Proc Natl Acad Sci U S A 118

Klecker T, Westermann B (2021) Pathways shaping the mitochondrial inner membrane. Open Biol 11: 210238

Kleele T, Rey T, Winter J, Zaganelli S, Mahecic D, Perreten Lambert H, Ruberto FP, Nemir M, Wai T, Pedrazzini T, Manley S (2021) Distinct fission signatures predict mitochondrial degradation or biogenesis. Nature 593: 435-439

Kohl JB, Mellis AT, Schwarz G (2019) Homeostatic impact of sulfite and hydrogen sulfide on cysteine catabolism. Br J Pharmacol 176: 554-570

Kovalčíková J, Vrbacký M, Pecina P, Tauchmannová K, Nůsková H, Kaplanová V, Brázdová A, Alán L, Eliáš J, Čunátová K, Kořínek V, Sedlacek R, Mráček T, Houštěk J (2019) TMEM70 facilitates biogenesis of mammalian ATP synthase by promoting subunit c incorporation into the rotor structure of the enzyme. FASEB J 33: 14103-14117

Kovářová N, Cížková Vrbacká A, Pecina P, Stránecký V, Pronicka E, Kmoch S, Houštěk J (2012) Adaptation of respiratory chain biogenesis to cytochrome c oxidase deficiency caused by SURF1 gene mutations. Biochimica et biophysica acta 1822: 1114-1124

Kratochvílová H, Hejzlarová K, Vrbacký M, Mráček T, Karbanová V, Tesařová M, Gombitová A, Cmarko D, Wittig I, Zeman J, Houštěk J (2014) Mitochondrial membrane assembly of TMEM70 protein. Mitochondrion 15: 1-9

Kucharczyk R, Giraud MF, Brèthes D, Wysocka-Kapcinska M, Ezkurdia N, Salin B, Velours J, Camougrand N, Haraux F, di Rago JP (2013) Defining the pathogenesis of human mtDNA mutations using a yeast model: the case of T8851C. Int J Biochem Cell Biol 45: 130-140

Lapuente-Brun E, Moreno-Loshuertos R, Acín-Pérez R, Latorre-Pellicer A, Colás C, Balsa E, Perales-Clemente E, Quirós PM, Calvo E, Rodríguez-Hernández MA, Navas P, Cruz R, Carracedo Á, López-Otín C, Pérez-Martos A, Fernández-Silva P, Fernández-Vizarra E, Enríquez JA (2013) Supercomplex assembly determines electron flux in the mitochondrial electron transport chain. Science 340: 1567-1570

Lazarou M, Thorburn DR, Ryan MT, McKenzie M (2009) Assembly of mitochondrial complex I and defects in disease. Biochimica et biophysica acta 1793: 78-88

Legati A, Reyes A, Nasca A, Invernizzi F, Lamantea E, Tiranti V, Garavaglia B, Lamperti C, Ardissone A, Moroni I, Robinson A, Ghezzi D, Zeviani M (2016) New genes and pathomechanisms in mitochondrial disorders unraveled by NGS technologies. Biochim Biophys Acta 1857: 1326-1335

Leif H, Weidner U, Berger A, Spehr V, Braun M, van Heek P, Friedrich T, Ohnishi T, Weiss H (1993) Escherichia coli NADH dehydrogenase I, a minimal form of the mitochondrial complex I. Biochem Soc Trans 21: 998-1001

Lemasters JJ, Theruvath TP, Zhong Z, Nieminen AL (2009) Mitochondrial calcium and the permeability transition in cell death. Biochimica et biophysica acta 1787: 1395-1401

Li Y, Jourdain AA, Calvo SE, Liu JS, Mootha VK (2017) CLIC, a tool for expanding biological pathways based on co-expression across thousands of datasets. PLoS Comput Biol 13: e1005653

Lichtenstein DA, Crispin AW, Sendamarai AK, Campagna DR, Schmitz-Abe K, Sousa CM, Kafina MD, Schmidt PJ, Niemeyer CM, Porter J, May A, Patnaik MM, Heeney MM, Kimmelman A, Bottomley SS, Paw BH, Markianos K, Fleming MD (2016) A recurring mutation in the respiratory complex 1 protein NDUFB11 is responsible for a novel form of X-linked sideroblastic anemia. Blood 128: 1913-1917

Lieber DS, Calvo SE, Shanahan K, Slate NG, Liu S, Hershman SG, Gold NB, Chapman BA, Thorburn DR, Berry GT, Schmahmann JD, Borowsky ML, Mueller DM, Sims KB, Mootha VK (2013) Targeted exome sequencing of suspected mitochondrial disorders. Neurology 80: 1762-1770

Lightowlers RN, Taylor RW, Turnbull DM (2015) Mutations causing mitochondrial disease: What is new and what challenges remain? Science 349: 1494-1499

Lines MA, Cuillerier A, Chakraborty P, Naas T, Duque Lasio ML, Michaud J, Pileggi C, Harper ME, Burelle Y, Toler TL, Sondheimer N, Crawford HP, Millan F, Geraghty MT (2021) A recurrent de novo ATP5F1A substitution associated with neonatal complex V deficiency. Eur J Hum Genet 29: 1719-1724

Lobo-Jarne T, Pérez-Pérez R, Fontanesi F, Timón-Gómez A, Wittig I, Peñas A, Serrano-Lorenzo P, García-Consuegra I, Arenas J, Martín MA, Barrientos A, Ugalde C (2020) Multiple pathways coordinate assembly of human mitochondrial complex IV and stabilization of respiratory supercomplexes. EMBO J 39: e103912

Lopez-Fabuel I, Le Douce J, Logan A, James AM, Bonvento G, Murphy MP, Almeida A, Bolaños JP (2016) Complex I assembly into supercomplexes determines differential mitochondrial ROS production in neurons and astrocytes. Proc Natl Acad Sci U S A 113: 13063-13068

Lott MT, Leipzig JN, Derbeneva O, Xie HM, Chalkia D, Sarmady M, Procaccio V, Wallace DC (2013) mtDNA Variation and Analysis Using Mitomap and Mitomaster. Curr Protoc Bioinformatics 44: 1.23.21-26

Ludwig B, Bender E, Arnold S, Hüttemann M, Lee I, Kadenbach B (2001) Cytochrome C oxidase and the regulation of oxidative phosphorylation. Chembiochem 2: 392-403

Luo S, Valencia CA, Zhang J, Lee NC, Slone J, Gui B, Wang X, Li Z, Dell S, Brown J, Chen SM, Chien YH, Hwu WL, Fan PC, Wong LJ, Atwal PS, Huang T (2018) Biparental Inheritance of Mitochondrial DNA in Humans. Proc Natl Acad Sci U S A 115: 13039-13044

Lussey-Lepoutre C, Hollinshead KE, Ludwig C, Menara M, Morin A, Castro-Vega LJ, Parker SJ, Janin M, Martinelli C, Ottolenghi C, Metallo C, Gimenez-Roqueplo AP, Favier J, Tennant DA (2015) Loss of succinate dehydrogenase activity results in dependency on pyruvate carboxylation for cellular anabolism. Nat Commun 6: 8784

Lynch M, Koskella B, Schaack S (2006) Mutation pressure and the evolution of organelle genomic architecture. Science 311: 1727-1730

López-Gallardo E, Solano A, Herrero-Martín MD, Martínez-Romero I, Castaño-Pérez MD, Andreu AL, Herrera A, López-Pérez MJ, Ruiz-Pesini E, Montoya J (2009) NARP syndrome in a patient harbouring an insertion in the MT-ATP6 gene that results in a truncated protein. J Med Genet 46: 64-67

Magner M, Dvorakova V, Tesarova M, Mazurova S, Hansikova H, Zahorec M, Brennerova K, Bzduch V, Spiegel R, Horovitz Y, Mandel H, Eminoğlu FT, Mayr JA, Koch J, Martinelli D, Bertini E, Konstantopoulou V, Smet J, Rahman S, Broomfield A, Stojanović V, Dionisi-Vici C, van Coster R, Morava-Kozicz E, Sperl W, Zeman J, Honzik T (2014) TMEM70 deficiency: long-term outcome of 48 patients. J Inherit Metab Dis

Mai N, Chrzanowska-Lightowlers ZM, Lightowlers RN (2017) The process of mammalian mitochondrial protein synthesis. Cell Tissue Res 367: 5-20

Maranzana E, Barbero G, Falasca AI, Lenaz G, Genova ML (2013) Mitochondrial respiratory supercomplex association limits production of reactive oxygen species from complex I. Antioxid Redox Signal 19: 1469-1480

Margulis L (1968) Evolutionary criteria in thallophytes: a radical alternative. Science 161: 1020-1022

Marković A, Tauchmannová K, Šimáková M, Mlejnek P, Kaplanová V, Pecina P, Pecinová A, Papoušek F, Liška F, Šilhavý J, Mikešová J, Neckář J, Houštěk J, Pravenec M, Mráček T (2022) Genetic Complementation of ATP Synthase Deficiency Due to Dysfunction of TMEM70 Assembly Factor in Rat. Biomedicines 10

Mayr JA, Haack TB, Freisinger P, Karall D, Makowski C, Koch J, Feichtinger RG, Zimmermann FA, Rolinski B, Ahting U, Meitinger T, Prokisch H, Sperl W (2015) Spectrum of combined respiratory chain defects. J Inherit Metab Dis 38: 629-640

Mayr JA, Havlícková V, Zimmermann F, Magler I, Kaplanová V, Jesina P, Pecinová A, Nusková H, Koch J, Sperl W, Houstek J (2010) Mitochondrial ATP synthase deficiency due to a mutation in the ATP5E gene for the F1 epsilon subunit. Hum Mol Genet 19: 3430-3439

McCormick EM, Zolkipli-Cunningham Z, Falk MJ (2018) Mitochondrial disease genetics update: recent insights into the molecular diagnosis and expanding phenotype of primary mitochondrial disease. Curr Opin Pediatr 30: 714-724

Meulemans A, Seneca S, Pribyl T, Smet J, Alderweirldt V, Waeytens A, Lissens W, Van Coster R, De Meirleir L, di Rago JP, Gatti DL, Ackerman SH (2010) Defining the pathogenesis of the human Atp12p W94R mutation using a Saccharomyces cerevisiae yeast model. J Biol Chem 285: 4099-4109

Meyer B, Wittig I, Trifilieff E, Karas M, Schägger H (2007) Identification of two proteins associated with mammalian ATP synthase. Mol Cell Proteomics 6: 1690-1699

Mizukami S, Yafune A, Watanabe Y, Nakajima K, Jin M, Yoshida T, Shibutani M (2017) Identification of epigenetically downregulated Tmem70 and Ube2e2 in rat liver after 28-day treatment with hepatocarcinogenic thioacetamide showing gene product downregulation in hepatocellular preneoplastic and neoplastic lesions produced by tumor promotion. Toxicol Lett 266: 13-22

Moe A, Di Trani J, Rubinstein JL, Brzezinski P (2021) Cryo-EM structure and kinetics reveal electron transfer by 2D diffusion of cytochrome. Proc Natl Acad Sci U S A 118

Mrácek T, Pecina P, Vojtísková A, Kalous M, Sebesta O, Houstek J (2006) Two components in pathogenic mechanism of mitochondrial ATPase deficiency: energy deprivation and ROS production. Exp Gerontol 41: 683-687

Mu W, Schiess N, Orthmann-Murphy JL, El-Hattab AW (2019) The utility of whole exome sequencing in diagnosing neurological disorders in adults from a highly consanguineous population. J Neurogenet 33: 21-26

Murphy E, Ardehali H, Balaban RS, DiLisa F, Dorn GW, Kitsis RN, Otsu K, Ping P, Rizzuto R, Sack MN, Wallace D, Youle RJ, American Heart Association Council on Basic Cardiovascular Sciences CuoCC, and Council on Functional Genomics and Translational Biology (2016) Mitochondrial Function, Biology, and Role in Disease: A Scientific Statement From the American Heart Association. Circ Res 118: 1960-1991

Nass S, Nass MM (1963) Intramitochondrial fibers with DNA characteristics. II. enzymatic and other hydrolytic treatments. J Cell Biol 19: 613-629

Neilson DE, Zech M, Hufnagel RB, Slone J, Wang X, Homan S, Gutzwiller LM, Leslie EJ, Leslie ND, Xiao J, Hedera P, LeDoux MS, Gebelein B, Wilbert F, Eckenweiler M, Winkelmann J, Gilbert DL, Huang T (2022) A Novel Variant of ATP5MC3 Associated with Both Dystonia and Spastic Paraplegia. Mov Disord 37: 375-383

Neupert W, Herrmann JM (2007) Translocation of proteins into mitochondria. Annu Rev Biochem 76: 723-749

Nijtmans LG, Klement P, Houstěk J, van den Bogert C (1995) Assembly of mitochondrial ATP synthase in cultured human cells: implications for mitochondrial diseases. Biochimica et biophysica acta 1272: 190-198

Ohsakaya S, Fujikawa M, Hisabori T, Yoshida M (2011) Knockdown of DAPIT (diabetes-associated protein in insulin-sensitive tissue) results in loss of ATP synthase in mitochondria. J Biol Chem 286: 20292-20296

Oláhová M, Yoon WH, Thompson K, Jangam S, Fernandez L, Davidson JM, Kyle JE, Grove ME, Fisk DG, Kohler JN, Holmes M, Dries AM, Huang Y, Zhao C, Contrepois K,

Zappala Z, Frésard L, Waggott D, Zink EM, Kim YM, Heyman HM, Stratton KG, Webb-Robertson BM, Snyder M, Merker JD, Montgomery SB, Fisher PG, Feichtinger RG, Mayr JA, Hall J, Barbosa IA, Simpson MA, Deshpande C, Waters KM, Koeller DM, Metz TO, Morris AA, Schelley S, Cowan T, Friederich MW, McFarland R, Van Hove JLK, Enns GM, Yamamoto S, Ashley EA, Wangler MF, Taylor RW, Bellen HJ, Bernstein JA, Wheeler MT, Network UD (2018) Biallelic Mutations in ATP5F1D, which Encodes a Subunit of ATP Synthase, Cause a Metabolic Disorder. Am J Hum Genet 102: 494-504

Pagliarini DJ, Calvo SE, Chang B, Sheth SA, Vafai SB, Ong SE, Walford GA, Sugiana C, Boneh A, Chen WK, Hill DE, Vidal M, Evans JG, Thorburn DR, Carr SA, Mootha VK (2008) A mitochondrial protein compendium elucidates complex I disease biology. Cell 134: 112-123

Pallotti F, Baracca A, Hernandez-Rosa E, Walker WF, Solaini G, Lenaz G, Melzi D'Eril GV, Dimauro S, Schon EA, Davidson MM (2004) Biochemical analysis of respiratory function in cybrid cell lines harbouring mitochondrial DNA mutations. Biochem J 384: 287-293

Papa S (1996) Mitochondrial oxidative phosphorylation changes in the life span. Molecular aspects and physiopathological implications. Biochim Biophys Acta 1276: 87-105

Parakatselaki ME, Ladoukakis ED (2021) mtDNA Heteroplasmy: Origin, Detection, Significance, and Evolutionary Consequences. Life (Basel) 11

Parey K, Wirth C, Vonck J, Zickermann V (2020) Respiratory complex I - structure, mechanism and evolution. Curr Opin Struct Biol 63: 1-9

Parsons DF (1963) Mitochondrial Structure: Two Types of Subunits on Negatively Stained Mitochondrial Membranes. Science 140: 985-987

Pernas L, Scorrano L (2016) Mito-Morphosis: Mitochondrial Fusion, Fission, and Cristae Remodeling as Key Mediators of Cellular Function. Annu Rev Physiol 78: 505-531

Pierron D, Wildman DE, Hüttemann M, Markondapatnaikuni GC, Aras S, Grossman LI (2012) Cytochrome c oxidase: evolution of control via nuclear subunit addition. Biochimica et biophysica acta 1817: 590-597

Pinke G, Zhou L, Sazanov LA (2020) Cryo-EM structure of the entire mammalian F-type ATP synthase. Nat Struct Mol Biol 27: 1077-1085

Pitceathly RDS, Taanman JW (2018) NDUFA4 (Renamed COXFA4) Is a Cytochrome-c Oxidase Subunit. Trends Endocrinol Metab 29: 452-454

Poole OV, Pizzamiglio C, Murphy D, Falabella M, Macken WL, Bugiardini E, Woodward CE, Labrum R, Efthymiou S, Salpietro V, Chelban V, Kaiyrzhanov R, Maroofian R, Amato AA, Gregory A, Hayflick SJ, Jonvik H, Wood N, Houlden H, Vandrovcova J, Hanna MG, Pittman A, Pitceathly RDS, Group SS, Genomics QS (2021) Mitochondrial DNA Analysis from Exome Sequencing Data Improves Diagnostic Yield in Neurological Diseases. Ann Neurol 89: 1240-1247

Protasoni M, Zeviani M (2021) Mitochondrial Structure and Bioenergetics in Normal and Disease Conditions. Int J Mol Sci 22

Pütz J, Dupuis B, Sissler M, Florentz C (2007) Mamit-tRNA, a database of mammalian mitochondrial tRNA primary and secondary structures. RNA 13: 1184-1190

Rabier D, Diry C, Rotig A, Rustin P, Heron B, Bardet J, Parvy P, Ponsot G, Marsac C, Saudubray JM, Munnich A, Kamoun P (1998) Persistent hypocitrullinaemia as a marker for mtDNA NARP T 8993 G mutation? J Inherit Metab Dis 21: 216-219

Rackham O, Filipovska A (2022) Organization and expression of the mammalian mitochondrial genome. Nat Rev Genet

Rahman S (2020) Mitochondrial disease in children. J Intern Med 287: 609-633

Rak M, Gokova S, Tzagoloff A (2011) Modular assembly of yeast mitochondrial ATP synthase. EMBO J 30: 920-930

Rath S, Sharma R, Gupta R, Ast T, Chan C, Durham TJ, Goodman RP, Grabarek Z, Haas ME, Hung WHW, Joshi PR, Jourdain AA, Kim SH, Kotrys AV, Lam SS, McCoy JG, Meisel JD, Miranda M, Panda A, Patgiri A, Rogers R, Sadre S, Shah H, Skinner OS, To TL, Walker MA, Wang H, Ward PS, Wengrod J, Yuan CC, Calvo SE, Mootha VK (2021) MitoCarta3.0: an updated mitochondrial proteome now with sub-organelle localization and pathway annotations. Nucleic Acids Res 49: D1541-D1547

Reyes A, Kazak L, Wood SR, Yasukawa T, Jacobs HT, Holt IJ (2013) Mitochondrial DNA replication proceeds via a 'bootlace' mechanism involving the incorporation of processed transcripts. Nucleic Acids Res 41: 5837-5850

Richter U, McFarland R, Taylor RW, Pickett SJ (2021) The molecular pathology of pathogenic mitochondrial tRNA variants. FEBS Lett 595: 1003-1024

Rieger B, Krajčová A, Duwe P, Busch KB (2019) ALCAT1 Overexpression Affects Supercomplex Formation and Increases ROS in Respiring Mitochondria. Oxid Med Cell Longev 2019: 9186469

Riley LG, Cooper S, Hickey P, Rudinger-Thirion J, McKenzie M, Compton A, Lim SC, Thorburn D, Ryan MT, Giegé R, Bahlo M, Christodoulou J (2010) Mutation of the mitochondrial tyrosyl-tRNA synthetase gene, YARS2, causes myopathy, lactic acidosis, and sideroblastic anemia--MLASA syndrome. Am J Hum Genet 87: 52-59

Riley LG, Rudinger-Thirion J, Schmitz-Abe K, Thorburn DR, Davis RL, Teo J, Arbuckle S, Cooper ST, Campagna DR, Frugier M, Markianos K, Sue CM, Fleming MD, Christodoulou J (2016) LARS2 Variants Associated with Hydrops, Lactic Acidosis, Sideroblastic Anemia, and Multisystem Failure. JIMD Rep 28: 49-57

Rizzuto R, Marchi S, Bonora M, Aguiari P, Bononi A, De Stefani D, Giorgi C, Leo S, Rimessi A, Siviero R, Zecchini E, Pinton P (2009) Ca(2+) transfer from the ER to mitochondria: when, how and why. Biochimica et biophysica acta 1787: 1342-1351

Rizzuto R, Pinton P, Carrington W, Fay FS, Fogarty KE, Lifshitz LM, Tuft RA, Pozzan T (1998) Close contacts with the endoplasmic reticulum as determinants of mitochondrial Ca2+ responses. Science 280: 1763-1766

Robin ED, Wong R (1988) Mitochondrial DNA molecules and virtual number of mitochondria per cell in mammalian cells. J Cell Physiol 136: 507-513

Ruby JR, Dyer RF, Skalko RG (1969) Continuities between mitochondria and endoplasmic reticulum in the mammalian ovary. Z Zellforsch Mikrosk Anat 97: 30-37

Russell OM, Gorman GS, Lightowlers RN, Turnbull DM (2020) Mitochondrial Diseases: Hope for the Future. Cell 181: 168-188

Rutter J, Winge DR, Schiffman JD (2010) Succinate dehydrogenase - Assembly, regulation and role in human disease. Mitochondrion 10: 393-401

Rühle T, Leister D (2015) Assembly of F1F0-ATP synthases. Biochimica et biophysica acta 1847: 849-860

Saada A (2004) Deoxyribonucleotides and disorders of mitochondrial DNA integrity. DNA Cell Biol 23: 797-806

Sarajlija A, Magner M, Djordjevic M, Kecman B, Grujic B, Tesarova M, Minic P (2017) Late-presenting congenital diaphragmatic hernia in a child with TMEM70 deficiency. Congenit Anom (Kyoto) 57: 64-65

Saraste M (1999) Oxidative phosphorylation at the fin de siècle. Science 283: 1488-1493

Scarpulla RC (2012) Nucleus-encoded regulators of mitochondrial function: integration of respiratory chain expression, nutrient sensing and metabolic stress. Biochimica et biophysica acta 1819: 1088-1097

Schmitz-Abe K, Ciesielski SJ, Schmidt PJ, Campagna DR, Rahimov F, Schilke BA, Cuijpers M, Rieneck K, Lausen B, Linenberger ML, Sendamarai AK, Guo C, Hofmann I, Newburger PE, Matthews D, Shimamura A, Snijders PJ, Towne MC, Niemeyer CM, Watson HG, Dziegiel MH, Heeney MM, May A, Bottomley SS, Swinkels DW, Markianos K, Craig EA, Fleming MD (2015) Congenital sideroblastic anemia due to mutations in the mitochondrial HSP70 homologue HSPA9. Blood 126: 2734-2738

Schoonen M, Smuts I, Louw R, Elson JL, van Dyk E, Jonck LM, Rodenburg RJT, van der Westhuizen FH (2019) Panel-Based Nuclear and Mitochondrial Next-Generation Sequencing Outcomes of an Ethnically Diverse Pediatric Patient Cohort with Mitochondrial Disease. J Mol Diagn 21: 503-513

Schägger H (2002) Respiratory chain supercomplexes of mitochondria and bacteria. Biochimica et biophysica acta 1555: 154-159

Schägger H, Link TA, Engel WD, von Jagow G (1986) Isolation of the eleven protein subunits of the bc1 complex from beef heart. Methods Enzymol 126: 224-237

Schägger H, Pfeiffer K (2000) Supercomplexes in the respiratory chains of yeast and mammalian mitochondria. EMBO J 19: 1777-1783

Schägger H, von Jagow G (1991) Blue native electrophoresis for isolation of membrane protein complexes in enzymatically active form. Anal Biochem 199: 223-231

Seifert EL, Ligeti E, Mayr JA, Sondheimer N, Hajnóczky G (2015) The mitochondrial phosphate carrier: Role in oxidative metabolism, calcium handling and mitochondrial disease. Biochem Biophys Res Commun 464: 369-375

Sgarbi G, Baracca A, Lenaz G, Valentino LM, Carelli V, Solaini G (2006) Inefficient coupling between proton transport and ATP synthesis may be the pathogenic mechanism for NARP and Leigh syndrome resulting from the T8993G mutation in mtDNA. Biochem J 395: 493-500

Sharma LK, Lu J, Bai Y (2009) Mitochondrial respiratory complex I: structure, function and implication in human diseases. Curr Med Chem 16: 1266-1277

Shchelochkov OA, Li FY, Wang J, Zhan H, Towbin JA, Jefferies JL, Wong LJ, Scaglia F (2010) Milder clinical course of Type IV 3-methylglutaconic aciduria due to a novel mutation in TMEM70. Mol Genet Metab 101: 282-285

Shi Y, Dierckx A, Wanrooij PH, Wanrooij S, Larsson NG, Wilhelmsson LM, Falkenberg M, Gustafsson CM (2012) Mammalian transcription factor A is a core component of the mitochondrial transcription machinery. Proc Natl Acad Sci U S A 109: 16510-16515

Shoubridge EA (2001) Nuclear genetic defects of oxidative phosphorylation. Hum Mol Genet 10: 2277-2284

Sibert BS, Patton JR (2012) Pseudouridine synthase 1: a site-specific synthase without strict sequence recognition requirements. Nucleic Acids Res 40: 2107-2118

Sikorska M, Sandhu JK, Simon DK, Pathiraja V, Sodja C, Li Y, Ribecco-Lutkiewicz M, Lanthier P, Borowy-Borowski H, Upton A, Raha S, Pulst SM, Tarnopolsky MA (2009) Identification of ataxia-associated mtDNA mutations (m.4052T>C and m.9035T>C) and evaluation of their pathogenicity in transmitochondrial cybrids. Muscle Nerve 40: 381-394

Sinkler CA, Kalpage H, Shay J, Lee I, Malek MH, Grossman LI, Hüttemann M (2017) Tissue- and Condition-Specific Isoforms of Mammalian Cytochrome. Oxid Med Cell Longev 2017: 1534056

Sládková J, Spáčilová J, Čapek M, Tesařová M, Hansíková H, Honzík T, Martínek J, Zámečník J, Kostková O, Zeman J (2015) Analysis of Mitochondrial Network Morphology in Cultured Myoblasts from Patients with Mitochondrial Disorders. Ultrastruct Pathol 39: 340-350

Soto IC, Fontanesi F, Liu J, Barrientos A (2012) Biogenesis and assembly of eukaryotic cytochrome c oxidase catalytic core. Biochimica et biophysica acta 1817: 883-897

Sperl W, Jesina P, Zeman J, Mayr JA, Demeirleir L, VanCoster R, Pícková A, Hansíková H, Houst'ková H, Krejcík Z, Koch J, Smet J, Muss W, Holme E, Houstek J (2006) Deficiency of mitochondrial ATP synthase of nuclear genetic origin. Neuromuscul Disord 16: 821-829

Spiegel R, Khayat M, Shalev SA, Horovitz Y, Mandel H, Hershkovitz E, Barghuti F, Shaag A, Saada A, Korman SH, Elpeleg O, Yatsiv I (2011) TMEM70 mutations are a common cause of nuclear encoded ATP synthase assembly defect: further delineation of a new syndrome. J Med Genet 48: 177-182

Spikes TE, Montgomery MG, Walker JE (2020) Structure of the dimeric ATP synthase from bovine mitochondria. Proc Natl Acad Sci U S A 117: 23519-23526

Staretz-Chacham O, Wormser O, Manor E, Birk OS, Ferreira CR (2019) TMEM70 deficiency: Novel mutation and hypercitrullinemia during metabolic decompensation. Am J Med Genet A 179: 1293-1298

Stenson PD, Ball EV, Mort M, Phillips AD, Shiel JA, Thomas NS, Abeysinghe S, Krawczak M, Cooper DN (2003) Human Gene Mutation Database (HGMD): 2003 update. Hum Mutat 21: 577-581

Stenton S, Masaru S, Piekutowska-Abramczuk D, Freisinger P, Distelmaier F, Mayr JA, Makowski C, Büchner B, Alhaddad B, Alston CL, Ardissone A, Ban R, Barić I, Berutti R, Brunet T, Ciara E, Deen D, Gagneur J, Ghezzi D, Gusic M, Haack TB, Hempel M, Husain RA, Karall D, Kölker S, Kotzaeridou U, Klopstock T, Kopajtich R, Konstantopoulou V, Liez St, Lenz D, Lim AZ, Mandel H, Müller-Felber W, Muñoz-Pujol G, Ohtake A, Okazaki Y, Olsen R, Pronicka E, Pyle A, Ribes A, Rokicki D, Santer R, Schiff M, Schuelke M, Smirnov D, Sperl W, Strom T, Tort F, Tsygankova P, Coster Rv (2022) Diagnosing pediatric mitochondrial disease: lessons from 2,000 exomes. Preprint. Genetic and Genomic Medicine,

Stewart JB, Chinnery PF (2015) The dynamics of mitochondrial DNA heteroplasmy: implications for human health and disease. Nat Rev Genet 16: 530-542

Stiburek L, Vesela K, Hansikova H, Pecina P, Tesarova M, Cerna L, Houstek J, Zeman J (2005) Tissue-specific cytochrome c oxidase assembly defects due to mutations in SCO2 and SURF1. Biochem J 392: 625-632

Stojanović V, Doronjski A (2013) Mild form of 3-methylglutaconic aciduria type IV and mutation in the TMEM70 genes. J Pediatr Endocrinol Metab 26: 151-154

Strauss M, Hofhaus G, Schröder RR, Kühlbrandt W (2008) Dimer ribbons of ATP synthase shape the inner mitochondrial membrane. EMBO J 27: 1154-1160

Stroud DA, Surgenor EE, Formosa LE, Reljic B, Frazier AE, Dibley MG, Osellame LD, Stait T, Beilharz TH, Thorburn DR, Salim A, Ryan MT (2016) Accessory subunits are integral for assembly and function of human mitochondrial complex I. Nature 538: 123-126

Štufková H, Kolářová H, Lokvencová K, Honzík T, Zeman J, Hansíková H, Tesařová M (2022) A Novel *MTTK* GeneVariant m.8315A > C as a Cause of MERRF Syndrome. Genes (Basel) 13

Su J, Liu D, Yang F, Zuo MQ, Li C, Dong MQ, Sun S, Sui SF (2022) Structural basis of Tom20 and Tom22 cytosolic domains as the human TOM complex receptors. Proc Natl Acad Sci U S A 119: e2200158119

Sun F, Huo X, Zhai Y, Wang A, Xu J, Su D, Bartlam M, Rao Z (2005) Crystal structure of mitochondrial respiratory membrane protein complex II. Cell 121: 1043-1057

Sánchez-Caballero L, Elurbe DM, Baertling F, Guerrero-Castillo S, van den Brand M, van Strien J, van Dam TJP, Rodenburg R, Brandt U, Huynen MA, Nijtmans LGJ (2020) TMEM70 functions in the assembly of complexes I and V. Biochim Biophys Acta Bioenerg 1861: 148202

Tang S, Wang J, Zhang VW, Li FY, Landsverk M, Cui H, Truong CK, Wang G, Chen LC, Graham B, Scaglia F, Schmitt ES, Craigen WJ, Wong LJ (2013) Transition to next generation analysis of the whole mitochondrial genome: a summary of molecular defects. Hum Mutat 34: 882-893

Tang T, Zheng B, Chen SH, Murphy AN, Kudlicka K, Zhou H, Farquhar MG (2009) hNOA1 interacts with complex I and DAP3 and regulates mitochondrial respiration and apoptosis. J Biol Chem 284: 5414-5424

Tesarova M, Vondrackova A, Stufkova H, Veprekova L, Stranecky V, Berankova K, Hansikova H, Magner M, Galoova N, Honzik T, Vodickova E, Stary J, Zeman J (2019) Sideroblastic anemia associated with multisystem mitochondrial disorders. Pediatr Blood Cancer 66: e27591

Theunissen TEJ, Nguyen M, Kamps R, Hendrickx AT, Sallevelt SCEH, Gottschalk RWH, Calis CM, Stassen APM, de Koning B, Mulder-Den Hartog ENM, Schoonderwoerd K, Fuchs SA, Hilhorst-Hofstee Y, de Visser M, Vanoevelen J, Szklarczyk R, Gerards M, de Coo IFM, Hellebrekers DMEI, Smeets HJM (2018) Whole Exome Sequencing Is the Preferred Strategy to Identify the Genetic Defect in Patients With a Probable or Possible Mitochondrial Cause. Front Genet 9: 400

Thompson K, Collier JJ, Glasgow RIC, Robertson FM, Pyle A, Blakely EL, Alston CL, Oláhová M, McFarland R, Taylor RW (2020) Recent advances in understanding the molecular genetic basis of mitochondrial disease. J Inherit Metab Dis 43: 36-50

Tomecki R, Dmochowska A, Gewartowski K, Dziembowski A, Stepien PP (2004) Identification of a novel human nuclear-encoded mitochondrial poly(A) polymerase. Nucleic Acids Res 32: 6001-6014

Torraco A, Verrigni D, Rizza T, Meschini MC, Vazquez-Memije ME, Martinelli D, Bianchi M, Piemonte F, Dionisi-Vici C, Santorelli FM, Bertini E, Carrozzo R (2012) TMEM70: a mutational hot spot in nuclear ATP synthase deficiency with a pivotal role in complex V biogenesis. Neurogenetics 13: 375-386

Tort F, Del Toro M, Lissens W, Montoya J, Fernàndez-Burriel M, Font A, Buján N, Navarro-Sastre A, López-Gallardo E, Arranz JA, Riudor E, Briones P, Ribes A (2011) Screening for nuclear genetic defects in the ATP synthase-associated genes TMEM70, ATP12 and ATP5E in patients with 3-methylglutaconic aciduria. Clin Genet 80: 297-300

Tsukihara T, Aoyama H, Yamashita E, Tomizaki T, Yamaguchi H, Shinzawa-Itoh K, Nakashima R, Yaono R, Yoshikawa S (1996) The whole structure of the 13-subunit oxidized cytochrome c oxidase at 2.8 A. Science 272: 1136-1144

Tucker K, Park E (2019) Cryo-EM structure of the mitochondrial protein-import channel TOM complex at near-atomic resolution. Nat Struct Mol Biol 26: 1158-1166

Valnot I, von Kleist-Retzow JC, Barrientos A, Gorbatyuk M, Taanman JW, Mehaye B, Rustin P, Tzagoloff A, Munnich A, Rötig A (2000) A mutation in the human heme A:farnesyltransferase gene (COX10) causes cytochrome c oxidase deficiency. Hum Mol Genet 9: 1245-1249

Valpadashi A, Callegari S, Linden A, Neumann P, Ficner R, Urlaub H, Deckers M, Rehling P (2021) Defining the architecture of the human TIM22 complex by chemical crosslinking. FEBS Lett 595: 157-168

van Belzen R, Kotlyar AB, Moon N, Dunham WR, Albracht SP (1997) The iron-sulfur clusters 2 and ubisemiquinone radicals of NADH:ubiquinone oxidoreductase are involved in energy coupling in submitochondrial particles. Biochemistry 36: 886-893

van der Bliek AM, Shen Q, Kawajiri S (2013) Mechanisms of mitochondrial fission and fusion. Cold Spring Harb Perspect Biol 5

Vercellino I, Sazanov LA (2021) Structure and assembly of the mammalian mitochondrial supercomplex CIII. Nature 598: 364-367

Vercellino I, Sazanov LA (2022) The assembly, regulation and function of the mitochondrial respiratory chain. Nat Rev Mol Cell Biol 23: 141-161

Verny C, Guegen N, Desquiret V, Chevrollier A, Prundean A, Dubas F, Cassereau J, Ferre M, Amati-Bonneau P, Bonneau D, Reynier P, Procaccio V (2011) Hereditary spastic paraplegia-like disorder due to a mitochondrial ATP6 gene point mutation. Mitochondrion 11: 70-75

Vinothkumar KR, Zhu J, Hirst J (2014) Architecture of mammalian respiratory complex I. Nature 515: 80-84

Vogel RO, van den Brand MA, Rodenburg RJ, van den Heuvel LP, Tsuneoka M, Smeitink JA, Nijtmans LG (2007) Investigation of the complex I assembly chaperones B17.2L and NDUFAF1 in a cohort of CI deficient patients. Mol Genet Metab 91: 176-182

Vrbacký M, Kovalčíková J, Chawengsaksophak K, Beck IM, Mráček T, Nůsková H, Sedmera D, Papoušek F, Kolář F, Sobol M, Hozák P, Sedlacek R, Houštěk J (2016) Knockout of Tmem70 alters biogenesis of ATP synthase and leads to embryonal lethality in mice. Hum Mol Genet 25: 4674-4685

Wagner K, Perschil I, Fichter CD, van der Laan M (2010) Stepwise assembly of dimeric F(1)F(o)-ATP synthase in mitochondria involves the small F(o)-subunits k and i. Mol Biol Cell 21: 1494-1504

Walker JE (2013) The ATP synthase: the understood, the uncertain and the unknown. Biochem Soc Trans 41: 1-16

Wang T, Liu H, Itoh K, Oh S, Zhao L, Murata D, Sesaki H, Hartung T, Na CH, Wang J (2021) C9orf72 regulates energy homeostasis by stabilizing mitochondrial complex I assembly. Cell Metab 33: 531-546.e539

Wang ZG, White PS, Ackerman SH (2001) Atp11p and Atp12p are assembly factors for the F(1)-ATPase in human mitochondria. J Biol Chem 276: 30773-30778

Wasilewski M, Chojnacka K, Chacinska A (2017) Protein trafficking at the crossroads to mitochondria. Biochim Biophys Acta Mol Cell Res 1864: 125-137

Watson E, Davis R, Sue C (2020) New diagnostic pathways for mitochondrial disease. *J Transl Genet Genom* 4: 188-202

Weinberg SE, Sena LA, Chandel NS (2015) Mitochondria in the regulation of innate and adaptive immunity. Immunity 42: 406-417

Westermann B (2012) Bioenergetic role of mitochondrial fusion and fission. Biochimica et biophysica acta 1817: 1833-1838

Wirth C, Brandt U, Hunte C, Zickermann V (2016) Structure and function of mitochondrial complex I. Biochimica et biophysica acta 1857: 902-914

Wiseman DH, May A, Jolles S, Connor P, Powell C, Heeney MM, Giardina PJ, Klaassen RJ, Chakraborty P, Geraghty MT, Major-Cook N, Kannengiesser C, Thuret I, Thompson AA, Marques L, Hughes S, Bonney DK, Bottomley SS, Fleming MD, Wynn RF (2013) A novel syndrome of congenital sideroblastic anemia, B-cell immunodeficiency, periodic fevers, and developmental delay (SIFD). Blood 122: 112-123

Wittig I, Meyer B, Heide H, Steger M, Bleier L, Wumaier Z, Karas M, Schägger H (2010) Assembly and oligomerization of human ATP synthase lacking mitochondrial subunits a and A6L. Biochimica et biophysica acta 1797: 1004-1011

Wittig I, Schägger H (2005) Advantages and limitations of clear-native PAGE. Proteomics 5: 4338-4346

Wittig I, Schägger H (2008) Structural organization of mitochondrial ATP synthase. Biochimica et biophysica acta 1777: 592-598

Wong LC, Chen T, Schmitt ES, Wang J, Tang S, Landsverk M, Li F, Zhang S, Wang Y, Zhang VW, Craigen WJ (2020) Clinical and laboratory interpretation of mitochondrial mRNA variants. Hum Mutat 41: 1783-1796

Wortmann SB, Rodenburg RJ, Jonckheere A, de Vries MC, Huizing M, Heldt K, van den Heuvel LP, Wendel U, Kluijtmans LA, Engelke UF, Wevers RA, Smeitink JA, Morava E (2009) Biochemical and genetic analysis of 3-methylglutaconic aciduria type IV: a diagnostic strategy. Brain 132: 136-146

Xia D, Esser L, Tang WK, Zhou F, Zhou Y, Yu L, Yu CA (2013) Structural analysis of cytochrome bc1 complexes: implications to the mechanism of function. Biochim Biophys Acta 1827: 1278-1294

Yang XH, Trumpower BL (1986) Purification of a three-subunit ubiquinol-cytochrome c oxidoreductase complex from Paracoccus denitrificans. J Biol Chem 261: 12282-12289

Yang Z, Slone J, Huang T (2022) Next-Generation Sequencing to Characterize Mitochondrial Genomic DNA Heteroplasmy. Curr Protoc 2: e412

Yin Z, Burger N, Kula-Alwar D, Aksentijević D, Bridges HR, Prag HA, Grba DN, Viscomi C, James AM, Mottahedin A, Krieg T, Murphy MP, Hirst J (2021) Structural basis for a complex I mutation that blocks pathological ROS production. Nat Commun 12: 707

Young MJ, Copeland WC (2016) Human mitochondrial DNA replication machinery and disease. Curr Opin Genet Dev 38: 52-62

Yu C, Zhao J, Yan L, Qi Y, Guo X, Lou Z, Hu J, Rao Z (2020) Structural insights into G domain dimerization and pathogenic mutation of OPA1. J Cell Biol 219

Zech M, Kopajtich R, Steinbrücker K, Bris C, Gueguen N, Feichtinger RG, Achleitner MT, Duzkale N, Périvier M, Koch J, Engelhardt H, Freisinger P, Wagner M, Brunet T, Berutti R, Smirnov D, Navaratnarajah T, Rodenburg RJT, Pais LS, Austin-Tse C, O'Leary M, Boesch S, Jech R, Bakhtiari S, Jin SC, Wilbert F, Kruer MC, Wortmann SB, Eckenweiler M, Mayr JA, Distelmaier F, Steinfeld R, Winkelmann J, Prokisch H (2022) Variants in Mitochondrial ATP Synthase Cause Variable Neurologic Phenotypes. Ann Neurol 91: 225-237

Zhang J, Shang J, Wang F, Huo X, Sun R, Ren Z, Wang W, Yang M, Li G, Gao D, Liu R, Bai P, Wang S, Wang Y, Yan X (2022) Decreased mitochondrial D-loop region methylation mediates an increase in mitochondrial DNA copy number in CADASIL. Clin Epigenetics 14: 2

Zhu J, Vinothkumar KR, Hirst J (2016) Structure of mammalian respiratory complex I. Nature 536: 354-358

10. SUPPLEMENTS

Supplement 1)

Hejzlarová, K., Tesařová, M., Vrbacká-Čížková, A., Vrbacký, M., Hartmannová, H., Kaplanová, V., Nosková, L., **Kratochvílová, H**., Buzková, J., Havlíčková, V., Zeman, J., Kmoch, S., Houštěk, J. (2011). **Expression and processing of the TMEM70 protein.** Biochimica et biophysica acta 1807, 144-149. IF = 4.843, Quartile Score = Q1 (2011).

Biochimica et Biophysica Acta 1807 (2011) 144–149

Contents lists available at ScienceDirect

Biochimica et Biophysica Acta

journal homepage: www.elsevier.com/locate/bbabio

Expression and processing of the TMEM70 protein

Kateřina Hejzlarová [a], Markéta Tesařová [b], Alena Vrbacká-Čížková [a,c], Marek Vrbacký [a], Hana Hartmannová [c], Vilma Kaplanová [a], Lenka Nosková [c], Hana Kratochvílová [b], Jana Buzková [b], Vendula Havlíčková [a], Jiří Zeman [b], Stanislav Kmoch [c], Josef Houštěk [a,*]

[a] Institute of Physiology Academy of Sciences of the Czech Republic, 142 20 Prague, Czech Republic
[b] Department of Pediatrics and Adolescent Medicine, 1st Faculty of Medicine, Charles University and General University Hospital, 120 00 Prague, Czech Republic
[c] Institute for Inherited Metabolic Diseases, 1st Faculty of Medicine, Charles University and General University Hospital, 120 00 Prague, Czech Republic

ARTICLE INFO

Article history:
Received 21 July 2010
Received in revised form 30 September 2010
Accepted 5 October 2010
Available online 16 October 2010

Keywords:
Mitochondria
ATP synthase
TMEM70
Biogenesis

ABSTRACT

TMEM70 protein represents a novel ancillary factor of mammalian ATP synthase. We have investigated import and processing of this factor in human cells using GFP- and FLAG-tagged forms of TMEM70 and specific antibodies. TMEM70 is synthesized as a 29 kDa precursor protein that is processed to a 21 kDa mature form. Immunocytochemical detection of TMEM70 showed mitochondrial colocalization with MitoTracker Red and ATP synthase. Western blot of subcellular fractions revealed the highest signal of TMEM70 in isolated mitochondria and mitochondrial location was confirmed by mass spectrometry analysis. Based on analysis of submitochondrial fractions, TMEM70 appears to be located in the inner mitochondrial membrane, in accordance with predicated transmembrane regions in the central part of the TMEM70 sequence. Two-dimensional electrophoretic analysis did not show direct interaction of TMEM70 with assembled ATP synthase but indicated the presence of dimeric form of TMEM70. No TMEM70 protein could be found in cells and isolated mitochondria from patients with ATP synthase deficiency due to TMEM70 c.317-2A>G mutation thus confirming that TMEM70 biosynthesis is prevented in these patients.

1. Introduction

Biogenesis of eukaryotic ATP synthase is a stepwise process, in which 16 different subunits assemble the structure of the enzyme consisting of the F_1 catalytic part and the membranous F_o part connected together by two stalks [1,2]. The biosynthesis of individual subunits and formation of the ATP synthase holoenzyme depend on several specific helper proteins that are partly common to, and partly unique to, higher and lower eukaryotes. Several yeast-specific factors (NCA1-3, NAM1, AEP1-3 ATP22 and ATP25) are involved in mRNA stability, translation and processing of mtDNA encoded subunits ATP6 and ATP9 [1,3–5] or their assembly (ATP10, ATP22). Additional factor ATP23 [5,6], the metalloprotease with chaperone activity is implicated in processing of ATP6 and its association with ATP9 oligomer. There exists mammalian ortholog of ATP23 which contains a HEXXH motif of the protease active site, but its function is unknown. The only two yeast factors that are found in mammals [1,7,8], having identical function are the F_1 chaperones, ATPAF1 and ATPAF2, interacting with F_1 subunits β and α. Both are absolutely essential for assembly of the functional $\alpha_3\beta_3$ heterooligomer. The FMC1, the third factor involved in F_1 assembly in yeast at high temperature [9] is again specific for yeast. Till now, only one essential ancillary factor, the TMEM70 protein, has been found in mammals being absent in yeast and fungi [10,11]. The mutations in *TMEM70* gene were found to be responsible for isolated deficiency of ATP synthase leading to a severe mitochondrial disease [10,12]. The enzyme defect was rescued by the wtTMEM70. The TMEM70 protein was identified as a putative mitochondrial protein that fulfils the criteria of MITOCARTA [13,14]. The biological roles, as well as biogenesis of this protein remain unknown. In this study we attempted to use tagged forms of TMEM70 and specific antibodies for characterization of expression, processing and localization of this factor.

2. Materials and methods

2.1. Cell cultures

Human embryonic kidney cells (HEK293, CRL-1573, ATCC) were grown in high-glucose DMEM medium (PAA) supplemented with 10% (v/v) fetal calf serum (PAA) at 37 °C in 5% CO_2 in air. Fibroblasts were grown in DMEM medium (Sigma) containing 10% fetal calf serum (Sigma), penicillin (100 U/mL) and streptomycin (100 μg/mL), at 37 °C in 5% CO_2 in air. Confluent cells were harvested by trypsinization

Abbreviations: DDM, dodecyl maltoside; F_1, catalytic part of ATP synthase; F_o, membrane embedded part of ATP synthase; PDH, pyruvate dehydrogenase

* Corresponding author. Institute of Physiology, Academy of Sciences of the Czech Republic, Vídeňská 1083, 142 20 Prague 4, Czech Republic. Tel.: +420 2 4106 2434; fax: +420 2 4106 2149.
E-mail address: houstek@biomed.cas.cz (J. Houštěk).

0005-2728/$ – see front matter © 2010 Elsevier B.V. All rights reserved.
doi:10.1016/j.bbabio.2010.10.005

and washed twice with PBS (8 g/L NaCl, 0.2 g/L KCl, 1.15 g/L Na_2HPO_4, 0.20 g/L KH_2PO_4).

2.2. Expression vectors

TMEM70 cDNA clone MHS1011-60493 was obtained from Open Biosystems. Following the sequence verification, the insert was transferred into the mammalian expression vector pEF-DEST51 using the Gateway technology (Invitrogen). Resulting plasmids TMEM70-pEF-DEST51 were propagated in *Escherichia coli*, isolated and fully sequenced before the transfection. *TMEM70-Flag* cDNA expression vector—the full-length human *TMEM70* coding sequence was amplified from the IMAGE clone 3631570 and inserted into the C-FLAG fusion mammalian expression vector pCMV-Tag4 (Stratagene). The fidelity of the construct was confirmed by sequencing. *TMEM70-GFP* cDNA expression vector [13] was kindly provided by Dr V.K. Mootha.

2.3. Transfections

Vectors were transfected into the fibroblast or HEK293 cell lines (2 μg of DNA/5×10^5 cells) using Nucleofector device and NHDF nucleofection kit (Amaxa/Lonza), following the standard protocol. For the transient expression of the TMEM70-FLAG fusion protein, cell transfection was carried out with Express-In Transfection Reagent (Open Biosystems). Transfected cell lines were cultured for 48 h on BD Falcon 4-well CultureSlides.

2.4. Isolation of mitochondria

HEK293 cells (1×10^7) were harvested by trypsinization, washed twice in PBS, re-suspended in isotonic STE buffer (250 mM sucrose, 10 mM Tris–HCl, pH 7.4, 1 mM EDTA, 0.2% (v/v) Protease Inhibitor Cocktail (PIC, Sigma P8340)), and disrupted on ice using Dounce homogenizer. Homogenate was centrifuged for 15 min at 600*g* and 4 °C, the post-nuclear supernatant was centrifuged for 25 min at 10,000*g* and 4 °C. The resulting supernatant corresponding to the cytoplasm fraction was collected and the mitochondrial pellet was washed by centrifugation with STE buffer.

Fibroblast mitochondria were isolated by the method utilizing the hypotonic shock cell disruption [15]. To avoid proteolytic degradation, the isolation medium (250 mM sucrose, 40 mM KCl, 20 mM Tris–HCl, 2 mM EGTA, pH 7.6) was supplemented with the 0.2% PIC. The isolated mitochondria were stored at −80 °C.

Rat liver mitochondria for import studies were isolated by the method of Enriquez et al. [16].

2.5. Submitochondrial fractionation

Fractionation of mitochondria from HEK293 cells was carried out according to Satoh et al. [17] with slight modifications. Briefly, isolated mitochondria were re-suspended in STE buffer at final concentration 1 mg/mL and disrupted by repeated freezing-thawing 3 times followed by sonication on ice for 5 s at 20% amplitude and 0.5 cycle using an UP 200S Ultrasonic Processor (Hielscher, Germany). Unbroken mitochondria were removed by centrifugation at 10,000*g* for 10 min. The soluble mitochondrial proteins and membranes were separated by centrifugation of the supernatant at 100,000*g* for 35 min. The pellet was re-suspended in 100 mM sodium carbonate, pH 11.5, and incubated at 4 °C and continuous vortexing for 30 min followed by centrifugation at 100,000*g* and 4 °C for 40 min. Supernatant containing membrane associated proteins was collected and the pellet was re-suspended in STE buffer. All collected fractions were kept at −80 °C until analysis.

2.6. TMEM70 antibodies

The cDNA sequence encoding 50–260 AA of human TMEM70, corresponding to expected mature part of the protein was cloned into pMAL-c2 expression vector (New England Biolabs). The construct with the correct sequence was introduced into the *E. coli* MAX Efficiency DH5αF'IQ cells and the fusion protein MBP-TMEM70 was expressed upon IPTG induction. Fusion protein was isolated from sonicated and detergent solubilized cell lysate (20 mM Tris–HCl, 0.2 M NaCl, 1 mM EDTA, 1% Nonidet P-40) using amylose resin column (New England Biolabs). The protein was eluted from the column by 50 mM maltose and directly used for rabbit immunization (Open Biosystems).

2.7. Electrophoresis and Western blot analysis

SDS-PAGE, two-dimensional BN/SDS-PAGE and Western blot analysis were performed by standard protocols as previously [18,19] using specific primary antibodies against GFP (Santa Cruz Biotechnology), FLAG (Sigma), cytochrome *c* oxidase subunit Cox1, ATPase β subunit, PDH E1 α subunit (Mitosciences), MtHSP70 (Alexis Biochemicals), α-Tubulin (Cell Signaling), a mixture of antibodies to respiratory chain proteins (MS603 to ATPase α, Core2, NDUFA9, SDH70, Cox4; Mitosciences), or the polyclonal rabbit antibody to TMEM70. The immunoblots were detected with peroxidase-conjugated secondary antibodies and SuperSignal West Femto Maximum Sensitivity Substrate (Thermo Scientific) using VersaDoc 4000 Imaging System (Bio-Rad), or with fluorescent secondary antibodies (Alexa Fluor 680, Molecular Probes) on an Odyssey infrared imaging system (LI-COR).

2.8. Immunocytochemistry

Fibroblast cells were grown on glass chamber slides (BD Falcon 4-well CultureSlides). After 48 h, the cells were washed with PBS, fixed and permeabilized for 10 min with methanol at −20 °C or with paraformaldehyde for 10 min at 4 °C. After blocking unspecific sites with 5% FBS, cells were incubated overnight at 4 °C with indicated antibody in 5% FBS followed by 60 min incubation at 37 °C with fluorophore-conjugated secondary antibody (1 μg/mL, Molecular Probes). The following primary antibodies were used: mouse monoclonal (MS503, Mitosciences) or polyclonal [20] to F_1 β subunit, mouse monoclonal to FLAG (Sigma), or rabbit polyclonal antibody to TMEM70.

When using MitoTracker Red (Molecular Probes), cells were incubated in 300 nM prewarmed medium solution of MitoTracker Red at 37 °C for 15 min, washed with fresh prewarmed medium, fixed and permeabilized. Nuclei were stained with 4',6-diamidino-2-phenylindole (DAPI). Prepared slides were mounted in fluorescence mounting medium Immu-Mount (ShandonLipshaw) and analyzed by confocal microscopy (Nikon Eclipse TE2000, Leica AOBS—Acusto-Optical Beam Splitter) and/or epifluorescent microscopy (widefield epifluorescent microscope Nikon Eclipse E400).

2.9. Mitochondrial import

Protein precursor was synthesized in the presence of ^{35}S-methionine using TNT T7 Quick Coupled Transcription/Translation System (Promega) with plasmid vector or PCR product as a DNA template, according to manufacturer's recommendation. Translation product was centrifuged at 13,000*g* for 2 min and supernatant was used for import to isolated rat liver mitochondria or human HEK293 mitochondria.

The import reaction was carried out in 50 μL of a medium containing 25 mM sucrose, 75 mM sorbitol, 100 mM KCl, 10 mM KH_2PO_4, 0.05 mM EDTA, 5 mM $MgCl_2$, 10 mM Tris–HCl, 1 mg BSA/mL,

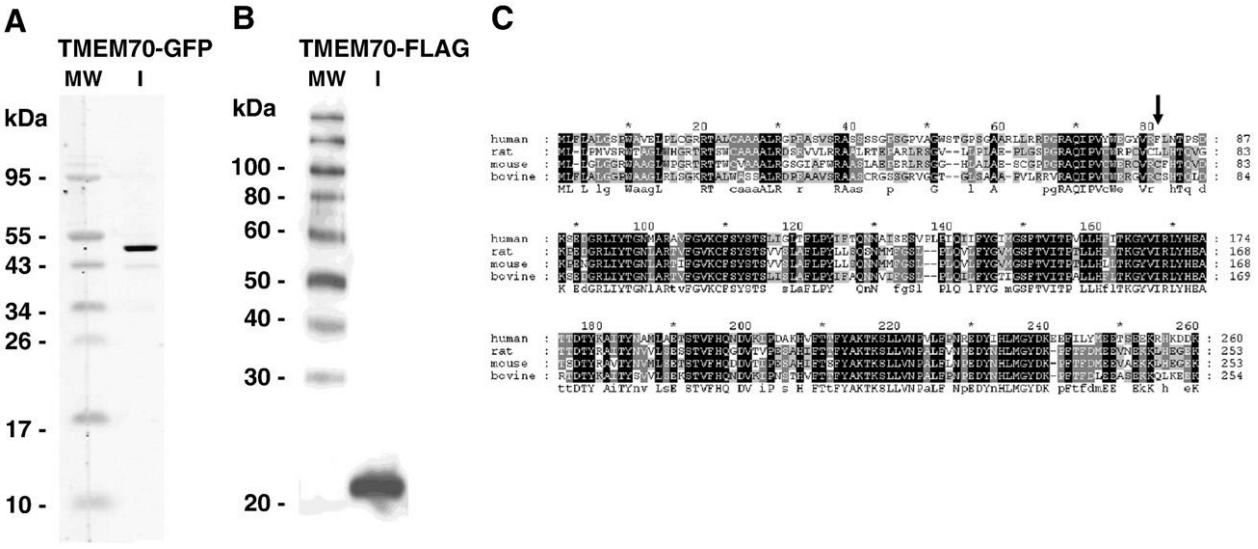

Fig. 1. The size of mature TMEM70. Western blot analysis of TMEM70-GFP (A) and TMEM70-FLAG (B) expressed in fibroblast and HEK293 cells. (C) Alignment of human (NCBI GI: 34147498), rat (157823940), mouse (15030135) and bovine (148878159) TMEM70 protein sequence; arrow indicates predicted cleavage site of the TMEM70 precursor protein.

1 mM methionine, pH 7.4, [21] and 2 mg protein/mL of freshly isolated mitochondria. Incubation with ^{35}S labeled-translation product was performed for 30 min at 30 °C, in presence or absence of 4 μM FCCP. Indicated samples were treated with 0.16 mg trypsin/mL for 20 min on ice. Then 4 μM PMSF (phenylmethanesulfonyl fluoride) was added to all samples and mitochondria were sedimented and washed twice by centrifugation at 13,000*g* for 2 min at 4 °C. Samples were analyzed by SDS-PAGE and radioactivity was detected using BAS-5000 system (Fuji).

2.10. Ethics

The project was approved by the Scientific Ethics Committees of the 1st Faculty of Medicine of Charles University in Prague and Institute of Physiology, Academy of Sciences of the Czech Republic. Patient participation in the project was made on a voluntary basis after oral and written information and consent according to the Helsinki V Declaration.

3. Results and discussion

As shown in Fig. 1A, the *TMEM70-GFP* construct is well expressed in human fibroblasts or HEK293 cells yielding a protein band of about 46 kDa. The *TMEM70* gene encodes 260 amino acids protein of expected MW of 29.0 kDa and the tagged TMEM70-GFP protein of 260 + 238 amino acids has calculated MW of 55.9 kDa. The difference between calculated and observed size of the TMEM70-GFP is ~10 kDa and corresponds well with predicted cleavable N-terminal sequence of 81 amino acids (Fig. 1C). Similar experiment using *TMEM70-FLAG* construct (Fig. 1B) revealed the size of expressed protein of approximately 22 kDa and thus both tagged forms of the TMEM70 supported the conclusion that this protein is synthesized as a precursor that is processed into a ~21 kDa mature form of 179 AA.

To obtain specific antibodies to TMEM70 protein, we have expressed mature part of TMEM70 in a form of a fusion protein with maltose binding protein (MBP-TMEM70) in *E. coli*. Resulting protein was isolated and used for immunization. As shown by SDS-PAGE/WB analysis in Fig. 2, the anti-TMEM70 antibody recognized a

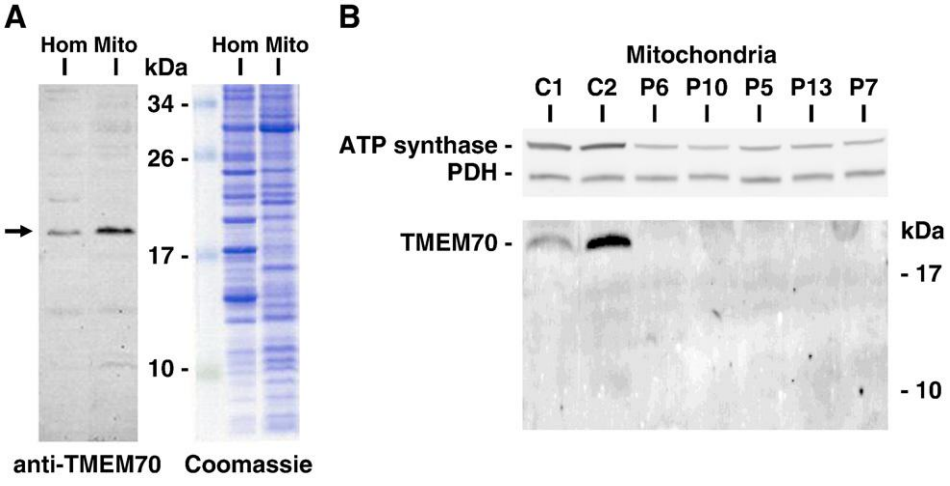

Fig. 2. Mature TMEM70 of ~21 kDa is absent in patients with ATP synthase deficiency. (A) Western blot detection of TMEM70 by polyclonal antibody in human heart homogenate and mitochondria. (B) Western blot detection of ATP synthase (β subunit), PDH (E1 α subunit) and TMEM70 in fibroblast mitochondria from control (C1, C2) and indicated patients (P) with *TMEM70* c.317-2A>G mutation.

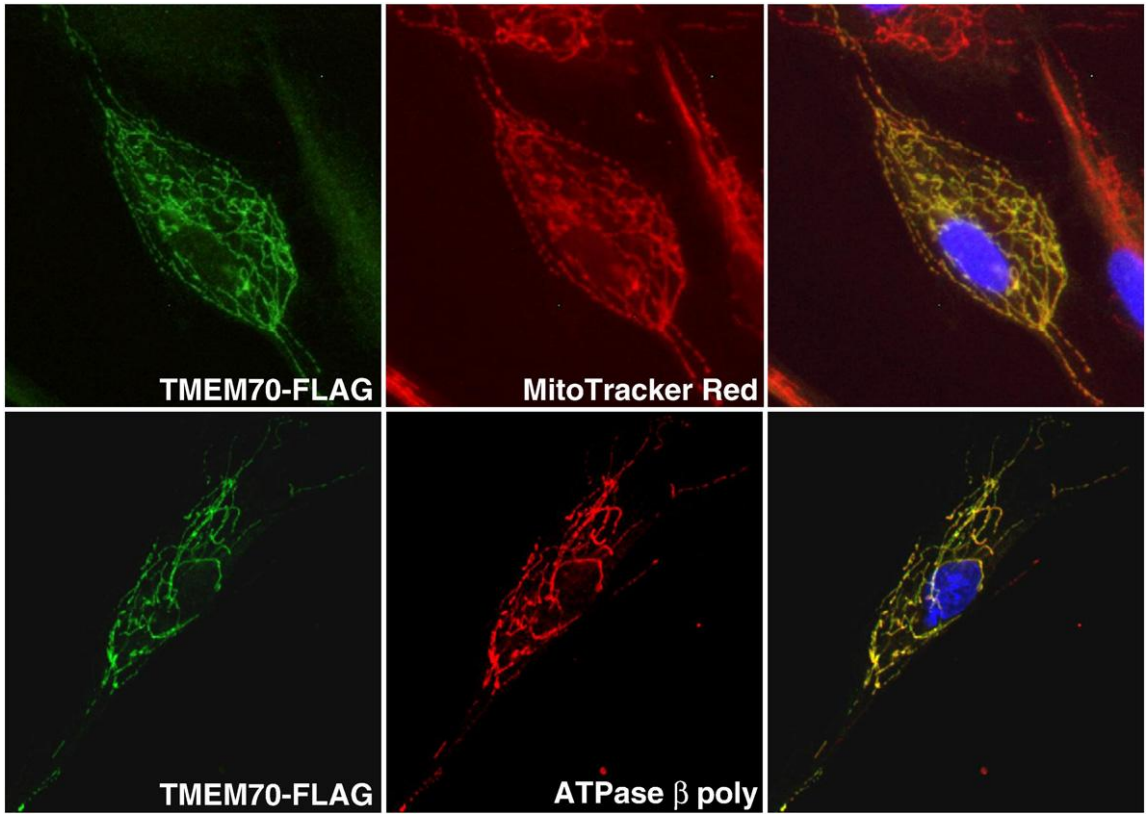

Fig. 3. Subcellular localization of TMEM70-FLAG with respect to MitoTracker Red or ATP synthase in human fibroblasts. Last column represents an overlay of the first two columns and shows cell nuclei stained with DAPI (blue).

20 kDa band in tissue homogenate of control human heart that was concentrated in isolated mitochondria (10,000*g*). The immunoreactive band was absent in fibroblast mitochondria (Fig. 2B) of the patients with ATP synthase deficiency due to the homozygous *TMEM70* mutation c.317-2A>G. This mutation at the second intron of TMEM70 gene has been shown to results in aberrant splicing and loss of *TMEM70* mRNA [10]. WB with anti-TMEM70 antibody thus confirmed previous conclusion that normal TMEM70 protein is absent in patient mitochondria. There was no immunoreactive band at lower molecular weight region indicating that no aberrant TMEM70 protein is produced in patient cells.

The presence of TMEM70 protein was also verified by mass spectrometry. LC-MS/MS analysis performed on mitochondria, whole tissue homogenates or 100,000*g* microsomal fraction from human heart and mouse heart or liver did not detect the TMEM70 protein. However, when a targeted approach was used (Supplementary Fig. S1), based on the knowledge of the retention time, precise mass and fragmentation spectrum of the human TMEM70 protein (MS/MS analysis of MBP-humanTMEM70 fusion protein), TMEM70 HVFTTFYAK tryptic peptide that is not present in any other human protein was found in the approximately 18–23 kDa region sample of isolated human heart mitochondria. MS analysis thus confirmed mitochondrial location of TMEM70 and further indicated that the cellular content of the TMEM70 is very low.

This conclusion is also supported by existing expression profile data (http://biogps.gnf.org/), which show that the level of *TMEM70* transcripts is extremely low in human cells and tissues (Supplementary Fig. S2), being several orders of magnitude lower than the level of mRNAs for structural subunits of ATP synthase (e.g. *ATP5B* mRNA for F_1 β subunit). The *TMEM70* mRNA levels are thus similarly low as the levels of transcripts of *ATPAF1* and *ATPAF2* assembly factors [1], the content of which is very small in mammalian tissues (Supplementary Fig. S2 and [22]). Furthermore, *TMEM70* transcripts show very small variation among various tissues, similarly as *ATPAF2*, characteristic for housekeeping genes. All these data thus support the view that the TMEM70 protein, ancillary factor of ATP synthase biogenesis is a low abundant mitochondrial protein, not exerting tissue-specificity.

Cellular localization of TMEM70 protein was further analyzed at a morphological level in cultured fibroblasts. For experiments the cells transfected with tagged *TMEM70* or control cells expressing the *wtTMEM70* were used. As shown in Fig. 3, in cells transfected with

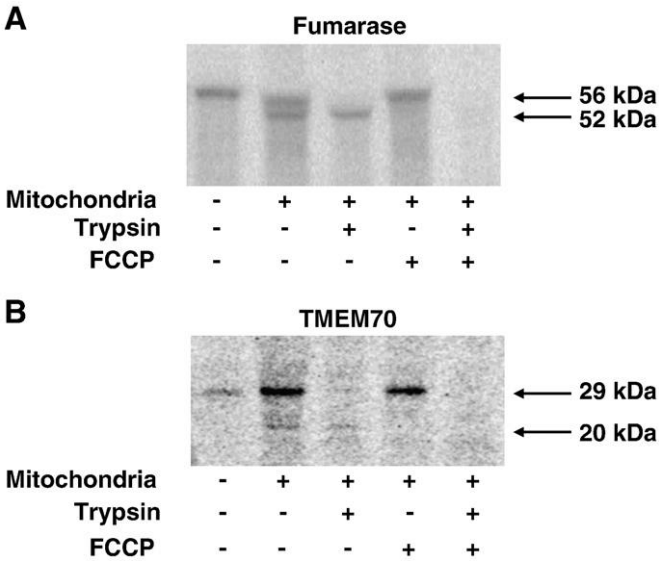

Fig. 4. Import of TMEM70 to mitochondria. *In vitro* translated human fumarase (A) and TMEM70 (B) were processed and imported to isolated rat liver mitochondria. Upon the import, the mature forms of both proteins resisted to trypsin and their import was prevented by uncoupler of oxidative phosphorylation FCCP.

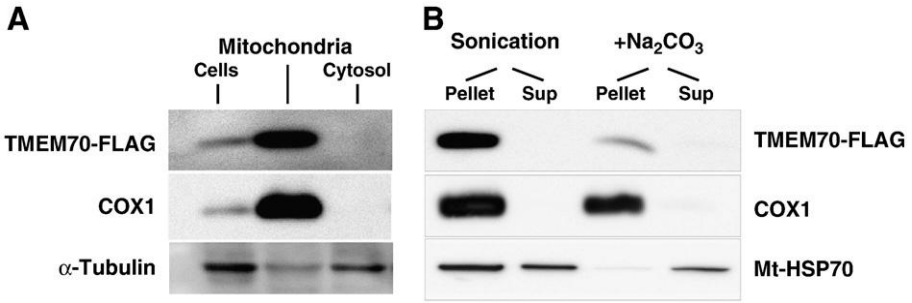

Fig. 5. TMEM70 is a membrane bound mitochondrial protein. HEK293 cells were transfected with *TMEM70-FLAG* and (A) cell homogenate, isolated mitochondria and cytosolic fractions were analyzed. (B) Isolated mitochondria were sonicated and extracted with Na_2CO_3 and 100,000*g* pellet and supernatant were prepared. Western blot was performed with indicated antibodies.

TMEM70-FLAG the tagged TMEM70 signal detected by anti-FLAG antibody colocalized with the signal of MitoTracker Red and with the signal of mitochondrial ATP synthase, detected with antibody to β subunit of the F_1 catalytic part, in accordance with previously demonstrated mitochondrial localization of TMEM70-GFP [13]. Antibody to TMEM70 protein also confirmed mitochondrial localization in control cells, but it was less specific in immunocytochemical experiments (not shown).

To assess further the basic properties of TMEM70 import to mitochondria, we have synthesized radioactive TMEM70 *in vitro* using coupled transcription-translation system and followed its import to isolated mitochondria. For comparison, we analyzed import of matrix located fumarase, as an example of mitochondrial protein that is synthesized with cleavable N-terminal sequence. As shown in Fig. 4A, the import analyses with isolated liver mitochondria showed a 56 kDa precursor and a 52 kDa mature form of fumarase, with expected sensitivity to trypsin and/or uncoupler. Analysis of TMEM70 protein revealed ~29 kDa band produced by *in vitro* translation and additional band of ~20 kDa present in the mitochondrial pellet. The 29 kDa band was sensitive to protease indicating its extramitochondrial localization typical for a precursor form. The 20 kDa band was resistant to protease but it disappeared in the presence of uncoupler, thus confirming the intramitochondrial localization of the TMEM70 mature form. Interestingly, there was only small amount of the mature 20 kDa protein found relative to the amount of precursor added. These data indicate that upon cleavage of the N-terminal part, the mature TMEM70 is rather labile at the conditions of *in vitro* import assay, or that additional cellular components are required for its import *in vivo*. However, similar pattern was observed when using mitochondria of human origin isolated from HEK293 cells or in co-translational import assay.

To characterize further the mitochondrial localization of TMEM70, we have investigated HEK293 cells expressing the *TMEM70-FLAG* construct, which is only slightly larger than the *wtTMEM70*. When we have isolated mitochondria from the cells expressing the TMEM70-FLAG protein, we found that the TMEM70-FLAG was fully recovered in mitochondria while it was absent in the cytosolic fraction (Fig. 5A). Then we fractionated the isolated mitochondria by sonication and treated the mitochondrial membranes with Na_2CO_3. Analysis of 100,000*g* pellet and supernatant by SDS-PAGE and WB (Fig. 5B) fully recovered the TMEM70-FLAG in the sediment, similarly as cytochrome *c* oxidase (COX), indicating its localization in the mitochondrial membrane. Efficiency of the treatments was verified by antibody to matrix located HSP70 that was quantitatively recovered in the soluble fractions.

Finally, to search for native conformation of TMEM70, we have extracted fibroblast mitochondria with mild detergent dodecyl maltoside (DDM) and analyzed the solubilized proteins by two-dimensional BN-PAGE/SDS-PAGE and WB. As demonstrated in Fig. 6, TMEM70 was found as two spots of identical mobility in the second

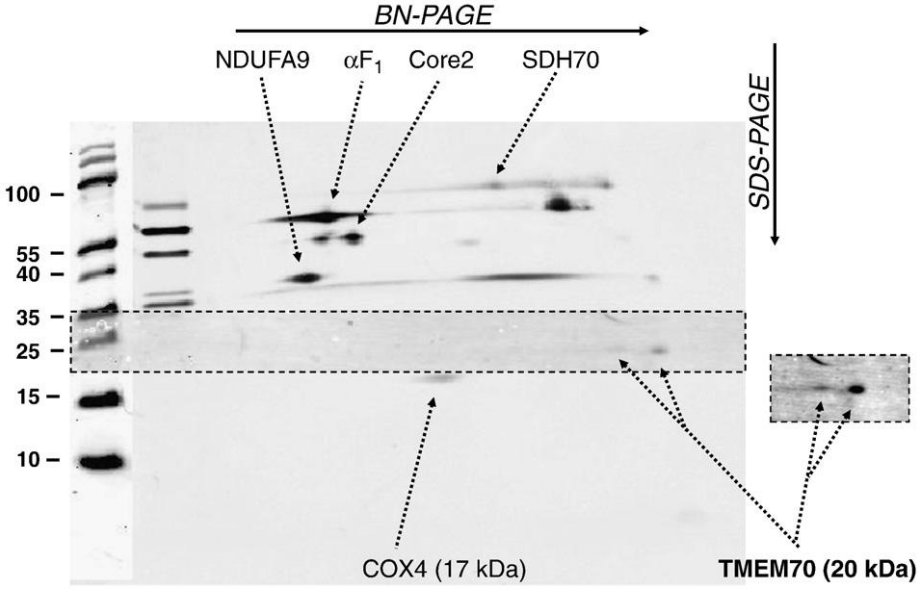

Fig. 6. DDM-solubilized mitochondrial proteins reveal a dimeric form of TMEM70. Fibroblast mitochondria were solubilized with DDM (1 g/g protein) and 30,000*g* supernatant was analyzed by two-dimensional electrophoresis (BN/SDS-PAGE) and WB using antibodies to indicated proteins. Dashed line frames the region probed with anti-TMEM70 antibody (higher intensity signal shown on the right).

dimension, corresponding to 21 kDa. Their mobility in the first dimension BN-PAGE gel was approximately 20 and 40 kDa. Parallel detection of ATP synthase and respiratory chain complexes did not reveal any association of TMEM70 with the assembled ATP synthase complex or free α or β subunits and indicated that TMEM70 exists in monomeric and dimeric forms when solubilized with detergent DDM.

Taken together, our experiments convincingly demonstrated that TMEM70 is a membrane bound 21 kDa mitochondrial protein that is synthesized as a 29 kDa precursor. TMEM70 is firmly associated with inner mitochondrial membrane and it does not interact directly with the ATP synthase complex. Very low cellular content of this protein, analogous to low content of ATPAF1 and ATPAF2 chaperones [23] supports the view of a regulatory — catalytic role of TMEM70 in ATP synthase biogenesis. It also indicates that putative interacting partner of TMEM70 might be similarly low-abundant protein(s), as are for example F_1 assembly intermediates [24]. A larger form of TMEM70 on two-dimensional gels appears to be a dimer according to calculated molecular weight, but we cannot exclude that it represents TMEM70 interacting with some other protein, although it cannot be the large ATP synthase subunits. Absence of TMEM70 in patient cells containing small amounts of functional ATP synthase complex [10,11] indicates that TMEM70 is not absolutely essential for ATP synthase biogenesis. Further studies are needed to elucidate the biological role of this factor. A unique specificity of TMEM70 to higher eukaryotes prevents the use of yeast cells, but the studies utilizing overexpression of TMEM70, various tagged forms as well as crosslinking and preparation of antibodies allowing for specific immunoprecipitation may represent a perspective strategy.

Acknowledgments

Dr. Miloslav Šanda is acknowledged for performing mass spectrometry analysis and Jana Sovová for assisting with immunocytochemical analysis. This work was supported by the Grant Agency of the Czech Republic (303/11/0970), Ministry of Health of the Czech Republic (NS9759), the Grant Agency of the Charles University of Prague (259089, 56209, 37710) and Ministry of Education, Youth and Sports of the Czech Republic (AV0Z 50110509, MSM0021620806, 1M6837805002).

Appendix A. Supplementary data

Supplementary data to this article can be found online at doi:10.1016/j.bbabio.2010.10.005.

References

[1] S.H. Ackerman, A. Tzagoloff, Function, structure, and biogenesis of mitochondrial ATP synthase, Prog. Nucleic Acid Res. Mol. Biol. 80 (2005) 95–133.
[2] I. Wittig, H. Schagger, Structural organization of mitochondrial ATP synthase, Biochim. Biophys. Acta 1777 (2008) 592–598.
[3] X. Zeng, M.H. Barros, T. Shulman, A. Tzagoloff, ATP25, a new nuclear gene of *Saccharomyces cerevisiae* required for expression and assembly of the Atp9p subunit of mitochondrial ATPase, Mol. Biol. Cell 19 (2008) 1366–1377.
[4] X. Zeng, A. Hourset, A. Tzagoloff, The *Saccharomyces cerevisiae* ATP22 gene codes for the mitochondrial ATPase subunit 6-specific translation factor, Genetics 175 (2007) 55–63.
[5] X. Zeng, W. Neupert, A. Tzagoloff, The metalloprotease encoded by ATP23 has a dual function in processing and assembly of subunit 6 of mitochondrial ATPase, Mol. Biol. Cell 18 (2007) 617–626.
[6] C. Osman, C. Wilmes, T. Tatsuta, T. Langer, Prohibitins interact genetically with Atp23, a novel processing peptidase and chaperone for the F1Fo-ATP synthase, Mol. Biol. Cell 18 (2007) 627–635.
[7] A. Pickova, M. Potocky, J. Houstek, Assembly factors of F1Fo-ATP synthase across genomes, Proteins 59 (2005) 393–402.
[8] Z.G. Wang, P.S. White, S.H. Ackerman, Atp11p and Atp12p are assembly factors for the F(1)-ATPase in human mitochondria, J. Biol. Chem. 276 (2001) 30773–30778.
[9] L. Lefebvre-Legendre, J. Vaillier, H. Benabdelhak, J. Velours, P.P. Slonimski, J.P. di Rago, Identification of a nuclear gene (FMC1) required for the assembly/stability of yeast mitochondrial F(1)-ATPase in heat stress conditions, J. Biol. Chem. 276 (2001) 6789–6796.
[10] A. Cizkova, V. Stranecky, J.A. Mayr, M. Tesarova, V. Havlickova, J. Paul, R. Ivanek, A. W. Kuss, H. Hansikova, V. Kaplanova, M. Vrbacky, H. Hartmannova, L. Noskova, T. Honzik, Z. Drahota, M. Magner, K. Hejzlarova, W. Sperl, J. Zeman, J. Houstek, S. Kmoch, TMEM70 mutations cause isolated ATP synthase deficiency and neonatal mitochondrial encephalocardiomyopathy, Nat. Genet. 40 (2008) 1288–1290.
[11] J. Houstek, S. Kmoch, J. Zeman, TMEM70 protein—a novel ancillary factor of mammalian ATP synthase, Biochim. Biophys. Acta 1787 (2009) 529–532.
[12] T. Honzik, M. Tesarova, J.A. Mayr, H. Hansikova, P. Jesina, O. Bodamer, J. Koch, M. Magner, P. Freisinger, M. Huemer, O. Kostkova, R. van Coster, S. Kmoch, J. Houstek, W. Sperl, J. Zeman, Mitochondrial encephalocardio-myopathy with early neonatal onset due to TMEM70 mutation, Arch. Dis. Child. 95 (2010) 296–301.
[13] S. Calvo, M. Jain, X. Xie, S.A. Sheth, B. Chang, O.A. Goldberger, A. Spinazzola, M. Zeviani, S.A. Carr, V.K. Mootha, Systematic identification of human mitochondrial disease genes through integrative genomics, Nat. Genet. 38 (2006) 576–582.
[14] D.J. Pagliarini, S.E. Calvo, B. Chang, S.A. Sheth, S.B. Vafai, S.E. Ong, G.A. Walford, C. Sugiana, A. Boneh, W.K. Chen, D.E. Hill, M. Vidal, J.G. Evans, D.R. Thorburn, S.A. Carr, V.K. Mootha, A mitochondrial protein compendium elucidates complex I disease biology, Cell 134 (2008) 112–123.
[15] H.A. Bentlage, U. Wendel, H. Schagger, H.J. ter Laak, A.J. Janssen, J.M. Trijbels, Lethal infantile mitochondrial disease with isolated complex I deficiency in fibroblasts but with combined complex I and IV deficiencies in muscle, Neurology 47 (1996) 243–248.
[16] J.A. Enriquez, P. Fernandez-Silva, A. Perez-Martos, M.J. Lopez-Perez, J. Montoya, The synthesis of mRNA in isolated mitochondria can be maintained for several hours and is inhibited by high levels of ATP, Eur. J. Biochem. 237 (1996) 601–610.
[17] M. Satoh, T. Hamamoto, N. Seo, Y. Kagawa, H. Endo, Differential sublocalization of the dynamin-related protein OPA1 isoforms in mitochondria, Biochem. Biophys. Res. Commun. 300 (2003) 482–493.
[18] P. Jesina, M. Tesarova, D. Fornuskova, A. Vojtiskova, P. Pecina, V. Kaplanova, H. Hansikova, J. Zeman, J. Houstek, Diminished synthesis of subunit a (ATP6) and altered function of ATP synthase and cytochrome c oxidase due to the mtDNA 2 bp microdeletion of TA at positions 9205 and 9206, Biochem. J. 383 (2004) 561–571.
[19] L. Stiburek, K. Vesela, H. Hansikova, P. Pecina, M. Tesarova, L. Cerna, J. Houstek, J. Zeman, Tissue-specific cytochrome c oxidase assembly defects due to mutations in SCO2 and SURF1, Biochem. J. 392 (2005) 625–632.
[20] J. Houstek, P. Klement, D. Floryk, H. Antonicka, J. Hermanska, M. Kalous, H. Hansikova, H. Houstkova, S.K. Chowdhury, T. Rosipal, S. Kmoch, L. Stratilova, J. Zeman, A novel deficiency of mitochondrial ATPase of nuclear origin, Hum. Mol. Genet. 8 (1999) 1967–1974.
[21] N.A. Steenaart, G.C. Shore, Alteration of a mitochondrial outer membrane signal anchor sequence that permits its insertion into the inner membrane. Contribution of hydrophobic residues, J. Biol. Chem. 272 (1997) 12057–12061.
[22] A. Pickova, J. Paul, V. Petruzzella, J. Houstek, Differential expression of ATPAF1 and ATPAF2 genes encoding F(1)-ATPase assembly proteins in mouse tissues, FEBS Lett. 551 (2003) 42–46.
[23] Z.G. Wang, D. Sheluho, D.L. Gatti, S.H. Ackerman, The alpha-subunit of the mitochondrial F(1) ATPase interacts directly with the assembly factor Atp12p, EMBO J. 19 (2000) 1486–1493.
[24] D.J. Burns, A.S. Lewin, The rate of import and assembly of F1-ATPase in *Saccharomyces cerevisiae*, J. Biol. Chem. 261 (1986) 12066–12073.

Supplement 2)

Kratochvílová, H. *, Hejzlarová, K. *, Vrbacký, M., Mráček, T., Karbanová, V., Tesařová, M., Gombitová, A., Cmarko, D., Wittig, I., Zeman, J., Houštěk, J. (2014). **Mitochondrial membrane assembly of TMEM70 protein.** Mitochondrion 15, 1-9. * Equal contribution, IF = 3.249, Quartile Score = Q2 (2014).

Mitochondrion 15 (2014) 1–9

Contents lists available at ScienceDirect

Mitochondrion

journal homepage: www.elsevier.com/locate/mito

Mitochondrial membrane assembly of TMEM70 protein

Hana Kratochvílová [a,b,1], Kateřina Hejzlarová [b,c,1], Marek Vrbacký [c], Tomáš Mráček [c], Vendula Karbanová [c], Markéta Tesařová [a], Adriána Gombitová [d], Dušan Cmarko [d], Ilka Wittig [e], Jiří Zeman [a], Josef Houštěk [c,*]

[a] Department of Pediatrics and Adolescent Medicine, First Faculty of Medicine, Charles University in Prague and General University Hospital in Prague, 12108 Prague, Czech Republic
[b] Charles University in Prague, First Faculty of Medicine, 12108 Prague, Czech Republic
[c] Institute of Physiology Academy of Sciences of the Czech Republic v.v.i., 14220 Prague, Czech Republic
[d] Institute of Cellular Biology and Pathology, First Faculty of Medicine, Charles University in Prague, 12108 Prague, Czech Republic
[e] Functional Proteomics, SFB 815 Core Unit, Faculty of Medicine, Goethe-University, 60590 Frankfurt am Main, Germany

ARTICLE INFO

Article history:
Received 21 October 2013
Received in revised form 4 February 2014
Accepted 18 February 2014
Available online 25 February 2014

Keywords:
Mitochondria
ATP synthase
TMEM70
Biogenesis

ABSTRACT

Dysfunction of TMEM70 disrupts the biogenesis of ATP synthase and represents the frequent cause of autosomal recessive encephalocardiomyopathy. We used tagged forms of TMEM70 and demonstrated that it has a hairpin structure with the N- and C-termini oriented towards the mitochondrial matrix. On BN-PAGE TMEM70 was detected in multiple forms including dimers and displayed partial overlap with assembled ATP synthase. Immunoprecipitation studies confirmed mutual interactions between TMEM70 molecules but, together with immunogold electron microscopy, not direct interaction with ATP synthase subunits. This indicates that the biological function of TMEM70 in the ATP synthase biogenesis may be mediated through interaction with other protein(s).

1. Introduction

Mitochondrial ATP synthase is a multisubunit protein formed by F_1 catalytic part and membrane embedded F_o part, that are connected via two stalks. The biosynthesis and assembly of ATP synthase is a complex, stepwise process requiring several specific helper proteins (Ackerman and Tzagoloff, 2005). Although the structure of ATP synthase is highly similar between lower and higher eukaryotes, the biogenesis of the enzyme is rather different reflecting differences in number, expression and processing of mtDNA encoded subunits. Thus 12 specific factors involved in the biosynthesis and assembly of the mtDNA encoded subunits ATP6, ATP8 and ATP9 of the F_o part of the enzyme have been described in *Saccharomyces cerevisiae* (Ackerman and Tzagoloff, 2005; Osman et al., 2007; Zeng et al., 2007a, 2007b, 2008) and none of them has functional homologs in higher eukaryotes. In addition, 3 factors are involved in the assembly of yeast F_1 catalytic part of ATP synthase and two of them have their functional homologs in mammals — Atp11p and Atp12p chaperones for F_1-β and F_1-α subunits respectively (Wang et al., 2001). Recently TMEM70 protein has been described as another ancillary factor in the ATP synthase biogenesis (Cizkova et al., 2008). In contrast to the above-mentioned factors, TMEM70 is only present in higher eukaryotes and is lacking in *S. cerevisiae* and many other lower eukaryotes (Cizkova et al., 2008; Jonckheere et al., 2011).

The functional role of TMEM70 protein was discovered while searching for the disease causing gene responsible for the fatal mitochondrial disease caused by isolated deficiency of ATP synthase (Cizkova et al., 2008; Houstek et al., 1999). Mutation c.317-2A>G in *TMEM70* gene preventing the synthesis of the protein was found to be the cause of ATP synthase deficiency in the group of patients with severe neonatal encephalocardiomyopathy. Since then, several other *TMEM70* mutations have been described (c.118_119insGT, c.494G>A, c.336T>A, c.316+1G>T, c.238C>T, c.578_579delCA, c.211-450_317-568del, c.580G>A, g.2436–3789, c.628A>C and c.535C>T (Atay et al., 2013; Cameron et al., 2011; Cizkova et al., 2008; Jonckheere et al., 2011; Shchelochkov et al., 2010; Spiegel et al., 2011; Torraco et al., 2012; Tort et al., 2011)), demonstrating that *TMEM70* gene is rather prone to mutations and represents the most frequent cause of ATP synthase deficiency.

We have previously described that the 30 kDa precursor of TMEM70 is processed upon import to mitochondria to 21 kDa mature protein with two putative transmembrane domains, and it behaves as an inner mitochondrial membrane protein capable to form dimers or aggregates with some other protein(s) (Hejzlarova et al., 2011). While our previous studies pointed to the involvement of TMEM70 in the early stages of ATP synthase biogenesis, possibly the F_1 formation (Houstek et al., 1999, 2009), Torraco et al. (2012) recently suggested

Abbreviations: AA, amino acids; DDM, n-dodecyl-β-D-maltoside; F_1, catalytic part of ATP synthase; F_o, membrane embedded part of ATP synthase; TX-100, Triton X-100; PIC, protease inhibitor cocktail.

* Corresponding author at: Institute of Physiology Academy of Sciences of the Czech Republic v.v.i., Vídeňská 1083, 14220 Prague 4, Czech Republic. Tel.: +420 2 4106 2434; fax: +420 2 4106 2149.
E-mail address: houstek@biomed.cas.cz (J. Houštěk).

[1] These authors contributed equally to this study.

http://dx.doi.org/10.1016/j.mito.2014.02.010
1567-7249/

the association of TMEM70 protein with ATP synthase subcomplex and the role of TMEM70 in the last steps of ATP synthase assembly — incorporation of the mtDNA encoded subunits F_o-a and A6L. However, the proper conformation of TMEM70 in the membrane as well as its function remain unknown.

In the present study we aimed to characterize structural properties of TMEM70 protein, namely its orientation in the inner mitochondrial membrane, presence in protein complexes under native conditions and its possible direct interactions with ATP synthase or other mitochondrial proteins.

2. Materials and methods

2.1. Cell cultures

Human embryonic kidney cells (HEK293, CRL-1573, ATCC) were grown in high glucose DMEM medium (PAA) supplemented with 10% (v/v) fetal bovine serum (Gold, PAA) at 37 °C in 5% CO_2 atmosphere.

2.2. Expression vectors and transfection

TMEM70-FLAG cDNA was inserted into vector pIRESpuro3 (Clontech) (Hejzlarova et al., 2011) and transfected into the HEK293 cell lines by nucleofection Kit V (Amaxa/Lonza). *TMEM70-GFP* cDNA expression vector (Calvo et al., 2006) was kindly provided by Prof. V.K. Mootha. To generate *TMEM70-MYC-FLAG*, *TMEM70* ORF was PCR amplified from *TMEM70-GFP* cDNA and cloned into the pCMV6-Entry plasmid (Origene). Plasmids were transfected into the HEK293 cell lines using METAFECTENE PRO (Biontex). *TMEM70-GFP* cDNA expression vector was transiently transfected into the HEK293 cells expressing TMEM70-FLAG by Express-In Transfection Reagent (Open Biosystems).

2.3. Isolation of mitochondria

Mitochondria were isolated from freshly harvested cells by hypo-osmotic shock method (Bentlage et al., 1996). Alternatively, for trypsin treatment experiment with TMEM70-FLAG, mitochondria isolated from cells homogenized by a Dounce homogenizer in isotonic medium (Stiburek et al., 2005) were used.

2.4. Trypsinization of the endogenous or C-terminal tagged TMEM70 protein in cells and mitochondria

Freshly harvested HEK293 cells constitutively expressing TMEM70-GFP, TMEM70-MYC-FLAG and control HEK293 cells were suspended in SEKT (0.25 M sucrose, 2 mM EGTA, 40 mM KCl and 20 mM Tris, pH 7.4) to a final protein concentration 5 mg/mL, mixed with the same volume of digitonin (1 mg/mL in SEKT) and incubated for 15 min on ice. The permeabilized cells were then incubated with trypsin (1 or 4 μg/100 μg of protein) in the presence or absence of 1% (v/v) Triton X-100 (TX-100) for 20 min at 37 °C. To stop digestion, SDS sample buffer (2% (v/v) 2-mercaptoethanol, 4% (w/v) SDS, 50 mM Tris (pH 7.0), 10% (v/v) glycerol) was added and the samples were incubated for 5 min at 90 °C. Samples were analyzed by 12% SDS-PAGE and WB using antibodies against TMEM70, FLAG, GFP, and compartment specific markers (intermembrane space — OPA1, matrix — PDH, loading control — porin). For details about antibodies used see Section 2.8.

To analyze the effect of trypsin on isolated organelle, mitochondria isolated from HEK293 cells constitutively expressing TMEM70-FLAG were exposed to hypotonic shock (Tang et al., 2009). Briefly, 150 μg of mitochondrial protein were resuspended in 100 μL of 5 mM MOPS-KOH, pH 7.2, and incubated for 20 min at 4 °C on a rotator. Swollen mitochondria with disrupted outer membrane were treated with trypsin (4 μg/100 μg of protein) for 20 min at 4 °C on a rotator in the presence or absence of 1% TX-100. Digestion was stopped with 100 μg/mL of soybean trypsin inhibitor and 1% (v/v) protease inhibitor cocktail (PIC, Sigma P8340). Samples were analyzed by 12% SDS-PAGE and WB using antibodies against FLAG and compartment specific markers (intermembrane space — OPA1, matrix — fumarate hydratase, inner membrane — Ndufb6).

2.5. Fluorescence microscopy analysis of TMEM70-GFP localization in intact cells and cells with permeabilized cytoplasmic and mitochondrial membrane

Selective permeabilization of the cytoplasmic and mitochondrial membranes by detergents as well as quenching of GFP fluorescence by Trypan blue was utilized as a tool to assess GFP tag orientation in mitochondria, essentially as in De Stefani et al. (2011). We used HEK293 cell lines transiently expressing TMEM70-GFP fusion protein, cells expressing GFP fusion protein localized in the cytosol (pMax-GFP, Amaxa/Lonza), or GFP fusion protein localized in the mitochondrial matrix (mt-GFP, Stratagene). Experiments were performed 48 h after transfection. The fluorescence signal was monitored on Leica DMI6000 wide field microscope with motorized z-stage equipped with Andor iXon897 photon counting camera. For each time point, image z-stack was collected (step optimized to 1 airy) and best focused plane was used for quantification. Cells were imaged in intracellular buffer containing 120 mM KCl, 3 mM HEPES, 5 mM KH_2PO_4, 3 mM $MgSO_4$ and 1 mM EGTA, pH 7.2. Each acquisition lasted for 10 min and subsequent additions were as follows: digitonin (0.2 g/g of protein, at 120 s), proteinase K (4 units, at 240 s), Trypan blue dye (0.05% (w/v), at 360 s) and TX-100 (1%, at 480 s). Total signal intensity from the whole cell at each timepoint was quantified in ImageJ software (FIJI package).

2.6. Immunoprecipitation

For TMEM70-FLAG immunoprecipitation, 1.3 mg protein of freshly isolated mitochondria from cultured cells were lysed with 0.35 mL buffer containing 0.5% TX-100, 150 mM NaCl and 50 mM Tris–HCl (pH 7.4) and 1% PIC for 30 min at 4 °C on a rotator and centrifuged at 12,000 *g* for 10 min. The lysate (0.32 mL) was incubated overnight at 4 °C with previously washed 40 μL of an EZ View ANTI-FLAG M2 affinity agarose resin (Sigma, F2426). Subsequently the resin was washed three times with buffer containing 150 mM NaCl and 50 mM Tris–HCl (pH 7.4). The bound protein was eluted by competition with 3× FLAG peptide (Sigma, F4799). The eluted immunoprecipitate was combined with SDS sample buffer and analyzed by 12% SDS-PAGE and Western blotting.

For ATP synthase immunoprecipitates, ATP Synthase Immunocapture Kit (Abcam, ab109715) was used. Freshly isolated mitochondria (0.45 mg protein) were solubilized with 2 g of n-dodecyl-β-D-maltoside (DDM)/g of protein in 90 μL PBS containing 0.2% PIC for 15 min on ice and centrifuged at 30,000 *g* for 20 min. Supernatant (80 μL) was mixed with ATP Synthase Immunocapture matrix. The mixture was incubated overnight at 4 °C on rotator and subsequently washed three times with PBS + PIC. Washed beads were mixed with SDS sample buffer and the sample subjected to 10% SDS-PAGE and Western blotting.

2.7. Polyacrylamide gel electrophoresis and Western blot immunodetection

SDS-PAGE (Schagger and von Jagow, 1987) was performed on 10% or 12% polyacrylamide minigels using Mini-Protean system (Bio-Rad).

BN-PAGE was performed on 8–15% polyacrylamide minigels (Schagger and von Jagow, 1991). Isolated mitochondria were solubilized with DDM (1 g/g of protein) or digitonin (2 g/g of protein) for 15 min on ice in 1.5 M aminohexanoic acid, 2 mM EDTA and 50 mM Bis-Tris, pH 7.0. The samples were centrifuged for 20 min at 4 °C and 30,000 *g* and Coomassie Brilliant Blue G-250 dye (Serva, 0.1 g/g of detergent) and 5% (v/v) glycerol were added to supernatants before electrophoresis.

For two dimensional BN/SDS-PAGE, strips of the first dimension gels were incubated in a 2D buffer containing 1% 2-mercaptoethanol and 1% SDS and then resolved in the second dimension on SDS-PAGE.

Western blot analysis using semidry electrotransfer of proteins was performed by standard protocols as previously described (Jesina et al., 2004; Stiburek et al., 2005). For immunodetection we used specific antibodies to FLAG (Sigma, F1804), OPA1 (BD Biosciences, 612606), fumarate hydratase (FH, Abnova, H00002271-M01), PDH E1-α subunit (Abcam, ab110334), GFP (Santa Cruz Biotechnology, sc-9996), TMEM70 (Proteintech Group, 20388-1-AP or 60195-1-Ig), Complex I subunit Ndufb6 (Abcam, ab110244), Complex II subunit Sdh70 (Abcam, ab14715), Complex III subunit Core2 (Abcam, ab14745), Complex IV subunit Cox1 (Abcam, ab14705), ATP synthase subunits F_1-α (Abcam, ab110273; or lot 20D6 (Moradi-Ameli and Godinot, 1983)), F_1-β (Abcam, ab14730), F_1-δ (GeneTex, GTX101503), F_o-c (Jesina et al., 2004), F_o-a (Jesina et al., 2004), OSCP (Abcam, ab110276), IF1 (Abcam, ab110277), F6 (Abcam, ab110279) and F_o-d (Abcam, ab110275). The immunoblots were detected with peroxidase conjugated secondary antibodies and SuperSignal West Femto Maximum Sensitivity Substrate (Thermo Scientific Pierce) using VersaDoc 4000 Imaging System (Bio-Rad), or with fluorescent secondary antibodies (Alexa Fluor 680, Life Technologies; IRDye800, Rockland Immunochemicals) on an Odyssey infrared imaging system (LI-COR).

2.8. Immunogold electron microscopy

Immunolabeling of TMEM70 protein and ATP synthase F_1-α at the ultrastructural level was performed directly on grids with the cell sections. Briefly, HEK293 cells grown on glass coverslips were fixed with freshly prepared formaldehyde, dehydrated and embedded in LR White resin. Ultrathin sections mounted on Formvar/carbon-coated nickel grids were incubated overnight with a mixture of primary antibodies: the rabbit polyclonal antibody to TMEM70 (Proteintech Group, 20388-1-AP) and the monoclonal antibody to ATP synthase F_1-α (Abcam, ab110273). After rinsing, the sections were incubated in secondary antibody for 30 min. Colloidal gold coupled secondary antibodies (anti-rabbit IgG — 6 nm gold particles, anti-mouse IgG — 12 nm gold particles, Jackson Immuno Research) were used. In the control specimens, sections were treated with the reaction mixture where the primary antibodies were omitted. Finally, the grids were contrasted with uranyl acetate followed by lead citrate. The labeled preparations were observed with a Zeiss 900 or Tecnai G^2 Sphera 20 electron microscopes at 80 and 100 kV, using a 30–40 μm objective aperture.

3. Results

3.1. Orientation of TMEM70 protein in the inner mitochondrial membrane

Previous studies demonstrated that TMEM70 is a mitochondrial protein localized in the inner mitochondrial membrane. Based on the two short and conserved transmembrane regions the protein has putative hairpin like fold with the short N-terminal and long C-terminal sequences oriented towards the same hydrophilic mitochondrial compartment (Jonckheere et al., 2011). To establish native orientation of TMEM70 protein in the inner membrane we tested accessibility of the C-terminal sequence to external protease- trypsin, at conditions when the protease can reach the intermembrane space or mitochondrial matrix. While the C-terminal sequence contains numerous lysines and arginines, no trypsin-cleavable sites are present in the predicted loop between the two transmembrane domains. For experiments we utilized HEK293 cells expressing the tagged forms of TMEM70 protein. Both tags used, i.e. MYC-FLAG and GFP, were attached to the noncleaved C-terminus of the sequence.

As summarized in Fig. 1, we tested the accessibility of TMEM70 in intact cells, after disruption of the plasma and outer mitochondrial membranes with digitonin and after permeabilization of the inner mitochondrial membrane by 1% TX-100. Low digitonin concentration (0.2 g/g of protein) is sufficient for permeabilization of the plasma and outer mitochondrial membranes but not for solubilization of the inner membrane proteins. Fig. 1A shows the behavior of the endogenous TMEM70 protein detected with specific antibody recognizing an epitope at the C-terminus of the protein. In digitonin-permeabilized cells addition of 1 or 4 μg of trypsin/100 μg of protein digested OPA1 protein localized in the intermembrane space and was without effect on matrix PDH as well as on TMEM70. Both TMEM70 and PDH became digested when TX-100 was added demonstrating that the TMEM70 antigen recognized by the antibody has to be located (similarly as PDH) in mitochondrial matrix. The same experiment was then performed with TMEM70-MYC-FLAG (Fig. 1B) and TMEM70-GFP (Fig. 1C). The MYC-FLAG attached to the TMEM70 C-terminus displayed analogous accessibility to trypsin and associated loss of the FLAG antigen; again in line with the matrix localization of the C-terminal sequence. This was further confirmed using TMEM70-GFP (Fig. 1C). The GFP signal at approx. 46 kDa was again resistant to trypsin unless Triton X-100 was added. Interestingly, the signal then moved to approx. 27 kDa and remained present even at the higher trypsin concentration (T4), while the TMEM70 signal completely disappeared. As GFP is highly resistant to trypsin digestion (Chiang et al., 2001) the 27 kDa signal most likely represents the whole GFP protein, which suggests that the cleavage site has to be at the very end of the TMEM70 C-terminus, close to the attached GFP molecule.

In further experiments we used isolated mitochondria from cells expressing TMEM70-FLAG to assess membrane topology of TMEM70. As shown in Fig. 2, when isolated mitochondria were swollen in hypotonic medium to disrupt the outer membrane, OPA1 protein of the intermembrane space was fully accessible and digested by trypsin, while the matrix enzyme, fumarate hydratase was protected from trypsin cleavage. At these conditions the C-terminal FLAG tag of TMEM70 protein was also unaffected by the protease. However, when TX-100 was added prior to trypsin treatment, both the fumarate hydratase and FLAG tag signals completely disappeared, thus confirming the matrix orientation of the TMEM70 C-terminus, in agreement with the data from the permeabilized cells.

As an independent approach to characterize the membrane topology of TMEM70 protein we used fluorescence microscopy of GFP protein and quenching of the GFP fluorescence by membrane impermeable dye Trypan blue. This approach was recently used to study the orientation of MCU protein from the inner mitochondrial membrane (De Stefani et al., 2011). As summarized in Fig. 3, we used HEK293 cells expressing TMEM70-GFP and compared them with HEK293 cells expressing two different forms of GFP — mt-GFP, i.e. a soluble GFP protein localized in the mitochondrial matrix, and pMax-GFP, which is localized in the cytosol. Cells were permeabilized with low digitonin concentration affecting only the cytoplasmic membrane and subsequently treated with proteinase K, Trypan blue and TX-100. As shown in Fig. 3A and B, in digitonin-permeabilized cells the cytosolic pMax-GFP fluorescence was completely lost by proteinase K digestion, as expected. In contrast, matrix mt-GFP and TMEM70-GFP were not affected by the addition of neither the proteinase K, which would digest proteins on the outer mitochondrial membrane nor by the Trypan blue, which would quench fluorescence of the GFP localized in the intermembrane space. However, rapid quenching of both the mt-GFP and TMEM70-GFP signals was induced by subsequent addition of TX-100 demonstrating that detergent solubilization of the inner mitochondrial membrane was essential for membrane impermeable Trypan blue and proteinase K to reach the GFP tag on TMEM70 or mt-GFP. Thus the morphological approach fully confirmed biochemical studies pointing to the matrix localization of the C-terminal sequence of TMEM70 protein.

3.2. Native organization of TMEM70 protein

We have previously found that TMEM70 was present on BN-PAGE as two spots possibly a monomer and dimer (Hejzlarova et al.,

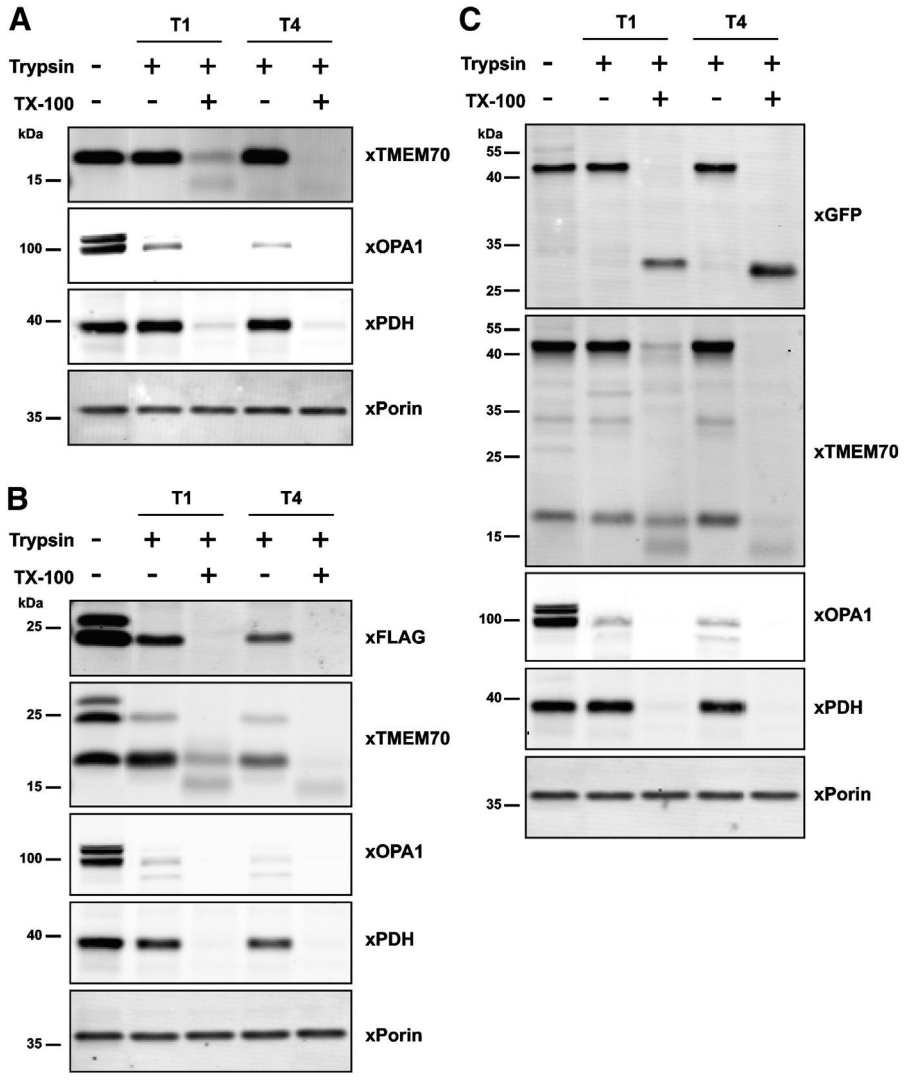

Fig. 1. Accessibility of TMEM70 to protease in digitonin-treated HEK293 cells expressing TMEM70, TMEM70-MYC-FLAG or TMEM70-GFP protein. After disruption of the cell and outer mitochondrial membranes by digitonin, HEK293 cells (A) with endogenous expression of TMEM70 protein, (B) constitutively expressing TMEM70-MYC-FLAG and (C) constitutively expressing TMEM70-GFP were treated with two different trypsin concentrations (T1, T4 — 1 and 4 μg of trypsin/100 μg of protein) in the presence or absence of 1% Triton X-100 (TX-100). Samples were separated by SDS-PAGE and probed with antibodies to TMEM70, FLAG, GFP, OPA1 (representative of intermembrane space proteins), PDH (representative of matrix proteins) and porin (loading control, as its beta barrel fold is well protected from protease digestion).

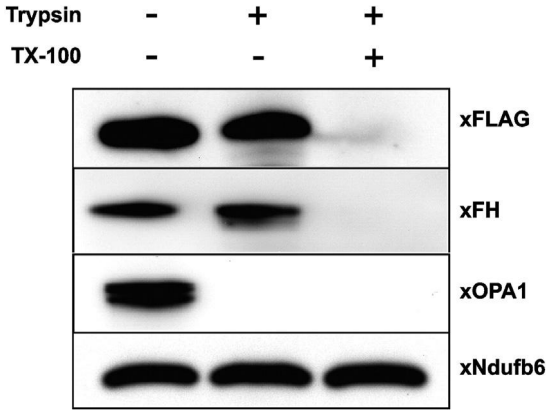

Fig. 2. Accessibility of the C-terminal FLAG to protease in mitochondria from HEK293 cells expressing TMEM70-FLAG. The outer membrane of isolated mitochondria was disrupted by hypotonic shock and mitochondria were treated with 4 μg of trypsin/100 μg of protein in the presence or absence of 1% Triton X-100 (TX-100) as indicated. Samples were separated by SDS-PAGE and probed with antibodies to FLAG, OPA1 (representative of intermembrane space proteins), fumarate hydratase (FH, representative of matrix proteins) and Ndufb6 (inner membrane protein protected from protease digestion).

2011). In further experiments we followed behavior of the detergent-solubilized tagged forms of TMEM70 by 2D analysis combining native and SDS electrophoreses and WB immunodetection with antibodies to the tags used (GFP, FLAG). As shown in Fig. 4A, the DDM-solubilized mitochondria from HEK293 cells expressing TMEM70-GFP (mature protein 46 kDa) revealed two distinct forms of the protein. Based on the migration pattern of free subunit F_1-α of 55 kDa, they should represent monomer and dimer of TMEM70-GFP. Relatively high portion of TMEM70-GFP could be detected in the high molecular weight region as an unfocused streak. In the cells expressing TMEM70-FLAG (mature protein 22 kDa) two major forms of the tagged protein were present (both migrating below F_1-α), while the migration of the single spot of TMEM70-MYC-FLAG (mature protein 24 kDa) was smaller than F_1-α subunit. These spots could represent TMEM70-FLAG monomer and dimer and TMEM70-MYC-FLAG dimer, respectively. A strong signal of TMEM70-MYC-FLAG was found also in the high molecular weight region, approximately between the position of ATP synthase monomers and dimers, but again this signal was rather unfocused. Distribution of tagged forms was further verified by using anti-TMEM70 antibody, which gave analogous patterns. Only discrepancy was in case of TMEM70-GFP, which was detected as two parallel lines of identical

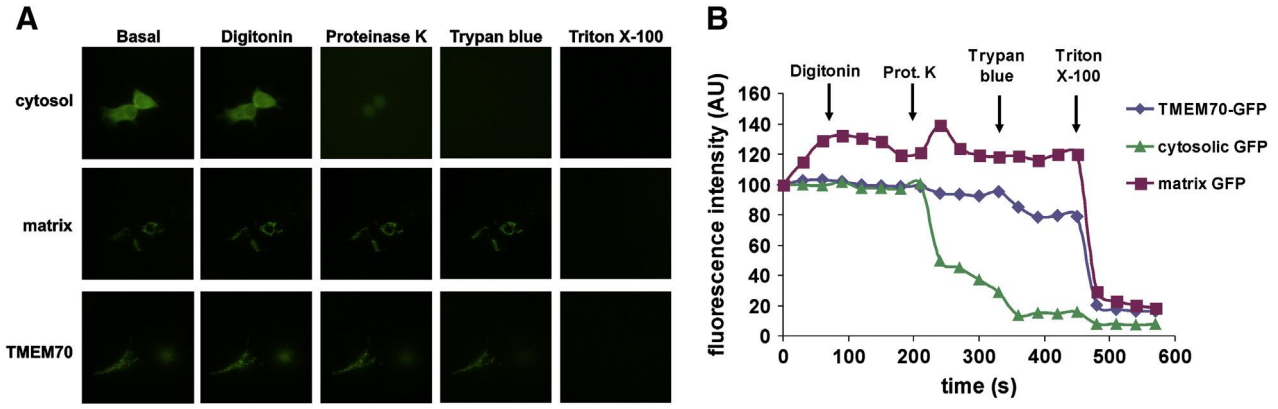

Fig. 3. Fluorescence detection of accessibility of C-terminal GFP to inner membrane impermeable Trypan blue dye in digitonin treated HEK293 cells expressing TMEM70-GFP protein. For experiment cell lines HEK293 pMax-GFP (GFP fusion protein localized in the cytosol), HEK293 mt-GFP (GFP fusion protein localized in the mitochondrial matrix) and HEK293 transiently expressing TMEM70-GFP were used. In the first step the cytoplasmic membranes of the cells were disrupted by low digitonin concentration treatment. Cells were subsequently incubated with proteinase K (digests cytosolic proteins) and Trypan blue dye. As a small molecule, Trypan blue gets into the intermembrane space inaccessible for proteinase K and quenches the GFP signal in this compartment. Afterwards Triton X-100 was added to disrupt all membranes. The fluorescence signal was monitored in HEK293 cells on Leica DMI6000 microscope. (A) GFP fluorescence images, (B) quantification of fluorescence data (n = 10 for each cell line).

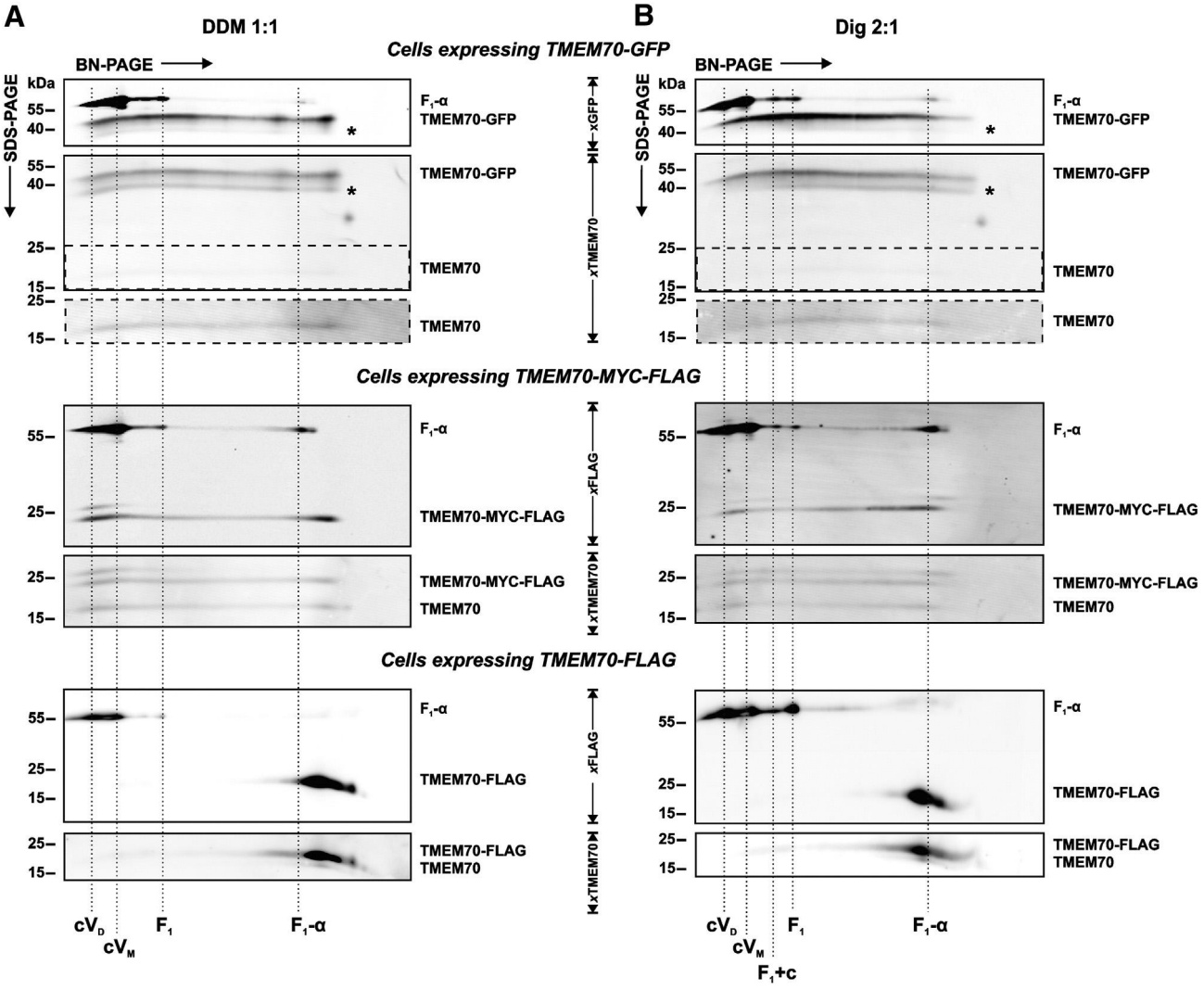

Fig. 4. Multiple forms of TMEM70 protein. Mitochondria isolated from HEK293 cells constitutively expressing TMEM70-GFP, TMEM70-MYC-FLAG or TMEM70-FLAG were solubilized with 1 g of DDM/g of protein (A) or with 2 g of digitonin/g of protein (B) and analyzed by two dimensional BN/SDS-PAGE and Western blot detection using antibodies to FLAG, GFP, TMEM70 and F_1-α subunit. Upper panels show detection of F_1-α subunit and GFP or FLAG, the lower panels show detection of TMEM70. cV_D, ATP synthase dimer; cV_M, ATP synthase monomer; F_1 + c, subcomplex of F_1 part and subunit c of ATP synthase; F_1, F_1 part alone; F_1-α, free F_1-α subunit. Dashed border line indicates higher intensity exposition of the relevant part of the membrane from the upper panel. Asterisks mark the proteolytic product of TMEM70-GFP.

profile. The lower (circa 40 kDa) line displayed only marginal reactivity with anti-GFP antibody and reflects some non-specific proteolysis of the GFP-tagged protein. Antibody to TMEM70 also clearly detected the endogenous TMEM70 protein. Its expression levels were considerably lower than those of the tagged forms, but showed similar distribution profile with low molecular weight forms as well as with the streaking signal up to the region of cV_D.

Since we detected all TMEM70-GFP, TMEM70-MYC-FLAG and native TMEM70 to partly overlap with ATP synthase (Fig. 4A), we used milder detergent digitonin instead of DDM for the solubilization of mitochondria, which may better preserve weak noncovalent interactions. In the region of putative monomers and dimers we observed a general shift to the higher molecular weights for TMEM70-GFP, TMEM70-MYC-FLAG as well as TMEM70, possibly due to the presence of the empty detergent micelles (Fig. 4B). More of the signal was found as unfocused streaks in the high molecular weight region, especially in the case of TMEM70-GFP. Nevertheless, no distinct spot pointing to specific association with the ATP synthase complex or the F_1 subcomplexes could be detected.

Expression of the tagged forms of TMEM70 was further used as an approach to find out whether TMEM70 can form oligomers. In Fig. 5 we have analyzed HEK293 cells expressing either TMEM70-GFP or TMEM70-FLAG alone or coexpressing both constructs simultaneously (TMEM70-FLAG + TMEM70-GFP). Mitochondria from these cells were solubilized with TX-100 and immunoprecipitation was performed with anti-FLAG antibody. As shown in Fig. 5, in the immunoprecipitate from cells coexpressing both tagged forms, the FLAG- and the GFP-tagged TMEM70 was detected. On the other hand, in cells expressing sole TMEM70-FLAG, only TMEM70-FLAG was detectable and no tagged TMEM70 was present in the immunoprecipitate from TMEM70-GFP expressing cells in accordance with the fact that anti-FLAG antibody was used for immunoprecipitation. Specific coimmunoprecipitation of TMEM70-GFP by anti-FLAG antibody from cells coexpressing both forms was further confirmed by the immunodetection with anti-GFP and anti-TMEM70 antibodies. In addition to the mature TMEM70-GFP (46 kDa) also a larger form, possibly yet unprocessed TMEM70-GFP was immunoprecipitated. These experiments clearly proved that TMEM70 protein can form oligomers, as previously suggested. On the other hand, they indicate that the interaction is weak and labile and/or may include only some copies of the protein.

3.3. No detectable interaction of TMEM70 with ATP synthase by immunoprecipitation and immunogold electron microscopy

Although the specific ancillary function of TMEM70 in the biosynthesis and assembly of functional ATP synthase is well established, its exact role in this process is still unclear (Cizkova et al., 2008; Honzik et al., 2010; Houstek et al., 1999; Torraco et al., 2012). An attractive hypothesis is that TMEM70 interacts directly with some of ATP synthase subunits, assembly intermediates or fully assembled enzyme. In Fig. 6 we addressed this question by further extension of immunoprecipitation experiments. We have expressed TMEM70-FLAG in HEK293 cells and used anti-FLAG antibody for immunoprecipitation of TX-100 solubilized mitochondria. The resulting immunoprecipitate was analyzed by SDS-PAGE and Western blot with a series of specific antibodies to subunits of ATP synthase. HEK293 cells expressing empty vector were used as a control. We have checked for the possible presence of F_1 subunits α, β, δ and IF1, as well as F_o subunits a, d, F6 and OSCP in the immunoprecipitate. However, none of them could be detected, although all antibodies were able to detect respective proteins in the whole mitochondria. In the case of subunit F_1-β, we found strongly reacting band that was somewhat higher than the mature F_1-β, but this reaction was unspecific as it was found in the immunoprecipitates from control cells not expressing TMEM70-FLAG as well (HEK293 cells with empty vector). In addition, we have also tested crossreactivity of the immunoprecipitates with antibodies to respiratory chain complexes II (Sdh70), III (Core2) and IV (Cox1), but with negative result. Efficiency of the immunoprecipitation was verified with antibodies to TMEM70 and FLAG.

In order to check whether the FLAG tag attached to TMEM70 did not affect its ability to interact with subunits of the ATP synthase in the FLAG-IP experiments, we took also the reverse approach. Here, we captured the ATP synthase by immunoprecipitation and looked for the presence of the endogenous TMEM70 protein. Fig. 7 illustrates, that

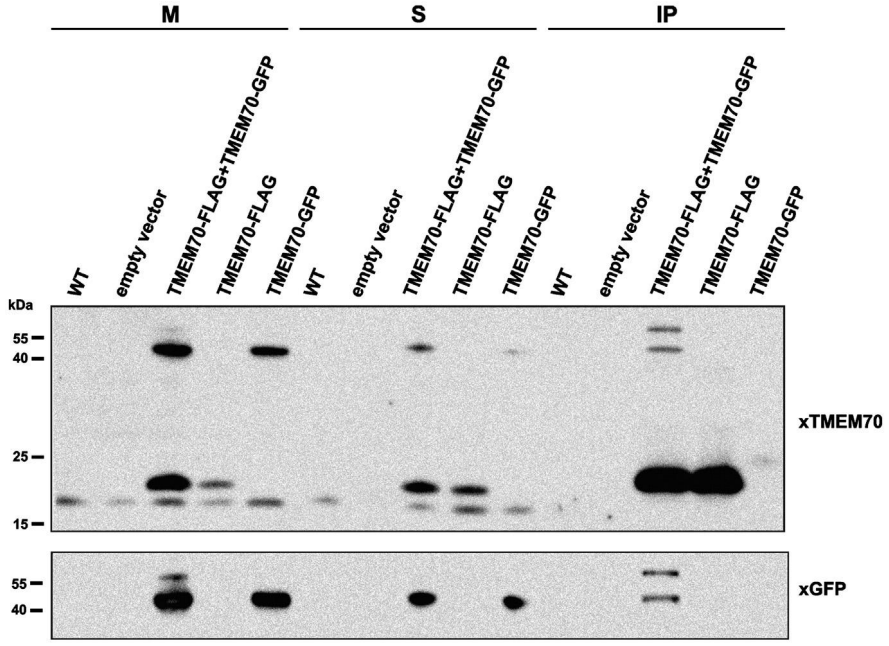

Fig. 5. Detection of TMEM70 oligomers by immunoprecipitation. Isolated mitochondria from parental HEK293 cells (WT), cells expressing TMEM70-FLAG, TMEM70-GFP, cells expressing both TMEM70-FLAG and TMEM70-GFP, as well as cells transfected with empty vector were solubilized with 0.5% Triton X-100 and for immunoprecipitation antibody to FLAG was used. Original mitochondria (M, 10 μg protein), solubilized proteins (S) and the immunoprecipitates (IP, obtained from ~290 μg protein of original mitochondria) were analyzed by SDS-PAGE and Western blot detection using antibodies to TMEM70 or GFP.

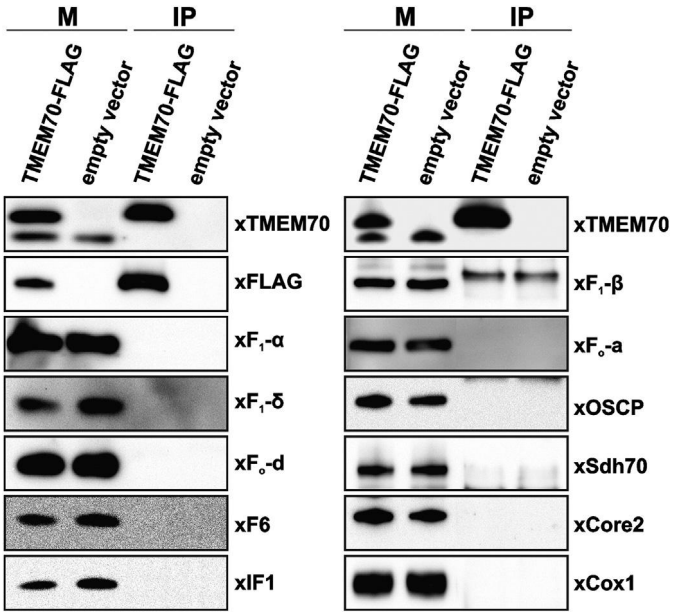

Fig. 6. Search for ATP synthase subunits in the TMEM70 immunoprecipitates. Mitochondria from HEK293 cells constitutively expressing TMEM70-FLAG and from HEK293 cells with empty vector were solubilized with 0.5% Triton X-100 and lysate proteins were immunoprecipitated using FLAG antibody. Original mitochondria (M, 10 μg protein) and the immunoprecipitate (IP, obtained from ~580 μg protein of original mitochondria) were analyzed by SDS-PAGE and Western blotting using indicated antibodies to TMEM70, FLAG, ATP synthase subunits (F_1-α, F_1-β, F_1-δ, IF1, F_o-a, F_o-d, OSCP, F6) and respiratory chain complexes II (Sdh70), III (Core2) and IV (Cox1).

using ATP Synthase Immunocapture antibody, ATP synthase was efficiently immunoprecipitated but no signal of TMEM70 protein could be observed, even when mild conditions of solubilization (2 g of DDM/g of protein) were used. The same results were obtained with other F_1 antibodies previously used for the immunoprecipitation (not shown) (Houstek et al., 1999).

Finally, to check for the possible interactions in the intact mitochondrial membrane, we have also performed electron microscopy studies by means of post embedding immunogold detection of TMEM70 protein and ATP synthase F_1-α. Immunolabeling of cellular constituents on ultrathin sections of intact cells is the method of choice for high resolution in situ localization of various proteins within the cell. Moreover,

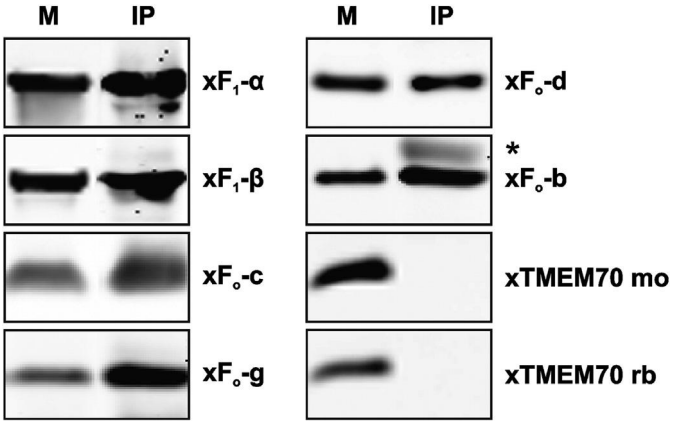

Fig. 7. Search for TMEM70 protein in the ATP synthase immunoprecipitates. Isolated mitochondria from wild type HEK293 cells were solubilized with 2 g of DDM/g of protein and immunoprecipitated with ATP Synthase Immunocapture Kit. Original mitochondria (M, 10 μg protein) and the immunoprecipitate (IP, obtained from ~40 μg protein of original mitochondria) were analyzed by SDS-PAGE and probed with mouse monoclonal (mo) or rabbit polyclonal (rb) antibody to TMEM70 and with antibodies to ATP synthase subunits F_1-α, F_1-β, F_o-c, F_o-g, F_o-d and F_o-b. Asterisk marks the light immunoglobulin chain.

such labeling circumvents the problem of the limited accessibility of antibodies into the cellular compartments, because the immunoreaction takes place on the surface of physically sectioned material. Fig. 8 shows the result of double immunogold analysis detecting ATP synthase with 12 nm colloidal gold particles and TMEM70 protein with 6 nm colloidal gold particles. Both signals were found inside of mitochondria, sometimes associated with the inner membrane. However, they were found in distinct regions and rather far from one another, thus arguing against close, intimate interaction of these two proteins.

4. Discussion

The ATP synthase biogenesis in mammalian mitochondria critically depends on TMEM70 protein, the lack of which diminishes the mitochondrial content of this enzyme far below the level needed for phosphorylation of ADP at physiological rates of substrate oxidation. While it is clear that TMEM70 protein is an important ancillary factor for de novo formation of ATP synthase complex, its exact role in this process remains unknown.

The aim of this study was to characterize the topology of TMEM70 protein within the inner mitochondrial membrane and to bring more light into the functional properties of TMEM70. We focused on its possible interaction with other protein(s), particularly ATP synthase subunits or assembly intermediates. The membrane topology of TMEM70 protein has previously been predicted by computational analysis (Jonckheere et al., 2011) of relatively high average accuracy (Klammer et al., 2009) but it was not experimentally verified. Therefore, in the first part of our study we have characterized the membrane topology of TMEM70 protein by several independent approaches using GFP and FLAG as the C-terminal tags of TMEM70 protein. Based on the accessibility to membrane impermeable protease or Trypan blue dye at differently permeabilized mitochondria we demonstrated that orientation of the C-terminus is towards the mitochondrial matrix.

TMEM70 protein sequence contains two highly conserved transmembrane domains spanning 21 amino acids (AA) each, separated by a short sequence of 18 mostly hydrophilic AA. Such structure should generate a hairpin like membrane assembly of the protein. Based on our results thus both the N- and C-termini of TMEM70 protein have to be located in the mitochondrial matrix. Such conformation is also in accordance with the previous computational prediction (Jonckheere et al., 2011). Additional evidence is also provided by the observation that the N-terminal presequence was cleaved upon import of nascent protein to the mitochondrial matrix (Hejzlarova et al., 2011), requiring the presence of the N-terminal part in the matrix during protein import. The matrix facing N-terminal is only 21 AA long and may not be critical for the protein function. On the other hand the matrix exposed C-terminal sequence is about 98 AA long with the first 40 AA highly conserved between species, indicating that this part of the sequence might be functionally important. TMEM70 could thus be involved in the matrix localized events in the ATP synthase biogenesis. Of interest is the phenotype of the recently reported c.578-579delCA mutation, predicted to yield truncated TMEM70 lacking the last 60 AA, but still containing the highly conserved region in the proximal part of the C-terminus. It was associated with rather long survival (24 years) of one of the siblings, which is unusual with other *TMEM70* mutations, although even here the phenotype was relatively severe (Spiegel et al., 2011).

Solubilization of membrane proteins in combination with analysis by native electrophoresis represents well established approach to characterize native forms of these proteins as well as their interactions with other components. Present analysis of different tagged forms of TMEM70 as well as previous studies of the wild type TMEM70 show that TMEM70 is presumably capable to form oligomers of different sizes, possibly dimers and larger forms; however, their pattern depends on solubilization conditions, attached tag, as well as electrophoretic system used for analysis. In contrast with our previous study (Hejzlarova

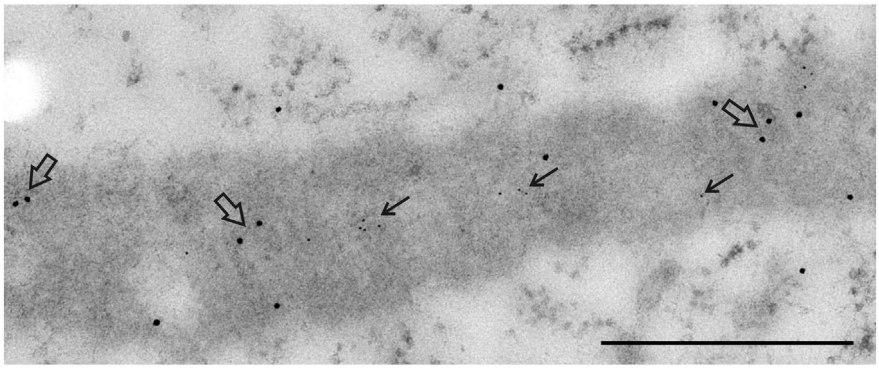

Fig. 8. Immunogold detection of TMEM70 protein and ATP synthase. Double immunolabeling for TMEM70 protein (small grains, arrows) and F_1-α subunit of ATP synthase (large grains, open arrows) on LR White resin sections showed that these factors do not colocalize inside of the mitochondrial space. Bar, 0.5 μm.

et al., 2011), which detected TMEM70 to form only monomers and dimers, here we used milder conditions for solubilization (half of the DDM concentrations or digitonin) and found also higher forms of TMEM70. Clearly a large portion of the solubilized TMEM70 that streaks up to the high molecular weight region (400–800 kDa) is mostly unfocused, especially in the digitonin solubilizates. However, such streaking is not uncommon for rather basic proteins and was observed for example also for AGP and MLQ subunits of ATP synthase (Meyer et al., 2007). We did not detect any specific overlap of TMEM70 with the signal of ATP synthase subunit F_1-α on 2D gels, where both proteins are very well detected. The direct interaction between TMEM70 molecules and formation of oligomeric forms was further confirmed by coimmunoprecipitation of TMEM70-FLAG and TMEM70-GFP from HEK293 cells coexpressing both tagged forms. The relative efficiencies of coimmunoprecipitation are similar to those observed by others in analogous experiments with other proteins of interest (Baughman et al., 2011) and demonstrate that oligomers of TMEM70 can be formed. On the other hand they do not provide hint about how quantitative this interaction is. Quite likely, only a part of all copies of TMEM70 protein is present as oligomers.

The key question to understand the biological role of TMEM70 is to uncover the physiological interaction with other components of the ATP synthase biogenesis, be it individual subunits, assembly intermediates or some other factors. Similar biochemical phenotype of ATP synthase deficiency, i.e. low content of otherwise functional enzyme, is observed not only in cells with *TMEM70* mutations (Cizkova et al., 2008), but also in the case of *ATP5A1*, *ATP5E* and *ATPAF2* mutations (De Meirleir et al., 2004; Jonckheere et al., 2013; Mayr et al., 2010). It suggests that the defect occurs at the early stage of the enzyme biogenesis, likely the formation and stabilization of F_1 part of the enzyme. Interestingly, very fast synthesis and degradation of the F_1-β subunit were found in the patient with *TMEM70* mutation (Houstek et al., 1999), suggesting the disturbance in the assembly of this subunit and thus of F_1 part of ATP synthase. The reason could be the problem at the level of the central stalk F_1 subunits γ, δ or ε, as their knockdown in HEK293 cells downregulates the ATP synthase biogenesis (Havlickova et al., 2010; Pecina et al., 2012). On the other hand the lack of F_1-γ, δ or ε subunits is associated with the accumulation of subunit F_o-c, a phenomenon absent in cells harboring *TMEM70* mutation (Havlickova et al., 2010).

The last stage in stepwise process of the ATP synthase assembly appears to be the addition of mtDNA encoded subunits. When the synthesis of subunits F_o-a and A6L (ATP6 and ATP8) is abolished due to the absence or depletion of mtDNA (Carrozzo et al., 2006), inhibition of mitochondrial protein synthesis (Nijtmans et al., 1995) or when *MT-ATP6* gene is mutated (Houstek et al., 1995; Jesina et al., 2004), a near complete but labile ATP synthase forms. However, it disintegrates upon solubilization and separation by BN-PAGE, which results in apparent accumulation of F_1 + c and F_1 subcomplexes. Recently the potential role for TMEM70 protein in the incorporation of mtDNA encoded subunits was suggested by Torraco et al. (2012). In TMEM70 patient cells they did not find full size ATP synthase, but by activity staining on BN-PAGE they detected a 550 kDa subcomplex, which should represent ATP synthase lacking mtDNA encoded subunits. However, the true nature of this complex is not obvious, since the authors detected it also in control cells, where it has not been shown in any of the previous studies. Also rather surprisingly, they did not observe OSCP signal in these subcomplexes, although OSCP should be present at least in the 550 kDa subcomplex. Nevertheless, they proposed that TMEM70 may bind to F_1, stabilize it to form F_1 + IF1 + c subassembly of 470 kDa and assist the insertion of subunits F_o-a and A6L at the ultimate stage of biogenesis. While this would support the above view of TMEM70 interacting with the whole F_1 or with F_1 subunits, neither they were successful in an attempt to identify any ATP synthase subunit directly interacting with TMEM70.

As revealed by our studies presented herein, some overlap between the endogenous or tagged TMEM70 protein and assembled ATP synthase or smaller F_1 containing assemblies can be found on native as well as 2D gels, which could be specific or just coincidental. Despite extensive attempts to find such specific interaction by means of several approaches, we were unable to detect a direct interaction with ATP synthase subunits. When we immunoprecipitated ATP synthase from the DDM solubilizates of mitochondria with different anti-F_1 antibodies there was no coimmunoprecipitation of TMEM70 protein. Vice versa, efficient immunoprecipitation of TMEM70 did not contain either F_1 or F_o subunits in the resulting immunoprecipitate. Finally, the third independent approach, morphological analysis by immunogold electron microscopy also indicated rather distant localizations of the ATP synthase subunit F_1-α antigen and the TMEM70 antigen in the mitochondrial membrane.

At the present stage the assembly of TMEM70 itself is well established while further studies are needed to find out TMEM70 interacting partners. These could be ATP synthase subunits, some chaperone, mitochondrial protease or some other protein through which TMEM70 participates in the biogenesis of ATP synthase.

Acknowledgment

This work was supported by the Grant Agency of the Czech Republic (P303/11/0970, 14-36804G), the Grant Agency of the Charles University in Prague (37710, 370411), Charles University in Prague (PRVOUK P24/LF1/3, P27/LF1/1 and UNCE 204011, 204022), Ministry of Education, Youth and Sports of the Czech Republic (LL1204, RVO:67985823), by the 2011 L'Oreal-UNESCO fellowship for Women in Science (M.T.), by the Deutsche Forschungsgemeinschaft, Sonderforschungsbereich 815, project Z1 (I.W.) and by the BMBF mitoNET — German Network for Mitochondrial Disorders 01GM1113B (I.W.).

References

Ackerman, S.H., Tzagoloff, A., 2005. Function, structure, and biogenesis of mitochondrial ATP synthase. Prog. Nucleic Acid Res. Mol. Biol. 80, 95–133.

Atay, Z., Bereket, A., Turan, S., Haliloglu, B., Memisoglu, A., Khayat, M., Shalev, S.A., Spiegel, R., 2013. A novel homozygous TMEM70 mutation results in congenital cataract and neonatal mitochondrial encephalo-cardiomyopathy. Gene 515, 197–199.

Baughman, J.M., Perocchi, F., Girgis, H.S., Plovanich, M., Belcher-Timme, C.A., Sancak, Y., Bao, X.R., Strittmatter, L., Goldberger, O., Bogorad, R.L., Koteliansky, V., Mootha, V.K., 2011. Integrative genomics identifies MCU as an essential component of the mitochondrial calcium uniporter. Nature 476, 341–345.

Bentlage, H.A., Wendel, U., Schagger, H., ter Laak, H.J., Janssen, A.J., Trijbels, J.M., 1996. Lethal infantile mitochondrial disease with isolated complex I deficiency in fibroblasts but with combined complex I and IV deficiencies in muscle. Neurology 47, 243–248.

Calvo, S., Jain, M., Xie, X., Sheth, S.A., Chang, B., Goldberger, O.A., Spinazzola, A., Zeviani, M., Carr, S.A., Mootha, V.K., 2006. Systematic identification of human mitochondrial disease genes through integrative genomics. Nat. Genet. 38, 576–582.

Cameron, J.M., Levandovskiy, V., Mackay, N., Ackerley, C., Chitayat, D., Raiman, J., Halliday, W.H., Schulze, A., Robinson, B.H., 2011. Complex V TMEM70 deficiency results in mitochondrial nucleoid disorganization. Mitochondrion 11, 191–199.

Carrozzo, R., Wittig, I., Santorelli, F.M., Bertini, E., Hofmann, S., Brandt, U., Schagger, H., 2006. Subcomplexes of human ATP synthase mark mitochondrial biosynthesis disorders. Ann. Neurol. 59, 265–275.

Chiang, C.F., Okou, D.T., Griffin, T.B., Verret, C.R., Williams, M.N., 2001. Green fluorescent protein rendered susceptible to proteolysis: positions for protease-sensitive insertions. Arch. Biochem. Biophys. 394, 229–235.

Cizkova, A., Stranecky, V., Mayr, J.A., Tesarova, M., Havlickova, V., Paul, J., Ivanek, R., Kuss, A.W., Hansikova, H., Kaplanova, V., Vrbacky, M., Hartmannova, H., Noskova, L., Honzik, T., Drahota, Z., Magner, M., Hejzlarova, K., Sperl, W., Zeman, J., Houstek, J., Kmoch, S., 2008. TMEM70 mutations cause isolated ATP synthase deficiency and neonatal mitochondrial encephalocardiomyopathy. Nat. Genet. 40, 1288–1290.

De Meirleir, L., Seneca, S., Lissens, W., De Clercq, I., Eyskens, F., Gerlo, E., Smet, J., Van Coster, R., 2004. Respiratory chain complex V deficiency due to a mutation in the assembly gene ATP12. J. Med. Genet. 41, 120–124.

De Stefani, D., Raffaello, A., Teardo, E., Szabo, I., Rizzuto, R., 2011. A forty-kilodalton protein of the inner membrane is the mitochondrial calcium uniporter. Nature 476, 336–340.

Havlickova, V., Kaplanova, V., Nuskova, H., Drahota, Z., Houstek, J., 2010. Knockdown of F1 epsilon subunit decreases mitochondrial content of ATP synthase and leads to accumulation of subunit c. Biochim. Biophys. Acta 1797, 1124–1129.

Hejzlarova, K., Tesarova, M., Vrbacka-Cizkova, A., Vrbacky, M., Hartmannova, H., Kaplanova, V., Noskova, L., Kratochvilova, H., Buzkova, J., Havlickova, V., Zeman, J., Kmoch, S., Houstek, J., 2011. Expression and processing of the TMEM70 protein. Biochim. Biophys. Acta 1807, 144–149.

Honzik, T., Tesarova, M., Mayr, J.A., Hansikova, H., Jesina, P., Bodamer, O., Koch, J., Magner, M., Freisinger, P., Huemer, M., Kostkova, O., van Coster, R., Kmoch, S., Houstek, J., Sperl, W., Zeman, J., 2010. Mitochondrial encephalocardio-myopathy with early neonatal onset due to TMEM70 mutation. Arch. Dis. Child. 95, 296–301.

Houstek, J., Klement, P., Hermanska, J., Houstkova, H., Hansikova, H., Van den Bogert, C., Zeman, J., 1995. Altered properties of mitochondrial ATP-synthase in patients with a T → G mutation in the ATPase 6 (subunit a) gene at position 8993 of mtDNA. Biochim. Biophys. Acta 1271, 349–357.

Houstek, J., Klement, P., Floryk, D., Antonicka, H., Hermanska, J., Kalous, M., Hansikova, H., Houstkova, H., Chowdhury, S.K., Rosipal, T., Kmoch, S., Stratilova, L., Zeman, J., 1999. A novel deficiency of mitochondrial ATPase of nuclear origin. Hum. Mol. Genet. 8, 1967–1974.

Houstek, J., Kmoch, S., Zeman, J., 2009. TMEM70 protein — a novel ancillary factor of mammalian ATP synthase. Biochim. Biophys. Acta 1787, 529–532.

Jesina, P., Tesarova, M., Fornuskova, D., Vojtiskova, A., Pecina, P., Kaplanova, V., Hansikova, H., Zeman, J., Houstek, J., 2004. Diminished synthesis of subunit a (ATP6) and altered function of ATP synthase and cytochrome c oxidase due to the mtDNA 2 bp microdeletion of TA at positions 9205 and 9206. Biochem. J. 383, 561–571.

Jonckheere, A.I., Huigsloot, M., Lammens, M., Jansen, J., van den Heuvel, L.P., Spiekerkoetter, U., von Kleist-Retzow, J.C., Forkink, M., Koopman, W.J., Szklarczyk, R., Huynen, M.A., Fransen, J.A., Smeitink, J.A., Rodenburg, R.J., 2011. Restoration of complex V deficiency caused by a novel deletion in the human TMEM70 gene normalizes mitochondrial morphology. Mitochondrion 11, 954–963.

Jonckheere, A.I., Renkema, G.H., Bras, M., van den Heuvel, L.P., Hoischen, A., Gilissen, C., Nabuurs, S.B., Huynen, M.A., de Vries, M.C., Smeitink, J.A., Rodenburg, R.J., 2013. A complex V ATP5A1 defect causes fatal neonatal mitochondrial encephalopathy. Brain 136, 1544–1554.

Klammer, M., Messina, D.N., Schmitt, T., Sonnhammer, E.L., 2009. MetaTM — a consensus method for transmembrane protein topology prediction. BMC Bioinforma. 10, 314.

Mayr, J.A., Havlickova, V., Zimmermann, F., Magler, I., Kaplanova, V., Jesina, P., Pecinova, A., Nuskova, H., Koch, J., Sperl, W., Houstek, J., 2010. Mitochondrial ATP synthase deficiency due to a mutation in the ATP5E gene for the F1 epsilon subunit. Hum. Mol. Genet. 19, 3430–3439.

Meyer, B., Wittig, I., Trifilieff, E., Karas, M., Schagger, H., 2007. Identification of two proteins associated with mammalian ATP synthase. Mol. Cell. Proteomics 6, 1690–1699.

Moradi-Ameli, M., Godinot, C., 1983. Characterization of monoclonal antibodies against mitochondrial F1-ATPase. Proc. Natl. Acad. Sci. U. S. A. 80, 6167–6171.

Nijtmans, L.G., Klement, P., Houstek, J., van den Bogert, C., 1995. Assembly of mitochondrial ATP synthase in cultured human cells: implications for mitochondrial diseases. Biochim. Biophys. Acta 1272, 190–198.

Osman, C., Wilmes, C., Tatsuta, T., Langer, T., 2007. Prohibitins interact genetically with Atp23, a novel processing peptidase and chaperone for the F1Fo-ATP synthase. Mol. Biol. Cell 18, 627–635.

Pecina, P., Nůsková, H., Havlíčková, V., Houštěk, J., 2012. Role of the mitochondrial ATP synthase central stalk subunits γ and δ in the activity and assembly of the mammalian enzyme. Biochim. Biophys. Acta 1917, S20.

Schagger, H., von Jagow, G., 1987. Tricine-sodium dodecyl sulfate-polyacrylamide gel electrophoresis for the separation of proteins in the range from 1 to 100 kDa. Anal. Biochem. 166, 368–379.

Schagger, H., von Jagow, G., 1991. Blue native electrophoresis for isolation of membrane protein complexes in enzymatically active form. Anal. Biochem. 199, 223–231.

Shchelochkov, O.A., Li, F.Y., Wang, J., Zhan, H., Towbin, J.A., Jefferies, J.L., Wong, L.J., Scaglia, F., 2010. Milder clinical course of Type IV 3-methylglutaconic aciduria due to a novel mutation in TMEM70. Mol. Genet. Metab. 101, 282–285.

Spiegel, R., Khayat, M., Shalev, S.A., Horovitz, Y., Mandel, H., Hershkovitz, E., Barghuti, F., Shaag, A., Saada, A., Korman, S.H., Elpeleg, O., Yatsiv, I., 2011. TMEM70 mutations are a common cause of nuclear encoded ATP synthase assembly defect: further delineation of a new syndrome. J. Med. Genet. 48, 177–182.

Stiburek, L., Vesela, K., Hansikova, H., Pecina, P., Tesarova, M., Cerna, L., Houstek, J., Zeman, J., 2005. Tissue-specific cytochrome c oxidase assembly defects due to mutations in SCO2 and SURF1. Biochem. J. 392, 625–632.

Tang, T., Zheng, B., Chen, S.H., Murphy, A.N., Kudlicka, K., Zhou, H., Farquhar, M.G., 2009. hNOA1 interacts with complex I and DAP3 and regulates mitochondrial respiration and apoptosis. J. Biol. Chem. 284, 5414–5424.

Torraco, A., Verrigni, D., Rizza, T., Meschini, M.C., Vazquez-Memije, M.E., Martinelli, D., Bianchi, M., Piemonte, F., Dionisi-Vici, C., Santorelli, F.M., Bertini, E., Carrozzo, R., 2012. TMEM70: a mutational hot spot in nuclear ATP synthase deficiency with a pivotal role in complex V biogenesis. Neurogenetics 13, 375–386.

Tort, F., Del Toro, M., Lissens, W., Montoya, J., Fernandez-Burriel, M., Font, A., Bujan, N., Navarro-Sastre, A., Lopez-Gallardo, E., Arranz, J.A., Riudor, E., Briones, P., Ribes, A., 2011. Screening for nuclear genetic defects in the ATP synthase-associated genes TMEM70, ATP12 and ATP5E in patients with 3-methylglutaconic aciduria. Clin. Genet. 80, 297–300.

Wang, Z.G., White, P.S., Ackerman, S.H., 2001. Atp11p and Atp12p are assembly factors for the F(1)-ATPase in human mitochondria. J. Biol. Chem. 276, 30773–30778.

Zeng, X., Hourset, A., Tzagoloff, A., 2007a. The Saccharomyces cerevisiae ATP22 gene codes for the mitochondrial ATPase subunit 6-specific translation factor. Genetics 175, 55–63.

Zeng, X., Neupert, W., Tzagoloff, A., 2007b. The metalloprotease encoded by ATP23 has a dual function in processing and assembly of subunit 6 of mitochondrial ATPase. Mol. Biol. Cell 18, 617–626.

Zeng, X., Barros, M.H., Shulman, T., Tzagoloff, A., 2008. ATP25, a new nuclear gene of Saccharomyces cerevisiae required for expression and assembly of the Atp9p subunit of mitochondrial ATPase. Mol. Biol. Cell 19, 1366–1377.

Supplement 3)

Štufková, H., Hůlková, H., Stránecký, V., Smíšková, Z., Pavrovská, S., Wenchich, L., Honzík, T., Hansíková, H., Honzík, T., Mráček, T., Houštěk, J., Zeman, J., Tesařová, M. **The impact of prevalent homozygous splicing c.317-2A>G TMEM70 mutation on OXPHOS complexes, mitochondrial reticulum, and ultrastructure in patient tissues, fibroblasts, and myoblasts** (manuscript prepared for submission).

The impact of prevalent homozygous splicing c.317-2A>G *TMEM70* mutation on OXPHOS complexes, mitochondrial reticulum, and ultrastructure in patient tissues, fibroblasts, and myoblasts

Hana Štufková[1], Helena Hůlková[1,2], Viktor Stránecký[1], Zuzana Smíšková[1], Sabina Pavrovská[1], Laszlo Wenchich[1], Hana Hansiková[1], Tomáš Honzík[1], Tomáš Mráček[3], Josef Houštěk[3], Jiří Zeman[1], Markéta Tesařová[1,*]

[1]Department of Pediatrics and Inherited Metabolic Disorders, First Faculty of Medicine, Charles University and General University Hospital in Prague, 128 00, Prague, Czech Republic.

[2]Institute of Pathology, First Faculty of Medicine, Charles University and General University Hospital in Prague, 128 00, Prague, Czech Republic.

[3]Laboratory of Bioenergetics, Institute of Physiology, Czech Academy of Sciences, 142 00 Prague, Czech Republic.

*corresponding author: marketa.tesarova@lf1.cuni.cz (Markéta Tesařová)

Abstract

Pathogenic variants in the assembly factor *TMEM70* gene are one of the most common causes of ATP synthase disorders. Our study represents a detailed analysis of the impact of prevalent, homozygous splicing c.317-2A>G mutation in *TMEM 70* on the amount, stability, and activity of OXPHOS complexes and mitochondrial ultrastructure in predominantly affected tissues (brain, muscle, heart, and liver) in myoblasts, and fibroblasts. Our results demonstrate that *TMEM70* prevalent mutation results in some stage of adaptive/compensatory effect, which is especially evident in fibroblasts and influence the mitochondrial reticulum and ultrastructure. The absence of TMEM70 protein always leads to an isolated deficiency of complex V, but only to the inconsistent form of a combined defect in OXPHOS complexes.

Keywords: TMEM70, ATP synthase, OXPHOS complexes, mitochondrial ultrastructure, mitochondrial reticulum

1. Introduction

The mitochondrial diseases due to ATP synthase defects might be caused by mtDNA mutations in *MT-ATP6* or *MT-ATP8* [1] genes, as well as mutations in nuclear genes encode structural subunits, subunit α (*ATP5FA1*) [2-5], subunit ε (*ATP5F1E*) [5,6], subunit δ (*ATP5F1D*) [7], subunit DAPIT (*ATP5MK*) [8], subunit c (*ATP5MC3)* [5,9], subunit OSCP (*ATP5O*) [5] or specific assembly factors ATPAF2 (*ATPAF2*) [10] and TMEM70 (*TMEM70*) [11]. Nuclear-caused ATP synthase defects are extremely rare, to this day only several patients were reported. In contrast, mutations in *TMEM70* gene are frequent [12-17].

Patient with *TMEM70* mutation, resulting in a neonatal-onset, muscular hypotonia, encephalo-cardiomyopathy, facial dysmorphism, psychomotor and mental retardation accompanied by elevated plasma lactate level, 3-methylglutaconic aciduria and hyperammonemia [15,16,18,19]. On a cellular level, TMEM70 defects caused diminished content and activity of ATP synthase [11,20,21] and affected a mitochondrial reticulum and ultrastructure [22-26].

TMEM70 protein has been studied for more than a decade. Over the last few years, its function in model organisms and cell lines has been studied [26-29]. It has been revealed that TMEM70 is involved in the assembly of the c8 ring in the inner mitochondrial membrane. In further studies [28,29], the authors suggested that TMEM70 is not only involved in the assembly of complex V but also has a role in the stabilization and assembly of complex I.

Herein, we report the impact of prevalent homozygous splicing c.317-2A>G *TMEM70* mutation on patients´ bioptic/autoptic tissues and cultured fibroblast and myoblast. The aims of our study were to verify a possible compensatory effect in tissues from patients with the prevalent c.317-2A>G *TMEM70* mutation, which has been previously described in fibroblasts [21] and described the ultrastructure in myoblast, fibroblasts and cardiomyocytes.

2. Material and Methods

2.1.Ethics

The present study was carried out in accordance with the Declaration of Helsinki of the World Medical Association and was approved by the Committee of Medical Ethics of the General University Hospital and First Faculty of Medicine, Charles University in Prague. Informed parental consent was obtained for all biopsies and autopsies.

2.2.Patients

The clinical phenotype of patients were described previously (Table 1). Patient 12 (P12) was not included in any previous study and therefore her clinic is listed below.

Table 1: The identification of patients in this article and previous study [15]

	P1	**P2**	**P3**	**P4**	**P5**	**P6**	**P7**	**P8**	**P9**	**P10**	**P11**	**P12**
(Honzík et al., 2010)	P13	P7	P6	P12	P9	P11	P1	P17	P14	P18	P15	-

The girl was born in the 39th week of gestation with birth weight 2250 g (< 3rd percentile), length 45 cm (17th percentile), head circumference 31,5 cm (< 3rd percentile), mild facial dysmorphy and Apgar score 9 in the 5th and 10th minute. Both parents and three sisters are healthy, but her brother with fatal neonatal lactic acidosis died in the age of 5 days. Within the first hour after birth, the girl developed hypotony with decreased skin blood perfusion and pale skin. Capillary refeelling was 3 seconds and O2 saturation was 81-84% non-responding to oxygenotherapy. Echocardiography revealed hypertrophic cardiomyopathy (HCMP) with mild decreased contractility, open foramen ovale and patent ductus arteriosus. She had mild hypoglycaemia 2,8 mmol/l, hypocholesterolaemia 2.1 mmol/l and moderate metabolic acidosis (pH 7,24, HCO3 16,6, base excess - 9,3). Lactate was elevated in blood (8,5 mmol/l, reference range < 2,3), urine (3942 mmol/mol creatine, age related reference range < 150) and cerebrospinal fluid (8,26 mmol/L, reference range < 2.1) and urinary excretion of 3-methylglutaconic acid was increased (131 mg/g creatinine, reference range < 15). In addition, alanine in blood and cerebrospinal fluid was elevated 782 µmol/l (reference range < 500) and 92 µmol/l (reference range < 35), respectively. She died in the age of 17 months during acute respiratory infection with vomiting, brain oedema and heart failure with hyperammonaemia 391 µmol/l (reference range 40-80) and hyperuricaemia 1005 µmol/l (reference range < 350).

2.3.Mutation Detection

The homozygous splicing c.317-2A>G mutation in *TMEM70* was found by sequencing the corresponding region of nuclear DNA.

2.4.Tissues and Cell Cultures

The studies were performed in available stored material from skeletal muscle, heart, liver, and brain (frontal cortex). Open muscle biopsies from the tibialis anterior muscle were immediately frozen in liquid nitrogen and stored at -80°C. Post-mortem tissue specimens (muscle, liver, heart, brain) were obtained at autopsy of patients and age-related controls were frozen in liquid nitrogen less than 2 hours after death. The heart sample of P7 was obtained during cardiac surgery.

The primary skin fibroblasts were established from forearm skin biopsy obtained during muscle biopsy or autopsy. Fibroblasts were cultivated high-glucose DMEM medium (Dulbecco's Modified Eagle Medium; PanBiotech) supplemented with 10% (v/v) Fetal Bovine Serum (GE Healthcare) and Antibiotic-Antimycotic (Biosera) at 37°C in 5% CO_2 atmosphere.

Isolation and culturing of myoblast were described previously [22]. Muscle biopsies samples were incubated in Skeletal Muscle Cell Growth and Differentiation Medium with Supplement Mix Promo Cell GmbH (Promega) at 37°C in 5% CO_2 atmosphere. Over 5–10 days, the growing myoblasts migrated, scattered, and fused spontaneously. Myoblasts were isolated using the ''pre-plating'' method [30].

2.5.Mitochondria Isolation

Skeletal muscle and brain mitochondria were isolated according to standard differential centrifugation procedures [31] in a buffer comprising 150 mM KCl, 10 mM Tris/HCl, 2mM EDTA, and 2 µg/ml aprotinin (pH 7.4) at 4°C. Heart and liver mitochondria were isolated in buffer comprising 250 mM sucrose, 20 mM Tris/HCl, 2 mM EDTA, and 2 µg/ml aprotinin (pH 7.4) at 4°C. Protein concentration was determined by the Lowry method [32] and the isolated mitochondria were stored at -80°C.

Fibroblasts were harvested by trypsinization, washed three times with phosphate-buffered saline, re-suspended in an isotonic STE buffer (250 mM sucrose, 10 mM Tris–HCl (pH 7.4), 1 mM EDTA, 1% (v/v) Protease Inhibitor Cocktail (PIC, Sigma-Aldrich)), and disrupted on ice using a Dounce homogenizer. To remove unbroken cells and nuclei, the homogenate was centrifuged at 600 g and 4°C for 15 min. The post-nuclear supernatant was

centrifuged at 10 000 g and 4°C for 25 min. The resulting mitochondrial pellet was twice washed with STE buffer. Protein concentration was determined with the Bio-Rad Protein Assay Kit (Bio-Rad Laboratories). The isolated mitochondria were stored at -80°C.

2.6. Electrophoresis and Immunoblot Analysis

BN-PAGE (Blue Native-Polyacrylamide gel electrophoresis) [33] was used for the separation of mitochondrial membrane complexes on polyacrylamide 6-15% (w/v) gradient gels using a MiniProtean®3 System (Bio-Rad Laboratories). Isolated mitochondria were solubilized with DDM (n-dodecyl β-D-maltoside) with a final concentration DDM/protein ratio of 2 mg/mg in buffer containing 1,5 M aminocaproic acid, 2 mM EDTA, and 50 mM Bis-Tris (pH 7.0). Serva Blue G was added to solubilized protein at a concentration of 0,1 mg/mg of detergent. 2-20 μg of protein prepared as described previously was loaded in each lane. Serial dilutions of the control sample (10%-100%) were loaded on the same gels.

Tricine SDS-PAGE (Sodium Dodecyl Sulfate–Polyacrylamide gel electrophoresis) was carried out under standard conditions with 12% polyacrylamide, 0,1% (w/v) SDS gels. Mitochondria or tissue/cell homogenates were incubated for 20 min on ice with RIPA buffer (50 mM Tris/HCl (pH 7.4), 150 mM NaCl, 1 mM PMSF, 1 mM EDTA, 1% Triton X-100 and 0,1% SDS (v/v), 1% (v/v) Protease Inhibitor Cocktail (PIC, Sigma-Aldrich)) and centrifuged at 51 000 g for 25 min, 4°C. Samples were dissociated in 50 mM Tris/HCl (pH 6.8), 12% (v/v) glycerol, 4% SDS, 2% (v/v) 2-mercaptoethanol, and 0,01% (w/v) Bromphenol Blue for 30 min at 37°C. 2,5-20 μg of protein was loaded in each lane. Serial dilutions of control sample (25-100%) were loaded on the same gels.

Proteins were electroblotted from the gels onto Immobilon^{TM-P} PVDF Membranes (Merck-Millipore) using semi-dry transfer for 1 h at a constant current of 0,6 mA/cm^2. Membranes were air-dried overnight, rinsed with 100% methanol (v/v) and blocked in TBS buffer with 5% non-fat dried milk for 2 hours. The primary detection was performed with mouse or rabbit monoclonal antibodies NDUFA9 (ab14713, Abcam, dilution 1:2 000), NDUFB6 (ab 110244, Abcam, dilution 1:4 000), SDH70 (ab14715, Abcam, dilution 1:20 000), SDH30 (ab14714, Abcam dilution 1:1 000), CORE2 (ab14745, Abcam, dilution 1:20 000), COX1 (ab14705, Abcam, dilution 1:10 000), COX2 (ab110258, Abcam, dilution 1:10 000), COX5a (ab110262, Abcam, dilution 1:2 000), F_1-α (ab110273, Abcam, dilution 1:4 000), F_1-β (ab14730, Abcam, dilution 1:4 000), OSCP (ab110276, Abcam, dilution 1:10 000), F_o-c (ab181243, Abcam, dilution 1:1 000), VDAC1 (ab14734, Abcam, dilution 1:2 000), α-Tubulin (2125S, Cell Signaling, dilution 1:2 000), and rabbit polyclonal primary antibody

TMEM70 (20388-1-AP, Proteintech Group, dilution 1:4 000). Blots were incubated with primary antibodies in TBS 0,1 % (v/v) Tween 20 and 1% non-fat dried milk for 2 hours. The secondary detection was carried out with Mouse IgG (whole molecule)–Peroxidase antibody produced in goat antibody (A8924, Sigma-Aldrich, dilution 1:2 000) or Rabbit IgG (whole molecule)–Peroxidase antibody produced in goat antibody (A0454, Sigma-Aldrich, dilution 1:2 000) in TBS, 0,1% Tween 20 and 1% non-fat dried milk for 1 hour. The blots were visualized with SuperSignal™ West Femto Maximum Sensitivity Substrate (TermoFisher Scientific) using VersaDoc 4000 Imaging System (Bio-Rad Laboratories) or Syngene G:Box (Syngene).

2.7.Epifluorescence Microscopy

Cells for mitochondrial network staining were cultivated on glass coverslips (22x22x0.17mm) in the experimental medium. The mitochondrial network was further visualized using fluorescence vital probe 10nM Mitotracker Red CMX Ros (Molecular Probes) for 15 min at 37°C. Cells were washed with PBS, the mitochondrial network was detected by Nikon Diaphot 200 inverted microscope (Nikon) and images were taken with an Olympus DP50 CCD camera and Viewfinder Lite 1.0 software (Pixera).

2.8.Electron Microscopy in heart, cultured skin fibroblasts and myoblasts

Tissues for electron microscopy were fixed with 3% glutaraldehyde, then post-fixed with 1% osmium tetraoxide, dehydrated with an ethanol series and propylene oxide and embedded in Durcupan-Epon mixture (Electron Microscopy Sciences). Ultrathin sections were cut by Ultracut Microtome (Reichert), mounted on copper grids, doubled contrasted with uranyl acetate and lead nitrate, and then examined using a transmission electron microscope (JEOL JEM-1200 EX).

Fibroblasts or myoblast were fixed by a modified method of Luft [34] as described previously [35]. Cells were incubated in PBS containing 2% potassium permanganate for 15 min, washed with PBS, and dehydrated with an ethanol series. The samples were embedded in Durcupan-Epon mixture (Electron Microscopy Sciences), sectioned by Ultracut Microtome (Reichert) to thicknesses ranging from 600 to 900 Å, and stained with lead citrate and uranyl acetate. A JEOL JEM-1200 EX transmission electron microscope was used for imaging.

4.10.Histology, Immunohistochemistry and Histochemistry

Formaldehyde-fixed, paraffin-embedded tissue specimens were cut at 4 μm thick paraffin sections and treated with conventional histological stains. Immunohistochemical detection of mitochondria was performed with mouse IgG1 anti-prohibitin antibody (LabVision) after heat antigen retrieval (10 mM citrate buffer, pH 7.6). The bound primary antibody was detected using a DAKO EnVision+ Peroxidase Mouse System (DAKO) with diaminobenzidine as a chromogen.

Cryostat sections 10 μm (for cytochrome c oxidase histochemistry) or 5 μm (for histochemistry of other respiratory enzymes) prepared from frozen tissues were stained for cytochrome c oxidase (COX), NADH-tetrazolium reductase (NADH-TR) and succinate dehydrogenase (SDH) activities according to standard histochemical protocols [36,37].

3. Results

3.1. Steady-state levels of OXPHOS complexes in TMEM70 deficient muscle, heart, liver, and brain mitochondria and protein level of TMEM70 in human control tissues

The protein content of individual OXPHOS complexes in mitochondria using BN-PAGE and Western blotting in the set of patient´s tissues (muscle, heart, liver, brain) was determined (Figure 1A-D). Serial dilutions of controls were loaded on the same gel in order to assess the residual steady-state levels of the complexes.

In skeletal muscle mitochondria (Figure 1A), a pronounced deficiency of complex V was found in all patients. Traces of free F_1 subassembly intermediates were detected in P1, P6, and control. The amount of complex I was reduced in all samples. The level of complex III was slightly increased in P4 and P6. Interestingly, a significantly increased amount of complex IV was detected in P1 and P6. The amount of complex II was comparable to controls.

In heart mitochondria (Figure 1B), markedly diminished amounts of complex V were found in all samples. Moreover, free F_1 was detected in the P7 sample as well as in the control material. A mild increase in steady-state levels of complex I was found for P1, P2 and a slight decrease for P3. The steady-state levels of complex IV were mostly comparable to the control. Nevertheless, an intermediate of complex IV, presumably intermediate S3, was detected in P1 and P3. Normal native amounts of complex II and complex III were observed.

In liver mitochondria (Figure 1C), a pronounced deficiency of complex V was detected in all analyzed samples. In addition, free F_1 intermediates were detected in P2. In P2, P3, and P7, the amount of complex I was slightly reduced. On the contrary, elevated steady-state level of complex I was observed in P1. Levels of complex IV were increased mainly in P3 and P7. The amount of complex II and complex III was normal or mildly elevated.

In brain mitochondria (Figure 1D), steady-state levels of complex V were markedly reduced, as in mitochondria of other tissues. Slight reductions in complex I and complex II levels were detected in P2 and P3.

The TMEM70 protein level profile in a set of the control human tissues (brain, heart, muscle, and liver) was analyzed by SDS-PAGE, western blot and immunodetection (Figure 2). Due to the same genetic background, the set of isolated mitochondria from one control was used. The amount of the protein loaded per line was normalized to protein concentration. VDAC1 was used as a relative control of mitochondrial enrichment [38]. While the highest protein level of TMEM70 was observed in the liver, the smallest in muscle mitochondria

(Figure 2A). The same profile of TMEM70 protein level using tissues from several different controls was observed (Figure 2B).

TMEM70 mRNA/protein levels using an online database www.proteinatlas.org have been studied [39]. mRNA according to the database was found in all human tissues with low human brain regional specificity. mRNA expression levels in the skeletal muscle has been identified as "tissues enhanced" this means that the level in the muscle is at least four times elevated to the other tissue. The database shows that the second-highest mRNA expression was found in the liver and among other tissues the mRNA level was at a similar level. The protein level in the database was derived from antibody-based protein profiling using immunohistochemical staining. However, low consistency between antibody staining and mRNA expression data was detected, because the TMEM70 protein level was constant in all analyzed tissues.

3.2. Steady-state levels of TMEM70 protein and selected OXPHOS complex subunits in muscle and heart mitochondria and fibroblast and myoblast cell lysate

To monitor possible changes in protein levels, we performed SDS-PAGE and Western blot analysis for OXPHOS complex subunits in fibroblasts, myoblasts, muscle, and heart (Figure 3, Figure A1). TMEM70 protein signal was not detectable in any of the analyzed patient´s samples. The amounts of ATP synthase subunits F_1-α and OSCP were significantly reduced in fibroblast, heart, and muscle patient samples. In fibroblast cell lysate, the same pattern in the amount of other OXPHOS complex subunits was detected. The level of subunits NDUFA9, SDH70, SDH30, CORE2, COX1, COX2, and COX5a were slightly or significantly increased. Moreover, on further electrophoresis, we analyzed the level of the complex V subunit c. Like the subunit F_1-β, the level was significantly reduced in samples from patient fibroblasts (Figure A1, D). Mildly decreased levels of complex I NDUFA9 subunits were observed in heart mitochondria. An increased COX5a signal was detected in P1 compared to a slightly reduced level in P2. A slight reduction of SDH30 was present in P2. All other studied proteins remained unchanged. Significant increases in steady-state levels of complex IV subunits COX1, COX2, and COX5a were observed in muscle mitochondria in both patients (P3, P1). Similarly, a pronounced rise in the amount of complex II subunit SDH30 was detected. However, the amount of the other analyzed complex II subunit SDH70 was comparable to controls.

Our laboratory has a very well optimized process for preparing myoblast cell lines [22]. Therefore, we generated patient myoblasts that were compared with fibroblasts as a classical

diagnostic material. To analyze possible changes in mitochondrial OXPHOS complexes, we determined by SDS-PAGE and western blotting the protein content of individual OXPHOS complex subunits in homogenates in fibroblast and myoblast of the same patient (P12) (Figure 3). All OXPHOS complex subunits studied (NDUFB6, COX1, COX2, F_1-α, OSCP) were decreased in the patient.

3.3.Enzyme activities of OXPHOS complexes in fibroblast, muscle, and heart mitochondria

The functional consequences of the prevalent homozygous splicing c.317-2A>G mutation in *TMEM70* gene were analyzed by spectrophotometric measurement of the enzymatic activities of OXPHOS complexes and the mitochondrial control enzyme citrate synthase (CS) in fibroblast, heart, and muscle mitochondria (Tabule 2).

In fibroblast mitochondria, oligomycin-sensitive ATP hydrolytic activity was significantly decreased in all samples (P2, P3, P6, and P8). The activities of other analyzed respiratory chain complexes as well as activity of citrate synthase were distinctly elevated compared to the range of control values. The results from our study revealed a wide range of values of respiratory chain complexes activities in muscle and heart mitochondria, nevertheless, general patterns were observed even if we measured activities from biopsy or autopsy samples. NQR (NADH: coenzyme Q reductase (rotenone sensitive) (complex I) activities were decreased or low limit values in almost all patients (P1, P2, P4, and P6) in muscle mitochondria. On the contrary activities of QCCR (QH2: cytochrome c reductase (complex III)) were elevated in all bioptic muscle (P2, P4, and P6). Furthermore, in heart mitochondria, CS (citrate synthase) activity was high or markedly increased in all samples (P1, P2, and P7).

3.4.Mitochondrial reticulum and electron microscopical analysis in myoblast, fibroblast and cardiomyocytes

Fluorescence microscopy revealed differences in the mitochondria reticulum among patients and controls in myoblast (Figure 4A) and fibroblast (Figure 4B). MitoTracker-based visualization in myoblast (P12) showed increased fragmentation compared to controls, the mitochondrial reticulum was rather scattered and irregularly distributed, moreover, ‘‘megamitochondria’’ (visible as enlarged spherical or oval mitochondria) were observed (Figure 4A). Native visualization of the mitochondrial network in fibroblasts (P2, P3, P6) by

MitoTracker Red CMX Ros Probe showed fragmentation and unequally distributed mitochondrial network through the cell were present (Figure 4B).

Electron microscopic analysis was performed in a heart sample obtained during cardiac surgery in patient P7 and in autoptic heart tissue in patient P10 revealed multiplication and abnormal ultrastructure of mitochondria in cardiomyocytes (Figure 5). Mitochondrial swelling with sparse cristae and profound cristae distorsion were the prevalent features. Several mitochondria with concentric cristae ("onion-ring" like morphology) were detected. Some mitochondria contained electron dense globular inclusions or parallel stacked formations possibly based on cristae fragments. Multiplied and structurally aberrant mitochondria in cardiomyocytes were clearly detectable in both, a 1 month old P7 and a 3 years old patient P10.

Mitochondrial ultrastructure was also analyzed in patient myoblasts (P12) (Figure 5). Elongated mitochondria were predominant in control myoblasts, whereas structural changes, including unusually aberrant and sparse cristae, were frequent in patient myoblasts. Moreover, mitochondria with concentric cristae were also found in the myoblasts of patient P12.

Mitochondrial ultrastructure in skin fibroblasts of three patients (P11, P1, P5) was also analyzed by transmission electron microscopy (Figure 5). In cells, a heterogeneous mixture of mainly abnormal mitochondria was observed, although a few mitochondria with normal shape and ultrastructure were present. The mitochondria were partially swollen with unusual and sparse cristae compared to the fibrous mitochondria with numerous cristae of control cells.

3.5.Histological and immunohistochemical analysis performed in a set of fixed autoptic and bioptic tissues.

Cardiac hypertrophy of both ventricles with increased heart weight compared to age matched controls (Tabule A3) was a constantly present but variably pronounced feature. Gross examination described obstructive hypertrophic cardiomyopathy in two cases P5, P7. Patient P7 was diagnosed with a ventricular septal defect. The histology showed cardiomyocytes with enlarged hyperchromatic and often doubled nuclei and variably increased number of mitochondria in their cytoplasm (Figure 6). Signs of hypertrophic cardiomyopathy were most conspicuous in patients P5, P6, and P4. Less pronounced cardiac hypertrophy was detected in P1 patient. P10 patient hypertrophy was associated with foci of cardiomyocyte disarray and shrunken hyperchromatic nuclei were occasionally present in cardiomyocytes.

Histologic examination of skeletal muscle available in 5 cases did not reveal any significant structural abnormalities apart from varying fibres size in two patients (P5, P10). No ragged red fibres were detected in any case.

Mild hepatopathy characterized predominantly by microvesicular steatosis was compatible with a mitochondrial disorder. Mild microvesicular steatosis was present in 4 patients (P4, P5, P6, and P10), and in one of them (P6) it was also associated with mild cholestasis. Incipient periportal fibrosis was detected in two patients (P6, P10). In one patient (P7) centrolobular venostasis was a dominant histological feature. Histology was without any substantial abnormalities in one case (P1). The immunohistochemical analysis did not reveal a markedly increased number of mitochondria in hepatocytes.

Histochemical analysis of NADH-tetrazolium reductase (NADH-TR), succinate dehydrogenase (SDH), and cytochrome c oxidase (COX) activities was performed in frozen autoptic heart, skeletal muscle, and liver tissues of a patient P10. Histochemical staining of all three OXPHOS enzymes was generally strong, either comparable with those seen in controls or exceeding them and often displaying the coarsely granular character. Increased histochemical activity and coarsely granular staining pattern of COX and SDH were most pronounced in cardiomyocytes and to a lesser degree in skeletal muscle fibres and in hepatocytes (Figure 7). Most intensive COX and SDH positivities in cardiomyocytes were detected in the perinuclear localization and corresponded with the multiplication of mitochondria (Figure 7D).

4. Discussion

Our study represents a detailed analysis of the impact of prevalent homozygous splicing c.317-2A>G *TMEM70* mutation on the amount, stability, and activity of OXPHOS complexes, mitochondrial ultrastructure, and reticulum. The key question is how ATP synthase deficiency caused by the *TMEM70* mutations affects OXPHOS in various patients´ tissues (brain, muscle, heart, and liver) and patient derived cells (myoblasts and fibroblasts). In addition, we have assessed an amount of TMEM70 protein in four human control tissues, which could help us uncover tissue specific impact of TMEM70 protein.

To date, over 20 different *TMEM70* mutations have been described leading to a broad range of clinical manifestations [14-16,23,40]. The prevalent mutation leads to aberrant splicing and loss of transcript thus preventing the TMEM70 protein synthesis [11].

A dimerization of complex V plays a pivotal role in shaping the cristae, hence in establishing the morphology of the inner mitochondrial membrane [41]. The role of ATP synthase dimers in mitochondria cristae formation was first described in yeast models, where a downregulation of ATP synthase [42] or altered formation of ATP synthase dimers due to deficiency of the subunits e or g [43] led to the absence of cristae and formation of concentric ("onion-like") membrane structures. Severely altered mitochondrial cristae as well as "onion-like" mitochondria were present both in patient´s tissues and cultured cells. Our data confirmed previously published findings in TMEM70 patients [20,22-24,26,44]. A similar mitochondrial ultrastructure changes has been demonstrated also in models of TMEM70 deficiency [26,45]. Mitophilin protein deficiency resulted in aberrant mitochondrial morphology and the formation of concentric cristae („onion-like" morphology) in HeLa cells [46], thus this morphological feature is not exclusive to TMEM70 defects.

We have studied activities of OXPHOS complexes, their steady-state levels, and amount of their representative subunits. In the case of fibroblasts, a compensatory effect was observed in almost all cases, but this phenomenon was not apparent in all available tissues. An increase in mitochondrial mass in cardiomyocytes and increased OXPHOS activity based on SDH, COX staining was observed. The elevated levels and activities of OXPHOS complexes, associated with compensatory effect, was previously reported in several mitochondrial defects [6,47]. The adaptive response is probably enabled by post-transcriptional events [21] in addition a compensatory effect was also observed in the TMEM70 mouse model [27,45].

To further understand the impact of TMEM70 deficiency in different tissues, we analyzed the protein level profile in various human control tissues (brain, heart, liver, muscle).

The expression profile of mRNA using database searching, with low levels and slight variations in the amount of transcript, characteristic for other assembly helper factors, was reported [48,49]. Mass spectrometry (MS) analysis revealed very low cellular content of the TMEM70 protein in human heart mitochondria in our previous study [48]. Comparison of protein levels between control tissues in our study showed a low abundance of TMEM70 protein in the heart and further in muscle mitochondria compared to the highest amount in liver mitochondria. The same data were obtained in the experiment with one individual control and the analysis with four different controls. Our study is in agreement with the results of a previous findings where the level of TMEM70 protein was lower in the human heart than in the liver [27]. Database search (https://www.proteinatlas.org/) [39] revealed inconsistent data between mRNA and final TMEM70 protein levels in skeletal muscle tissue. This may indicate that although there is increased expression of mRNA, it is not translated into the protein itself. In contrast, low levels of TMEM70 mRNA were detected in the heart according to the database but the protein levels were then comparable with other tissues. The difference between mRNA and protein levels in muscle tissue was also observed in the case of another ATP synthase assembly factor, ATPAF1.

It is typical for isolated ATP synthase defects of nuclear origin that complex V remains functional, but its quantity is greatly reduced [50-52], furthmore, the membrane potential is increased and reactive oxygen species (ROS) production is stimulated [53,54]. The pathogenic mechanism of mitochondrial diseases caused by isolated defects of ATP synthase originates clearly from defective mitochondrial ATP provision. The energy deprivation and oxidative stress then become main pathogenic factors [51]. However, it is complicated to establish how the ATP synthase dysfunction correlates with the biochemical and clinical phenotypes in different types of ATP synthase disorders [52].

To date, >60 patients with TMEM70 deficiency have been described. Interestingly, these cases vary significantly in life expectancy from neonatal death to survival of almost two decades, even in patients harbouring identical *TMEM70* mutation. The most plausible explanation lies in the different levels of antioxidant defense mechanisms and/or compensatory changes at the level of OXPHOS system [55]. The other determinant for long term patients survival depends on how they manage the metabolic crisis including adaptation on extrauterine life after birth [15].

The role of the TMEM70 protein has been intensively studied in recent years, but its precise molecular function remains largely unknown. Several studies have demonstrated the presence of binding between TMEM70 and the subunit c [26-28]. Bahri et al. [26] provide evidence

that TMEM70 localization is restricted to cristae where it assembles in large oligomers that interact specifically with subunit c of ATP synthase and provide a scaffold for the assembly of the c-ring before its incorporation into functional complex. Similarly to others [6,26], we detected significantly reduced level of subunit c in skin fibroblasts (Figure A1 D). Kovalčíková at el. suggested that TMEM70 is involved in c-ring formation [27]. Moreover, they showed that subunit c import and synthesis is not affected in TMEM70 defective cells [27].

Other studies on model lines and organisms have attributed a function to TMEM70 protein in the association of the F_1 subcomplex with the c-ring [28,45]. Interestingly, the animal model shows an improvement in the impact of TMEM70 defect on complex V levels when the c subunit is overexpressed [27]. A clear link between TMEM70 protein function and the c subunit is also evidenced by the fact that in cells lacking mitochondrial DNA (rho^0), the c subunit and TMEM70 protein levels are significantly reduced. When TMEM70 is overexpressed in those cells, the c subunit is upregulated again. When F1 subunits were affected by a mutation [6] or were knocked down [56] an accumulation of subunit c was detected.

The important question remains, how at least some residual amount of functional ATP synthase is always assembled even if TMEM70 protein is not present. Is there another functional partner for TMEM70 protein? The hypothesis of a second protein required for c-ring assembly was recently confirmed by the Walker group [29]. Carroll and coauthors showed that the assembly of the c-ring requires not only TMEM70 but also a second protein TMEM242. TMEM242 is directly involved in the assembly of ATP synthase and both TMEM242 and TMEM70 interact specifically with subunit c [29]. TMEM70 and TMEM242 have similar overlapping functions in the assembly of c-ring, but additionally TMEM242 might influence the incorporation of subunits ATP6, ATP8, j, and k [29]. Finally, in our previous study [57], we obtained gene expression data in a set of 10 TMEM70 patient fibroblasts. In this group, we analysed the mRNA expression level of TMEM242. However, data does not show any specific trend in patients in the level of TMEM242 expression.

Furthermore, TMEM70 and TMEM242 interact with subunit c and also with the mitochondrial assembly intermediates of complex I [28,29]. Nevertheless, this functional connection needs to be further studied because the reduction of complex I is not consistent feature [21,27] including present study. Across various types of patient tissues, a decreased level of complex I was rather individual and seem to be tissue specific. Moreover, no assembly intermediates were observed.

Conclusion:

In summary, this study provides insight into TMEM70 protein deficiency in four different patient tissues and patient derived fibroblast and myoblasts. Our results demonstrate that isolated ATP synthase deficiency due to absence of TMEM70 triggers an adaptive/compensatory effect which is especially evident in fibroblasts.

Tab. 2: Oligomycin-sensitive ATP hydrolytic activity of ATP synthase (nmol/min/mg $_{protein}$), citrate synthase (CS) and respiratory chain complex activities (nmol/min/mg $_{protein}$) in fibroblast, muscle, and heart mitochondria. *NQR, NADH: coenzyme Q reductase (rotenone sensitive) (complex I), SQR, succinate: coenzyme Q reductase (complex II), QCCR, QH2:cytochrome c reductase (complex III), NCCR, NADH:cytochrome c reductase (rotenone sensitive) (complex I-III), SCCR, succinate:cytochrom c reductase (complex II-III), COX cytochrome c oxidase (complex IV), ATP, ATP synthase (complex V), CS citrate synthase*. Bold values indicate increased activities and italic values indicated decreased activities, nd (not detected).

Tissue		Pacient	nmol/min/mg $_{protein}$							
			NQR	**SQR**	**QCCR**	**NCCR**	**SCCR**	**COX**	**ATP**	**CS**
Fibroblasts		P2	nd	**68**	**126**	**224**	**62**	**123**	*77*	**264**
		P3	nd	**70**	**151**	**286**	**96**	**110**	*38*	**156**
		P6	nd	**93**	**217**	**199**	**85**	**174**	*37*	**236**
		P8	nd	**60**	**173**	nd	**59**	**163**	*67*	**271**
		controls (n=4)	-	28-51	65-104	119-168	36-52	30-75	97-153	86-139
Muscle	Biopsy	P2	*19*	56	**543**	62	137	336	nd	344
		P4	*133*	56	**296**	69	81	**1232**	nd	534
		P6	196	31	**576**	nd	63	*225*	nd	234
		controls (n=20)	194-354	20-108	100-217	42-156	50-206	287-1077	-	200-640
	Autopsy	P1	119	73	190	53	58	**1324**	nd	484
		P7	231	**133**	341	61	55	*323*	nd	372
		controls (n=12)	118-282	56-104	170-494	40-86	27-73	506-1002	nd	223-498
Heart	Biopsy	P7	325	**195**	**408**	534	**322**	*635*	nd	1608
		controls (n=6)	150-430	70-170	280-340	110-540	130-250	1100-2800	-	900-1700
	Autopsy	P1	238	*46*	484	38	77	**2153**	nd	**1183**
		P2	*173*	117	*74*	69	52	1032	nd	**1447**
		controls (n=8)	180-352	80-240	177-573	31-165	45-165	942-1638	nd	347-727

Tabule A3: Weights of hearts of TMEM70 deficient patients

Patient	**Age**	**Heart weight (gm)**	**Means of heart weight of age matched infants (gm)**
P1	4 years	99	73
P4	2 years	Not weighted [2]	-
P5	32 days	40	18
P6	2 months	50	23
P7	1 month	Not weighted [1]	-
P10	3 years	104	59

[1] gross examination described obstructive hypertrophic cardiomyopathy.

[2] gross examination described hypertrophy of both cardiac ventricles.

Figures:

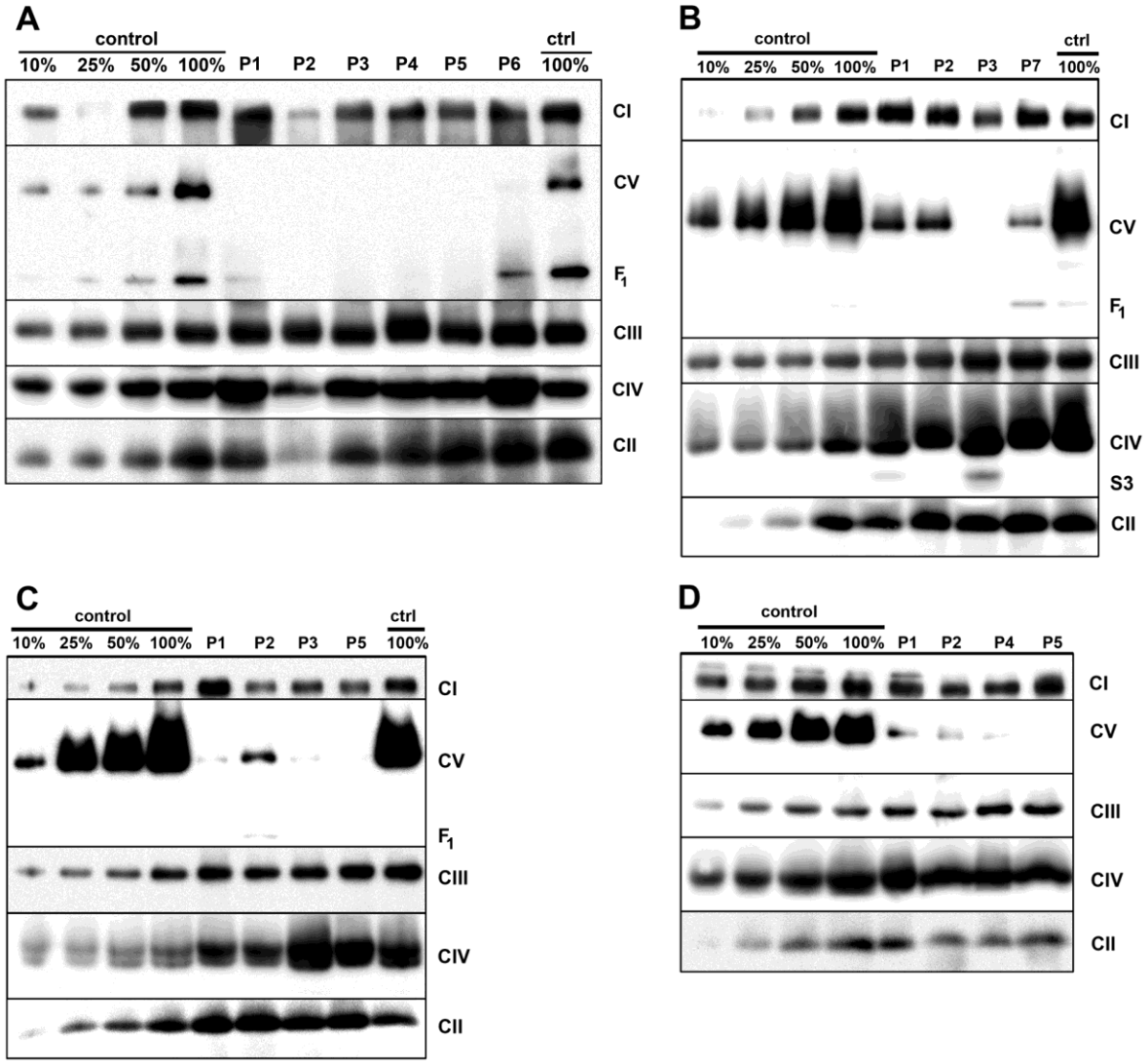

Figure 1: Steady-state levels of OXPHOS complexes in muscle, heart, liver and brain mitochondria: Mitochondrial fraction (2-20 µg) from the muscle (A), heart (B), liver (C) and brain (D) from patients carrying c.317-2A>G homozygous *TMEM70* mutation were resolved using 6-15% BN-PAGE, electroblotted and probed with specific antibodies (CI: NDUFB6, CII: SDH70, CIII: CORE2, CIV: COX1, CV: F1-α).

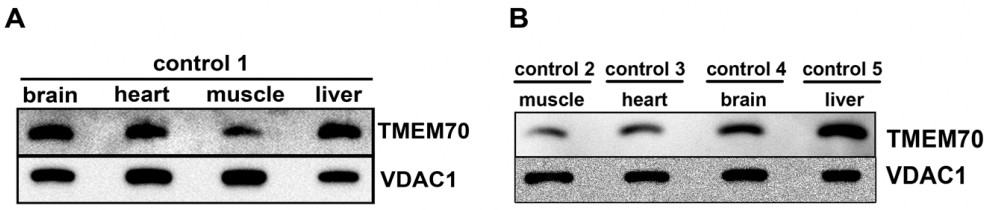

Figure 2. A) TMEM70 protein level in the various control tissues. Mitochondria fraction (10µg) from the brain (frontal cortex), heart, muscle, and liver from one control individual were resolved by 12% SDS-PAGE electroblotted and explored with specific antibodies (TMEM70 and VDAC1). The amount of the protein loaded per line was normalized to protein concentration**. B)** TMEM70 protein level in the various control tissues. Mitochondria fraction (10µg) from the muscle, heart, brain and liver from four different controls were resolved by 12% SDS-PAGE electroblotted and explored with specific antibodies (TMEM70 and VDAC1). The amount of the protein loaded per line was normalized to protein concentration.

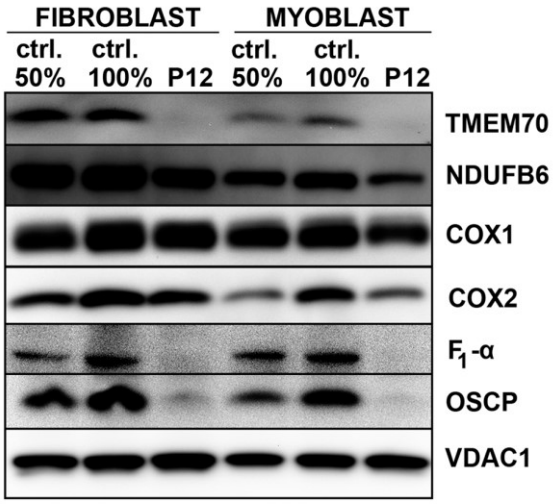

Figure 3: Comparison of protein amount of OXPHOS complex subunits in fibroblast and myoblast (P12). 5-10µg fibroblast and myoblast cell lysate were resolved by 12% SDS-PAGE electroblotted on the membrane and explored with specific antibodies for OXPHOS complex subunits.

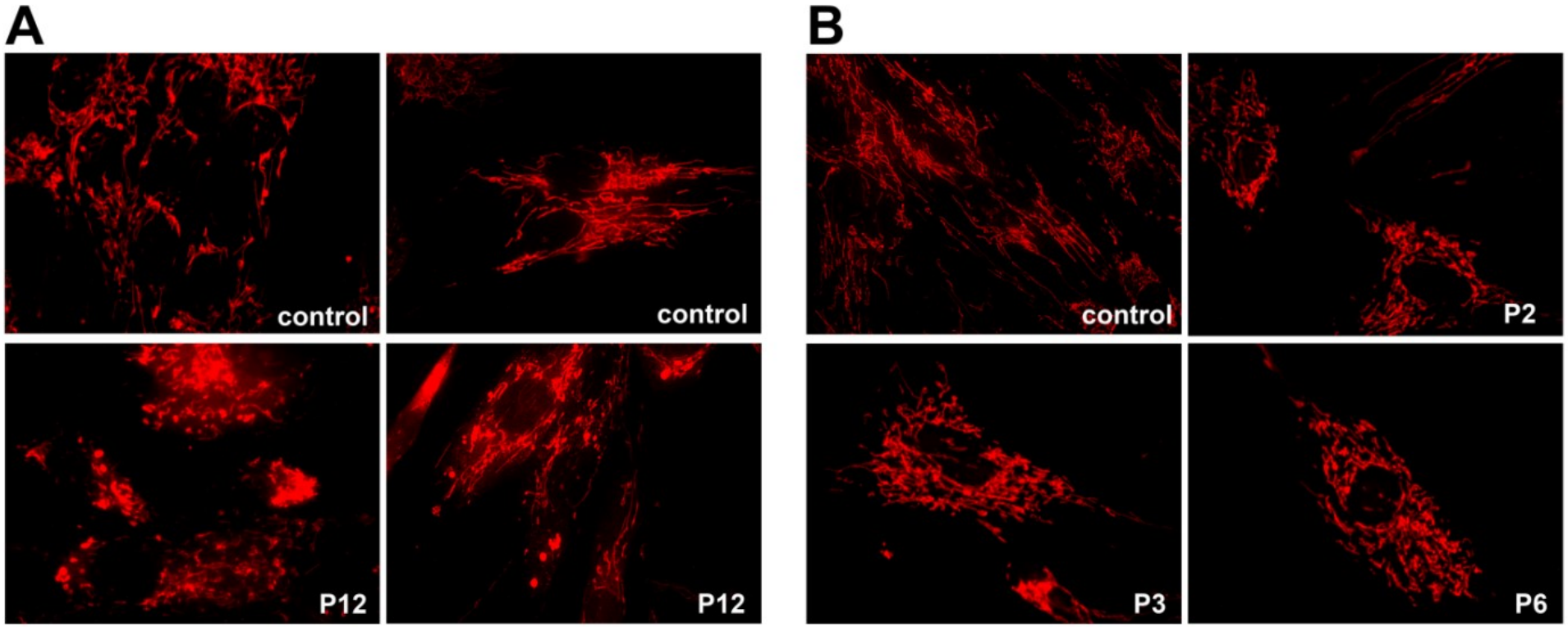

Figure 4: Native staining of the mitochondrial network in myoblast (A) and fibroblasts (B) of TMEM70 patients and controls. Myoblast and fibroblast were visualized in 10 nM MTR (MitoTracker-RED) for 15 min at 37°C. Original magnification: 600x.

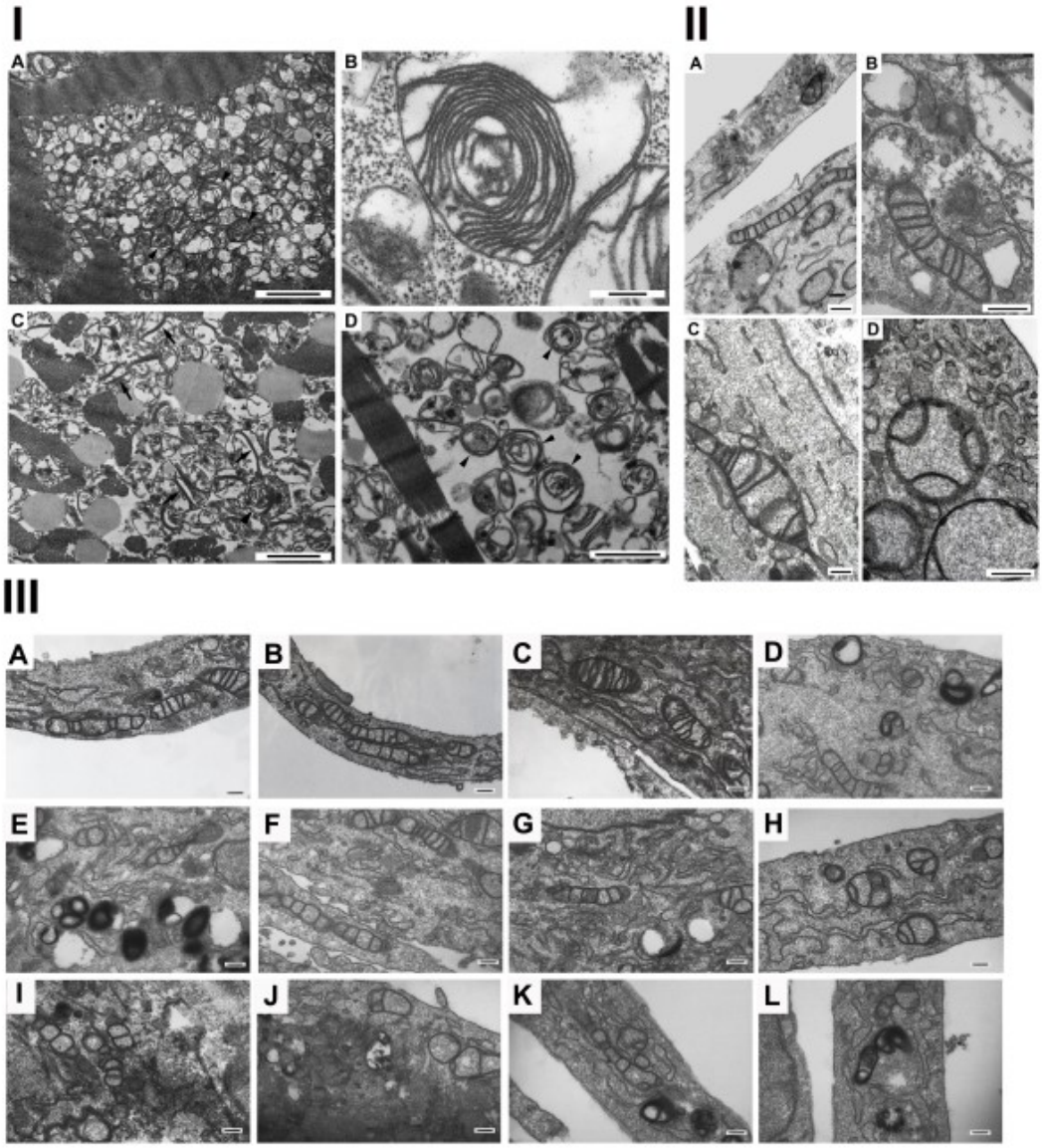

Figure 5: Mitochondrial abnormal ultrasctructure in cells and heart tissue**. I) Mitochondrial ultrastructural abnormalities in cardiomyocytes of TMEM70 deficient patients:** (A) Multiplied swollen mitochondria with reduced (asterisks) and distorted (arrowheads) cristae in a cardiomyocyte in P7. (B) Detailed view of an abnormal mitochondrion with circular concentric cristae in a cardiomyocyte in the same patient (P7). (C) Cardiomyocyte in P10, mitochondria increased in number and size display swelling and abnormal cristae configuration with the formation of parallel stacked (arrows) and circular structures (an arrowhead). Several neutral lipid droplets are present in the cytoplasm. (D) Mitochondria with prevailed "onion-ring" like morphology (arrowheads) in a cardiomyocyte in the same patient. Scale bars in (A, C, and D) represent 2µm, scale bar in (B) represents 250nm. **II) Mitochondrial ultrastructure in myoblast in TMEM70 deficient patients**: The normal mitochondria with number of cristae were observed in the control cell (A, B). In patient P12 (C, D) enlarged sphere mitochondria with the concentric shape of cristae were observed. Scale bars represent 250 nm. **II) Mitochondrial ultrastructure in cultivated TMEM70 deficient patient fibroblasts**: The normal filamentous shape mitochondria with many cristea represent control cells (A, B, C). In patient cell (D-F: P11; G-I: P1; J-L: P5) abnormal mitochondria were observed. The partially swollen mitochondria (D-H) and several mitochondria with unusual spare cristae were present (G, I, K). The mitochondria with normal shape and ultrastructure were present even in patient samples (F). Scale bars represent 250 nm.

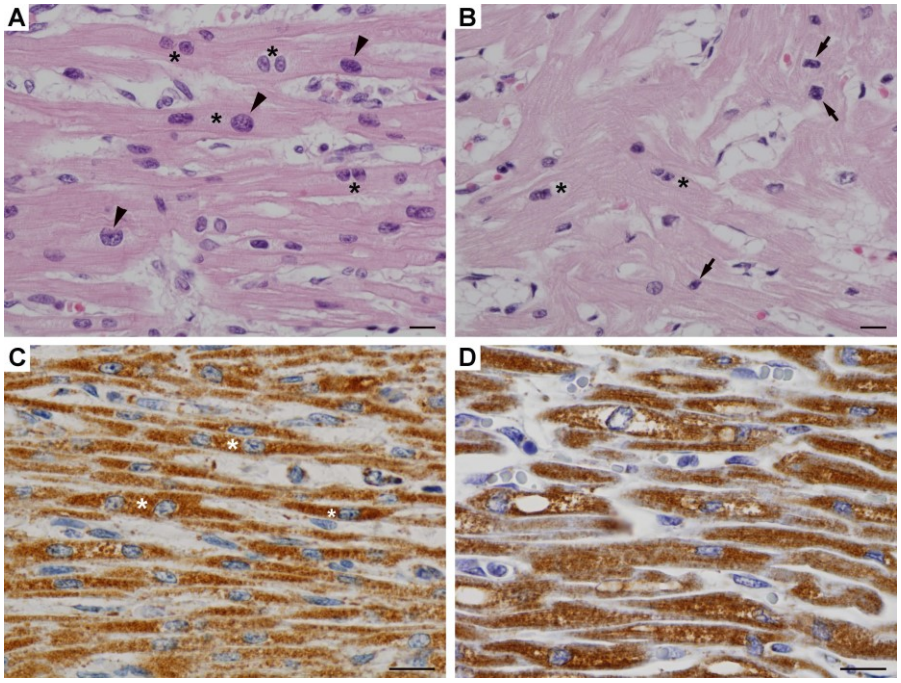

Figure 6. Hypertrophic cardiomyopathy in TMEM70 deficient patients: (A) Cardiomyocytes with enlarged hyperchromatic nuclei (arrowheads), doubled nuclei (asterisks), and finely granular cytoplasm in P7, H&E stain. (B) The disarray of cardiomyocytes, occasionally with double nuclei (asterisks) and presence of shrunken hyperchromatic nuclei in some cardiomyocytes in P10, H&E stain. (C, D) Immunohistochemical detection of prohibitin in the myocardium of TMEM deficient patients. Increased number of mitochondria in the cytoplasm of individual cardiomyocytes (asterisks) in P7 (C) and almost uniform expansion of the mitochondrial compartment in cardiomyocytes of P10 (D). Scale bars in (A, B) represent 25μm, bars in (C, D) represent 30μm.

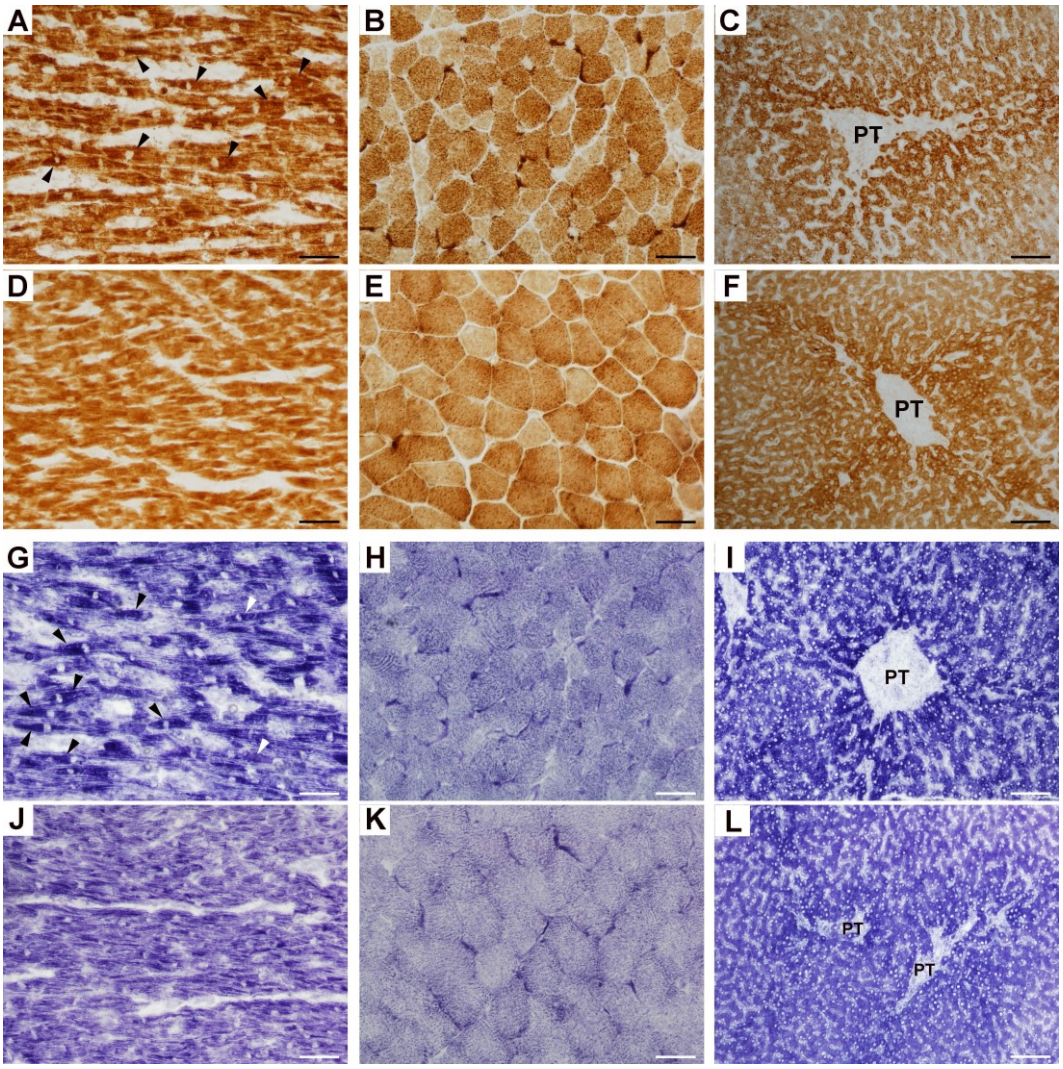

Figure. 7: Histochemical detection of COX and SDH in heart, skeletal muscle, and liver in TMEM70 deficient patient P10 and a control: Strong coarsely granular COX staining in cardiomyocytes (A), skeletal muscle fibres (B), and periportal hepatocytes (C) in patient P10, and less intensive finely granular staining in their control counterparts (D, E, and F). Analogous differences between patient´s myocardium (G), skeletal muscle (H) and liver (I), and control tissues (J, K, and L) were seen in SDH staining. Massive COX (A) and SDH (G) reaction in the perinuclear region of patient's cardiomyocytes is marked by arrowheads. Accented subsarcolemmal staining for COX (B) and less so for SDH (H) in skeletal muscle fibres were more prominent in the patient. Scale bars in (A, D, G, and J) represent 100µm, in (B, E, H, and K) 50µm, and in (C, F, I, and L) 200µm. PT-portal tracts.

Supplements:

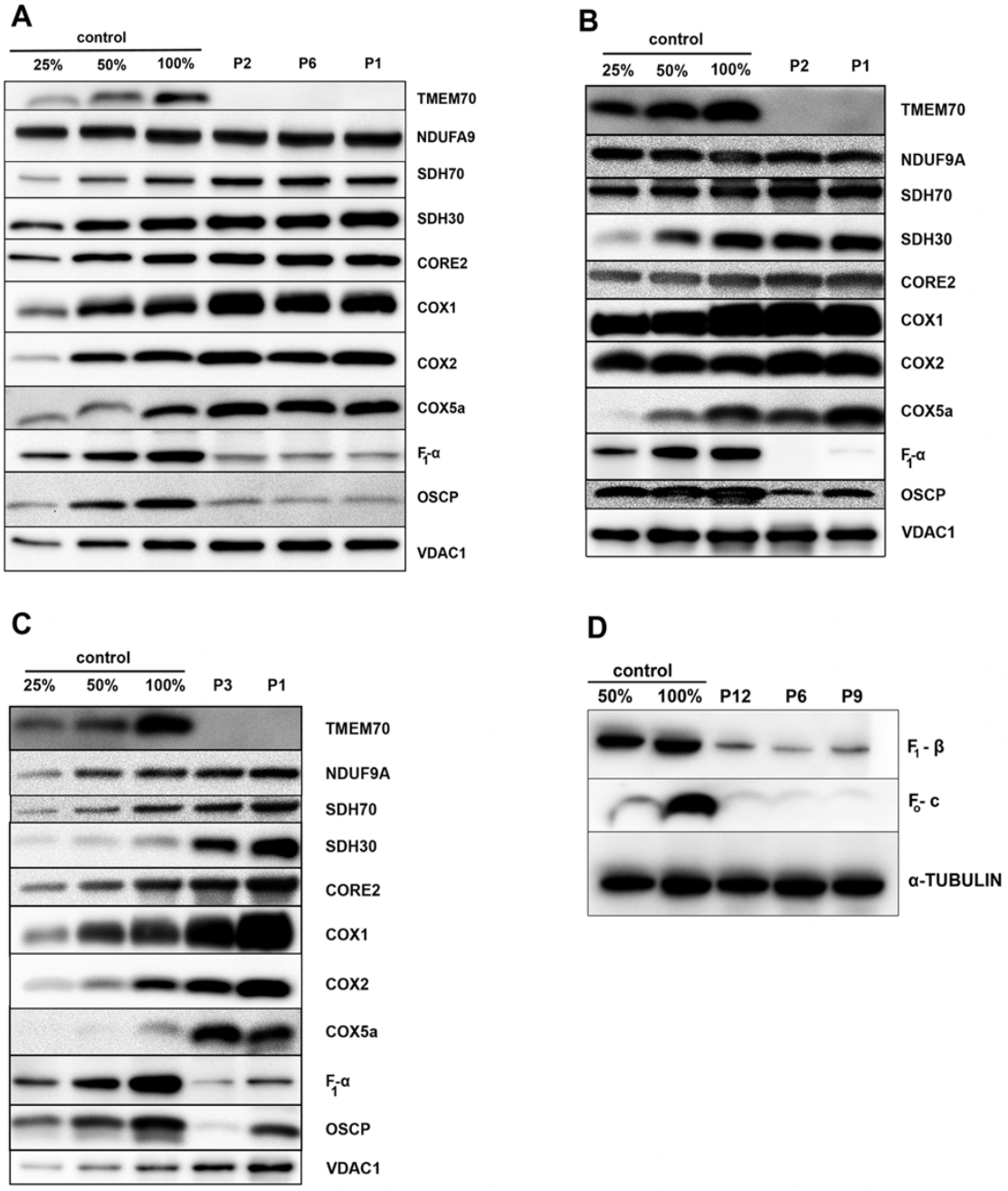

Figure A1: The steady-state levels of selected OXPHOS complex subunits in fibroblast cell lysate (A, D), heart (B), and muscle (C) mitochondria. (5-20µg) proteins were resolved using 12% SDS-PAGE, electroblotted and probed with specific antibodies.

Fundings: This work was supported by the Ministry of Health of the Czech Republic [grant numbers AZV NV19-07-00149, RVO-VFN-64165]; and Charles University [grant numbers SVV260516, UNCE 204064, Cooperatio Program, research area Paediatrics]. The funding bodies were not involved in the study's design, collection, analysis, and interpretation of data and the writing of the manuscript.

Author Contributions: Conceptualization, H.S. and M.T.; methodology, H.S. and M.T.; formal analysis, H.S., H.Hu. and M.T..; investigation, H.S., H.Hu., Z.S., S.P., L.W. and H.Ha; resources, H.S. and M.T., ; writing—original draft preparation, H.S.; writing—review and editing, H.S., M.T., T.H., V.S. and J.Z.; visualization, H.S. and H. Hu.; supervision, M.T.; project administration, H.S. and M.T.; funding acquisition, M.T., T.H., H.Ha. and J.Z. All authors have read and agreed to the published version of the manuscript. Please turn to the CRediT taxonomy for the term explanation. Authorship must be limited to those who have contributed substantially to the work reported.

Conflicts of Interest: The authors declare no conflict of interest. The funders had no role in the design of the study; in the collection, analyses, or interpretation of data; in the writing of thfe manuscript, or in the decision to publish the results.

Institutional Review Board Statement: The study was conducted according to the guidelines of the Declaration of Helsinki, and approved by the Institutional Research Ethics Committee (First faculty of Medicine, Charles University in Prague).

Informed Consent Statement: Informed consent was obtained from all subjects involved in the study.

Data Availability Statement: The data presented in this study are available upon request from the corresponding author.

Acknowledgments: We would like to acknowledge S. Knopová (First Faculty of Medicine, Charles University, Prague, Czech Republic) for her assistance with the spectrophotometric analysis and M. Elleder (First Faculty of Medicine, Charles University, Prague, Czech Republic) and J. Sladkova (First Faculty of Medicine, Charles University, Prague, Czech Republic) for their assistance with the electron microscopy.

Reference

1. Lott, M.T., Leipzig, J.N., Derbeneva, O., Xie, H.M., Chalkia, D., Sarmady, M., Procaccio, V., and Wallace, D.C. (2013). mtDNA Variation and Analysis Using Mitomap and Mitomaster. Curr Protoc Bioinformatics *44*, 1.23.21-26. 10.1002/0471250953.bi0123s44.

2. Jonckheere, A.I., Renkema, G.H., Bras, M., van den Heuvel, L.P., Hoischen, A., Gilissen, C., Nabuurs, S.B., Huynen, M.A., de Vries, M.C., Smeitink, J.A., and Rodenburg, R.J. (2013). A complex V ATP5A1 defect causes fatal neonatal mitochondrial encephalopathy. Brain *136*, 1544-1554. 10.1093/brain/awt086.

3. Lines, M.A., Cuillerier, A., Chakraborty, P., Naas, T., Duque Lasio, M.L., Michaud, J., Pileggi, C., Harper, M.E., Burelle, Y., Toler, T.L., et al. (2021). A recurrent de novo ATP5F1A substitution associated with neonatal complex V deficiency. Eur J Hum Genet *29*, 1719-1724. 10.1038/s41431-021-00956-0.

4. Lieber, D.S., Calvo, S.E., Shanahan, K., Slate, N.G., Liu, S., Hershman, S.G., Gold, N.B., Chapman, B.A., Thorburn, D.R., Berry, G.T., et al. (2013). Targeted exome sequencing of suspected mitochondrial disorders. Neurology *80*, 1762-1770. 10.1212/WNL.0b013e3182918c40.

5. Zech, M., Kopajtich, R., Steinbrücker, K., Bris, C., Gueguen, N., Feichtinger, R.G., Achleitner, M.T., Duzkale, N., Périvier, M., Koch, J., et al. (2022). Variants in Mitochondrial ATP Synthase Cause Variable Neurologic Phenotypes. Ann Neurol *91*, 225-237. 10.1002/ana.26293.

6. Mayr, J.A., Havlícková, V., Zimmermann, F., Magler, I., Kaplanová, V., Jesina, P., Pecinová, A., Nusková, H., Koch, J., Sperl, W., and Houstek, J. (2010). Mitochondrial ATP synthase deficiency due to a mutation in the ATP5E gene for the F1 epsilon subunit. Hum Mol Genet *19*, 3430-3439. 10.1093/hmg/ddq254.

7. Oláhová, M., Yoon, W.H., Thompson, K., Jangam, S., Fernandez, L., Davidson, J.M., Kyle, J.E., Grove, M.E., Fisk, D.G., Kohler, J.N., et al. (2018). Biallelic Mutations in ATP5F1D, which Encodes a Subunit of ATP Synthase, Cause a Metabolic Disorder. Am J Hum Genet *102*, 494-504. 10.1016/j.ajhg.2018.01.020.

8. Barca, E., Ganetzky, R.D., Potluri, P., Juanola-Falgarona, M., Gai, X., Li, D., Jalas, C., Hirsch, Y., Emmanuele, V., Tadesse, S., et al. (2018). USMG5 Ashkenazi Jewish founder mutation impairs mitochondrial complex V dimerization and ATP synthesis. Hum Mol Genet *27*, 3305-3312. 10.1093/hmg/ddy231.

9. Neilson, D.E., Zech, M., Hufnagel, R.B., Slone, J., Wang, X., Homan, S., Gutzwiller, L.M., Leslie, E.J., Leslie, N.D., Xiao, J., et al. (2022). A Novel Variant of ATP5MC3 Associated with Both Dystonia and Spastic Paraplegia. Mov Disord *37*, 375-383. 10.1002/mds.28821.

10. De Meirleir, L., Seneca, S., Lissens, W., De Clercq, I., Eyskens, F., Gerlo, E., Smet, J., and Van Coster, R. (2004). Respiratory chain complex V deficiency due to a mutation in the assembly gene ATP12. J Med Genet *41*, 120-124.

11. Cízková, A., Stránecký, V., Mayr, J.A., Tesarová, M., Havlícková, V., Paul, J., Ivánek, R., Kuss, A.W., Hansíková, H., Kaplanová, V., et al. (2008). TMEM70 mutations cause isolated ATP synthase deficiency and neonatal mitochondrial encephalocardiomyopathy. Nat Genet *40*, 1288-1290. 10.1038/ng.246.

12. Baban, A., Adorisio, R., Corica, B., Rizzo, C., Calì, F., Semeraro, M., Taurisano, R., Magliozzi, M., Carrozzo, R., Parisi, F., et al. (2020). Delayed appearance of 3-methylglutaconic aciduria in neonates with early onset metabolic cardiomyopathies: A potential pitfall for the diagnosis. Am J Med Genet A *182*, 64-70. 10.1002/ajmg.a.61383.

13. Diodato, D., Invernizzi, F., Lamantea, E., Fagiolari, G., Parini, R., Menni, F., Parenti, G., Bollani, L., Pasquini, E., Donati, M.A., et al. (2015). Common and Novel TMEM70 Mutations in a Cohort of Italian Patients with Mitochondrial Encephalocardiomyopathy. JIMD Rep *15*, 71-78. 10.1007/8904_2014_300.

14. Hirono, K., Ichida, F., Nishio, N., Ogawa-Tominaga, M., Fushimi, T., Feichtinger, R.G., Mayr, J.A., Kohda, M., Kishita, Y., Okazaki, Y., et al. (2019). Mitochondrial complex deficiency by novel compound heterozygous. Clin Case Rep *7*, 553-557. 10.1002/ccr3.2050.

15. Honzík, T., Tesarová, M., Mayr, J.A., Hansíková, H., Jesina, P., Bodamer, O., Koch, J., Magner, M., Freisinger, P., Huemer, M., et al. (2010). Mitochondrial encephalocardio-myopathy with early neonatal onset due to TMEM70 mutation. Arch Dis Child *95*, 296-301. 10.1136/adc.2009.168096.

16. Magner, M., Dvorakova, V., Tesarova, M., Mazurova, S., Hansikova, H., Zahorec, M., Brennerova, K., Bzduch, V., Spiegel, R., Horovitz, Y., et al. (2014). TMEM70 deficiency: long-term outcome of 48 patients. J Inherit Metab Dis. 10.1007/s10545-014-9774-8.

17. Torraco, A., Verrigni, D., Rizza, T., Meschini, M.C., Vazquez-Memije, M.E., Martinelli, D., Bianchi, M., Piemonte, F., Dionisi-Vici, C., Santorelli, F.M., et al. (2012). TMEM70: a mutational hot spot in nuclear ATP synthase deficiency with a pivotal role in complex V biogenesis. Neurogenetics *13*, 375-386. 10.1007/s10048-012-0343-8.

18. Wortmann, S.B., Rodenburg, R.J., Jonckheere, A., de Vries, M.C., Huizing, M., Heldt, K., van den Heuvel, L.P., Wendel, U., Kluijtmans, L.A., Engelke, U.F., et al. (2009). Biochemical and genetic analysis of 3-methylglutaconic aciduria type IV: a diagnostic strategy. Brain *132*, 136-146. 10.1093/brain/awn296.

19. Hejzlarová, K., Mráček, T., Vrbacký, M., Kaplanová, V., Karbanová, V., Nůsková, H., Pecina, P., and Houštěk, J. (2014). Nuclear genetic defects of mitochondrial ATP synthase. Physiol Res *63 Suppl 1*, S57-71.

20. Cameron, J.M., Levandovskiy, V., Mackay, N., Ackerley, C., Chitayat, D., Raiman, J., Halliday, W.H., Schulze, A., and Robinson, B.H. (2011). Complex V TMEM70 deficiency results in mitochondrial nucleoid disorganization. Mitochondrion *11*, 191-199. 10.1016/j.mito.2010.09.008.

21. Havlickova Karbanova, V., Cizkova Vrbacka, A., Hejzlarova, K., Nuskova, H., Stranecky, V., Potocka, A., Kmoch, S., and Houstek, J. (2012). Compensatory upregulation of respiratory chain complexes III and IV in isolated deficiency of ATP synthase due to TMEM70 mutation. Biochim Biophys Acta *1817*, 1037-1043. 10.1016/j.bbabio.2012.03.004.

22. Sládková, J., Spáčilová, J., Čapek, M., Tesařová, M., Hansíková, H., Honzík, T., Martínek, J., Zámečník, J., Kostková, O., and Zeman, J. (2015). Analysis of Mitochondrial Network Morphology in Cultured Myoblasts from Patients with Mitochondrial Disorders. Ultrastruct Pathol *39*, 340-350. 10.3109/01913123.2015.1054013.

23. Braczynski, A.K., Vlaho, S., Müller, K., Wittig, I., Blank, A.E., Tews, D.S., Drott, U., Kleinle, S., Abicht, A., Horvath, R., et al. (2015). ATP synthase deficiency due to TMEM70 mutation leads to ultrastructural mitochondrial degeneration and is amenable to treatment. Biomed Res Int *2015*, 462592. 10.1155/2015/462592.

24. Diodato, D., Invernizzi, F., Lamantea, E., Fagiolari, G., Parini, R., Menni, F., Parenti, G., Bollani, L., Pasquini, E., Donati, M.A., et al. (2014). Common and Novel TMEM70 Mutations in a Cohort of Italian Patients with Mitochondrial Encephalocardiomyopathy. JIMD Rep. 10.1007/8904_2014_300.

25. Jonckheere, A.I., Huigsloot, M., Lammens, M., Jansen, J., van den Heuvel, L.P., Spiekerkoetter, U., von Kleist-Retzow, J.C., Forkink, M., Koopman, W.J., Szklarczyk, R., et al. (2011). Restoration of complex V deficiency caused by a novel deletion in the human TMEM70 gene normalizes mitochondrial morphology. Mitochondrion *11*, 954-963. 10.1016/j.mito.2011.08.012.

26. Bahri, H., Buratto, J., Rojo, M., Dompierre, J.P., Salin, B., Blancard, C., Cuvellier, S., Rose, M., Ben Ammar Elgaaied, A., Tetaud, E., et al. (2021). TMEM70 forms oligomeric scaffolds within mitochondrial cristae promoting in situ assembly of mammalian ATP synthase proton channel. Biochim Biophys Acta Mol Cell Res *1868*, 118942. 10.1016/j.bbamcr.2020.118942.

27. Kovalčíková, J., Vrbacký, M., Pecina, P., Tauchmannová, K., Nůsková, H., Kaplanová, V., Brázdová, A., Alán, L., Eliáš, J., Čunátová, K., et al. (2019). TMEM70 facilitates biogenesis of mammalian ATP synthase by promoting subunit c incorporation into the rotor structure of the enzyme. FASEB J *33*, 14103-14117. 10.1096/fj.201900685RR.

28. Sánchez-Caballero, L., Elurbe, D.M., Baertling, F., Guerrero-Castillo, S., van den Brand, M., van Strien, J., van Dam, T.J.P., Rodenburg, R., Brandt, U., Huynen, M.A., and Nijtmans, L.G.J. (2020). TMEM70 functions in the assembly of complexes I and V. Biochim Biophys Acta Bioenerg *1861*, 148202. 10.1016/j.bbabio.2020.148202.

29. Carroll, J., He, J., Ding, S., Fearnley, I.M., and Walker, J.E. (2021). TMEM70 and TMEM242 help to assemble the rotor ring of human ATP synthase and interact with assembly factors for complex I. Proc Natl Acad Sci U S A *118*. 10.1073/pnas.2100558118.

30. Richler, C., and Yaffe, D. (1970). The in vitro cultivation and differentiation capacities of myogenic cell lines. Dev Biol *23*, 1-22. 10.1016/s0012-1606(70)80004-5.

31. Rickwood, D., Wilson, M.T., Darley-Usmar, W.M. (1987). Isolation and characteristics of intact mitochondria. In Mitochondria: A Practical Approach, V.M. Darley-Usmar, Rickwood, D. and Wilson, M. T., ed. (IRL Press), pp. 3-5.

32. Lowry, O.H., Rosebrough, N.J., Farr, A.L., and Randall, R.J. (1951). Protein measurement with the Folin phenol reagent. J Biol Chem *193*, 265-275.

33. Schägger, H., and von Jagow, G. (1991). Blue native electrophoresis for isolation of membrane protein complexes in enzymatically active form. Anal Biochem *199*, 223-231.

34. Luft, J.H. (1956). Permanganate—A New Fixative for Electron Microscopy. The Journal of Biophysical and Biochemical Cytology *2*, 799-802. 10.1083/jcb.2.6.799.

35. Brantova, O., Tesarova, M., Hansikova, H., Elleder, M., Zeman, J., and Sladkova, J. (2006). Ultrastructural changes of mitochondria in the cultivated skin fibroblasts of patients with point mutations in mitochondrial DNA. Ultrastruct Pathol *30*, 239-245.

36. Lojda, Z., Kociánová, J., and Maratka, Z. (1979). Histochemistry of the human duodenal mucosa with special reference to the gradient of activities of the brush border enzymes. Scand J Gastroenterol Suppl *54*, 7-13.

37. Dubowitz, V. (2007). Musle Biopsy: A Practical Approach. In C. Sewry, ed. Elsevier.

38. Stiburek, L., Vesela, K., Hansikova, H., Pecina, P., Tesarova, M., Cerna, L., Houstek, J., and Zeman, J. (2005). Tissue-specific cytochrome c oxidase assembly defects due to mutations in SCO2 and SURF1. Biochem J *392*, 625-632.

39. Uhlén, M., Karlsson, M.J., Hober, A., Svensson, A.S., Scheffel, J., Kotol, D., Zhong, W., Tebani, A., Strandberg, L., Edfors, F., et al. (2019). The human secretome. Sci Signal *12*. 10.1126/scisignal.aaz0274.

40. Catteruccia, M., Verrigni, D., Martinelli, D., Torraco, A., Agovino, T., Bonafé, L., D'Amico, A., Donati, M.A., Adorisio, R., Santorelli, F.M., et al. (2014). Persistent pulmonary arterial hypertension in the newborn (PPHN): a frequent manifestation of TMEM70 defective patients. Mol Genet Metab *111*, 353-359. 10.1016/j.ymgme.2014.01.001.

41. Davies, K.M., Anselmi, C., Wittig, I., Faraldo-Gómez, J.D., and Kühlbrandt, W. (2012). Structure of the yeast F1Fo-ATP synthase dimer and its role in shaping the mitochondrial cristae. Proc Natl Acad Sci U S A *109*, 13602-13607. 10.1073/pnas.1204593109.

42. Lefebvre-Legendre, L., Salin, B., Schaëffer, J., Brèthes, D., Dautant, A., Ackerman, S.H., and di Rago, J.P. (2005). Failure to assemble the alpha 3 beta 3 subcomplex of the ATP synthase leads to accumulation of the alpha and beta subunits within inclusion bodies and the loss of mitochondrial cristae in Saccharomyces cerevisiae. J Biol Chem *280*, 18386-18392. 10.1074/jbc.M410789200.

43. Paumard, P., Vaillier, J., Coulary, B., Schaeffer, J., Soubannier, V., Mueller, D.M., Brèthes, D., di Rago, J.P., and Velours, J. (2002). The ATP synthase is involved in generating mitochondrial cristae morphology. EMBO J *21*, 221-230. 10.1093/emboj/21.3.221.

44. Holme, E., Greter, J., Jacobson, C.E., Larsson, N.G., Lindstedt, S., Nilsson, K.O., Oldfors, A., and Tulinius, M. (1992). Mitochondrial ATP-synthase deficiency in a child with 3-methylglutaconic aciduria. Pediatr Res *32*, 731-735. 10.1203/00006450-199212000-00022.

45. Vrbacký, M., Kovalčíková, J., Chawengsaksophak, K., Beck, I.M., Mráček, T., Nůsková, H., Sedmera, D., Papoušek, F., Kolář, F., Sobol, M., et al. (2016). Knockout of Tmem70 alters biogenesis of ATP synthase and leads to embryonal lethality in mice. Hum Mol Genet *25*, 4674-4685. 10.1093/hmg/ddw295.

46. John, G.B., Shang, Y., Li, L., Renken, C., Mannella, C.A., Selker, J.M., Rangell, L., Bennett, M.J., and Zha, J. (2005). The mitochondrial inner membrane protein mitofilin controls cristae morphology. Mol Biol Cell *16*, 1543-1554. 10.1091/mbc.e04-08-0697.

47. Kovářová, N., Cížková Vrbacká, A., Pecina, P., Stránecký, V., Pronicka, E., Kmoch, S., and Houštěk, J. (2012). Adaptation of respiratory chain biogenesis to cytochrome c oxidase deficiency caused by SURF1 gene mutations. Biochimica et biophysica acta *1822*, 1114-1124. 10.1016/j.bbadis.2012.03.007.

48. Hejzlarová, K., Tesařová, M., Vrbacká-Čížková, A., Vrbacký, M., Hartmannová, H., Kaplanová, V., Nosková, L., Kratochvílová, H., Buzková, J., Havlíčková, V., et al. (2011). Expression and processing of the TMEM70 protein. Biochim Biophys Acta *1807*, 144-149. 10.1016/j.bbabio.2010.10.005.

49. Picková, A., Paul, J., Petruzzella, V., and Houstek, J. (2003). Differential expression of ATPAF1 and ATPAF2 genes encoding F(1)-ATPase assembly proteins in mouse tissues. FEBS Lett *551*, 42-46.

50. Houstek, J., Pícková, A., Vojtísková, A., Mrácek, T., Pecina, P., and Jesina, P. (2006). Mitochondrial diseases and genetic defects of ATP synthase. Biochim Biophys Acta *1757*, 1400-1405. 10.1016/j.bbabio.2006.04.006.

51. Mrácek, T., Pecina, P., Vojtísková, A., Kalous, M., Sebesta, O., and Houstek, J. (2006). Two components in pathogenic mechanism of mitochondrial ATPase deficiency: energy deprivation and ROS production. Exp Gerontol *41*, 683-687. 10.1016/j.exger.2006.02.009.

52. Nuskova, H., Mikesova, J., Efimova, I., Pecinova, A., Pecina, P., Drahota, Z., Houstek, J., and Mracek, T. (2020). Biochemical thresholds for pathological presentation of ATP synthase deficiencies. Biochem Biophys Res Commun *521*, 1036-1041. 10.1016/j.bbrc.2019.11.033.

53. Baracca, A., Sgarbi, G., Mattiazzi, M., Casalena, G., Pagnotta, E., Valentino, M.L., Moggio, M., Lenaz, G., Carelli, V., and Solaini, G. (2007). Biochemical phenotypes associated with the mitochondrial ATP6 gene mutations at nt8993. Biochim Biophys Acta *1767*, 913-919. 10.1016/j.bbabio.2007.05.005.

54. Mattiazzi, M., Vijayvergiya, C., Gajewski, C.D., DeVivo, D.C., Lenaz, G., Wiedmann, M., and Manfredi, G. (2004). The mtDNA T8993G (NARP) mutation results in an impairment of oxidative phosphorylation that can be improved by antioxidants. Hum Mol Genet *13*, 869-879. 10.1093/hmg/ddh103.

55. Havlíčková Karbanová, V., Cížková Vrbacká, A., Hejzlarová, K., Nůsková, H., Stránecký, V., Potocká, A., Kmoch, S., and Houštěk, J. (2012). Compensatory upregulation of respiratory chain complexes III and IV in isolated deficiency of ATP synthase due to TMEM70 mutation. Biochim Biophys Acta *1817*, 1037-1043. 10.1016/j.bbabio.2012.03.004.

56. Pecina, P., Nůsková, H., Karbanová, V., Kaplanová, V., Mráček, T., and Houštěk, J. (2018). Role of the mitochondrial ATP synthase central stalk subunits γ and δ in the activity and assembly of the mammalian enzyme. Biochim Biophys Acta Bioenerg *1859*, 374-381. 10.1016/j.bbabio.2018.02.007.

57. Cízková, A., Stránecký, V., Ivánek, R., Hartmannová, H., Nosková, L., Piherová, L., Tesarová, M., Hansíková, H., Honzík, T., Zeman, J., et al. (2008). Development of a human mitochondrial oligonucleotide microarray (h-MitoArray) and gene expression analysis of fibroblast cell lines from 13 patients with isolated F1Fo ATP synthase deficiency. BMC Genomics *9*, 38. 10.1186/1471-2164-9-38.

Supplement 4)

Honzík, T., Tesařová, M., Vinšová, K., Hansíková, H., Magner, M., **Kratochvílová, H.**, Zámečník, J., Zeman, J., and Ješina, P. (2013). **Different laboratory and muscle biopsy findings in a family with an m.8851T>C mutation in the mitochondrial *MTATP6* gene**. Mol Genet Metab 108, 102-105. IF = 2.827, Quartile Score = Q2 (2013).

Molecular Genetics and Metabolism 108 (2013) 102–105

Contents lists available at SciVerse ScienceDirect

Molecular Genetics and Metabolism

journal homepage: www.elsevier.com/locate/ymgme

Brief Communication

Different laboratory and muscle biopsy findings in a family with an m.8851T>C mutation in the mitochondrial *MTATP6* gene☆,☆☆,★,★★

Tomas Honzik [a], Marketa Tesarova [a], Kamila Vinsova [a], Hana Hansikova [a], Martin Magner [a], Hana Kratochvilova [a], Josef Zamecnik [c], Jiri Zeman [a], Pavel Jesina [b,*]

[a] Department of Pediatrics and Adolescent Medicine, First Faculty of Medicine, Charles University in Prague and General University Hospital in Prague, Czech Republic
[b] Institute of Inherited Metabolic Diseases, First Faculty of Medicine, Charles University in Prague and General University Hospital in Prague, Czech Republic
[c] Department of Pathology and Molecular Medicine, 2nd Faculty of Medicine, Charles University in Prague and Teaching Hospital Motol in Prague, Czech Republic

ARTICLE INFO

Article history:
Received 31 August 2012
Received in revised form 5 November 2012
Accepted 5 November 2012
Available online 13 November 2012

Keywords:
Leigh syndrome
ATP synthase
Mitochondrial DNA m.8851T>C mutation

ABSTRACT

We report the second known family with a very rare, maternally inherited missense m.8851T>C mutation in the mitochondrial *MTATP6* gene. A failure to thrive, microcephaly, psychomotor retardation and hypotonia were present in a 3-year-old girl with a high mtDNA mutation load (87–97%). Ataxia and Leigh syndrome were subsequently documented in a neurological examination and brain MRI. A muscle biopsy demonstrated decreased ATP synthase and an accumulation of succinate dehydrogenase products, indicating mitochondrial myopathy. Her 36-year-old mother (68% blood heteroplasmy) developed peripheral neuropathy and muscle weakness at the age of 22 years. Our findings extend the clinical and laboratory phenotype associated with the m.8851T>C mutation.

1. Introduction

Mitochondrial disorders due to isolated ATPase deficiency represent, on the molecular level, a heterogeneous group of disorders caused by mutations in nuclear or mitochondrial genes for structural subunits or nuclearly encoded genes for assembly factors [1]. Mutations in mtDNA have been primarily found in the ATP6 subunits of the ATPase (gene *MTATP6*). Although the *MTATP6* gene is highly polymorphic in the normal population, its pathogenic mutations can lead to severe symptoms. This gene is considered as a "hotspot" for mutations resulting in Leigh syndrome and the pathogenically similar entity of bilateral striatal necrosis. The most common and best studied of the pathogenic *MTATP6* mutations is the m.8993T>G mutation, which is clinically described as maternally inherited Leigh syndrome (MILS) or NARP syndrome (neuropathy, ataxia and retinitis pigmentosa). However, seven other mutations in this gene have also been associated with Leigh syndrome [reviewed in 2].

Leigh syndrome, a subacute necrotizing encephalopathy, is a progressive neurodegenerative disease. Its symptoms typically occur in early childhood and are heterogeneous, including hypotonia, psychomotor regression, ataxia, ocular movement abnormalities, seizures, dystonia, swallowing dysfunction, intention tremor, and an elevated lactate level in blood and cerebrospinal fluid. The clinical diagnosis is supported by symmetric abnormalities in the basal ganglia on a magnetic resonance imaging (MRI) [3].

One of the rare mutations in Leigh syndrome is the mutation m.8851T>C in the mitochondrial *MTATP6* gene. The first genetically proven case was published in 1995 by De Meirleir [4]. Herein, we report on the second family diagnosed with this very rare mtDNA m.8851T>C mutation and a high level of heteroplasmy in various tissues (87–97%). We observed novel laboratory and muscle biopsy findings in the patient and a new clinical presentation in her mother. Our findings extend the clinical and laboratory phenotypes associated with this mtDNA mutation.

2. Laboratory methods — see electronic supplement (Supplement 1)

2.1. Patients

2.1.1. Case report — girl

The 3-year-old female patient was born at term following an uncomplicated vaginal delivery and uneventful pregnancy; she was the

Abbreviations: BN-PAGE, Blue Native Polyacrylamide Gel Electrophoresis; CSF, cerebrospinal fluid; DCCD, Dicyclohexylcarbodiimide; MTATP6, mitochondrial ATP 6 subunit; OXPHOS, oxidative phosphorylation.

☆ The author serving as a guarantor for the article: Pavel Jesina, M.D., MSc., Ph.D.

☆☆ Competing interest statement: all authors confirm that they have no competing interests to declare.

★ Details of funding: the authors confirm independence from the sponsors; the content of the article has not been influenced by the sponsors.

★★ Details of ethics approval: the study was performed in accordance with the Declaration of Helsinki of the World Medical Association. Due to the nature of the study, no ethical approval was requested from the local ethics committee.

* Corresponding author at: Institute of Inherited Metabolic Diseases, First Faculty of Medicine, Charles University in Prague and General University Hospital in Prague, Ke Karlovu 2, 128 08 Prague 2, Czech Republic. Fax: +420 224 967 168.
E-mail address: pavel.jesina@vfn.cz (P. Jesina).

1096-7192/$ – see front matter © 2012 Elsevier Inc. All rights reserved.
http://dx.doi.org/10.1016/j.ymgme.2012.11.002

5th child of non-consanguineous parents of Roma origin. Her weight was 3290 g, length was 48 cm and had a head circumference of 32 cm (10th centile). Her postnatal adaptation was uncomplicated with an Apgar score of 9 at both the 5th and 10th minutes. Her development was uneventful until she was 8 months old. At that time, hypotonia and loss of responsive smiling were observed. In the second year of her life, she demonstrated a developmental delay corresponding to the level of a seven-month-old infant. At the age of 14 months, her weight and head circumference were below the third percentile, while her length was in the 25th centile. A neurological examination revealed central hypotonia, ataxia, and a poor hearing response. Electroencephalography and electromyography demonstrated that her somato-sensory evoked potentials on the n. tibialis and n. medianus were normal. Her visual and brain auditory evoked potentials documented pathological responses. An ophthalmological examination showed no optic atrophy or retinopathy. Electrocardiography and echocardiography were normal.

Brain MRI demonstrated diffuse symmetric hyperintensity on a T2-weighted image of the bilateral basal ganglia, including the caudate nuclei. The white matter, brainstem, and spinal cord did not show any abnormalities. Ultrasonography found neither hepato- nor splenomegaly. The girl had a mild metabolic acidosis with a base excess of −4 mmol/L (reference range ±2 mmol/L), an elevated blood lactate level of 2.7 mmol/L (reference range 0.5–2.2 mmol/L) and an elevated CSF-lactate level of 3.8–6.4 mmol/L (reference range 1.2–2.1 mmol/L) without hyperlactaciduria. Gas chromatography mass spectrometry showed elevated ethyl malonate in her urine (22 mg/g of creatinine; reference range <15 mg/g). The amino acid profiles in the CSF and urine were normal, but an elevated alanine blood level of 649 μmol/L (reference range 150–500 μmol/L) was observed.

Muscle biopsy was performed and the histology of muscle biopsy did not reveal myopathic or neurogenic changes. But, the enzyme histochemistry revealed focal subsarcolemmal accumulation of SDH reaction product in up to 5% of muscle fibers (Fig. 1). The typical COX-negative fibers were not observed. The electron microscopy reveals focal increase of subsarcolemmal mitochondria without altered morphology. In a muscle sample, OXPHOS energy-generating capacity indicated diminished OXPHOS activity due to a disturbed complex V. The respiratory chain enzyme activities in a muscle homogenate and isolated mitochondria showed normal or even increased activities of respiratory chain complexes I, II, III, I + III, II + III, and IV and citrate synthase (CS) in comparison to age-related controls (for details see supplementary Table 1). Muscle mitochondrial proteins were separated by blue native electrophoresis (BN-PAGE) according to a standard protocol described elsewhere [5]. A marked decrease of the steady state level of complex V and the accumulation of its disintegrated parts were found (Fig. 2A). In skin fibroblasts, BN-PAGE followed by Western blot and immunodetection revealed a mild decrease (80% of controls) in complex V. However, free F_1-part and free F_1-alpha subunits were not observed (Fig. 2B). Sequencing of the whole mtDNA molecule from a muscle biopsy sample revealed a T-to-C transition at position 8851 in the *MTATP6* gene. Heteroplasmy of the mutation was tested in several tissues, and its presence was very high in muscle (97%), hair follicles (95%), blood (92%), buccal cells (92%) and urinary sediment cells (87%).

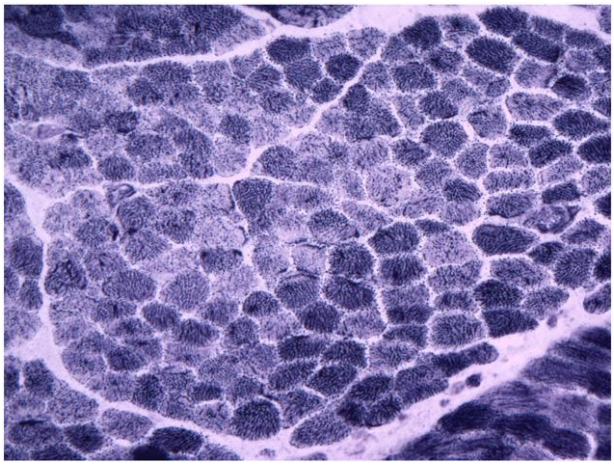

Fig. 1. Focal subsarcolemmal accumulation of succinate dehydrogenase (SDH) reaction product. SDH histochemistry, with original magnification of 400x.

2.2. Case report — the mother of the girl

The 36-year-old woman was healthy until 22 years of age. She then developed muscle weakness and pain in her legs. Her parents were healthy. Her difficulties were progressive, and a subsequent neurological examination revealed pes cavus, reduced vibration detection, hyporeflexia, mild proximal lower limb weakness (hip flexion 4+). Babinski test was with mild extensor plantar response. The gait was ataxic and speech slow. Pregnancy did not affect her clinical symptoms. Peripheral nerve conduction studies showed motor-predominant axonal neuropathy compactible with motor-predominant Charcot-Marie-Tooth type 2 (CMT2). Somato-sensory evoked potentials on the n. tibialis were normal. Hereditary motor and sensory neuropathy (HMSN II; CMT2) was excluded. A cardiological examination, including ECG and echocardiography, documented normal findings. Brain MRI was normal. A laboratory analysis showed normal levels of lactate in the blood, CSF and urine, a normal organic acid profile in the urine and physiological levels of amino acids in the blood. A PCR-RFLP analysis confirmed the presence of the pathogenic mutation m.8851T>C in her mtDNA. Heteroplasmy was observed in her buccal cells (85%), hair follicles (96%), blood (68%) and urinary sediment cells (69%).

2.3. Case report — the sister of the girl

Mutation load was also determined in healthy asymptomatic 20-years old sister of the girl. Heteroplasmy of mutation m.8851T>C was 60% in blood and 52% buccal cells.

3. Discussion

The current report expands the clinical and biochemical phenotypes of the m.8851T>C mutation in the *MTATP6* gene. We report the second known family with this very rare mutation. The first published case and our patient had very similar clinical symptoms with normal development during the first 8 months of life, followed by failure to thrive, microcephaly, psychomotor retardation, hypotonia, and ataxia. The MRI findings of Leigh syndrome were documented. This presentation is consistent with the high level of heteroplasmy observed in many tissues analyzed in both cases. However, contrary to this clinical observation, some discrepancies in biochemical measurements were recognized to suggest mitochondrial disorders. In addition, we documented a pathological image in a muscle biopsy sample. Furthermore, we demonstrated the novel finding of decreased full-size ATPase complex content in the muscle, and functional studies revealed diminished OXPHOS activity, particularly ATPase. Thus, our patient had more typical histological, structural and functional markers for mitochondrial disorders. Furthermore, significant differences were found in the clinical presentations of their mothers. The mother of our patient developed profound neurological symptoms, including progressive peripheral neuropathy, muscle weakness and ataxic gait, despite having lower heteroplasmy levels than the asymptomatic mother of the first published patient.

All of these findings unambiguously support pathogenicity of the m.8851T>C mutation. The m.8851T>C mutation in the *MTATP6* gene resulted in an amino acid change of a highly conserved tryptophan to an arginine at codon 109 in subunit ATP6 of the mitochondrial ATPase

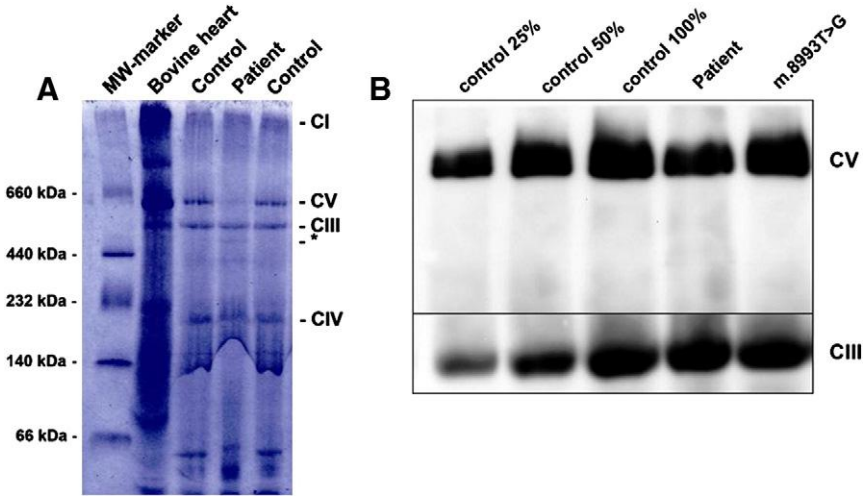

Fig. 2. A — Blue native polyacrylamide gel electrophoresis (BN-PAGE). Isolated defect of ATP synthase in patient muscle. A marked decrease of the steady state level of complex V (CV) and the accumulation of its disintegrated parts (*) was found. Levels of complex I (CI), complex III (CIII) and cytochrome *c* oxidase (complex IV — CIV) showed identical pattern in patient and control samples. The migration of molecular mass standards is indicated on the left side. B — BN-PAGE Western blot (WB) with monoclonal antibody against F_1-alpha subunit in skin fibroblasts showed a mild decrease (80% of control) in complex V (CV). Free F_1-part and/or free F_1-alpha subunit were not detected. Complex III (CIII) was normal content in patient and control. Series of dilution control sample is indicated.

[4]. The functional consequences of the change are still unknown, but a recent study of this mutation in an *Escherichia coli* model showed altered DCCD sensitivity of the ATPase activity but no other effects on the function of the ATPase [6].

Differences in clinical and biochemical phenotype can be explained by "threshold effect" showing that phenotypic manifestation of the genetic defect occurs only when a threshold level of mutation load is exceeded. Inhibition or deficiency of the activity of a respiratory chain complex up to a critical value may not affect the rate of mitochondrial respiration or ATP production without phenotypic presentation [7]. Various phenotypical manifestations have been largely depending on mtDNA heteroplasmy and related threshold effects. Furthermore, differences in mtDNA heteroplasmy among tissues may affect phenotypic presentation of mtDNA mutation and its severity [2]. We propose that correlation between mtDNA heteroplasmy level and clinical presentation is necessary. Mutation load in several easily accessible tissues must be considered. Since mtDNA heteroplasmy may change with age in blood [8]. This is partly supported by our findings of motor-predominant axonal neuropathy in mother of our patient in whom heteroplasmy level was found within interval of 68–96% (blood-hair follicles) in contrast with totally asymptomatic mother from previous case harboring higher mutation load (85%) in blood, however other tissues remained uninvestigated. Since heteroplasmy levels in the patient's sister (52–60%) are close to the values observed in their mother, her thorough clinical follow-up including regular neurological examinations will be necessary.

A different phenotype may be observed in cases with other *MTATP6* gene mutations, depending on the mutation load. A very unusual late onset of Leigh syndrome and/or ataxia has also been published in seven family members with a heteroplasmic m.9185T>C mtDNA mutation. Patients with high heteroplasmy (more than 90% in lymphoblasts) typically have Leigh syndrome that begins in infancy. Patients with a lower heteroplasmy level (80%–90% in lymphoblast) present milder symptoms, such as peripheral neuropathy, muscle weakness, walking difficulties, and dysfluent speech that begin in the late teenage years or a young adult age [2]. Moslemi and colleagues [9] described two new mutations in the *MTATP6* gene that are associated with Leigh syndrome. A patient with 97% m.9185T>C mutant mtDNA developed symptoms at the age of 7 years, while his mother was asymptomatic with a lower mutation load (85% in blood). Our findings in patients with m.8851T>C mutation are similar to observation to patients with m.9185T>C mutation recently reported [10], in which it is not clear why some patients harboring same mutation level had other neurological phenotype.

A correlation between the mutation load and clinical manifestations was also speculated in the case of an *MTATP6* m.9176T>G mutation leading to Leigh syndrome [11]. We previously described a family with another rare *MTATP6* mutation (the microdeletion 9205delTA) in a severely affected boy with a homoplasmic load in all tissues tested [12]. His mother and grandmother, who had heteroplasmy in blood (82% and 16%, respectively), were asymptomatic.

From these studies, we can conclude that minor variations in mutant mtDNA in tissue heteroplasmy influence the clinical and biochemical phenotypes and that other factors must also be considered. For example, the threshold effect shows that the phenotypic manifestation of the genetic defect occurs only when a threshold mutation load is exceeded [2]. Furthermore, the mtDNA background plays an important role in modulating the biochemical phenotype of mtDNA mutations [13].

In summary, we describe the second family with a very rare, maternally inherited, m.8851T>C missense mitochondrial *MTATP6* mutation associated with Leigh syndrome, ataxia, and progressive peripheral neuropathy that was dependent on the heteroplasmy load. Our findings extend the clinical and laboratory phenotypes associated with this mutation. A more complete understanding of the structural and functional effects of the m.8851T>C mtDNA mutation will be required before accurate correlations can be made between a patient's genotype and phenotype.

In study of patients with CMT2, it was recently shown that about 1% of genetically undefined cases with inherited axonal neuropathies harbored mutation in the *MTATP6* gene [10]. Although *MTATP6* mutations are very rare cause of peripheral neuropathies, ataxia and/or muscle weakness, as a practical consequence of the observation, we recommend that a sequence analysis of the *MTATP6* gene should be performed in adolescents and adults with this phenotype of unknown etiology.

Acknowledgments

Institutional support was provided by the research program PRVOUK-P24/LF1/3 and the institutional research project RVO-VFN64165/2012.

Appendix A. Supplementary data

Supplementary data to this article can be found online at http://dx.doi.org/10.1016/j.ymgme.2012.11.002.

References

[1] J. Houstek, A. Pícková, A. Vojtísková, T. Mrácek, P. Pecina, P. Jesina, Mitochondrial diseases and genetic defects of ATP synthase, Biochim. Biophys. Acta 1757 (9–10) (2006) 1400–1405.

[2] A.E. Castagna, J. Addis, R.R. McInnes, J.T. Clarke, P. Ashby, S. Blaser, B.H. Robinson, Late onset Leigh syndrome and ataxia due to a T to C mutation at bp 9,185 of mitochondrial DNA, Am. J. Med. Genet. A 143A (8) (2007) 808–816.

[3] H.F. Lee, C.R. Tsai, C.S. Chi, H.J. Lee, C.C. Chen, Leigh syndrome: clinical and neuroimaging follow-up, Pediatr. Neurol. 40 (2) (2009) 88–93.

[4] L. De Meirleir, S. Seneca, W. Lissens, E. Schoentjes, B. Desprechins, Bilateral striatal necrosis with a novel point mutation in the mitochondrial ATPase 6 gene, Pediatr. Neurol. 13 (3) (1995) 242–246.

[5] A.J. Janssen, F.J. Trijbels, R.C. Sengers, L.T. Wintjes, W. Ruitenbeek, J.A. Smeitink, E. Morava, B.G. van Engelen, L.P. van den Heuvel, R.J. Rodenburg, Measurement of the energy-generating capacity of human muscle mitochondria: diagnostic procedure and application to human pathology, Clin. Chem. 52 (5) (2006) 860–871.

[6] I. Ogilvie, R.A. Capaldi, Mutation of the mitochrondrially encoded ATPase 6 gene modeled in the ATP synthase of *Escherichia coli*, FEBS Lett. 453 (1–2) (1999) 179–182.

[7] R. Rossignol, B. Faustin, C. Rocher, M. Malgat, J.P. Mazat, T. Letellier, Mitochondrial threshold effects, Biochem. J. 370 (3) (2003) 751–762.

[8] H.K. Rajasimha, P.F. Chinnery, D.C. Samuels, Selection against pathogenic mtDNA mutations in a stem cell population leads to the loss of the 3243A–>G mutation in blood, Am. J. Hum. Genet. 82 (2) (2008) 333–343.

[9] A.R. Moslemi, N. Darin, M. Tulinius, A. Oldfors, E. Holme, Two new mutations in the MTATP6 gene associated with Leigh syndrome, Neuropediatrics 36 (5) (2005) 314–318.

[10] R.D.S. Pitceathly, S.M. Murphy, E. Cottenie, A. Chalasani, M.G. Sweeney, C. Woodward, E.E. Mudanohwo, I. Hargreaves, S. Heales, J. Land, J.L. Holton, H. Houlden, J. Blake, M. Champion, F. Flinter, S.A. Robb, R. Page, M. Rose, J. Palace, C. Crowe, C. Longman, M.P. Lunn, S. Rahman, M.M. Reilly, M.G. Hanna, Genetic dysfunction of MT-ATP6 causes axonal Charcot–Marie–Tooth disease, Neurology 79 (2012) 1145–1154.

[11] M. Akagi, K. Inui, H. Tsukamoto, N. Sakai, T. Muramatsu, M. Yamada, K. Matsuzaki, Y. Goto, I. Nonaka, S. Okada, Point mutation of mitochondrial ATPase 6 gene in Leigh syndrome, Neuromuscul. Disord. 12 (1) (2002) 53–55.

[12] P. Jesina, M. Tesarová, D. Fornusková, A. Vojtísková, P. Pecina, V. Kaplanová, H. Hansíková, J. Zeman, J. Houstek, Diminished synthesis of subunit a (ATP6) and altered function of ATP synthase and cytochrome c oxidase due to the mtDNA 2 bp microdeletion of TA at positions 9205 and 9206, Biochem. J. 383 (Pt. 3) (2004) 561–571.

[13] M. D'Aurelio, C. Vives-Bauza, M.M. Davidson, G. Manfredi, Mitochondrial DNA background modifies the bioenergetics of NARP/MILS ATP6 mutant cells, Hum. Mol. Genet. 19 (2) (2010) 374–386.

Supplement 5)

Štufková, H., Kelifová, S., Kousal, B., Lokvencová, K., Hansíková, H., Zámečník, J., Vaněčková, M., Zeman, J., Lišková, P., Honzík, T., Tesařová, M. **Clinical and laboratory findings in a rare maternally inherited variant m.8719G>A in *MT-ATP6* gene** (manuscript prepared for submission).

Clinical and laboratory findings in a rare maternally inherited variant m.8719G>A in *MT-ATP6* gene

Hana Štufková[1], Silvie Kelifová[1], Bohdan Kousal[2], Kateřina Lokvencová[1], Hana Hansíková[1], Josef Zámečník[3], Manuela Vaněčková[4], Jiří Zeman[1], Petra Lišková[1,2], Tomáš Honzík[1], Markéta Tesařová[1,*]

[1]Department of Pediatrics and Inherited Metabolic Disorders, First Faculty of Medicine, Charles University and General University Hospital in Prague, Prague, Czech Republic.
[2]Department of Ophthalmology, First Faculty of Medicine, Charles University and General University Hospital in Prague, Prague, Czech Republic.
[3]Department of Pathology and Molecular Medicine, Second Faculty of Medicine, Charles University and Motol University Hospital, Prague, Czech Republic.
[4]Department of Radiology, First Faculty of Medicine, Charles University and General University Hospital in Prague, Prague, Czech Republic.
*corresponding author: marketa.tesarova@lf1.cuni.cz (Markéta Tesařová)

Acknowledgment

This work was supported by the Ministry of Health of the Czech Republic [grant numbers AZV NV19-07-00149, RVO-VFN-64165]; and Charles University [grant numbers SVV260516, UNCE 204064, Cooperatio Program, research area Paediatrics]. The funding bodies were not involved in the study's design, collection, analysis, and interpretation of data and the writing of the manuscript.

Conflict of Interest

The authors declare no conflict of interest

Abbreviations

ADP: adenosine diphosphate, ATP: adenosine triphosphate, BCVA: best corrected visual acuity, BN-PAGE: blue native polyacrylamide gel electrophoresis, CCCP: carbonyl cyanide m-chlorophenylhydrazone, CME, CS: citrate synthase, EMG, HPLC: high performance liquid chromatography, IOL, LE: left eye, LHON: Leber hereditary optic neuropathy, LS: Leigh syndrome, MEGS: mitochondrial energy-generating system, MILS: maternally inherited Leigh syndrome, MRI: magnetic resonance imaging, mtDNA: mitochondrial DNA, Leigh

syndrome, NARP: neuropathy, ataxia, retinitis pigmentosa, SD-OCT: spectral domain optical coherence tomography, OXPHOS: mitochondrial oxidative phosphorylation system, RE: right eye, SDS-PAGE: sodium dodecyl sulfate polyacrylamide gel electrophoresis, SNHL: sensorineural hearing loss

Abstract

We report a case of a 57-year-old man with cataract, pigmentary retinopathy, hearing loss, and leukoencephalopathy. Mitochondrial DNA sequencing revealed extremely rare, maternally inherited missense m.8719G>A variant in *MT-ATP6*, which leads to the formation of a premature stop codon (p.Gly65*). Tested tissues (blood, buccal swab, skin fibroblasts, skeletal muscle) showed a variable load of the variant ranging from 9% in fibroblasts to 70% in muscle. Normal or elevated activities of respiratory chain complexes were observed in muscle mitochondria. The mitochondrial energy-generating system analysis indicated a complex V deficiency. A decrease in complex IV steady-state level and a profound reduction of complex V in muscle mitochondria was found. In addition, ATP synthase subcomplexes, V^* (F_1-part with c8-ring), and free F_1-part were detected. Our findings provide, for the first time, a detailed clinical and laboratory phenotype associated with the m.8719G>A pathogenic variant.

Keywords: mtDNA, *MT-ATP6*, OXPHOS, heteroplasmy

Introduction:

F_1F_O-ATPsynthase (ATP synthase, complex V, CV) synthesizes ATP in the mitochondrial matrix using energy provided by a proton electrochemical gradient. The ATP synthase consists of 17 structural subunits, of which only two (*MT-ATP6* and *MT-ATP8*) are encoded by mitochondrial DNA (mtDNA) (Fearnley and Walker 1986).

The *MT-ATP6* gene encodes subunit *a*, which is a critical component of the proton channel and plays a direct role in the translocation of protons across the inner mitochondrial membrane (Pinke et al. 2020). Over 70 different *MT-ATP6* mutations with a confirmed or suspected pathogenic character are summarized in Mitomap database (Lott et al. 2013). The mtDNA defects of ATP synthase most often clinically manifest as neuropathy, ataxia, retinitis pigmentosa (NARP), Leigh syndrome (LS) or maternally inherited LS (MILS), Leber hereditary optic neuropathy (LHON) (Baracca et al. 2007), or hypertrophic cardiomyopathy (Jonckheere et al. 2008).

The heteroplasmic variant m.8719G>A in the *MT-ATP6* gene, which leads to a premature stop codon (p.Gly65*), has so far been reported only once in a patient (without clinical and laboratory specification) from a cohort of more than 10000 patients suspected of mitochondrial disease (Tang et al. 2013). Herein, we report the second case with mutation load ranging from 9% to 70% in tested tissues and cells. For the first time, our findings thus provide the clinical and biochemical phenotypes associated with this pathogenic mtDNA variant.

Material and Methods:

Ethics

The present study was carried out by the Declaration of Helsinki. It was approved by the Committee of Medical Ethics of the General University Hospital and First Faculty of Medicine, Charles University in Prague. Informed consent was obtained for all biopsies.

Mitochondrial DNA sequencing and heteroplasmy

Total genomic DNA was isolated from blood, muscle biopsy, fibroblasts, and buccal swab cells using following kits: Gentra Puregene Blood Kit, QIAamp DNA Mini Kit, and QIAamp DNA Micro Kit, respectively (all Qiagen, USA). For a mutation analysis, SeqCap EZ Design: Mitochondrial Genome Design (Roche NimbleGen, Pleasonton, CA, USA) enrichment kit was used for preparation of sequencing library, followed by analysis on MiSeq (Illumina, San Diego, CA, USA) system using MiSeq Reagent Sequencing kit v3. The revised Cambridge Reference Sequence (NC_012920.1) was used for variant annotation.

Material and Mitochondria Isolation

Open muscle biopsy from the *m.gastrocnemius* was immediately transported on ice (at 4°C) to laboratory and mitochondria were isolated according to standard differential centrifugation procedures (Makinen et al. 1968) in a buffer containing 150mM KCl, 50mM Tris/HCl, 2mM EDTA and 2 μg/ml aprotinin (pH 7.5) at 4 °C (Jesina et al. 2004). The homogenate was centrifuged for 10 min at 4 °C and 600 *g*, the postnuclear supernatant was filtered through a 100 μm nylon membrane, and mitochondria were sedimented by centrifugation for 10 min at 4 °C and 10 000 *g*. The mitochondrial pellet was washed by centrifugation and resuspended to a final protein concentration of 20–25 mg/ml. Protein concentration was determined by the Lowry method (Lowry et al. 1951), the isolated mitochondria were stored at -80°C.

The primary skin fibroblasts were established from skin obtained during muscle biopsy procedure. Fibroblasts were cultured in high-glucose DMEM medium (Dulbecco's Modified Eagle Medium; PanBiotech) supplemented with 10% (v/v) fetal bovine serum (GE Healthcare) and Antibiotic-Antimycotic (Biosera) at 37°C in 5% CO_2 atmosphere.

Spectrophotometry

The activities of respiratory chain complexes (complex I − NADH:coenzyme Q oxidoreductase, CI, EC 1.6.5.3; complex I + III − NADH:cytochrome c oxidoreductase, CI +

III; complex II − succinate:coenzyme Q oxidoreductase, CII, EC 1.3.5.1; complex II + III − succinate:cytochrome c oxidoreductase, CII + III; complex III − coenzyme Q:cytochrome c oxidoreductase, CIII, EC 7.1.1.8; complex IV − cytochrome c oxidase, CIV, EC 1.9.3.1) were measured according to (Rustin et al. 1994) in fresh isolated mitochondria and fibroblast homogenate. The activity of citrate synthase (CS, EC 2.3.3.1), serving as the control enzyme to avoid assay variability, was measured according to (Srere and John 1969). Protein concentrations were measured by the Lowry method (Lowry et al. 1951).

Total coenzyme Q10 content

The total coenzyme Q10 content in muscle homogenate was determined using high performance liquid chromatography with UV detection at 275 nm according to the method of Mosca et al. (Mosca et al. 2002).

Histochemistry and immunohistology

The cryostat sections were prepared from frozen muscle *m. gastrocnemius* (10 μm in thickness for CIV histochemistry and 5 μm in thickness for CII histochemistry) and stained for CIV and CII activity using standard protocols (Lojda et al. 1979).

Electrophoresis and Immunoblot analysis

To analyse the steady-state levels of mitochondrial oxidative phosphorylation system (OXPHOS) protein complexes, Blue Native Polyacrylamide Gel Electrophoresis (BN-PAGE) of n-dodecyl β-d-maltoside (DDM) solubilized isolated mitochondria was used (final ratio 2 DDM/ mg protein) (Schägger and von Jagow 1991). Protein concentration was determined by BCA assay (Thermo Scientific™, Waltham, MA, USA). A total 10 μg of protein was loaded per lane and separated by 6-15% polyacrylamide gradient gels (MinProtean® 3 system; Bio-Rad, Herciles, CA, USA). For 2D (two-dimensional) analysis BN/SDS-PAGE (Sodium Dodecyl Sulfate–Polyacrylamide gel electrophoresis), strips of the first-dimension BN-PAGE gel were incubated for 1 h in 1% (w/v) SDS and 1% (v/v) mercaptoethanol and then subjected to SDS/PAGE (12% polyacrylamide) for separation in the second dimension as describe previously (Stiburek et al. 2005). BN-PAGE or BN/SDS-PAGE gels were transferred onto Immobilon-P PVDF Membrane (Millipore, Burlington, MA, USA) by semi-dry electroblotting using the Hoefer semi-dry transfer unit (Hoefer, Harvard Bioscience, Hollistion, MA, USA). Primary detection of blots was performed using mouse monoclonal antibodies against the CI subunit NDUFA9 (1:2 000), complex II subunit SDH70 protein (1:

20 000), complex III subunit CORE 2 (1:20 000), complex IV subunit COX1 (1:10 000), ATP synthase subunit β (1:2 000), ATP synthase subunit d (1:2 000), ATP synthase subunit c (1:1 000), ATP synthase subunit a (1:1 000) (Abcam, Cambridge, UK). The immunoblots were detected with peroxidase-conjugated secondary antibodies and SuperSignal West Femto Maximum Sensitivity Substrate (Thermo Fisher Scientific) using G:Box (Syngene, Cambridge, UK).

Mitochondrial Energy-Generating System analysis (MEGS)

The analysis of the MEGS capacity in fresh postnuclear muscle supernatant was determined by measuring the oxidation rates of ^{14}C-labelled pyruvate malate and succinate, donors and acceptors of Acetyl-CoA and inhibitors of tricarboxylic acid cycle, according to Janssen *et al.* (Janssen et al. 2006), using ten different incubations. The rate of each individual reaction was normalized according to both the protein concentration and the CS activity. The incubation ratios were compared to evaluate the OXPHOS activity and the functioning of the Krebs cycle and the pyruvate dehydrogenase complex (Burska et al. 2021).

Results

Case report

A 53-year-old male patient was referred to the Department of Pediatrics and Inherited Metabolic Disorders for further diagnostics because of suspected mitochondrial disorder manifesting as pigmentary retinopathy and sensorineural hearing loss (SNHL).

The patient underwent several surgeries due to traumatic injury of right eye (RE) in childhood including cataract removal. At the age of 28 he had a secondary anterior chamber intraocular lens implantation in the RE and at the age of 50 phacoemulsification with intraocular lens implantation in the left eye (LE). The patient noticed nyctalopia at the age of 25 years, with a more significant worsening after 44 years of age when the first evidence of bilateral retinopathy was noticed during a routine check-up. At the age of 53, ophthalmic examination revealed decreased best corrected visual acuity (BCVA) in the RE to 0.063 (Snellen charts, converted to decimal value); this was however attributed to the past injury and 0.8 in the LE. Fundus examination in the RE was limited due to the anterior chamber lens not allowing dilation. In the LE, there was mild peripheral pigmentary retinopathy and cystoid macular edema which responded to topical dorzolamide three times a day (Figure 1). Static perimetry (M700, Medmont International, Nunawading, Australia) showed only mild narrowing of the visual field in the LE (Figure 1). At the last examination performed, aged 57, BCVA remained stable.

At the age of 43, bilateral SNHL developed accompanied by tinnitus; after 6 years the patient required hearing aids because of progression, recent examination at the age of 56 revealed severe impairment. A genetic examination was performed to exclude hereditary causes of hearing loss. Additionally, he has been followed for essential hypertension, dyslipidaemia, and mitral regurgitation (grade 1-2), and impaired glucose tolerance which progressed to diabetes mellitus treated by oral antidiabetic agents at the age of 56.

Clinical examination of the patient showed lean, short stature (168 cm) with physiological topical neurological examination and normal muscular strength without eyelid ptosis or progressive external ophthalmoplegia. However, electromyography revealed incipient distal sensorimotor axonal and demyelinating polyneuropathy. Magnetic resonance imaging (MRI) of the brain at the age of 43 was with findings of mild cortical and cerebellar atrophy and unilateral T2-weighted lesions in putamen and capsula interna, as well as fine demyelination lesions in white matter not fulfilling multiple sclerosis criteria; cerebrospinal fluid

examination was without pathology (Figure 2). Psychological evaluation at the age of 56 showed mild cognitive decline over the course of disease with significantly impaired auditory short-term memory, working memory and ability to concentrate; the executive component was also disturbed

Laboratory blood tests including complete blood count, comprehensive metabolic panel, muscle enzymes, acid-base balance, thyroid function test were without pathology; as well as investigation of blood and urine lactate levels and urine organic acids; only in blood amino acids borderline elevated alanine (559; 597 μmol/l, controls <500 μmol/l) was detected.

Family history is insignificant. The patient's mother died at the age of 89, and she was diagnosed with a mild hearing loss after 70 years of age. The patient's two brothers (62 years and 66 years old) are healthy.

MtDNA analysis

The mtDNA sequencing in patient material revealed heteroplasmic variant m.8719G>A in *MT-ATP6* gene, which leads to the formation of a premature stop codon (p.Gly65*). The highest level of heteroplasmy was found in muscle 70%. Overall low levels of heteroplasmy were detected in buccal swab (16%), blood (11%) and fibroblasts (9%). The variant was not detected in blood DNA of his both brothers.

Biochemical and histochemical analysis

In a muscle homogenate, MEGS analysis indicated slightly increased oxidation in incubation containing uncoupler CCCP (Table 1) as well as ratio of reactions 4/1 that indicate disturbance of complex V. The spectrophotometric activities of complex I, I+III and the control enzyme CS were normal, the CIV/CS ratio was at the upper limit and the activities of complexes II, II+III, III and IV were significantly increased in muscle mitochondria (Table 1). The total coenzyme Q10 content in muscle homogenate was normal (Table 1). Histochemistry in muscle, revealed very mild dispersion size variation of muscle fibers with slight focal subsarcolemmal accumulation of the succinate dehydrogenase reaction product. The respiratory chain enzyme activities in fibroblasts showed normal values in comparison to age-related controls (Table 1).

Separation of muscle mitochondria by BN-PAGE followed by Western blot and immunodetection revealed reduced amounts of complex V (approx. 20% of controls) with accumulated subcomplexes, V* (F_1-part with c8-ring) and free F_1-part (Figure 3A). In

addition, the steady-state level of complex IV holoenzyme was also diminished in patient mitochondria (approx. 70% of control, Figure 3A).

To better characterize the complex V subcomplexes in patient muscle mitochondria, 2D-PAGE was applied (Figure 3B). In the control sample, the signal of individual antibodies was present in the monomer and the dimer of complex V. Only a minor amount of the subunit β was present in the F_1-part. While more variability was observed in the patient muscle mitochondria. All the subunits were present in the monomer and some were additionally detected in the dimer as well. A strong signal of subunit β (F_1- β) was revealed in the V* subcomplex, which contains the F_1-part connected to the c8-ring, and in the F1-part as well. However, the signal of subunit c was detected only in subcomplex V*, as a free c8-ring and lower oligomers. In the patient´s mitochondria, the level of subunit *a* (F_o-a) was significantly reduced compared to the control (same exposure) and it was detected only in the complex V monomer.

Discussion

In this study, we identified an extremely rare mtDNA mutation m.8719G>A in human *MT-ATP6* gene, which leads to premature stop codon (p.Gly65*) in patient with cataract, hearing loss, and leukoencephalopathy. Clinical manifestation of pathogenic variants in *MT-ATP6* includes LS, subacute necrotizing encephalomyelopathy, and NARP syndrome characterised by sensory neuropathy, ataxia and pigmentary retinopathy as firstly described in 1990 by Holt *et al.*; apart from those two well-defined syndromes patients with other phenotypic features were identified (Ganetzky et al. 2019; Holt et al. 1990; Stendel et al. 2020). The age at onset is primarily in early childhood with 75% of patients younger than 6 years of age at symptom onset in the largest retrospective multicentric study of cohort of *MT-ATP6* carriers by Stendel *et al.* in comparison, adult onset was observed only in 12% patients (Stendel et al. 2020) Interestingly, in adult-onset patients with *MT-ATP6* mutations were not rare oligosymptomatic presentations of isolated ataxia, as well as asymptomatic carriers were identified (Stendel et al. 2020). In general, to frequent symptoms in *MT-ATP6* patients belong ataxia, neuropathy, cognitive impairment, seizures, retinopathy; the most common manifestation is LS, described in more than half of the patients. Surprisingly, NARP syndrome, considered one of the classic manifestations of *MT-ATP6* was identified in only 8% of patients in the multicentre cohort by Stendel *et al*. (Stendel et al. 2020).

Retinopathy and hearing impairment in our patient were leading symptoms that raised suspicion from mitochondrial disease. During the following years developed neurological, psychiatric, and ocular symptoms are consistent with phenotypic spectrum of patients with *MT-ATP6* mutations, even diabetes mellitus is high probably associated symptom of mitochondrial disease as there are no other risk factors in our patient. As well as cataracts probably represents one of the accompanied symptoms, as seen in several patients with *MT-ATP6* mutation (Bugiardini et al. 2020; Stendel et al. 2020). Interestingly, our patient has not developed cerebellar symptomatology – one of the most frequent symptoms seen in patients with *MT-ATP6* mutation - over the curse of 15 years since first symptoms (Stendel et al. 2020). Neuroimaging in our patient were compatible with described brain MRI findings in patients with mutations in *MT-ATP6*, especially cerebellar and cortical atrophy, even white matter lesions that are rarer in those patients (Stendel et al. 2020). However, unilateral lesions in the caudate and in the internal capsule were rather surprising as bilateral impairment is usually seen in patients with mitochondrial disorders and the patient did not suffer any known

stroke-like episode (Gropman 2013). Unfortunately, more recent brain MRI for a comparison and evaluation of progression was not available.

A wide range of heteroplasmy levels were present in different tissues of the patient. The highest level of heteroplasmy was found in muscle 70% while the lowest in fibroblast 9%. Our data underscores the necessity of muscle biopsy especially for characterization of mtDNA variants pathogenicity. In fibroblasts, no disturbances in ATP synthase function and protein amount was expected due to low levels of heteroplasmy.

In muscle, we detected changes at the activity of OXPHOS complexes using MEGS, histochemistry, and spectrophotometry. Analysis of the steady-state levels of muscle mitochondria revealed a reduction in the amount of complex IV while its activity was significantly increased. This may be due to the high reserve capacity of complex IV (Gnaiger et al. 1998). In our previous study, *MT-ATP6* patient with the m.8851T>C (p.Trp109Arg) variant, a slight decrease in the native amount of complex IV was observed, but its activity was normal (Honzik et al. 2013). This trend was also observed in the case of homoplasmic cybrids generated from patient with *MT-ATP6* variant m.8993T>C (p. Leu156Pro), where the amount of complex IV was reduced, but the activity was slightly increased (D'Aurelio et al. 2010).

Analysis of the steady-state levels of muscle mitochondria revealed decrease amount of complex V and the presence of several complex V subcomplexes. It was previously described that the subunit *a* plays a role in the stabilization and dimerization of the complex V (Wittig et al. 2010). The similar subcomplexes were repeatedly described in *MT-ATP6* patients and Rho^0 cells (Carrozzo et al. 2006; Jesina et al. 2004; López-Gallardo et al. 2014; López-Gallardo et al. 2009; Smet et al. 2009). However, the absence of these subcomplexes in *MT-ATP6* patients´ tissues/cells have also been demonstrated (Honzik et al. 2013; Verny et al. 2011). The discrepancies in complex V assembly/stability among patients with the same genotype at similar levels of heteroplasmy points to biochemical variability caused by slight changes in heteroplasmy of *MT-ATP6* pathogenic variants and the overall unique aspect of each patient

The analysis of the composition of assembly/stability subcomplexes is performed by 2D electrophoresis. The approximately 390 kDa subcomplex containing the subunit β presumably the F_1-part of ATP synthase, a larger 460 kDa subcomplex containing the subunit β and the subunit c were found in muscle mitochondria. Additionally, other complex containing only

the subunit c was observed with a molecular mass of approximately 120 kDa, which likely represents the c8-ring itself. In addition, the presence of lower oligomers of the subunit c was detected. However, none of the above complexes showed detectable presence of the subunit *a* or the subunit d as well. The similar profile was found in a patient carrying 2 bp microdeletion m.9205_9206delTA in mtDNA (Jesina et al. 2004). Based on the findings in patient´s muscle, 30% of wild-type mtDNA is not sufficient to provide enough full-length subunit *a* for complex V assembly. However, mtDNA heteroplasmy represents only one of the conditions, which manifest threshold behavior. Others may include impairment of mitochondrial protein synthesis, stability of the OXPHOS complexes and other (Nuskova et al. 2020).

Conclusion: Our report confirms the pathogenicity of a very rare variant m.8719G>A resulting in a premature stop-codon in the subunit *a* followed by severely impaired ATP synthase assembly, and further extends the spectrum of *MT-ATP6* variants associated with mitochondrial encephalopathies in adults.

References

Baracca A, Sgarbi G, Mattiazzi M, Casalena G, Pagnotta E, Valentino ML, Moggio M, Lenaz G, Carelli V, Solaini G (2007) Biochemical phenotypes associated with the mitochondrial ATP6 gene mutations at nt8993. Biochimica et biophysica acta 1767: 913-919

Bugiardini E, Bottani E, Marchet S, Poole OV, Beninca C, Horga A, Woodward C, Lam A, Hargreaves I, Chalasani A, Valerio A, Lamantea E, Venner K, Holton JL, Zeviani M, Houlden H, Quinlivan R, Lamperti C, Hanna MG, Pitceathly RDS (2020) Expanding the molecular and phenotypic spectrum of truncating. Neurol Genet 6: e381

Burska D, Stiburek L, Krizova J, Vanisova M, Martinek V, Sladkova J, Zamecnik J, Honzik T, Zeman J, Hansikova H, Tesarova M (2021) Homozygous missense mutation in UQCRC2 associated with severe encephalomyopathy, mitochondrial complex III assembly defect and activation of mitochondrial protein quality control. Biochim Biophys Acta Mol Basis Dis 1867: 166147

Carrozzo R, Wittig I, Santorelli FM, Bertini E, Hofmann S, Brandt U, Schägger H (2006) Subcomplexes of human ATP synthase mark mitochondrial biosynthesis disorders. Ann Neurol 59: 265-275

D'Aurelio M, Vives-Bauza C, Davidson MM, Manfredi G (2010) Mitochondrial DNA background modifies the bioenergetics of NARP/MILS ATP6 mutant cells. Hum Mol Genet 19: 374-386

Fearnley IM, Walker JE (1986) Two overlapping genes in bovine mitochondrial DNA encode membrane components of ATP synthase. EMBO J 5: 2003-2008

Ganetzky RD, Stendel C, McCormick EM, Zolkipli-Cunningham Z, Goldstein AC, Klopstock T, Falk MJ (2019) MT-ATP6 mitochondrial disease variants: Phenotypic and biochemical features analysis in 218 published cases and cohort of 14 new cases. Hum Mutat 40: 499-515

Gnaiger E, Lassnig B, Kuznetsov A, Rieger G, Margreiter R (1998) Mitochondrial oxygen affinity, respiratory flux control and excess capacity of cytochrome c oxidase. J Exp Biol 201: 1129-1139

Gropman AL (2013) Neuroimaging in mitochondrial disorders. Neurotherapeutics 10: 273-285

Holt IJ, Harding AE, Petty RK, Morgan-Hughes JA (1990) A new mitochondrial disease associated with mitochondrial DNA heteroplasmy. Am J Hum Genet 46: 428-433

Honzik T, Tesarova M, Vinsova K, Hansikova H, Magner M, Kratochvilova H, Zamecnik J, Zeman J, Jesina P (2013) Different laboratory and muscle biopsy findings in a family with an m.8851T>C mutation in the mitochondrial MTATP6 gene. Mol Genet Metab 108: 102-105

Janssen AJ, Trijbels FJ, Sengers RC, Wintjes LT, Ruitenbeek W, Smeitink JA, Morava E, van Engelen BG, van den Heuvel LP, Rodenburg RJ (2006) Measurement of the energy-generating capacity of human muscle mitochondria: diagnostic procedure and application to human pathology. Clin Chem 52: 860-871

Jesina P, Tesarova M, Fornuskova D, Vojtiskova A, Pecina P, Kaplanova V, Hansikova H, Zeman J, Houstek J (2004) Diminished synthesis of subunit a (ATP6) and altered function of ATP synthase and cytochrome c oxidase due to the mtDNA 2 bp microdeletion of TA at positions 9205 and 9206. Biochem J 383: 561-571

Jonckheere AI, Hogeveen M, Nijtmans LG, van den Brand MA, Janssen AJ, Diepstra JH, van den Brandt FC, van den Heuvel LP, Hol FA, Hofste TG, Kapusta L, Dillmann U, Shamdeen MG, Smeitink JA, Rodenburg RJ (2008) A novel mitochondrial ATP8 gene mutation in a patient with apical hypertrophic cardiomyopathy and neuropathy. J Med Genet 45: 129-133

Lojda Z, Kociánová J, Maratka Z (1979) Histochemistry of the human duodenal mucosa with special reference to the gradient of activities of the brush border enzymes. Scand J Gastroenterol Suppl 54: 7-13

Lott MT, Leipzig JN, Derbeneva O, Xie HM, Chalkia D, Sarmady M, Procaccio V, Wallace DC (2013) mtDNA Variation and Analysis Using Mitomap and Mitomaster. Curr Protoc Bioinformatics 44: 1.23.21-26

Lowry OH, Rosebrough NJ, Farr AL, Randall RJ (1951) Protein measurement with the Folin phenol reagent. J Biol Chem 193: 265-275

López-Gallardo E, Emperador S, Solano A, Llobet L, Martín-Navarro A, López-Pérez MJ, Briones P, Pineda M, Artuch R, Barraquer E, Jericó I, Ruiz-Pesini E, Montoya J (2014) Expanding the clinical phenotypes of MT-ATP6 mutations. Hum Mol Genet 23: 6191-6200

López-Gallardo E, Solano A, Herrero-Martín MD, Martínez-Romero I, Castaño-Pérez MD, Andreu AL, Herrera A, López-Pérez MJ, Ruiz-Pesini E, Montoya J (2009) NARP syndrome in a patient harbouring an insertion in the MT-ATP6 gene that results in a truncated protein. J Med Genet 46: 64-67

Makinen MW, Lee CP, Shy GM (1968) Microanalysis of cytochrome content, oxidative and phosphorylative activities of human skeletal muscle mitochondria. Neurology 18: 299

Mosca F, Fattorini D, Bompadre S, Littarru GP (2002) Assay of coenzyme Q(10) in plasma by a single dilution step. Anal Biochem 305: 49-54

Nuskova H, Mikesova J, Efimova I, Pecinova A, Pecina P, Drahota Z, Houstek J, Mracek T (2020) Biochemical thresholds for pathological presentation of ATP synthase deficiencies. Biochem Biophys Res Commun 521: 1036-1041

Pinke G, Zhou L, Sazanov LA (2020) Cryo-EM structure of the entire mammalian F-type ATP synthase. Nat Struct Mol Biol 27: 1077-1085

Rustin P, Chretien D, Bourgeron T, Gerard B, Rotig A, Saudubray JM, Munnich A (1994) Biochemical and molecular investigations in respiratory chain deficiencies. Clin Chim Acta 228: 35-51

Schägger H, von Jagow G (1991) Blue native electrophoresis for isolation of membrane protein complexes in enzymatically active form. Anal Biochem 199: 223-231

Smet J, Seneca S, De Paepe B, Meulemans A, Verhelst H, Leroy J, De Meirleir L, Lissens W, Van Coster R (2009) Subcomplexes of mitochondrial complex V reveal mutations in mitochondrial DNA. Electrophoresis 30: 3565-3572

Srere PA, John ML (1969) Citrate synthase : [EC 4.1.3.7. Citrate oxaloacetate-lyase (CoA-acetylating)]. Methods in Enzymology, Academic Press, pp 3-11

Stendel C, Neuhofer C, Floride E, Yuqing S, Ganetzky RD, Park J, Freisinger P, Kornblum C, Kleinle S, Schöls L, Distelmaier F, Stettner GM, Büchner B, Falk MJ, Mayr JA, Synofzik M, Abicht A, Haack TB, Prokisch H, Wortmann SB, Murayama K, Fang F, Klopstock T, Group AS (2020) Delineating *MT-ATP6*-associated disease: From isolated neuropathy to early onset neurodegeneration. Neurol Genet 6: e393

Stiburek L, Vesela K, Hansikova H, Pecina P, Tesarova M, Cerna L, Houstek J, Zeman J (2005) Tissue-specific cytochrome c oxidase assembly defects due to mutations in SCO2 and SURF1. Biochem J 392: 625-632

Tang S, Wang J, Zhang VW, Li FY, Landsverk M, Cui H, Truong CK, Wang G, Chen LC, Graham B, Scaglia F, Schmitt ES, Craigen WJ, Wong LJ (2013) Transition to next generation analysis of the whole mitochondrial genome: a summary of molecular defects. Hum Mutat 34: 882-893

Verny C, Guegen N, Desquiret V, Chevrollier A, Prundean A, Dubas F, Cassereau J, Ferre M, Amati-Bonneau P, Bonneau D, Reynier P, Procaccio V (2011) Hereditary spastic paraplegia-like disorder due to a mitochondrial ATP6 gene point mutation. Mitochondrion 11: 70-75

Wittig I, Meyer B, Heide H, Steger M, Bleier L, Wumaier Z, Karas M, Schägger H (2010) Assembly and oligomerization of human ATP synthase lacking mitochondrial subunits a and A6L. Biochim Biophys Acta 1797: 1004-1011

Table 1: Energetic metabolism in *MT-ATP6* m.8719G>A patient´s muscle and fibroblasts

Skeletal muscle, isolated mitochondria		
Enzymatic activities - (nmol/min/mg protein)		
	Patient	Controls (n=30)
NQR (CI)	169	110-290
QCCR (CIII)	**926**	321-640
NCCR (CI+III)	266	126-316
SQR (CII)	**142**	21-93
SCCR (CII+III)	**530**	82-251
COX (CIV)	**2078**	658-1552
CS	855	435-1234
COX/CS ratio	**2,43**	0,66-2,25
Skeletal muscle, homogetate		
Coenzyme Q10 content	Patient	Controls (n=18)
Coenzyme Q10 (pmol/mg protein)	232	180-460
Coenzyme Q10/CS ratio	2,11	1,5-3,9
Skeletal muscle, postnuclear supernatant		
Substrate oxidation rates normalized to CS and ratios of indicated reations		
	Patient	Controls (n=10)
1 [1-14C]Pyruvate+Malate+ADP	5,32	1,2-5,2
2 [1-14C]Pyruvate+Carnitine+ADP	5,37	1,22-5,66
3 [1-14C]Pyruvate+Malate(-ADP)	0,82	0,18-0,8
4 [1-14C]Pyruvate+Malate-ADP+CCCP	**6,75**	1,39-5,19
5 [1-14C]Pyruvate+Malate+ADP+atractyloside	1,36	0,1-1,14
6 [U-14C]Malate+Pyruvate+Malonate+ADP	0,85	0,24-1,52
7 [U-14C]Malate+Acetylcarnitine+Malonate+ADP	0,72	0,41-1,17
8 [U-14C]Malate+Acetylcarnitine+Arsenite+ADP	1,29	0,09-0,63
9 [1,4-14C]Succinate+Acetylcarnitine+ADP	0,86	0,38-1,36
Ratio of reactions 1/3	6,5	3,58-9,62
Ratio of reactions 2/1	1,01	0,93-1,21
Ratio of reactions 4/1	**1,27**	0,7-1,26
Ratio of reactions 3/5	0,6	0,6-2,1
Ratio of reactions 6/1	0,16	0,14-0,37
Ratio of reactions 7/6	0,85	0,41-1,83
Ratio of reactions 7/8	1,19	0,49-4,47
Cultured fibroblast		
Enzymatic activities - (nmol/min/mg protein)		
	Patient	Controls (n=30)
NQR (CI)	43,83	12.66
SQR (CII)	16,42	5.29
COX (CIV)	9,42	5.26
CS	23,23	13-46
COX/CS ratio	0,41	0,12-1,44

NQR, NADH: coenzyme Q reductase (rotenone sensitive) (CI), QCCR, QH2: cytochrome c reductase (CIII), NCCR, NADH:cytochrome c reductase (rotenone sensitive) (CI+III), SQR, succinate: coenzyme Q reductase (CII), SCCR, succinate:cytochrom c reductase (CII+III), COX cytochrome c oxidase (CIV), CS citrate synthase.

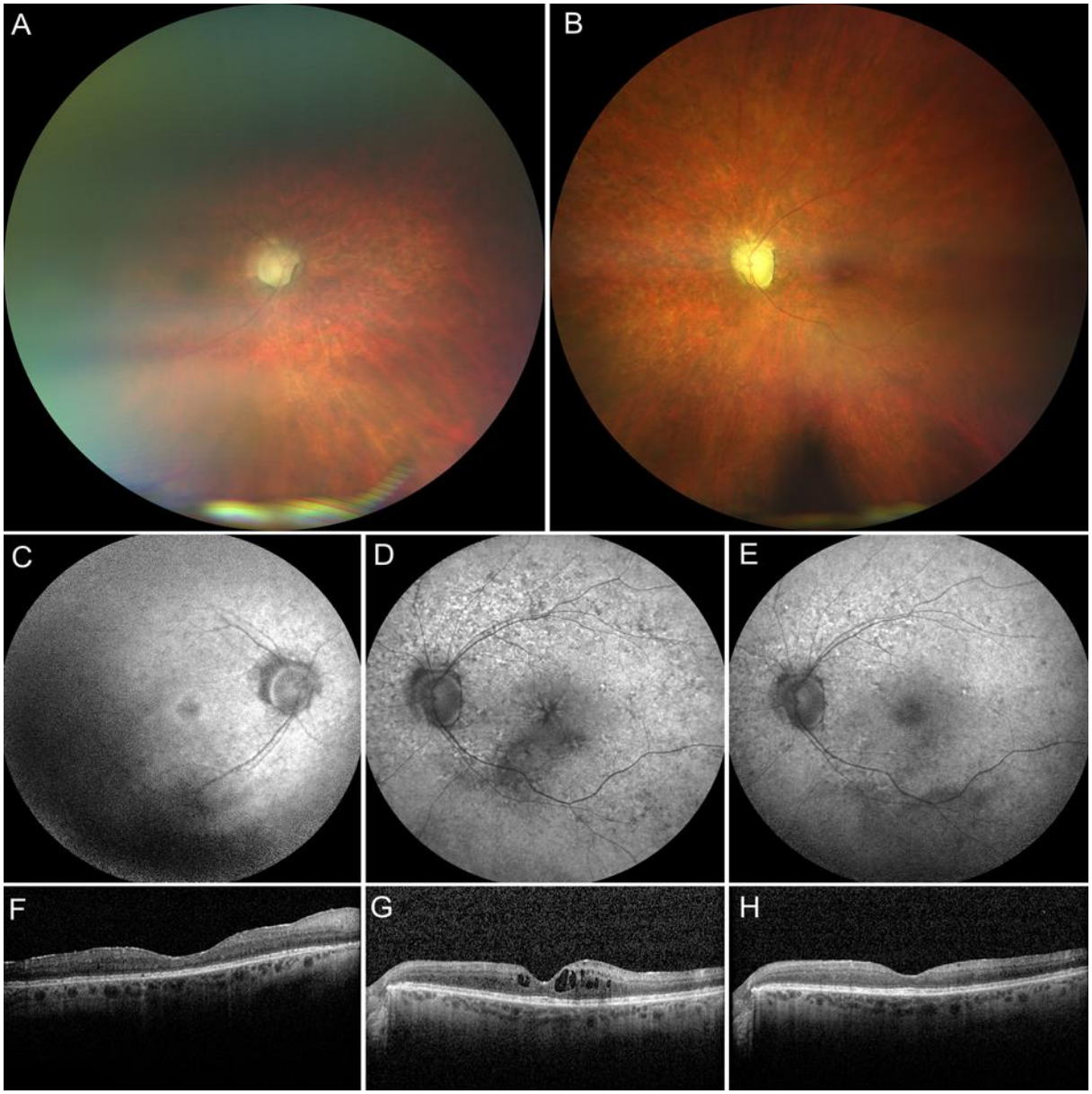

Figure 1: Wide-field fundus photograph of the right (A) and left (B) eye taken at the age of 56 years showing pigmentary retinopathy and optic disc pallor. Fundus autofluorescence of the right (C) and left (D) eye aged 52 years. SD-OCT horizontal transfoveal scan of the right (F) and left macula (G) aged 52 years demonstrate retinal thinning in both eyes, as well as cystoid macular edema in the left eye. Effect of topical dorzolamide treatment three times a day within 4 months is shown in the fundus autofluorescence (E) and SD-OCT (H) of the left eye.

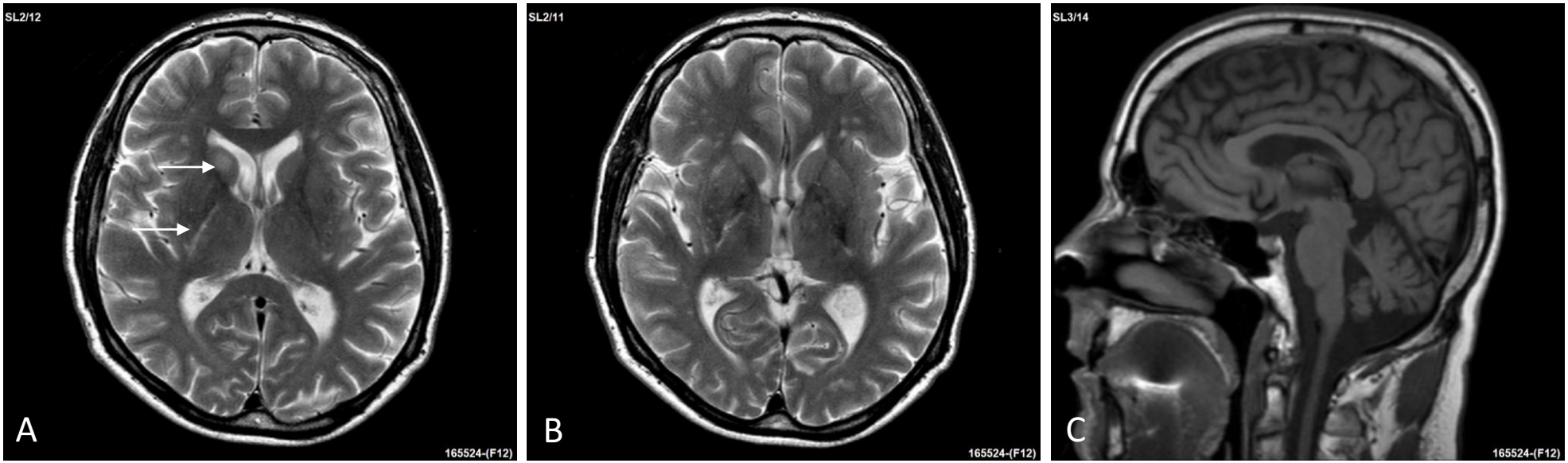

Figure 2: Brain MRI of patient with m.8719G>A mutation in MT-ATP6 gene at the age of 43. Axial T2-weighted images show a hypersignal lesion in the right caudate and right dorsal limb of the capsula interna (arrows, A). In addition, nonspecific small hypersignal foci in the white matter and mild cortical atrophy are present (A, B). Sagittal view of the T1-weighted image also shows mild cerebellar atrophy (C).

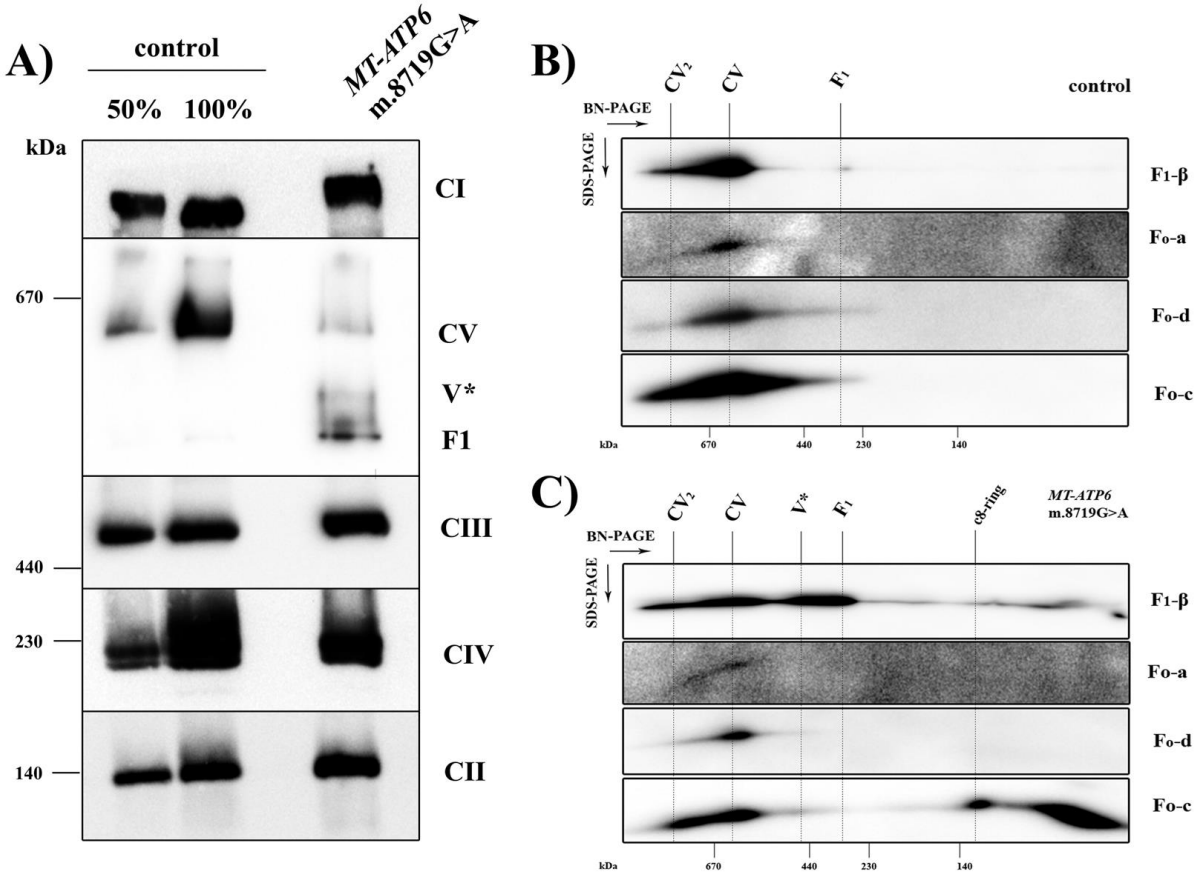

Figure 3: A) Steady-state levels of OXPHOS complexes in muscle mitochondria in *MT-ATP6* m.8719G>A patient and control. The mitochondrial fractions (5-10 µg) were resolved using 6-15% BN-PAGE, electroblotted, and probed with specific antibodies (CI-NDUFA9, CII-SDH70, CIII-CORE2, CIV-COX1, CV-F_1-β). Two aliquots of control mitochondria corresponding to the indicated dilutions of control samples were loaded on the same gels. B) and C) 2D electrophoretic analysis and immunodetection of selected ATP synthase subunits in control (B) and patient (C) (*MT-ATP6* m.8719G>A) muscle mitochondria. Mitochondrial muscle fractions (10 µg) were separated in the first dimension by BN-PAGE and in the second dimension by SDS-PAGE. Final gels were electroblotted and probed with specific antibodies against the ATP synthase β (F_1-β), subunit a (F_o-a), subunit d (F_o-d) and subunit c (F_o-c).

Supplement 6)

Tesařová, M., Vondráčková, A., **Štufková, H**., Vepřeková, L., Stránecký, V., Beránková, K., Hansíková, H., Magner, M., Gáloová, N., Honzík, T., Vodičková, E., Starý, J., Zeman, J. (2019). **Sideroblastic anemia associated with multisystem mitochondrial disorders.** Pediatr Blood Cancer 66, e27591. IF = 2.355, Quartile Score = Q2 (2019).

Received: 10 August 2018 | Revised: 18 November 2018 | Accepted: 29 November 2018

DOI: 10.1002/pbc.27591

RESEARCH ARTICLE

WILEY Pediatric Blood & Cancer | SIOP INTERNATIONAL SOCIETY OF PAEDIATRIC ONCOLOGY | aspho The American Society of Pediatric Hematology/Oncology

Sideroblastic anemia associated with multisystem mitochondrial disorders

Marketa Tesarova[1] | Alzbeta Vondrackova[1] | Hana Stufkova[1] | Lenka Veprekova[1] | Viktor Stranecky[1] | Kamila Berankova[1] | Hana Hansikova[1] | Martin Magner[1] | Natalia Galoova[2] | Tomas Honzik[1] | Elena Vodickova[3] | Jan Stary[4] | Jiri Zeman[1]

[1]Department of Paediatrics and Adolescent Medicine, First Faculty of Medicine, Charles University and General University Hospital, Prague, Czech Republic

[2]Department of Paediatric Oncology and Haematology, Children's University Hospital, Kosice, Slovakia

[3]Department of Haematology, Motol University Hospital, Prague, Czech Republic

[4]Department of Paediatric Haematology and Oncology, Second Faculty of Medicine, Charles University and Motol University Hospital, Prague, Czech Republic

Correspondence
Jiri Zeman, Department of Paediatrics and Adolescent Medicine, First Faculty of Medicine, Charles University and General University Hospital, Ke Karlovu 2, Prague 2, 12808, Czech Republic.
Email: jzem@lf1.cuni.cz

Funding information
Ministerstvo Zdravotnictví Ceské Republiky, Grant/Award Numbers: AZV 17-30965A, RVO VFN 64165; Univerzita Karlova v Praze, Grant/Award Numbers: Progres Q26/LF1, UNCE 204064; Grantová Agentura Ceské Republiky, Grant/Award Number: GACR 14-36804G

Abstract

Background: Sideroblastic anemia represents a heterogeneous group of inherited or acquired diseases with disrupted erythroblast iron utilization, ineffective erythropoiesis, and variable systemic iron overload. In a cohort of 421 patients with multisystem mitochondrial diseases, refractory anemia was found in 8 children.

Results: Five children had sideroblastic anemia with increased numbers of ring sideroblasts >15%. Two of the children had a fatal course of MLASA1 syndrome (mitochondrial myopathy, lactic acidosis, and sideroblastic anemia [SA]) due to a homozygous, 6-kb deletion in the *PUS1* gene, part of the six-member family of pseudouridine synthases (pseudouridylases). Large homozygous deletions represent a novel cause of presumed *PUS1*-loss-of-function phenotype. The other three children with SA had Pearson syndrome (PS) due to mtDNA deletions of 4 to 8 kb; two of these children showed early onset of PS and died due to repeated sepsis; the other child had later onset of PS and survived as the hematological parameters normalized and the disease transitioned to Kearns–Sayre syndrome. In addition, anemia without ring sideroblasts was found in three other patients with mitochondrial disorders, including two children with later onset of PS and one child with failure to thrive, microcephaly, developmental delay, hypertrophic cardiomyopathy, and renal tubular acidosis due to the heterozygous mutations c.610A>G (p.Asn204Asp) and c.674C>T (p.Pro225Leu) in the *COX10* gene encoding the cytochrome *c* oxidase assembly factor.

Conclusions: Sideroblastic anemia was found in fewer than 1.2% of patients with multisystem mitochondrial disease, and it was usually associated with an unfavorable prognosis.

KEYWORDS
mitochondrial disorders, MLASA, mtDNA, Pearson syndrome, ring sideroblasts, sideroblastic anemia

1 | INTRODUCTION

Sideroblastic anemia (SA) represents a heterogeneous group of inherited or acquired diseases with disrupted utilization of iron in erythroblasts, ineffective erythropoiesis, and variable systemic iron overload.[1]

The most common acquired SA is refractory anemia with ring sideroblasts (RARS), as defined in the WHO classification of myelodysplastic syndrome (MDS). Variants of this condition include refractory cytopenia with multilineage dysplasia and ring sideroblasts and RARS, associated with marked thrombocytosis (combined myelodysplastic and myeloproliferative disorder). Somatic mutations in *SF3B1* are found in ≥80% of patients, sometimes in combination with mutations in other genes, including *JAK2V617F*, *ASXL1*, *DNMT3A*, *SETBP1*, and *TET2*.[2,3] Congenital SA is associated with mutations in nuclear genes involved in heme biosynthesis (*ALAS2* and *SLC25A38*), iron-sulfur-cluster biogenesis/transport (*ABCB7* and *GLRX5*), thiamine-transport

Abbreviations: ANC, absolute neutrophil count; BN-PAGE, blue-native polyacrylamide gel electrophoresis; CS, citrate synthase; EPO, erythropoietin; gDNA, genomic DNA; MCV, mean corpuscular volume; MD, mitochondrial disease; MLASA, mitochondrial myopathy, lactic acidosis, and sideroblastic anemia; mtDNA, mitochondrial DNA; PS, Pearson syndrome; RFLP, restriction fragment length polymorphism; RS, ring sideroblasts; SA, sideroblastic anemia; WBC, white blood cell

protein (*SLC19A1*), structural subunits of the respiratory chain complex (*NDUFB11*), and mitochondrial protein synthesis and chaperones (*PUS1*, *YARS2*, *LARS2*, and *HSPA9*) or with mutations in mitochondrial DNA (*MTATP6*, or large mtDNA deletions) involved in mitochondrial biogenesis.[4–11]

Although the association between hematological pathology and mitochondrial disorders is generally accepted, collaboration between hematologists and mitochondrial researchers is not common.

We report five children with SA and multisystem mitochondrial disorders, including three children with Pearson marrow–pancreas syndrome (PS) due to heteroplasmic mtDNA deletions and two children with MLASA1 syndrome (mitochondrial myopathy, lactic acidosis, and SA) due to a homozygous 6-kb deletion in the *PUS1* gene. In addition, refractory anemia without ring sideroblasts was found in three patients with mitochondrial disorders, including two children with later onset of PS and one child with mutations c.610A>G (p.Asn204Asp) and c.674C>T (p.Pro225Leu) in the *COX10* gene that encodes Cox10, the assembly factor for cytochrome c oxidase (respiratory chain complex IV).

2 | MATERIALS

During the last two decades, we diagnosed multisystem mitochondrial disease at the molecular and/or enzymatic level in 421 patients, including 25 patients with mtDNA deletions. The diagnosis in most patients was confirmed on the molecular level and, in the remainder, on the biochemical level if the activity of one or more respiratory chain complexes or ATP synthase was decreased to <30% of the mean of age-related controls, or if there was a decrease in the ratio between the mitochondrial complex and citrate synthase enzymatic activities.[12]

3 | METHODS

Genomic DNA (gDNA) from patients and parents was extracted from blood and/or other tissue specimens. Total RNA was isolated from lymphocytes and/or cultured fibroblasts (P1 and P2). Mutations in mtDNA were excluded by Sanger sequencing in 32 overlapping PCR fragments encompassing the whole mitochondrial genome using specifically designed primers (available upon request) based on the revised human mtDNA Cambridge reference sequence (NC_012920). Long-range PCR was used for analysis of mtDNA deletions.[13] The nuclear DNA of P1 was analyzed using a Genome-Wide Human SNP 6.0 microarray chip (Affymetrix, Santa Clara, USA), enabling the detection of deletions larger than 700 bp at the Centre for Applied Genomics (Hospital for Sick Children (SickKids), University of Toronto, Toronto, Canada). To determine the copy number of the *PUS1* gene, TaqMan probes were used (Hs01998936_cn, Hs01410383_cn; Applied Biosystems, Foster City, USA) according to the manufacturer's instructions. The *PUS1* gene (ENSG00000177192 and ENST00000376649) deletion was characterized both on the gDNA and cDNA level using specifically designed primers flanking the deleted region of the gene (gDNA primers: F 5′-TGGCCTGATTTTTCCTAGGTT-3′, R 5′-ACAAAGGGTTCCTCGCAGTA-3′; cDNA primers: F 5′-GTGCTGCTCATGGCCTATTC-3′, R 5′-GATGATGGTGGGGTAGATGTG-3′). The PCR product was sequenced in both directions. Targeted exome sequencing of the characterized mitochondrial-related genes was performed for P8 using 1.2 μg of gDNA.[14] *COX10* (ENSG00000006695 and ENST00000261643) mutations were confirmed by Sanger sequencing in the proband and her parents. The absence of deleterious mutations was confirmed by PCR-RFLP analysis in the Czech population using a set of 200 control samples (*COX10* and *PUS1*) and a set of 80 control gDNA samples of Roma origin (*PUS1* gene).

Mitochondria in patients P1–4 and P7–8 were isolated from muscle biopsies[15] and/or liver tissue[16] obtained at autopsy. Protein concentrations were measured by the Lowry method,[17] and the isolated mitochondria were stored at −80 °C. The activities of the respiratory chain complexes were measured spectrophotometrically.[18] Blue-native polyacrylamide gel electrophoresis (BN-PAGE)[19] separation of mitochondrial membrane complexes on polyacrylamide 6% to 15% (w/v) gradient gels[20] followed by immunoblot analysis was used to analyze the steady-state levels of oxidative phosphorylation system complexes.[21] Primary detection of BN/PAGE blots was performed using mouse monoclonal antibodies raised against the complex I subunit NDUFA9 (2 μg/mL), ATP synthase subunit alpha (2–3 μg/mL), complex III subunit Core 2 (0.5 μg/mL), complex IV subunit COX2 (0.5–1 μg/mL), and complex II subunit 70-kDa protein (1 μg/mL) (Abcam) at the indicated dilutions.

3.1 | Ethics

The study was approved by the ethics committee of the General University Hospital in Prague and was conducted in agreement with institutional guidelines. Written informed consent for molecular analyses was obtained from the parents of affected children.

3.2 | Results

SA with an increased number of ring sideroblasts >15% in bone marrow was found in five patients (P1–5) representing <1.2% of the mitochondrial cohort. In addition, refractory anemia without ring sideroblasts was found in three other children with mitochondrial disorders (P6–8). The clinical symptoms and results of the hematological and molecular analyses are shown in Tables 1 and 2. Most children showed growth that was below the third percentile, had hypotony, developmental delay, and mild to moderate hyperlactacidemia.

Two children (P1 and 2), both of Roma origin, developed SA with ring sideroblasts at the ages of three and six years, respectively. Both had MLASA syndrome due to a homozygous 6-kb deletion of all of exon 4, a partial deletion of exon 5 and a 9-bp insertion derived from intron 3 (c.896+2551_1061delinsATTTTACCA), resulting in a putative truncation of the PUS1 protein (p.Gly148ValfsX41). The parents of P1 are second cousins, but to the best of their knowledge, they are not related to P2's family, at least in the last three generations.

SA was also observed in three of five children with Pearson syndrome (PS) due to mtDNA deletions (4–8 kb) in various tissues, including blood (P3, 5, and 6), muscle (P3, 4, and 7), buccal cells

TABLE 1 Clinical data of 5 children with sideroblastic anemia (P1–5) and multisystem mitochondrial diseases and three other children with mitochondrial disorders with anemia without ring sideroblasts (P6–8)

Patient	P1 female	P2 male	P3 male	P4 female	P5 female	P6* female	P7 male	P8 female
Mutation	*PUS1***	*PUS1***	mtDNA 8 kb deletion	mtDNA 5.4 kb deletion (m.10382_15783del)	mtDNA 6 kb deletion	mtDNA 4 kb deletion	mtDNA 5 kb deletion (m.8483_13446del)	COX10****
Analysed tissues with mutation	Blood	Blood	Blood, muscle	Muscle, buccal cells, urinary cells	Blood	Blood, buccal cells	Muscle, buccal cells, urinary cells	Blood
Age at onset	Second day	5 years	First day	First day	3 months	3 months	18 months	Second day
First symptom	Apathy hypotony	Short stature, developmental delay	Tachypnoe, anaemia	Tachypnoe, anaemia	Anaemia	Hypotony, tachypnoe	Failure to thrive	Apathy, tachypnoe
Age at onset of anemia	3 years	6 years	First day	First day	3 months	3 months	3.5 years	7 days
Transfusion dependency	Every 3–4 weeks	During infections	Every 3–4 weeks	Every 4 weeks	Every 4 weeks till 2 years	Every 4 weeks till 4 years	–	Every 3 weeks
IUGR	–	–	–	+	–	+	–	–
Prematurity	–	+	–	+	–	+	–	–
Microcephaly < third percentile	+	+	–	+	–	+	+	+
Growth < third percentile	+	+	Third percentile	+	–	+	+	+
Failure to < third percentile		+	–	+	–	+	+	
Developmental delay	+	+	+	+	–	+	+	+
Intellectual disability	IQ 80	IQ 45	n.d.	Mild	DQ 100	IQ 50	IQ 65	n.d.
Strabismus	–	+	–		–	–	Ptosis	+
Hypotony	+	+	+	+	+	+	+	+
Adrenal insufficiency	–	–	–	–	**Since 3 years**	–	**Since 4 years**	–
Heart	**HCM**	Normal	Normal	Normal	Normal	Normal	Pacemaker since 10 years	**HCM**
B-lactate (controls < 2.3 mmol/l)	**2.4–4.3**	**4–19**	**5–13**	**4.1–5.1**	n.d.	**1.9–4.2**	**1.7–9.1**	**2.7–7.9**
CSF-protein (controls < 0.4 g/l)	n.d.	n.d.	**2.3**	n.d.	n.d.	n.d.	**3.5**	**1.5**
Age of death	**5 years**	**24 years**	**11 months**	**16 months**	Alive at 4 years	Alive at 5 years	Alive at 11 years	**8 months**

Abbreviations: B, blood; CSF, cerebrospinal fluid; DQ, developmental quotient; HCM, hypertrophic cardiomyopathy; IQ, intelligence quotient; IUGR, intrauterine growth retardation; n.d., not done.

*Complicated postnatal adaptation due to intracranial haemorrhage.

**PUS1 genotype c.[896+2551_1061delinsATTTTACCA]; [896+2551_1061delinsATTTTACCA].

***COX10 genotype c. [610A>G]; [674C>T].

(P4, 6, and 7), urinary epithelial cells (P4 and 7), and fibroblasts (P3 and 4). Two children with PS (P3 and 4) and very early onset of SA with severe thrombocytopenia since birth died after repeated sepsis at the ages of 11 and 16 months, and one patient (P5) with SA and mild thrombocytopenia since the third month of life survived similarly to the last two patients with PS (P6 and 7) and anemia but without ring sideroblasts. The hematological parameters in all three children subsequently normalized and their clinical symptoms transitioned to Kearns–Sayre syndrome. Two children developed adrenal insufficiency, and one received a pacemaker.

The last child (P8, female) with early neonatal onset of refractory anemia without ring sideroblasts had failure to thrive, microcephaly, mild hypertrophic cardiomyopathy, profound arrest of motor development, and renal tubular acidosis due to a combination of mutations in the *COX10* gene that have not been reported to date. The patient was a compound heterozygote for the novel mutation, c.610A>G (p.Asn204Asp), and the previously described mutation, c.674C>T (p.Pro225Leu).[22] She died at the age of eight months due to sepsis and renal failure. The novel mutation p.Asn204Asp was predicted to be pathogenic by several prediction algorithms (a 0.999 probability to be disease causing by Mutationtaster; a damaging probability score of 0.999 by PolyPhen2-HumVar; a deleterious score of −4.822 by Provean; and a pathogenic probability score of 0.815 by MutPred2).

3.3 | Hematological analyses

All children had anemia (Hb of 16–87 g/L), and all except one (P7) were transfusion dependent every three or four weeks. All children had a

TABLE 2 Hematological analyses in 5 children with sideroblastic anemia (P1–5) and multisystem mitochondrial diseases and three other children with mitochondrial disorders with anemia without ring sideroblasts (P6–8) at the time of diagnosis

Patient	P1 female	P2 male	P3 male	P4 female	P5 female	P6 female	P7 male	P8 female
Mutation	*PUS1**	*PUS1**	mtDNA 8 kb deletion	mtDNA 5.4 kb deletion (m.10382_15783del)	mtDNA 6 kb deletion	mtDNA 4 kb deletion	mtDNA 5 kb deletion (m.8483_13446del)	COX10**
Age at analysis	3 years	6 years	7 months	2 months	9 months	3 months	3 years	1 week
Hb (g/l)	**66**	**16**	**71**	**78**	**87**	**69**	**87**	**57**
Red blood cells ($\times 10^{12}$/l)	**2.45**	**0.53**	**2.4**	**2.6**	**2.5**	**1.8**	n.a.	**2.8**
MCV (fl)	88	**106**	90	98	**98**	**103**	**95**	**113**
WBC ($\times 10^9$/l)	6.1	8.1	5.2	8.2	5.0	8.4	**3.5**	6.9
ANC	3,782	4,293	**832**	**1,230**	1,600	**1,008**	1,925	**1,242**
Platelets ($\times 10^9$/l)	237	337	**46**	**50**	**98**	**19**	**75**	307
Bone marrow								
Sideroblasts	**44%**	**66%**	**78%**	**95%**	**76%**	**43%**	**20%**	**50%**
Ring sideroblasts	**28%**	**18%**	**51%**	**50%**	**24%**	0%	1%	0%
Myelodys plasia in cell lines	Erythroid, myeloid	Erythroid, myeloid, megacaryotic	Erythroid, myeloid	Erythroid, myeloid	Erythroid, myeloid, megacaryotic	Erythroid, myeloid	–	–
Vacuolisation in cell lines precursors	Erythroid	Erythroid	Erythroid, myeloid	Erythroid, myeloid	Erythroid, myeloid	Myeloid	Erythroid	Erythroid

Abbreviations: ANC, absolute neutrophil count (controls > 1500); Hb, haemoglobin; MCV, mean corpuscular volume; WBC, white blood cells; n.a., not available; n.d., not done.
*PUS1 genotype c.[896+2551_1061delinsATTTTACCA]; [896+2551_1061delinsATTTTACCA]).
**COX10 genotype c. [610A>G]; [674C>T].

borderline high or increased mean corpuscular volume (MCV) with normal levels of vitamin B12 and folates. Reticulocytes at the time of anemia were low in all four analyzed children (P1, 2, 3, and 5). Although the white blood cell (WBC) count was normal in all children except P7, the absolute neutrophil count (ANC) was $<1500 \times 10^9$/L in five children (P3, 4, 6, and 8). All children with PS (P3–7) had thrombocytopenia ($19–98 \times 10^9$/L), and all children with nuclear-encoded diseases (P1, 2, and 8) had normal platelet counts.

In the bone marrow, SA with sideroblasts (66%–95%) and ring sideroblasts (18%–51%) was found in four children (P2–P5), and one child (P1) had 44% sideroblasts but an increased number of ring sideroblasts (28%). SA was not found in the other three anemic children without ring sideroblasts (P6–8). Bone marrow dysplasia was present in six children, in all three cell lineages in two of them (P2 and 5), and in two cell lineages (erythroid and myeloid) in four children (P1, 3, 4, and 6). The erythroid abnormalities included megaloblastic changes, multinucleation, eccentric nuclei, nuclear fragments, and karyorrhexis. Dysmorphism of the myeloid lineage presented as the arrest of maturation at the myelocyte stage and defective granulation with abnormally large or absent granules. Megakaryocytic dysplasia was demonstrated by micromegakaryocytes or large and binuclear forms. The bone marrow of all children showed cytoplasmic vacuolization. The vacuoles in precursors of two cell lineages (erythroid and myeloid) were found in three children with PS (P3–5), vacuoles in the erythroid precursors were found only in all three children with nuclear-encoded mutations (P1, 2, and 8) and in one child with PS (P7), and vacuoles in the myeloid precursors were found only in P6 with PS. The bone marrow of P2 with SA and dysplastic changes is shown in Figure 1.

3.4 | Biochemical analyses

The activities of mitochondrial respiratory chain complexes in muscle are shown in Table 3. In P1 and P2, activities of complex I and citrate synthase (CS) were in the reference range, but activities of respiratory chain complexes III and IV were markedly decreased. In addition, P2 showed a decreased activity of complexes I + III. However, P2 was 11 years older than P1 at the time of muscle enzymatic analysis, and complex I enzymatic activity is known to be the highest in neonates and tends to decrease with age.[23] P8 showed low activities of complexes I + III and IV. The decreased activities of complexes I + III and IV were found in all three analyzed PS patients (P3, 4, and 7). All patients, except P3, had a very low ratio between complex IV and CS enzymatic activities.

Protein analyses of respiratory chain complexes revealed reduced amounts of complex IV in the muscle and liver mitochondria of P8. The protein levels of complexes I, III, IV, and V were noticeably reduced in the mitochondria of P1 and P2. The combined oxidative phosphorylation complex deficiency was more profound in the muscle mitochondria of these two patients. Although these results are similar to those of other studies, we also found an increased number of complex V assembly intermediates in both the muscle and liver tissues of patients P1 and P2 (Figure 2). The residual levels of oxidative phosphorylation

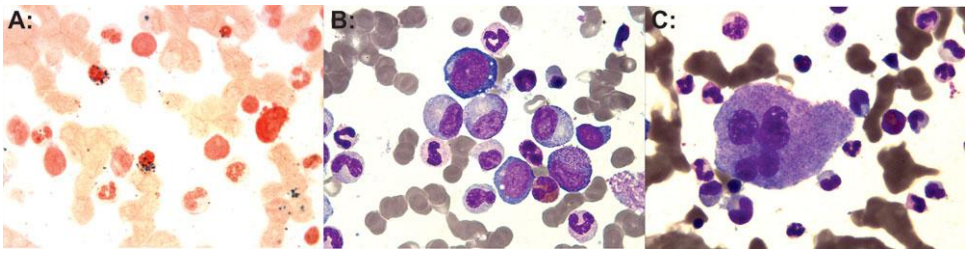

FIGURE 1 Patient 2 with SA and MLASA1 due to a homozygous, 6-kb deletion in the *PUS1* gene. (A) Bone marrow rich in iron and ring sideroblasts are present; (B) vacuolization of marrow precursors, dysplastic changes in neutrophil granulocytes (large and small granulocyte size, irregular maturation of nuclei and the cytoplasm, persistent basophilia of the cytoplasm, frequent hypo-/agranulation but also hypergranularity with irregularly distributed granules; (C) megakaryocytes with separated nuclei and agranular and hyposegmented neutrophils with bilobed and one with monolobed nuclei (pseudo-Pelger–Huët nuclear anomaly). A: Perls' Prussian Blue Iron stain, original magnification ×500, B and C: May–Grünwald Giemsa stain, original magnification ×500–1000

TABLE 3 Activities of mitochondrial respiratory chain complexes in isolated muscle mitochondria in four children with mitochondrial diseases and SA (P1–4) and two children with mitochondrial disorders with anemia without ring sideroblasts (P7 and 8)

Patient	P1 female	P2 male	P3 male	P4 female	P7 male	P8 female
Mutation	*PUS1*[a]	*PUS1*[a]	mtDNA 8-kb deletion	mtDNA 5.4-kb deletion (m.10382_15783del)	mtDNA 5-kb deletion (m.8483_13446del)	COX10[b]
Enzyme	nmol/minute/mg of protein (age-related reference range)					
CI	182 (63–315)	121.9 (110–290)	178 (63–315)	329 (194–354)	173 (118–282)	**101.3** (118–282)
CII	460 (21–93)	n.d.	44 (21–93)	84 (20–108)	49 (28–94)	50.2 (28–94)
CIII	**120** (>200)	**113** (>200)	**89** (>200)	995 (>200)	445 (>200)	317 (100–220)
CIV	**173** (658–1552)	**198** (658–1552)	**439** (658–1552)	**163** (290–1077)	**563** (825–1500)	**59.7** (290–1077)
CI + CIII	232 (126–316)	**69.5** (126–316)	**22** (126–316)	**25** (42–156)	**64** (100–287)	**37.7** (42–156)
CII + III	**64** (82–250)	n.d.	**71** (82–250)	65 (50–206)	258 (97–265)	120 (97–265)
CS	741 (435–1234)	893 (435–1234)	184 (435–1234)	278 (200–640)	767 (528–938)	426.0 (200–640)
CIV/CS	**0.23** (0.66–2.2)	**0.22** (0.66–2.2)	2.3 (0.66–2.2)	**0.59** (1.1–2.2)	**0.74** (1.16–2.13)	**0.14** (1.1–2.2)
PDHc	13.9 (10–40)	n.d.	3.9 (3.5–30)	14.9 (3–13)	n.d.	n.d.

Note: The activities were compared with values of age-matched control samples and CS was used as a reference enzyme.
Abbreviations: CI (complex I, NADH:coenzyme Q reductase); CII (complex II, succinate:coenzyme Q reductase); CIII (complex III, QH2:cytochrome c reductase); CIV (complex IV, cytochrome c oxidase); CI+CIII (NADH:cytochrome c reductase); CII+III (succinate:cytochrome c reductase); CS (citrate synthase); CIV/CS (ratio between CIV and CS); PDHc (pyruvate dehydrogenase complex).
[a]PUS1 genotype c. [896+2551_1061delinsATTTTACCA]; [896+2551_1061delinsATTTTACCA]).
[b]COX10 genotype c.[610A>G]; [674C>T].

complexes are in accordance with the roles of PUS1 and COX10 proteins in the cells.

4 | DISCUSSION

Although anemia is associated with many diseases, the combination of SA and mitochondrial disorders is rare. During the last two decades, we diagnosed 421 patients with multisystem mitochondrial diseases (MD), but SA was found only in five patients, representing <1.2% of patients with MD. Mitochondrial disorders can be caused by mutations in two genomes, which include >300 genes encoding structural subunits, assembly factors, and factors involved in mitochondrial biogenesis and mtDNA maintenance. Interestingly, the three children with anemia and normal levels of platelets had nuclear-encoded multisystem MD with autosomal recessive inheritance, and the five other children with anemia and thrombocytopenia had sporadic, single, large-scale deletions in mtDNA, which may cause a broad spectrum of symptoms ranging from almost fatal PS to multisystem Kearns–Sayre syndrome or attenuated progressive external ophthalmoplegia.[24] The size, location, and heteroplasmy of the mtDNA deletions may be responsible for the clinical phenotype.[25]

PS is characterized by macrocytic aregenerative SA with vacuolization of marrow progenitor cells, thrombocytopenia, and exocrine pancreatic dysfunction, but ring sideroblasts are not present in all children with PS. For example, among the seven children with aregenerative macrocytic anemia described by Bader-Meunier et al,[26] only four had ring sideroblasts, similar to our finding of RS in three of five children with PS. Children with PS are transfusion dependent every 3 to 4 weeks, but the transfusion frequency may gradually decline and even disappear in surviving children as they age.

PS is a sporadic disease due to single, large-scale mtDNA deletions ranging in size from 4 to 14 kb.[27] Most children with PS have failure to thrive and growth retardation; pancreatic insufficiency is present in approximately 25% of patients, and adrenal insufficiency is present in 18%. Diabetes mellitus is less common, and renal tubulopathy may progress to Fanconi syndrome. The prognosis of PS is poor. Eight of 11 children with PS in the study from Italy and 7 of 11 patients from

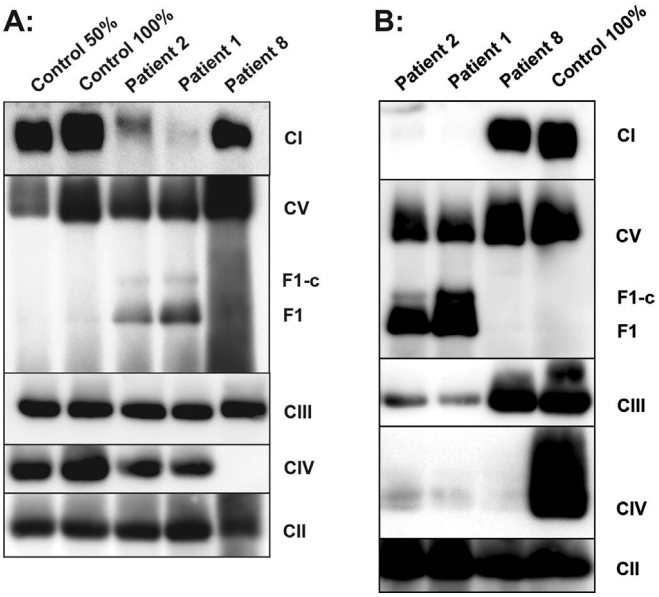

FIGURE 2 Oxidative phosphorylation complex levels in liver (A) and muscle (B) mitochondria of patients 1, 2, and 8 separated by BN-PAGE followed by immunoblotting. In both tissues of patients 1 and 2, a profound, combined oxidative phosphorylation complex deficiency (complexes I, III, IV, and V) was found with an accumulation of assembly intermediates of complex V (F1-part of the complex and F1-c, which is F1-part associated with the c-subunits). Patient 8 mitochondria revealed an isolated deficiency of complex IV in both tissues

the UK died due to sepsis or renal failure,[28,29] similar to our patients with neonatal onset of PS. It may be of importance that these patients had neutropenia and the highest percentage of sideroblasts and ring sideroblasts. The phenotype in surviving children with PS may transition to Kearns–Sayre syndrome, which is characterized by ptosis, exercise intolerance, chronic external ophthalmoplegia, and heart block. This finding was characteristic of the three surviving children with PS (P5–7) in our study, who presented symptoms during infancy or early childhood, but their hematological parameters gradually normalized. Symptoms of Kearns–Sayre syndrome developed, including adrenal insufficiency in two and heart block in one.

MLASA syndrome may present with a broad spectrum of clinical features, including microcephaly, micrognathia, high philtrum, high palate, and mental retardation.[30,31] MLASA was described in 1974, but the causative mutations in the affected genes *PUS1* (MLASA1), *YARS2* (MLASA2), and *MTATP6* (MLASA plus) have been identified in only a small number of patients worldwide.[5–7] Our two patients (P1 and 2) were homozygous for a 6-kb deletion in *PUS1* that leads to a truncated protein (p.Gly148ValfsX41).[32,33] The deletion was not present in 200 control samples or a set of 80 control gDNA samples of Roma origin. Currently, the Database of Genomic Variants identifies only one larger deletion (CNV-variation_8742) affecting exon 4 of *PUS1* with an assessed prevalence of 0.1%.[34] The long, homozygous, disease-causing deletion seems to be quite unique. To the best of our knowledge, this is the first report of the presumed PUS1 loss-of-function phenotype caused by large, homozygous deletions in humans. A previous study showed that various human PUS1 mutants harboring missense amino-acid replacements within catalytic sites are still viable.[35] The clinical severity of MLASA syndrome may be variable, but anemia, microcephaly, and mental insufficiency are typical.[36] Different courses of the disease were observed not only in our patients with the same deletion in the *PUS1* gene but also in their siblings.[36] Surprisingly, none of the reported patients manifested cardiomyopathy similar to our patient (P1), although it may be consistent with higher tissue-specific expression of PUS1 in skeletal muscle, heart, and brain.[5] Similarly, the sensorineural hearing loss presenting in P2 has never been previously reported in patients with PUS1 deficiency.

Iron is an essential trace element participating in erythropoiesis, completing the active sites of many redox enzymes and regulating gene expression via iron-responsive genetic machinery[37] and RNA modifications,[38] and is even likely to be engaged in lipid metabolism.[39] Disruption of iron homeostasis may cause iron overload or deficiency and contribute to anemia, hemochromatosis, and neurological impairments.[40] In patients with MLASA syndrome, SA and iron deposits within erythroblast mitochondria have been documented, thus pointing to faulty iron utilization and sensing.[41] This process seems to be affected by many factors, such as delayed clustering and exclusions of the transferrin receptor,[42] imbalanced regulation of iron trafficking, futile feedback regulation of heme synthesis via Fe–S clusters and/or defective hypoxia sensing.[37,40] Interestingly, very low levels of cytochromes (a, b, and c) were detected in patients' muscle mitochondria,[30] thereby providing more evidence of incorrect protein translation and incorporation of iron within vital molecules, as well as an additional explanation for the cytochrome c oxidase deficiency ordinarily observed in patients with PUS1 deficiency. In addition, secondary hemochromatosis and signs of iron overload has been observed in several PUS1-deficient patients due to chronic SA, requiring regular blood transfusions that may intensify and/or widen the clinical signs of MLASA syndrome (weakness, weight loss, abdominal pain, hepatomegaly, heart failure, retinopathy, and joint impairment). Additionally, experimental evidence also showed that iron overload could promote the UPR response.[43]

The *COX10* gene encodes the assembly factor Cox10, which is involved in the assembly of the heme a and heme a_3 prosthetic groups in subunit I of cytochrome *c* oxidase, the terminal enzyme of the respiratory chain.[44] To date, pathological mutations in the *COX10* gene have been reported in six children and one adult with failure to thrive and/or growth retardation and encephalomyopathy.[22,45–47] Two patients had tubulopathy and one had hypertrophic cardiomyopathy. Only one child was transfusion dependent, and anemia in the others was mild. Our patient with refractory anemia without RS and the mutations p.Asn204Asp and p.Pro225Leu in *COX10* (P8) had failure to thrive, microcephaly, arrested motor development, mild hypertrophic cardiomyopathy, renal tubular acidosis, and renal failure. This combination of missense variants had not yet been documented. Mutation p.Asn204Asp is a novel one and might account for an unexpected disease phenotype in our patient. The mutation is localized in the second transmembrane segment of the heme A:farnesyltransferase, at the II/III loop junction in the highly evolutionarily conserved domain ANSINQ among the vertebrates. Another mutation of Asn^{204} has been described in one of the first COX10 patients (p.Asn204Lys) and it

was predicted that substitution in this region leads to conformational change in the loop that cause adverse effects on heme A synthesis.[46]

When focusing on the cause of anemia in patients with the *COX10* mutation, coincidental occurrence of renal involvement and anemia may be considered due to disruptions in erythropoietin (EPO) synthesis.[48] Surprisingly, the specific cell type responsible for EPO production is still not firmly established, but several hypotheses have been proposed.[49,50] EPO is, to a lesser extent, also produced by the liver[51] and may cross the blood–brain barrier in several types of neuronal cells.[52] Our patient had profound cytochrome *c* oxidase deficiency in muscle and liver tissues. Although a sample of the patient's kidney was not available for analysis, we hypothesize that inefficient EPO generation might have contributed to the anemia because mitochondrial pathology has been found in renal diseases.[53,54] Recently, a new method has been introduced to detect liver and kidney EPO[55] that may help to assess disease severity.

5 | CONCLUSIONS

Identifying the molecular basis of inherited anemia is of the utmost importance, both for patient prognosis and for providing genetic counseling for their families.[56] In our group of 421 patients with multisystem mitochondrial diseases, SA was present in <1.2% of patients and was associated with an unfavorable prognosis in most of them.

ACKNOWLEDGMENTS

This study was supported by research grants from the Ministry of Health of the Czech Republic (AZV 17-30965A, RVO VFN 64165), the Czech Science Foundation (GACR 14-36804G), and Charles University (Progress Q26/LF1, UNCE 204064). We appreciate the assistance provided by Dr. I. Fatorova, University Hospital Hradec Kralove.

CONFLICTS OF INTEREST

The authors have no affiliations with or involvement in any organization or entity with any financial or nonfinancial interest in the subject matter or materials discussed in this article.

ORCID

Marketa Tesarova https://orcid.org/0000-0002-5141-2289

REFERENCES

1. Bottomley SS, Fleming MD. Sideroblastic anemia: diagnosis and management. *Hematol Oncol Clin North Am*. 2014;28:653–670.
2. Malcovati L, Cazzola M. Recent advances in the understanding of myelodysplastic syndromes with ring sideroblasts. *Br J Haematol*. 2016;174:847–858.
3. Patnaik MM, Tefferi A. Refractory anemia with ring sideroblasts (RARS) and RARS with thrombocytosis (RARS-T): 2017 update on diagnosis, risk-stratification, and management. *Am J Hematol*. 2017;92:297–310.
4. Wiseman DH, May A, Jolles S, et al. A novel syndrome of congenital sideroblastic anemia, B-cell immunodeficiency, periodic fevers, and developmental delay (SIFD). *Blood*. 2013;122:112–123.
5. Bykhovskaya Y, Casas K, Mengesha E, Inbal A, Fischel-Ghodsian N. Missense mutation in pseudouridine synthase 1 (PUS1) causes mitochondrial myopathy and sideroblastic anemia (MLASA). *Am J Hum Genet*. 2004;74:1303–1308.
6. Riley LG, Cooper S, Hickey P, et al. Mutation of the mitochondrial tyrosyl-tRNA synthetase gene, YARS2, causes myopathy, lactic acidosis, and sideroblastic anemia–MLASA syndrome. *Am J Hum Genet*. 2010;87:52–59.
7. Bergmann AK, Campagna DR, McLoughlin EM, et al. Systematic molecular genetic analysis of congenital sideroblastic anemia: evidence for genetic heterogeneity and identification of novel mutations. *Pediatr Blood Cancer*. 2010;54:273–278.
8. Diaz GA, Banikazemi M, Oishi K, Desnick RJ, Gelb BD. Mutations in a new gene encoding a thiamine transporter cause thiamine-responsive megaloblastic anaemia syndrome. *Nat Genet*. 1999;22:309–312.
9. Riley LG, Rudinger-Thirion J, Schmitz-Abe K, et al. LARS2 Variants associated with hydrops, lactic acidosis, sideroblastic anemia, and multisystem failure. *JIMD Rep*. 2016;28:49–57.
10. Schmitz-Abe K, Ciesielski SJ, Schmidt PJ, et al. Congenital sideroblastic anemia due to mutations in the mitochondrial HSP70 homologue HSPA9. *Blood*. 2015;126:2734–2738.
11. Lichtenstein DA, Crispin AW, Sendamarai AK, et al. A recurring mutation in the respiratory complex 1 protein NDUFB11 is responsible for a novel form of X-linked sideroblastic anemia. *Blood*. 2016;128:1913–1917.
12. Bohm M, Pronicka E, Karczmarewicz E, et al. Retrospective, multicentric study of 180 children with cytochrome C oxidase deficiency. *Pediatr Res*. 2006;59:21–26.
13. Amati-Bonneau P, Valentino ML, Reynier P, et al. OPA1 mutations induce mitochondrial DNA instability and optic atrophy 'plus' phenotypes. *Brain*. 2008;131(Pt 2):338–351.
14. Mazurova S, Magner M, Kucerova-Vidrova V, et al. Thymidine kinase 2 and alanyl-tRNA synthetase 2 deficiencies cause lethal mitochondrial cardiomyopathy: case reports and review of the literature. *Cardiol Young*. 2017;27:936–944.
15. Makinen MW, Lee CP. Biochemical studies of skeletal muscle mitochondria. I. Microanalysis of cytochrome content, oxidative and phosphorylative activities of mammalian skeletal muscle mitochondria. *Arch Biochem Biophys*. 1968;126:75–82.
16. Rickwood D, Wilson MT, Darley-Usmar WM. Isolation and characteristics of intact mitochondria. In: Darley-Usmar VM, Rickwood D, Wilson MT, eds. Mitochondria: A Practical Approach. Oxford, UK: IRL Press; 1987:3–5.
17. Lowry OH, Rosebrough NJ, Farr AL, Randall RJ. Protein measurement with the Folin phenol reagent. *J Biol Chem*. 1951;193:265–275.
18. Rustin P, Chretien D, Bourgeron T, et al. Biochemical and molecular investigations in respiratory chain deficiencies. *Clin Chim Acta*. 1994;228:35–51.
19. Schagger H, Cramer WA, von Jagow G. Analysis of molecular masses and oligomeric states of protein complexes by blue native electrophoresis and isolation of membrane protein complexes by two-dimensional native electrophoresis. *Anal Biochem*. 1994;217:220–230.
20. Stiburek L, Vesela K, Hansikova H, et al. Tissue-specific cytochrome c oxidase assembly defects due to mutations in SCO2 and SURF1. *Biochem J*. 2005;392(Pt 3):625–632.
21. Fornuskova D, Brantova O, Tesarova M, et al. The impact of mitochondrial tRNA mutations on the amount of ATP synthase differs in the brain compared to other tissues. *Biochim Biophys Acta*. 2008;1782:317–325.

22. Antonicka H, Leary SC, Guercin GH, et al. Mutations in COX10 result in a defect in mitochondrial heme A biosynthesis and account for multiple, early-onset clinical phenotypes associated with isolated COX deficiency. *Hum Mol Genet*. 2003;12:2693–2702.
23. Honzik T, Wenchich L, Bohm M, et al. Activities of respiratory chain complexes and pyruvate dehydrogenase in isolated muscle mitochondria in premature neonates. *Early human development*. 2008;84:269–276.
24. Mancuso M, Orsucci D, Angelini C, et al. Redefining phenotypes associated with mitochondrial DNA single deletion. *J Neurol*. 2015;262:1301–1309.
25. Grady JP, Campbell G, Ratnaike T, et al. Disease progression in patients with single, large-scale mitochondrial DNA deletions. *Brain*. 2014;137(Pt 2):323–334.
26. Bader-Meunier B, Mielot F, Breton-Gorius J, et al. Hematologic involvement in mitochondrial cytopathies in childhood: a retrospective study of bone marrow smears. *Pediatr Res*. 1999;46:158–162.
27. Rotig A, Bourgeron T, Chretien D, Rustin P, Munnich A. Spectrum of mitochondrial DNA rearrangements in the Pearson marrow-pancreas syndrome. *Hum Mol Genet*. 1995;4:1327–1330.
28. Farruggia P, Di Cataldo A, Pinto RM, et al. Pearson syndrome: a retrospective cohort study from the Marrow Failure Study Group of A.I.E.O.P. (Associazione Italiana Emato-Oncologia Pediatrica). *JIMD Rep*. 2016;26:37–43.
29. Broomfield A, Sweeney MG, Woodward CE, et al. Paediatric single mitochondrial DNA deletion disorders: an overlapping spectrum of disease. *J Inherit Metab Dis*. 2015;38:445–457.
30. Inbal A, Avissar N, Shaklai M, et al. Myopathy, lactic acidosis, and sideroblastic anemia: a new syndrome. *Am J Med Genet*. 1995;55:372–378.
31. Zeharia A, Fischel-Ghodsian N, Casas K, et al. Mitochondrial myopathy, sideroblastic anemia, and lactic acidosis: an autosomal recessive syndrome in Persian Jews caused by a mutation in the PUS1 gene. *J Child Neurol*. 2005;20:449–452.
32. Hamma T, Ferre-D'Amare AR. Pseudouridine synthases. *Chem Biol*. 2006;13:1125–1135.
33. Czudnochowski N, Wang AL, Finer-Moore J, Stroud RM. In human pseudouridine synthase 1 (hPus1), a C-terminal helical insert blocks tRNA from binding in the same orientation as in the Pus1 bacterial homologue TruA, consistent with their different target selectivities. *J Mol Biol*. 2013;425:3875–3887.
34. MacDonald JR, Ziman R, Yuen RK, Feuk L, Scherer SW. The Database of Genomic Variants: a curated collection of structural variation in the human genome. *Nucleic Acids Res*. 2014;42(Database issue):D986–992.
35. Sibert BS, Fischel-Ghodsian N, Patton JR. Partial activity is seen with many substitutions of highly conserved active site residues in human pseudouridine synthase 1. *RNA*. 2008;14:1895–1906.
36. Fernandez-Vizarra E, Berardinelli A, Valente L, Tiranti V, Zeviani M. Nonsense mutation in pseudouridylate synthase 1 (PUS1) in two brothers affected by myopathy, lactic acidosis and sideroblastic anaemia (MLASA). *J Med Genet*. 2007;44:173–180.
37. Anderson CP, Shen M, Eisenstein RS, Leibold EA. Mammalian iron metabolism and its control by iron regulatory proteins. *Biochim Biophys Acta*. 2012;1823:1468–1483.
38. Kimura S, Suzuki T. Iron-sulfur proteins responsible for RNA modifications. *Biochim Biophys Acta*. 2015;1853:1272–1283.
39. Klug L, Daum G. Yeast lipid metabolism at a glance. *FEMS Yeast Res*. 2014;14:369–388.
40. Chen C, Paw BH. Cellular and mitochondrial iron homeostasis in vertebrates. *Biochim Biophys Acta*. 2012;1823:1459–1467.
41. Yun S, Vincelette ND. Update on iron metabolism and molecular perspective of common genetic and acquired disorder, hemochromatosis. *Crit Rev Oncol Hematol*. 2015;95:12–25.
42. Ahlqvist KJ, Leoncini S, Pecorelli A, et al. MtDNA mutagenesis impairs elimination of mitochondria during erythroid maturation leading to enhanced erythrocyte destruction. *Nat Commun*. 2015;6:6494.
43. Henkel A, Green RM. The unfolded protein response in fatty liver disease. *Semin Liver Dis*. 2013;33:321–329.
44. Scaglia F, Towbin JA, Craigen WJ, et al. Clinical spectrum, morbidity, and mortality in 113 pediatric patients with mitochondrial disease. *Pediatrics*. 2004;114:925–931.
45. Coenen MJ, van den Heuvel LP, Ugalde C, et al. Cytochrome c oxidase biogenesis in a patient with a mutation in COX10 gene. *Ann Neurol*. 2004;56:560–564.
46. Valnot I, von Kleist-Retzow JC, Barrientos A, et al. A mutation in the human heme A:farnesyltransferase gene (COX10) causes cytochrome c oxidase deficiency. *Hum Mol Genet*. 2000;9:1245–1249.
47. Pitceathly RD, Taanman JW, Rahman S, et al. COX10 mutations resulting in complex multisystem mitochondrial disease that remains stable into adulthood. *JAMA Neurol*. 2013;70:1556–1561.
48. Suzuki N, Obara N, Pan X, et al. Specific contribution of the erythropoietin gene 3′ enhancer to hepatic erythropoiesis after late embryonic stages. *Mol Cell Biol*. 2011;31:3896–3905.
49. Nagai T, Yasuoka Y, Izumi Y, et al. Reevaluation of erythropoietin production by the nephron. *Biochem Biophys Res Commun*. 2014;449:222–228.
50. Maxwell PH, Ferguson DJ, Nicholls LG, et al. Sites of erythropoietin production. *Kidney Int*. 1997;51:393–401.
51. Benderro GF, LaManna JC. Kidney EPO expression during chronic hypoxia in aged mice. *Adv Exp Med Biol*. 2013;765:9–14.
52. Subiros N, Del Barco DG, Coro-Antich RM. Erythropoietin: still on the neuroprotection road. *Ther Adv Neurol Disord*. 2012;5:161–173.
53. Che R, Yuan Y, Huang S, Zhang A. Mitochondrial dysfunction in the pathophysiology of renal diseases. *Am J Physiol Renal Physiol*. 2014;306:F367–378.
54. O'Toole JF. Renal manifestations of genetic mitochondrial disease. *Int J Nephrol Renovasc Dis*. 2014;7:57–67.
55. Lonnberg M, Garle M, Lonnberg L, Birgegard G. Patients with anaemia can shift from kidney to liver production of erythropoietin as shown by glycoform analysis. *J Pharm Biomed Anal*. 2013;81-82:187–192.
56. Fujiwara T, Harigae H. Pathophysiology and genetic mutations in congenital sideroblastic anemia. *Pediatr Int*. 2013;55:675–679.

How to cite this article: Tesarova M, Vondrackova A, Stufkova H, et al. Sideroblastic anemia associated with multisystem mitochondrial disorders. *Pediatr Blood Cancer*. 2019;66:e27591. https://doi.org/10.1002/pbc.27591

Supplement 7)

Štufková, H., Kolářová, H., Lokvencová, K., Honzík, T., Zeman, J., Hansíková, H., and Tesařová, M. (2022). **A Novel *MTTK* Gene Variant m.8315A>C as a Cause of MERRF Syndrome.** Genes (Basel) 13 (7) 1245. IF = 4.141, Quartile Score = Q2 (2021).

genes

MDPI

Article

A Novel *MTTK* Gene Variant m.8315A>C as a Cause of MERRF Syndrome

Hana Štufková, Hana Kolářová, Kateřina Lokvencová, Tomáš Honzík, Jiří Zeman, Hana Hansíková and Markéta Tesařová *

Department of Pediatrics and Inherited Metabolic Disorders, First Faculty of Medicine, Charles University, and General University Hospital in Prague, 128 08 Prague, Czech Republic; hana.stufkova@lf1.cuni.cz (H.Š.); hana.kolarova@vfn.cz (H.K.); katerina.lokvencova@vfn.cz (K.L.); tomas.honzik@vfn.cz (T.H.); jzem@lf1.cuni.cz (J.Z.); hana.hansikova@lf1.cuni.cz (H.H.)
* Correspondence: marketa.tesarova@lf1.cuni.cz; Tel.: +420-224-967-748

Abstract: In this study, we report on a novel heteroplasmic pathogenic variant in mitochondrial DNA (mtDNA). The studied patient had myoclonus, epilepsy, muscle weakness, and hearing impairment and harbored a heteroplasmic m.8315A>C variant in the *MTTK* gene with a mutation load ranging from 71% to >96% in tested tissues. In muscle mitochondria, markedly decreased activities of respiratory chain complex I + III and complex IV were observed together with mildly reduced amounts of complex I and complex V (with the detection of V*- and free F1-subcomplexes) and a diminished level of complex IV holoenzyme. This pattern was previously seen in other *MTTK* pathogenic variants. The novel variant was not present in internal and publicly available control databases. Our report further expands the spectrum of *MTTK* variants associated with mitochondrial encephalopathies in adults.

Keywords: mtDNA; *MTTK* gene; OXPHOS; heteroplasmy; m.8315A>C

Citation: Štufková, H.; Kolářová, H.; Lokvencová, K.; Honzík, T.; Zeman, J.; Hansíková, H.; Tesařová, M. A Novel *MTTK* Gene Variant m.8315A>C as a Cause of MERRF Syndrome. *Genes* **2022**, *13*, 1245. https://doi.org/10.3390/genes13071245

Academic Editor: Wolfram S. Kunz

Received: 1 June 2022
Accepted: 11 July 2022
Published: 14 July 2022

1. Introduction

The analysis of mitochondrial DNA (mtDNA) is an essential step in the diagnosis of patients with mitochondrial disease (MD), and although variations in nuclear genes are increasingly being reported, mtDNA sequencing should precede more complex genomic analysis, especially in adults with suspected MD. Since their first description in 1990, the number of pathogenic variants in mitochondrial tRNA genes has steadily increased [1,2], and associations with a striking variety of clinical features have been reported [3]. Mitochondrial disease can present in infancy or adulthood in a multisystemic or highly tissue-specific manner. Many organ systems can be affected in varying combinations based on the heteroplasmy levels and energy demand in particular tissues. The *MTTK* gene, coding for mitochondrial tRNA-Lys, is the second most common site of mutations in mtDNA, and 28 pathogenic variants have been described [4]. Mitochondrial tRNA-Lys, similarly to other 21 tRNAs encoded by mtDNA, is essential for mitochondrial translation; thus, its mutations lead to a combined deficiency of oxidative phosphorylation (OXPHOS) complexes. Classically, patients present ataxia, myoclonus, or epilepsy, indicating CNS involvement and myopathy [5,6].

2. Materials and Methods

2.1. Patient

The patient, now a 39-year-old woman, is the only child of healthy, unrelated parents, and her early development was uneventful. Since the age of 10 years, the patient reported having increased fatigue and slightly altered postural stability. However, until her early adulthood, the patient's state was rather unremarkable, and she was able to complete her master's degree. At age of 30, the patient developed focal sensory seizures with

numerous multi-colored photopsias arising from the right occipital lobe and lasting several hours. She felt the progression of both fatigue and exercise intolerance and further balance deterioration. At the age of 35, focal motoric seizures in the left hemisphere occurred. She was never well-stabilized and required repeated hospitalizations due to repeated migrating myoclonias. During an intercurrent Candida sepsis, the seizures progressively increased in frequency and evolved to generalized convulsive status epilepticus refractory to acute first- and second-line antiepileptic drugs. Currently, she suffers from epilepsy partialis continua with daily myoclonic seizures in her left abdominal wall. At the latest clinical evaluation, she was severely atactic and dysarthric, and she reported occasional difficulty swallowing. There was moderate proximal and distal weakness in all extremities and postictal hypoesthesia in the left side of the face, left arm, and right leg. A recent audiology examination revealed mild mixed bilateral hearing impairment. The blood test results were normal, including serum CK and lactic acid concentrations, but her serum alanine level was mildly increased (538 μmol/L; controls < 500). Mild hyperlactaciduria was observed (76 mmol/mol of creatinine; controls < 30).

2.2. Mitochondrial DNA Sequencing

Total genomic DNA was isolated from blood, muscle biopsy, buccal swab cells, and hair follicles using the following kits: the Gentra Puregene Blood Kit, QIAamp DNA Mini Kit, and QIAamp DNA Micro Kit, respectively (all Qiagen, Hilden, Germany). For mutation analysis, the SeqCap EZ Design: Mitochondrial Genome Design (Roche NimbleGen, Pleasonton, CA, USA) enrichment kit was used for the preparation of the sequencing library, followed by analysis using the MiSeq (Illumina, San Diego, CA, USA) system, specifically, the MiSeq Reagent Sequencing kit v3. The revised Cambridge Reference Sequence (NC_012920) was used for variant annotation.

2.3. Mitochondria Isolation

A sample obtained by muscle biopsy was transported on ice (at 4 °C), and mitochondria were isolated immediately according to standard differential centrifugation procedures [7] in a buffer containing 150 mM KCl, 50 mM Tris/HCl, 2 mM EDTA, and 2 μg/mL aprotinin (pH 7.5) at 4 °C [8].

2.4. MEGS Analysis

The analysis of the mitochondrial energy-generating system (MEGS) capacity in fresh postnuclear muscle supernatant was determined by measuring the oxidation rates of 14C-labeled pyruvate malate and succinate, donors and acceptors of Acetyl-CoA, and inhibitors of TCA cycle according to Janssen et al. [9] using ten different incubations.

2.5. Spectrophotometry

The activities of respiratory chain complexes (complex I—NADH:coenzyme Q oxidoreductase, CI, EC 1.6.5.3; complex I + III—NADH:cytochrome c oxidoreductase, CI + III; complex II—succinate-coenzyme Q oxidoreductase, CII, EC 1.3.5.1; complex II + III—succinate:cytochrome c oxidoreductase, CII + III; complex III—coenzyme Q:cytochrome c oxidoreductase, CIII, EC 7.1.1.8; complex IV—cytochrome c oxidase, CIV, EC 1.9.3.1) were measured according to [10]. The activity of citrate synthase (CS, EC 2.3.3.1), serving as the control enzyme to avoid assay variability, was measured according to [11]. Protein concentrations were measured using the Lowry method.

2.6. Electrophoresis

Blue Native Polyacrylamide Gel Electrophoresis (BN-PAGE) separation [12] of mitochondrial membrane complexes on polyacrylamide 6–15% (*w*/*v*) gradient gels (MiniProtean® 3 System; Bio-Rad, Hercules, CA, USA) followed by immunoblot analysis was used to analyze the steady-state levels of the oxidative phosphorylation system complexes. The primary detection of BN-PAGE blots was performed using mouse monoclonal antibodies

against the CI subunit NDUFA9 (1:2000), complex II subunit SDH70 protein (1: 20,000), complex III subunit Core 2 (1:20,000), complex IV subunit COX2 (1:10,000), and ATP synthase subunit alpha (1:4000) (Abcam, Cambridge, UK). The immunoblots were detected with peroxidase-conjugated secondary antibodies and SuperSignal West Femto Maximum Sensitivity Substrate (Thermo Fisher Scientific, Waltham, MA, USA) using G:Box (Syngene, Cambridge, UK).

3. Results

MtDNA sequencing in blood revealed a heteroplasmic variant m.8315A>C in the *MTTK* gene. To further assess the variant, several tissues, including muscle biopsy, were collected, and mutation loads were determined. The highest level of heteroplasmy was found in hair follicles > 96%, followed by 86% in buccal swab cells, 85% in muscle, and 71% in blood leucocytes (Figure 1).

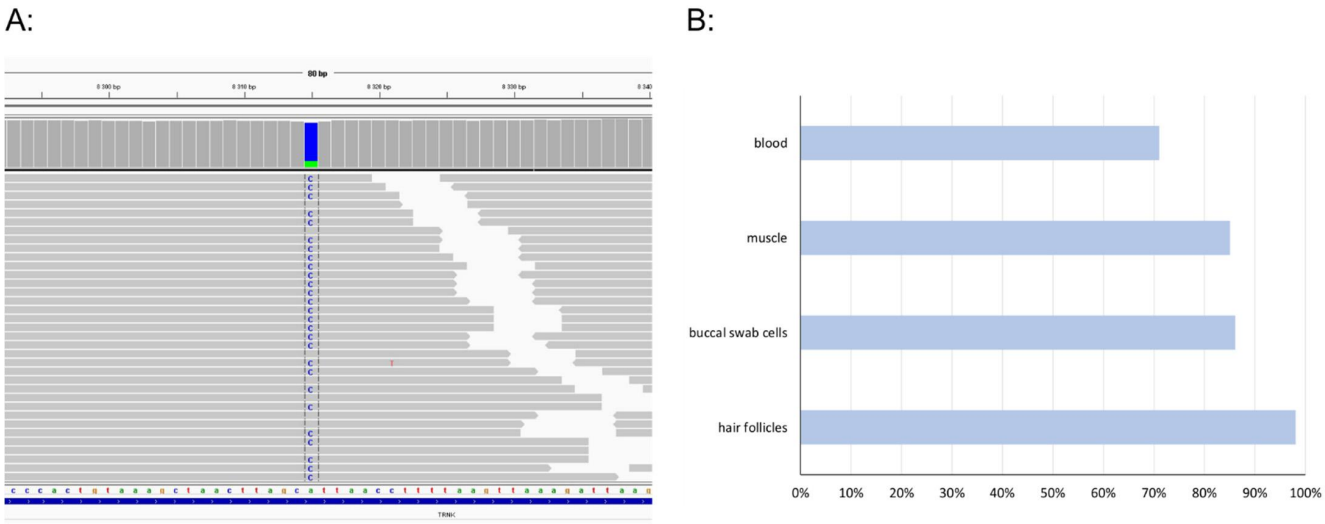

Figure 1. A *MTTK* gene variant m.8315A>C. IGV snapshot of mtDNA sequencing in patient's muscle (**A**); overview of heteroplasmy levels in patient tissues (**B**).

In a muscle sample obtained from a biopsy of the quadriceps, the analysis of the MEGS capacity indicated disturbed OXPHOS activity with decreased ADP stimulation. The respiratory chain enzyme activities in isolated mitochondria showed normal activities of respiratory chain complexes I and III. Markedly decreased were activities of complexes I + III and IV, as well as complex IV to the citrate synthase (CS) ratio in comparison to age-related controls (Table 1). Interestingly, the activities of respiratory chain complexes II and II + III were slightly increased, suggesting a compensation effect. However, no structural changes or RRF- or COX-negative fibers were detected.

Table 1. Activities of respiratory chain complexes in muscle mitochondria.

	Patient	**Controls (n = 26)**
	(nmol/min/mg Protein)	
Complex I	262.1	118–282
Complex I + III	**50.7**	100–287
Complex II	124.8	28–94
Complex II + III	320	97–267
Complex III	620.8	321–640
Complex IV	**112.9**	825–1500
Citrate Synthase (CS)	573.3	528–938
Complex IV/CS	**0.20**	1.16–2.13

The separation of muscle mitochondrial proteins using BN-PAGE followed by Western blotting and immunodetection revealed mildly reduced amounts of complex I (40% of the control) and complex V (approx. 50% of the control) with accumulated sub-complexes, most likely V* (F1-ATPase with several c-subunits) and F1-ATPase (α and β subunits hexamer with central stalk subunits). The steady-state level of complex IV holoenzyme was diminished in patient mitochondria (approx. 20% of the control, Figure 2).

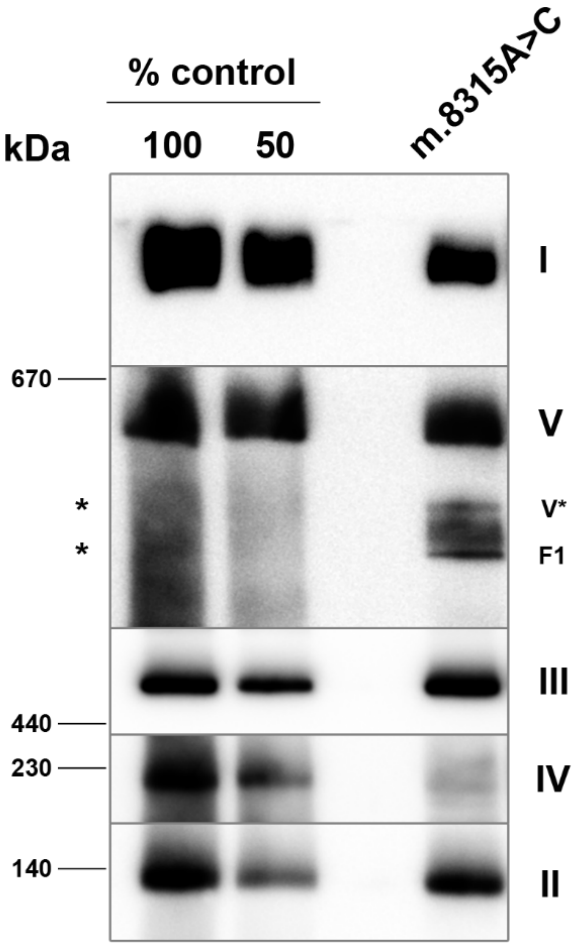

Figure 2. Analysis of the assembly of OXPHOS complexes by immunoblotting of BN-PAGE in muscle mitochondria. BN-PAGE of lauryl maltoside-solubilized mitochondria was electroblotted onto PVDF membranes and probed with monoclonal antibodies that detect the native forms of the OXPHOS complexes. Two aliquots of control mitochondria corresponding to the indicated dilutions of control samples were loaded on the same gels. I—complex I; II—complex II; III—complex III; IV—complex IV; V—complex V; V*—complex V subcomplex composed of F1-ATPase with several c-subunits; F1—F1-ATPase; *-expected migration of complex V subcomplexes.

4. Discussion

Mitochondrial tRNA pathogenic variants are associated with a wide range of clinical phenotypes. Over the years, almost 30 disease variants in the *MTTK* gene have been identified and their pathogenicity more or less assessed. We found an unreported heteroplasmic variant m.8315A>C localized between the D-stem and AC-stem of mitochondrial tRNA-Lys. Using ACMG/AMP criteria adapted for mitochondrial variants [13], the m.8315A>C variant was classified as a variant of unknown significance since it is absent from controls (PM2), the phenotype suggests a single gene etiology (PP4), and it was classified as likely benign by in silico analyses (BP4). Nonetheless, we provide several key arguments supporting the pathogenicity of the m.8315A>C variant. First, despite the linker between D- and AC- stems not having been previously predicted as a mutation hotspot among mt-

tRNAs [14], based on *MTTK* sequence alignment, there is only a single purine nucleotide, either A or G, found in this position among 40 species [15]. Thus, the substitution of adenine for cytosine at position m.8315 may disturb interactions stabilizing the secondary structure of mt-tRNA-Lys. The purine nucleotides are conserved in the linker between the D-stem and AC-stem of other five mt-tRNAs (mt-tRNA-Glu, mt-tRNA-Ile, mt-tRNA-Cys, mt-tRNA-Phe, and mt-tRNA-Tyr) [15]. Second, the m.8315A>C variant was absent from the available databases, Mitomap [4], GnomAD [16], and Helix [17], as well as our internal one. Interestingly, m.8315A>G occurred with a frequency of 0.002–0.037% in public databases, which is in accordance with the conservation of the purine nucleotide in this position. Third, the heteroplasmy levels differed in the tested tissues of the patient, with the lowest mutation load observed in the blood. Unfortunately, no maternal relatives were available for mutation testing since the patient has no siblings or children, and her mother is deceased. Fourth, the muscle biopsy provided significant support for the pathogenicity of the m.8315A>C variant. Despite the absence of ragged-red fibers, which is not unique for MERRF (myoclonic epilepsy with ragged-red fibres) patients [18], combined OXPHOS complexes deficiency was apparent in the patient´s muscle mitochondria. Based on the activity measurement and analysis of the steady-state levels of OXPHOS complexes, complex IV was the most severely affected, compared to a milder complex I and complex V deficiency. We observed this pattern in our previous study analyzing the impact of two *MTTK* genes' (m.8363G>A and m.8344A>G) and one *MTTL1* gene's (m.3243A>G) pathogenic variants on OXPHOS complexes in muscle, heart, liver, and brain mitochondria [19]. In muscle, both *MTTK* gene variants resulted in profoundly decreased levels of complex IV, with similar or milder decreases in complex I levels with markedly reduced levels of the complex V holoenzyme with accumulated sub-complexes containing F1-ATPase. Interestingly, each of the *MTTK* variants, including the novel m.8315A>C variant, are localized in different secondary structures of mitochondrial tRNA-Lys (m.8315—linker of D-stem and AC-stem, m.8344—T-loop, and m.8363—acceptor stem), which results in the same pattern of combined OXPHOS complex deficiency (diminished CIV levels, with a profound decrease in CI and CV, and accumulated CV sub-complexes), which is distinct from the *MTTL1* gene variant [19].

5. Conclusions

Our report provides solid evidence supporting the pathogenicity of a novel heteroplasmic variant, m.8315A>C, and further expands the spectrum of *MTTK* gene variants associated with mitochondrial encephalopathies in adults. It also highlights the substantial role of muscle biopsies in the evaluation of the pathogenicity of novel mtDNA variants. However, additional reports are necessary to definitively confirm the pathogenicity of the m.8315A>C variant.

Author Contributions: Conceptualization, M.T.; methodology, H.Š., H.H., K.L. and M.T.; investigation, H.Š., H.K., T.H., J.Z., H.H. and M.T.; writing—original draft preparation, H.Š., H.K. and M.T.; writing—review and editing, H.Š., H.K., K.L., T.H., J.Z., H.H. and M.T; funding acquisition, M.T. and J.Z. All authors have read and agreed to the published version of the manuscript.

Funding: This work was supported by the Ministry of Health of the Czech Republic (grant number: AZV 17-30965A).

Institutional Review Board Statement: This study was conducted in accordance with the Declaration of Helsinki and approved by the Ethics Committee of General University Hospital in Prague (reference nr. 69/16).

Informed Consent Statement: Informed consent was obtained from the subject involved in the study.

Data Availability Statement: Not applicable.

Conflicts of Interest: The authors declare no conflict of interest. The funders had no role in the design of the study; in the collection, analyses, or interpretation of data; in the writing of the manuscript, or in the decision to publish the results.

References

1. Shoffner, J.M.; Lott, M.T.; Lezza, A.M.; Seibel, P.; Ballinger, S.W.; Wallace, D.C. Myoclonic epilepsy and ragged-red fiber disease (MERRF) is associated with a mitochondrial DNA tRNA(Lys) mutation. *Cell* **1990**, *61*, 931–937. [CrossRef]
2. Richter, U.; McFarland, R.; Taylor, R.W.; Pickett, S.J. The molecular pathology of pathogenic mitochondrial tRNA variants. *FEBS Lett.* **2021**, *595*, 1003–1024. [CrossRef] [PubMed]
3. DiMauro, S.; Schon, E.A.; Carelli, V.; Hirano, M. The clinical maze of mitochondrial neurology. *Nat. Rev. Neurol.* **2013**, *9*, 429–444. [CrossRef] [PubMed]
4. MITOMAP: A Human Mitochondrial Genome Database 2019. Available online: http://www.mitomap.org (accessed on 26 May 2022).
5. Blakely, E.L.; Alston, C.L.; Lecky, B.; Chakrabarti, B.; Falkous, G.; Turnbull, D.M.; Taylor, R.W.; Gorman, G.S. Distal weakness with respiratory insufficiency caused by the m.8344A>G "MERRF" mutation. *Neuromuscul. Disord.* **2014**, *24*, 533–536. [CrossRef] [PubMed]
6. Mancuso, M.; Orsucci, D.; Angelini, C.; Bertini, E.; Carelli, V.; Comi, G.P.; Minetti, C.; Moggio, M.; Mongini, T.; Servidei, S.; et al. Phenotypic heterogeneity of the 8344A>G mtDNA "MERRF" mutation. *Neurology* **2013**, *80*, 2049–2054. [CrossRef] [PubMed]
7. Makinen, M.W.; Lee, C.P.; Shy, G.M. Microanalysis of cytochrome content, oxidative and phosphorylative activities of human skeletal muscle mitochondria. *Neurology* **1968**, *18*, 299. [PubMed]
8. Jesina, P.; Tesarova, M.; Fornuskova, D.; Vojtiskova, A.; Pecina, P.; Kaplanova, V.; Hansikova, H.; Zeman, J.; Houstek, J. Diminished synthesis of subunit a (ATP6) and altered function of ATP synthase and cytochrome c oxidase due to the mtDNA 2 bp microdeletion of TA at positions 9205 and 9206. *Biochem. J.* **2004**, *383*, 561–571. [CrossRef] [PubMed]
9. Janssen, A.J.; Trijbels, F.J.; Sengers, R.C.; Wintjes, L.T.; Ruitenbeek, W.; Smeitink, J.A.; Morava, E.; van Engelen, B.G.; van den Heuvel, L.P.; Rodenburg, R.J. Measurement of the energy-generating capacity of human muscle mitochondria: Diagnostic procedure and application to human pathology. *Clin. Chem.* **2006**, *52*, 860–871. [CrossRef] [PubMed]
10. Rustin, P.; Chretien, D.; Bourgeron, T.; Gerard, B.; Rotig, A.; Saudubray, J.M.; Munnich, A. Biochemical and molecular investigations in respiratory chain deficiencies. *Clin. Chim. Acta* **1994**, *228*, 35–51. [CrossRef]
11. Srere, P.A.; John, M.L. Citrate synthase: [EC 4.1.3.7. Citrate oxaloacetate-lyase (CoA-acetylating)]. In *Methods in Enzymology*; Academic Press: Cambridge, MA, USA, 1969; pp. 3–11.
12. Schagger, H.; Cramer, W.A.; von Jagow, G. Analysis of molecular masses and oligomeric states of protein complexes by blue native electrophoresis and isolation of membrane protein complexes by two-dimensional native electrophoresis. *Anal. Biochem.* **1994**, *217*, 220–230. [CrossRef]
13. McCormick, E.M.; Lott, M.T.; Dulik, M.C.; Shen, L.; Attimonelli, M.; Vitale, O.; Karaa, A.; Bai, R.; Pineda-Alvarez, D.E.; Singh, L.N.; et al. Specifications of the ACMG/AMP standards and guidelines for mitochondrial DNA variant interpretation. *Hum. Mutat.* **2020**, *41*, 2028–2057. [CrossRef] [PubMed]
14. Blakely, E.L.; Yarham, J.W.; Alston, C.L.; Craig, K.; Poulton, J.; Brierley, C.; Park, S.M.; Dean, A.; Xuereb, J.H.; Anderson, K.N.; et al. Pathogenic mitochondrial tRNA point mutations: Nine novel mutations affirm their importance as a cause of mitochondrial disease. *Hum. Mutat.* **2013**, *34*, 1260–1268. [CrossRef] [PubMed]
15. Putz, J.; Dupuis, B.; Sissler, M.; Florentz, C. Mamit-tRNA, a database of mammalian mitochondrial tRNA primary and secondary structures. *RNA* **2007**, *13*, 1184–1190. [CrossRef] [PubMed]
16. Laricchia, K.M.; Lake, N.J.; Watts, N.A.; Shand, M.; Haessly, A.; Gauthier, L.; Benjamin, D.; Banks, E.; Soto, J.; Garimella, K.; et al. Mitochondrial DNA variation across 56,434 individuals in gnomAD. *Genome Res.* **2022**, *32*, 569–582. [CrossRef] [PubMed]
17. Bolze, A.; Mendez, F.; White, S.; Tanudjaja, F.; Isaksson, M.; Jiang, R.; Rossi, A.D.; Cirulli, E.; Rashkin, M.; Metcalf, W.; et al. A catalog of homoplasmic and heteroplasmic mitochondrial DNA variants in humans. *bioRxiv* **2019**. [CrossRef]
18. Mancuso, M.; Petrozzi, L.; Filosto, M.; Nesti, C.; Rocchi, A.; Choub, A.; Pistolesi, S.; Massetani, R.; Fontanini, G.; Siciliano, G. MERRF syndrome without ragged-red fibers: The need for molecular diagnosis. *Biochem. Biophys. Res. Commun.* **2007**, *354*, 1058–1060. [CrossRef] [PubMed]
19. Fornuskova, D.; Brantova, O.; Tesarova, M.; Stiburek, L.; Honzik, T.; Wenchich, L.; Tietzeova, E.; Hansikova, H.; Zeman, J. The impact of mitochondrial tRNA mutations on the amount of ATP synthase differs in the brain compared to other tissues. *Biochim. Biophys. Acta* **2008**, *1782*, 317–325. [CrossRef] [PubMed]

Univerzita Karlova v Praze, 1. lékařská fakulta
Kateřinská 32, Praha 2

Prohlášení zájemce o nahlédnutí
do závěrečné práce absolventa studijního programu
uskutečňovaného na 1. lékařské fakultě Univerzity Karlovy v Praze

Jsem si vědom/a, že závěrečná práce je autorským dílem a že informace získané nahlédnutím do zpřístupněné závěrečné práce nemohou být použity k výdělečným účelům, ani nemohou být vydávány za studijní, vědeckou nebo jinou tvůrčí činnost jiné osoby než autora.

Byl/a jsem seznámen/a se skutečností, že si mohu pořizovat výpisy, opisy nebo kopie závěrečné práce, jsem však povinen/a s nimi nakládat jako s autorským dílem a zachovávat pravidla uvedená v předchozím odstavci.

Příjmení, jméno (hůlkovým písmem)	**Číslo dokladu totožnosti vypůjčitele (např. OP, cestovní pas)**	**Signatura závěrečné práce**	**Datum**	**Podpis**